Novel Interactions of Volatile Anaesthetics on O_2 Sensing and TASK Channels in Carotid Body Type-1 Cells

A thesis submitted for the degree of Doctor of Philosophy

Nicky Huskens

Wolfson College

University of Oxford

Trinity Term 2015

Dedicated to my parents

Abstract:

Novel Interactions of Volatile Anaesthetics on O_2 Sensing and TASK Channels in Carotid Body Type-1 Cells.

Nicky Huskens, Wolfson College, Trinity Term 2015

DPhil in Physiology, Anatomy and Genetics

Hypoxia elicits a carotid body-mediated increase in minute ventilation, called the chemoreflex. Volatile anaesthetics depress this chemoreflex, even at sub-anaesthetic doses. The broad aim of this thesis is to explore how these anaesthetics act on carotid body mechanisms to depress the chemoreflex. The agents studied in this thesis are halothane (a potent depressant of this reflex), isoflurane (a less potent depressant) and sevoflurane (a weak depressant).

Intracellular Ca^{2+} measurements, mitochondrial NADH and potential measurements, and single channel electrophysiology studies were performed on a primary culture of rat carotid body type-1 cells and HEK cells transiently expressing TASK channels. Cells were exposed to hypoxia and/or volatile anaesthetics.

The results reveal that on all levels studied, the same order of potency of anaesthetics was observed as seen in human ventilatory studies. Volatile anaesthetics depress the hypoxia evoked Ca^{2+} entry in the carotid body and increase the activity of K^+ background channels both in glomus and HEK cells expressing TASK. Furthermore, on all levels studied, when halothane and isoflurane were applied as a mixture, the effect evoked by the mix was of a lesser magnitude than that of the halothane alone, revealing a novel sub-additive observation, which has not been previously reported in the literature.

The anaesthetic action of glomus cells was not exclusive to the TASK channels as application of all three anaesthetics evoked an increase in mitochondrial NADH and caused mitochondrial depolarization in glomus cells. These effects of anaesthetics on mitochondria mimics the effects of hypoxia, the implications of which are discussed in this thesis. Two novel TASK blocking agents A1899 and PK-THPP were able to decrease glomus cell TASK channel activity, even in the presence of a clinically relevant concentration of isoflurane. These agents may be promising as future respiratory stimulants

Acknowledgements

This project was only possible through the help and support of many, in particular I would like to thank the following:

My supervisors, **Professor Jaideep Pandit** and **Professor Keith Buckler**: Jaideep for his infectious enthusiasm and undying commitment to the project, and I am very grateful for his valuable advice on matters not exclusive to the experiments. I have great memories regarding the many long chats we had, discussioning the implications and design of the experiments and was many times amazed at his extremely quick turnover of drafts of papers and chapters. Keith for his helpful advice, and teaching me to be critical of my own work. I will remember how I was at any time allowed to knock on his door when stuck with experiments. Many times I was left astonished when within seconds, my hour-long battle with the most persistent 60- cycle noise would disappear within seconds upon Keith's intervention.

The other members of the Buckler-Pandit lab, **Dr Phil Turner** and **Dr Peadar O' Donohoe**: Phil for teaching me all the techniques, his incredible patience, and offering me perspective to DPhil life. Peadar, as fellow DPhil student, for all the time we spent working together, and the many useful comments on experimental design and result interpretation. Peadar was also always able to elaborate on the clinical aspects of the project, bringing the science to life and putting the project in clinical perspective.

I also express my gratitude to **James Wickens** who assisted me with the chromatography experiments; **Dr David O'Connor**, who provided the technical support; and **Dr Emma Hodson** for her inspiration and support.

The staff of **Wolfson College** deserves a special mention for their academic support and for providing me throughout my DPhil with a home and supportive community. Especially many thanks to my college advisor **Professor Jonathan Austyn**.

The **British Journal of Anaesthesia/National Institute of Academic Anaesthesia** provided the PhD studentship award that made this project possible.

My parents, **Margret and Chris Huskens**, for their incredible support and love.

My dear friends **Emma Clifton** and **Stefany Wragg,** who supported me so much and with whom I have shared much more than the many rowing strokes and early mornings. I will remember the thesis writing days with Stef in the beautiful libraries and the all the adventures Emma and I embarked on during and after the trialling.

Lastly, I must profoundly thank my partner **Gregers Bangert**, for his round the clock support, encouragement and never ending understanding. I feel he heard me talk so much about this project that he would be capable of presenting my work at any time if needed.

List of abbreviations

4-AP 4-aminopyridine

AHVR acute hypoxia ventilatory response

AICAR 5-Aminoimidazole-4-carboxamide ribonucleotide

AMPK adenosine monophosphate activated protein kinase

BKca large-conductance Ca^{2+}-activated channel

[Ca2+]i intracellular Ca^{2+} concentration

DMSO dimethyl sulfoxide

EK equilibrium potential for K+ ions

FCCP carbonyl cyanide 4-(trifluoromethoxy) phenylhydrazone

GABA γ-aminobutyric acid ligand-gated ion channel

GC-MS gas chromatography–mass spectrometry

H_2S hydrogen sulphite

HEK human embryonic kidney

K_2P two pore K+ channel

KO knock out

LB-AMP Luria Bertani broth with Ampiciline

MAC Minimum alveolar concentration

NADH Nicotinamide adenine dinucleotide

NADPH nicotinamide adenine dinucleotide phosphate

NMDA N-methyl-D-aspartate

nPopen estimated channel open probability

PBS phosphate-buffered saline

PCR polymerase chain reaction

PIP_2 phosphatidylinositol 4,5-bisphosphate

PLC Phospholipase C

PMT photomultiplier tube

PNA peanut agglutinin

PO_2 partial pressure of oxygen

Rh123 rhodamine 123

ROS reactive oxygen species

SEM standard error of the mean

SCG superior cervical ganglion

TASK TWIK-related acid-sensing K+ channel

TEA tetraethylammonium

TRAAK TWIK-related arachidonic-acid-stimulated K+ channel

TREK TWIK-related K+-channel

TWIK tandem of p domains in a weak inward rectifying K+ channel

TABLE OF CONTENTS

Chapter 1. Introduction

1.1 Structure

This thesis focuses on how volatile anaesthetics act on oxygen sensing cells in the carotid body. The main aim is to gain further insight into how these anaesthetics act on, and interfere with, different mechanisms in the carotid body that are involved in oxygen sensing. Although most of the chapters investigate the anaesthetic and oxygen sensing pathways, the final part focusses on two novel TASK blocking compounds that show potential to overcome some of the undesired effects that anaesthetics have on the carotid body.

This introduction is divided into three main sections:

The first section addresses the clinical background regarding the use of volatile anaesthesia during surgery and introduces the volatile anaesthetics to be researched. There will also be an overview of how our understanding of the mechanism of action of volatile anaesthetics has evolved over the past 100 years. The section will conclude with an overview of hypoxia in the peri-operative environment and highlight the clinical reports showing that anaesthetics interfere with acute ventilatory response to hypoxia.

The second section focuses on the carotid body anatomy and discusses the excitation in response to hypoxia. These are the events that are well established and agreed upon in the literature. The second section will also elaborate on the different hypotheses of oxygen sensing in the carotid body

The third section will review the characteristics of the 2 pore K^+ channel (K_2P) family and will elaborate in further detail on the TASK channels in the carotid body. The section finishes

with an overview of what is known about the interaction between volatile anaesthetics and TASK channels.

The introduction will end with further explanation and justification for the experimental chapters in this thesis, together with the detailed aims for this chapter.

1.2 Volatile anaesthesia and hypoxia

1.2.1 The use of volatile anaesthetics during surgery

Modern surgery would be impossible to conduct without general anaesthesia. As Franks wrote: 'Every year, tens of millions of patients are exposed to general anaesthetics, drugs that remove the most precious human attribute - consciousness' (Franks, 2008). General anaesthetics are a mix of agents that have the ability to achieve analgesia, unconsciousness, immobility and amnesia. General anaesthetics have been used in medical procedures for approximately 160 years. Interestingly, despite its longstanding and widespread use, the mechanism of action of anaesthetics is still not completely elucidated, even though research in this area has been performed for over 100 years. This lack of complete understanding makes volatile anaesthesia all the more intriguing.

Nowadays, there are a number of different categories of anaesthesia available with quite some choice within each category. The mixture and type of anaesthetic can be adapted to the intended surgery and to the clinical, physiological and pathological condition of the patient in order to achieve the best outcome. Anaesthetics can be classified into intravenous anaesthetics; local and regional anaesthetics; and inhalational anaesthetics. The latter will be the main subject of this thesis (Schuttler and Schwilden, 2008).

The first inhalational anaesthetics were ether and chloroform. Ether is an airway irritant and also highly flammable, and is notorious for having caused fire in a significant number of procedures. Similarly, chloroform turned out to be very toxic and had an unacceptably high mortality rate. Therefore scientists looked for better and safer inhalational agents in the 1930s (Booth and Bixby, 1932). Following a paper published by Robbins on anaesthetic properties of fluorinated hydrocarbons, three fluorinated compounds were introduced into clinical practice (Robbins, 1946, Terrell, 2008). Amongst those three agents was halothane (2-bromo-2-chloro-1,1,1,-trifluoroethane), which quickly became the most used agent because of its potency and non-flammability. The major problems with halothane were its myocardial depression, negative inotropic effect (Schmidt et al., 1994) and hepatotoxicity; hence halothane is rarely used nowadays.

Later studies in the 1960s and 70s identified halogenated methyl ethyl ethers amongst which were enflurane, isoflurane, sevoflurane and desflurane (Terrell, 2008). Isoflurane is a l-chloro-2,2,2-trifluoroethyl difluoromethyl ether that was discovered in 1965 and was Food and Drug Administration (FDA) approved in 1979. Following approval, isoflurane was

introduced in the US, quickly becoming highly used (Evers et al., 2011). Isoflurane is still in frequent clinical use today.

Sevoflurane (fluoromethyl 2,2,2-trifluoro-1-(trifluoromethyl) ethyl ether) is also a frequently used anaesthetic in the UK. Sevoflurane was first synthesized in 1968 and its potential use was published in 1971 (Wallin R.F., 1971, Smith et al., 1996). It was first released for clinical use in 1990. A summary of some basic properties of halothane, isoflurane and sevoflurane can be found in Table 1.1.

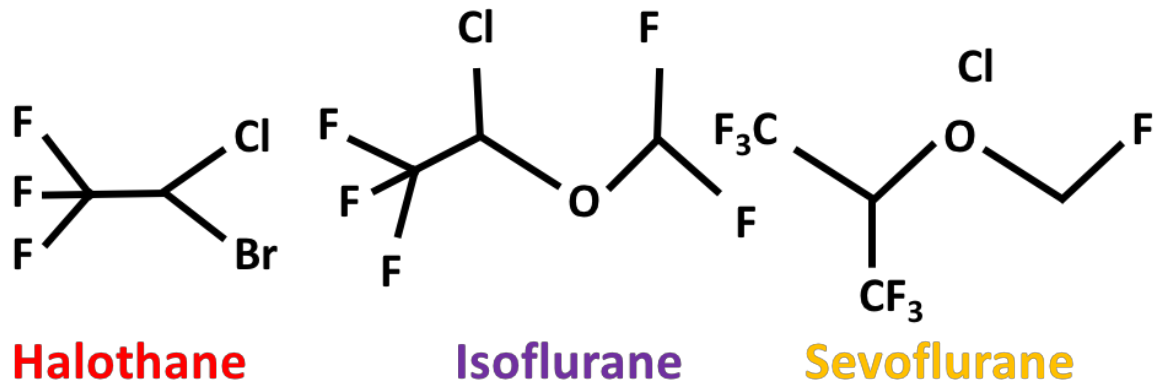

Figure 1.1: Molecular structure of halothane isoflurane and sevoflurane.

	Halothane	**Isoflurane**	**Sevoflurane**
Boiling point (℃)	50.2	48.5	58.6
*MAC (humans) (%)**	0.75	1.17	1.71 - 2.05
Blood:gas partition coefficient	2.4	1.43	0.69
Molecular weight	197.4	184.5	200.5

Table 1.1: Basic properties of halothane, isoflurane and sevoflurane. Table based on (Nathanson 1996), (Bovill, 2008), (Evers et al., 2011) *Human MAC in this table is defined as: the minimum alveolar concentration of an anaesthetic at one atmosphere ambient pressure that suppresses gross movement in response to a defined painful stimulus in 50% of subjects.

Characteristic of volatile agents like halothane, isoflurane and sevoflurane is their ability to rapidly induce loss of consciousness. On their own however, these agents lack sufficient pain relief and therefore an analgesic, such as an opioid, is commonly co-administered during the surgical procedure (Bovill, 2008).

The most recent survey conducted in the UK (NAP5) regarding the use of anaesthetics found that, for most adult patients, loss of consciousness is induced by an intravenous agent, (propofol in 88% of UK cases) after which it is switched to a vapour agent (in 92% of the cases). Sevoflurane is the most commonly used vapour agent (58.5% of all vapour agents). In 90% of all surgeries, patients also receive opioids (Sury et al., 2014). Therefore general anaesthesia-induced loss of consciousness in the modern day consists of a mixture of different agents (an induction agent, a maintenance agent and an opioid).

1.2.2 The development of our understanding of the mechanism of action of volatile anaesthetics

One of the first inhalational anaesthetics to be described and administered was diethyl-ether and nitrous oxide, with reports and letters describing these agents dating centuries back. Ether was mentioned by Paracelsus in 1500s and later in 1729 by Frobenius, who published an article named 'An Account of a Spiritus Vini Æthereus, Together with Several Experiments Tried'. In this paper Frobenius describes ether as a flammable but fragrant substance, able to dissolve in many different oily solutions (Frobenius, 1729, Bovill, 2008). It was not until the 1840s following the first public demonstration of ether anaesthesia during removal of a neck tumour at Massachusetts General Hospital in Boston, that the use of this agent as an anaesthetic became widely introduced. The use of ether was then published in 1846 in the

Boston Medical and Surgical Journal by Bigelow who reported the use of ether as an anaesthetic for surgical procedures such as leg amputations (Bigelow, 1846). Shortly after that, anaesthesia with ether, nitrous oxide and chloroform was rapidly introduced and used for surgery.

Following the publications indicating the use of these agents for surgery, the research on the mechanism of action of general anaesthesia really started. Von Bibra was the first, proposing a mechanism of anaesthetic action in 1847. He hypothesised that the agents dissolve in the fatty part of the brain and change brain activity (Harless and Von Bibra, 1847).

Within two years of each other Meyer and Overton published independently (1899 and 1901) a theory inspired by the work from Von Bibra, which then became known as the Meyer and Overton theory of anaesthesia. This theory is based on the fact that the more lipid soluble the agent is, the more potent the anaesthetic is, and that there is a near linear relationship between the potency and the oil partition coefficient (in which the olive oil was the approximation of the brain cell fatty acids). This hypothesis was based on experiments in which Meyer determined the concentration of agent needed to observe 'atypical' behaviour in tadpoles, which was then compared with the lipid partition coefficient (Meyer, 1899, Overton, 1901). This theory explains that the anaesthetic effect comes from non-specific perturbation of the lipid bilayer in neural cells, which is a physical-chemical interaction rather than interaction with receptors. For a long time through the 1900s this theory remained very popular and can be found in textbooks explaining the mechanisms of action of general anaesthetics.

However, this slowly changed when certain limitations of this theory came to light (Franks and Lieb, 1982). Franks and Lieb in the 80s were testing a novel hypothesis, suggesting that anaesthetics act on proteins. Franks showed that the activity of the soluble firefly luciferase can be inhibited by up to 50% at clinically relevant concentrations of anaesthetics such as halothane (Franks and Lieb, 1984). Moreover, there was competition between luciferin (the substrate) and halothane for binding. The authors proposed the novel theory that anaesthetics compete with endogenous ligands for binding to target proteins.

In 1988 Franks and Lieb first identified a novel anaesthetic-activated K^+ current in the pond snail (lymnea stagnalis), which it later turned out was mediated by K_2P channels (Franks and Lieb, 1988, 1991, Andres-Enguix et al., 2007). Thus the link between anaesthesia and channel interaction was initiated. Following this, considerable progress was made as more anaesthetic mediated currents were identified. This was then followed by the cloning and identification of the responsible channels. This was not exclusive to K^+ channels, but also other channels including γ-aminobutyric acid ligand-gated ion channel (GABA type A receptors), Na^+ channels and N-methyl-D-aspartate (NMDA) receptors were being identified.

Another piece of evidence against the lipid-pertubation hypothesis was also provided by Franks and Lieb in 1991. The authors demonstrated stereo-selective effects of the optical isomers of isoflurane on neuronal ion channels (Franks and Lieb, 1991). This further supports the protein/channel binding hypothesis as isomers should not have differential effects if their sole effect was a nonspecific effect of lipid-pertubation.

Franks' theory is thus different from the Meyer-Overton hypothesis in that according to the latter hypothesis, anaesthetics are thought to behave additively, whereas according to Franks' theory, anaesthetics should compete. However, to date, competition for a binding site between two volatile anaesthetics has not been demonstrated and only additive (or synergistic) interactions between agents have been reported (Hendrickx et al., 2008, Jenkins et al., 2008).

Similarly, targets have been identified for intravenous anaesthetics such as propofol and etomidate. Hales and Lambert (1991) studied bovine chromaffin cells and rat cortical neurones in cell culture and reported that propofol can potentiate the actions of GABA on GABA(A) receptors. Their single channel recordings revealed that although propofol had no significant effect on GABA single channel conductances, it greatly increased the probability of a single channel being in the conducting state. Other interesting evidence was found by Davies et al. (1997), who identified a human GABA(A) receptor subunit (epsilon) that can assemble with alpha- and beta-subunits and so confer an insensitivity to the potentiating effects of intravenous anaesthetic agents. In the same year, Belelli et al. (1997) also investigated the GABA(A) channel and its different subunits and reported a point mutation which strongly supressed GABA-modulatory effects of etomidate on the channel. These results together also show that ion channels are targets of intravenous anaesthetics.

To date, there are many channels identified that are modulated by anaesthesia. Examples include: Na^+, K^+, Ca^{2+}, GABA type a receptors, glycine and NMDA receptors. The most important channels seem to be GABA type a receptors, NMDA receptors and K_2P channels (Daniels and Smith, 1993, Franks and Lieb, 1994, Mihic et al., 1997).

Anaesthetics are also believed to have effects that extend beyond membrane channels. There are reports showing that anaesthetics act on mitochondrial respiration and cause a slowdown of the electron transport chain (Hanley et al., 2002, Morgan et al., 2002). There is also evidence for anaesthetics directly targeting second messenger molecules, thus interfering with the cellular signalling cascades (Rebecchi and Pentyala, 2002).

Although more and more targets of anaesthesia are being identified, it is not clear which of these mechanisms is truly responsible for hypnotic effects, immobility, analgesia and unconsciousness. A current popular hypothesis is the 'multisite hypothesis'. This hypothesis states that anaesthesia may have small actions on different channels and other targets in different tissues and that the sum of this causes the hypnotic effect of anaesthesia (Urban, 2002). Acknowledging that such theories exist, I will not be further focussing on hypnotic theories of anaesthesia in this thesis.

1.2.3 Hypoxia in the peri-operative environment

During surgery involving anaesthesia, one of the biggest risks is hypoxia, which is the main cause of anaesthetic-related death and morbidity (Craig, 1981, Ward et al., 2011). Hypoxia is a term referring to a state in which the body does not receive enough oxygen. Hypoxemia refers to an oxygen arterial partial pressure value lower than 80mmHg (Bateman and Leach, 1998). Hypoxia can be caused by many events, including anaesthesia or other drug induced depression of ventilation, obstructive airway diseases, or pulmonary oedema. Hypoxemia occurs frequently in the peri-operative environment, and recent studies have shown this can occur in up to 30% of all patients receiving a general anaesthetic (Dunham et al., 2014). With nearly 3 million general anaesthetics a year in the UK alone, this entails around 900,000

patients at risk (Sury et al., 2014). Particular groups of patients at risk include patients with obstructed sleep apnoea, cardio-respiratory disease and day case surgery patients (Kaw et al., 2012)

Hypoxia normally elicits a carotid body-mediated acute hypoxia ventilatory response (AHVR), which results in an increased minute ventilation and increased oxygen delivery to the lungs, and so mitigates against severe hypoxaemia. The AHVR is mediated by the oxygen sensing type-1 (glomus) cells in the carotid body (see below for detailed mechanism).

Volatile anaesthetic agents are known to interfere with the body's physiological response to hypoxia and can prevent an adequate increase in ventilation in response to hypoxia (Gelb and Knill, 1978, Knill and Gelb, 1982, Temp et al., 1994, Froese, 2014). Even at sub-anaesthetic doses (1/20th – 1/10th of that required for general anaesthesia) volatile anaesthetics depress the AHVR. As volatile anaesthetic agents persist in the body for many hours after surgery, patients are not only at risk during the surgery, but also post-operatively after administration, meaning that the patient is at risk in the recovery room or back home where they are less closely monitored (Lockwood, 2010).

Studies have provided an interesting observation when measuring the depression of the ventilatory response by volatile anaesthetics. This depression exhibits a specific order of potency which is halothane > isoflurane > sevoflurane (Dahan et al., 1994a, Dahan et al., 1994b, van den Elsen et al., 1994, van den Elsen et al., 1998, Pandit, 2002). Interestingly, this order of potency is also preserved in rat studies. Karanovic et al. (2010) studied the hypoxic response in adult male Sprague-Dawley rats and found a similar rank order of potency. This

finding further highlights that the rat may be a good animal model for studying the volatile anaesthesia evoked depression of the AHVR.

It is apposite here to review the chemical reflex control of breathing. Under normal circumstances in the body, breathing is a product of firing of semi-autonomous neural networks, called the central pattern generators. There is an important role for the Bötzinger and pre-Bötzinger complex, the retrotrapezoid nucleus and raphe compartments (Feldman and Del Negro, 2006, Smith et al., 2013). However central and peripheral chemo sensing can change the depth and frequency of breathing when a decrease in O_2 or an increase in CO_2 is sensed by stimulating the respiratory control centres (Kafer and Sugioka, 1981, West, 2012). Where central chemoreceptors are sensitive to H^+/CO_2, peripheral chemoreceptors are also oxygen sensitive. It is believed that the anaesthetic evoked depression of the AHVR is mediated through peripheral chemo sensing in the carotid body and not central chemo-sensing (Knill and Gelb, 1978, Kafer and Sugioka, 1981, Knill and Clement, 1984, Dahan et al., 1994a).

1.3 Carotid body anatomy and excitation

1.3.1 Anatomy

The carotid body is the principal arterial chemo-sensor for O_2, CO_2 and pH and is involved in the regulation of ventilation (Biscoe, 1971). The carotid body is perhaps the smallest organ in the human body and is located on both sides of the neck, at the rostral end of the left and right common carotid arteries at the point where these bifurcate into the external and internal carotid arteries (Kumar and Prabhakar, 2012). The size of the carotid body is approximately

2-3mm in humans and is highly vascularized (Heath et al., 1970). The carotid body consists of type-1 cells, called glomus cells and type-2 cells also called sustentacular cells.

Type-2 cells are thought to be supporting cells and usually represent less than 20% of the total cells within the carotid body (Kumar and Prabhakar, 2012). The major difference between type-1 and -2 cells is regarding their excitability. Type-2 cells do not respond to hypoxia in a way that type-1 cells do. It is thought that type-2 cells are 'support cells' for the type-1 cells, however, their functional significance remains largely unknown (Gonzalez et al., 1994).

In rats it is estimated that there are 120,000 type-1 cells each having a size of 8-15μm, whereas type-2 cells are thought to be 6μm (Urena et al., 1989). The type-1 cell is thought to be the major oxygen pH sensitive cell (Verna, 1979, Kumar and Prabhakar, 2012). Once dissociated, type-1 cells often present in small clusters and contain characteristic dense-cored vesicles (Duchen et al., 1988).

1.3.2 Overview of hypoxia evoked events in carotid body

A decrease in arterial PO_2 from 100–80 mmHg is enough to evoke afferent nerve activation in the carotid body (Biscoe et al., 1970, Prabhakar, 2006). In response to hypoxia the following events occur: The activity of K^+ channels setting the resting membrane potential decreases, which results in membrane depolarisation and opening of voltage gated L type Ca^{2+} channels. Ca^{2+} enters the cell, which in turn promotes fusion of vesicles with cell membrane and the release of neurotransmitters. The neurotransmitters excite afferent nerves projecting to the ventilatory control centres in the brainstem and so induce an increase in

breathing, both in depth and in frequency (Heymans C., 1930, Acker, 1994, Weir et al., 2005, Lopez-Barneo et al., 2015).

There are a wide variety of neurotransmitters released by the carotid body. Research in animals has shown that amongst them are: acetylcholine, ATP, dopamine, noradrenaline, and serotonin (Rigual et al., 1984, Gonzalez et al., 1994, Rong et al., 2003, Zhang and Nurse, 2004). It is thought that ATP is one of the key neurotransmitters, exciting afferent nerve endings via P2X2 and P2X3 receptors (Zhang and Nurse, 2004). A recent paper by Kahlin et al. (2014), investigated human carotid bodies to verify some of the animal research and found that in response to hypoxia, acetylcholine and ATP were released within 5 minutes.

The resting potential of the type-1 cell is believed to be between -48 and -60mV (Buckler and Vaughan-Jones, 1994, Buckler, 2012). Ca^{2+} channels become active at a voltage more positive than -50mV (Buckler and Vaughan-Jones, 1994). The rise of Ca^{2+} in response to hypoxia is inhibited in Ca^{2+}-free medium, indicating that the rise in hypoxia evoked Ca^{2+} comes from outside the cell. Studies with inhibitors revealed that both L- and N-type Ca^{2+} channels contribute to the facilitation of the Ca^{2+} influx (e Silva and Lewis, 1995). Although discussed in more detail later in this chapter, it is assumed that the channels closing in response to hypoxia and causing the depolarisation are the TASK channels (Buckler, 1997, Buckler et al., 2000, Kim et al., 2009a, Buckler, 2015).

Other channels in the rat carotid body are voltage-gated (delayed rectifier) K^+ channels (Kv), voltage-gated Na^+ channels and large conductance Ca^{2+}-activated K^+ channels (maxi K channels or BKCa) (Buckler, 2015). Interesting are the BKCa channels, which are thought to

be inhibited by hypoxia and acidosis (Peers, 1990). These channels are most likely not active at resting membrane potential, instead BKCa appears to come into play when the membrane potential of glomus cells is depolarized to levels more positive than ~ −30 mV (Kang et al., 2014). Similarly, Kv channels are assumed to mediate action potential repolarisation in rat carotid body and not responsible for the onset of the response to hypoxia.

1.3.3 Oxygen sensing mechanisms and hypotheses

Although there is agreement about the decrease in K^+ channel activity (such as TASK channels) and a rise of intracellular Ca^{2+} in response to hypoxia, there is uncertainty regarding how O_2 levels are sensed in order to decrease the K^+ channel activity in response to hypoxia.

The first question that arises is whether or not the carotid body K^+ channels are the oxygen sensing channels themselves, or whether the channel is regulated by another oxygen sensor. One way to test whether the TASK channel itself is oxygen sensitive, is by expressing TASK channels in HEK cells outside their native environment. Lewis et al. (2001) expressed human TASK-1 in HEK-293 cells and found that the pH sensitive K+ current in the transfected cells was greatly reduced in the presence of hypoxia. However, this result was not replicated when similar experiments were attempted by Buckler and Honore (Buckler and Honore, 2004). Another way to study if the channel is directly oxygen sensitive is by studying the channel in an excised patch, where the channel is isolated from its cellular environment. Under these conditions, no oxygen sensitivity was found (Buckler et al., 2000). To date, the direct oxygen sensitivity of the TASK channel therefore remains disputed.

A second oxygen sensing hypothesis postulates that the carotid body contains a source oxygen sensor. This sensor is capable of regulating TASK channel activity directly or indirectly through signal molecules or second messengers, which in turn can regulate TASK channel activity with or without an accessory molecule. There are a few hypotheses regarding the source and messenger molecules involved, which will be discussed together with evidence in favour and against the hypothesis.

Mitochondria in the carotid body are a convincing candidate for being the source oxygen sensor. Research suggests that the respiratory function of the mitochondria alters over the physiologically relevant PO_2 range, which is in contrast to the mitochondria of other tissues (Duchen and Biscoe, 1992a, b). Moreover, inhibitors of the mitochondrial transport chain significantly inhibit background K^+ currents in type-1 cells and evoke a Ca^{2+} influx, therefore mirroring the effect of hypoxia on the type-1 cell (Wyatt and Buckler (2004).

A number of metabolites that could potentially regulate TASK channels are ATP, Mg-ATP or AMP-activated protein kinase (AMPK) (Varas et al., 2007, Peers et al., 2010, Buckler, 2015). Some evidence in favour of this is that the rapid decline of TASK channel activity in inside-out patches can be rescued in large part by applying Mg-ATP (Varas et al., 2007). Evidence against a role of ATP activation is the absence of a nucleotide binding site in cloned TASK channels (Buckler 2015).

AMPK is an enzyme sensing a change in AMP/ATP ratio and upon activation can change cell metabolism. Evidence in favour of an important role for AMPK as a modulator is provided by Wyatt et al, who showed that AMPK activation by 5-Aminoimidazole-4-carboxamide ribonucleotide (AICAR) inhibited the O_2 -sensitive K+ currents carried by TASK-like leak K+ channels (Wyatt et al., 2007). Further evidence also shows that AICAR may contribute to regulation of expressed TASK-3 channels and other K+ channels (Evans et al., 2005, Evans et al., 2009). Conflicting evidence for the role of AMPK is provided by Kim et al. (2014). These authors report that activators of AMPK did not inhibit TASK activity or cause depolarization during acute or prolonged exposure in carotid body cells. Furthermore, the activators of AMPK also failed to evoke Ca^{2+} entry in glomus cells.

Other potential TASK channel modulators may be reactive oxygen species (ROS) as produced by nicotinamide adenine dinucleotide phosphate (NADPH) oxidases or mitochondria (Brunelle et al., 2005, Waypa et al., 2006). One theory is that a change in available oxygen leads to a change in ROS production by NADPH oxidase, with a subsequent decrease in TASK channel activity. For example, it was found that the absence of NADPH subunit p47 (phox) facilitates the ventilatory and chemoreceptor response to hypoxia in vivo and in vitro (Sanders et al., 2002). However, other studies show the opposite, and report an increase of ROS production in hypoxic conditions (He et al., 2005). Papreck et al. (2012) did find that H_2O_2 applied to inside-out patches activated transiently expressed TASK-1, TASK-3, and TASK-1/3 heterodimer, but this was only at high concentrations outside the physiological range.

A recent study by Bernardini et al found that, depending on the breeding conditions of mice, the ROS level in carotid bodies in response to hypoxia either decreased or increased and that there was no clear consistency. However, inhibitors of a NADPH oxidase subunit would always attenuate the hypoxia evoked membrane depolarisation (Bernardini et al., 2015). Interesting evidence in favour of the importance of ROS, comes from two studies by Teppema et al., who showed that application of an anti-oxidant (for example vitamin C) to healthy volunteers, resulted in a complete reversal of the anaesthetic evoked depression of the hypoxic ventilatory response. It is tempting to speculate that this may be due to an interaction with ROS, or a change in redox state of the carotid body, which reversed the anaesthetic induced depression of ventilation (Teppema et al., 2002, Teppema et al., 2005). However, with so many studies reporting opposite findings and conflicting views, the role of ROS in oxygen sensing remains unclear.

There are a few gaseous signalling molecules that have been extensively investigated with respect to oxygen sensing in the carotid body such as carbon monoxide (CO), nitric oxide (NO) and hydrogen sulphide (H_2S) (Lewis et al., 2002, Otsubo et al., 2006, Peers et al., 2010, Fandrey, 2015), which have been demonstrated to be chemo-excitants on their own, or through binding of haeme-proteins (Kemp and Telezhkin, 2014).

Another pathway that may play a role in regulating TASK channel activity is by mediation of G_{aq} proteins or one of its downstream signalling molecules such as Phospholipase C (PLC) and phosphatidylinositol 4,5-bisphosphate (PIP_2). Studies from two different groups have reported an effect of PIP_2 on TASK channels in heterologous expression systems (Chemin et al., 2003, Lopes et al., 2005). Later work performed by Chen et al. (2006) however, reported that TASK channel inhibition is independent of PLC activity and PIP_2 depletion and that activated Gαq subunits inhibit TASK-3 in excised inside-out macropatches. A similar result has been found in a study by Lindner et al. (2011).

1.4 K2P channels

1.4.1 Structure, characteristics and gating of K2P channels

TASK channels belong to the two-pore potassium (K_2P) channels. In mammals 15 genes are identified as KCNK genes encoding the K_2P channels, which are expressed in a variety of tissues such as the brain, heart, lung, kidney and carotid body (Goldstein et al., 2001, Goldstein et al., 2005).

On the basis of sequence homology, eukaryotic K_2P channels have been subdivided into six subgroups (Goldstein et al., 2001, Renigunta et al., 2015):

1. TWIK channels - weakly inwardly rectifying
2. TREK channels - lipid and mechano sensitive
3. TASK channels - acid pH-sensitive
4. TALK channels - alkaline pH-activated
5. THIK channels - halothane-inhibited
6. TRESK channels - spinal cord

K_2P channels are background channels, active around and/or involved in setting the cell's resting membrane potential. These channels are also called 'open rectifiers', which refers to the characteristic that their current-to-voltage relation can often be fairly well approximated by the Goldman-Hodgkin-Katz (GHK) equation. For a GHK- rectifying K^+ channel in physiological conditions (in which the inside K^+ concentration is higher than the outside K^+ concentration), an outward current is favored and hence the channels are leaking K+ ions at rest. With a symmetrical distribution of K+ ions, the rectification disappears and consequently the IV-relationship is often near linear (Bayliss and Barrett, 2008).

The structure and gating of most K_2P channels is not fully elucidated, because to date the structure remains unresolved for most channels. Over the past few years however, more insight has been gained as the first structures have been solved and detailed gating studies have been carried out. Brohawn et al. (2012) solved the crystal structure of TRAAK and Miller and Long (2012) solved the structure of TWIK-1. These two papers revealed that K_2P

channels assemble as a dimer and each subunit of the dimer consists of four trans-membrane domains (M1–M4), two pore-forming domains (P1 and P2) and two extracellular cap helices (C1 and C2). This is depicted in Figure 1.2.

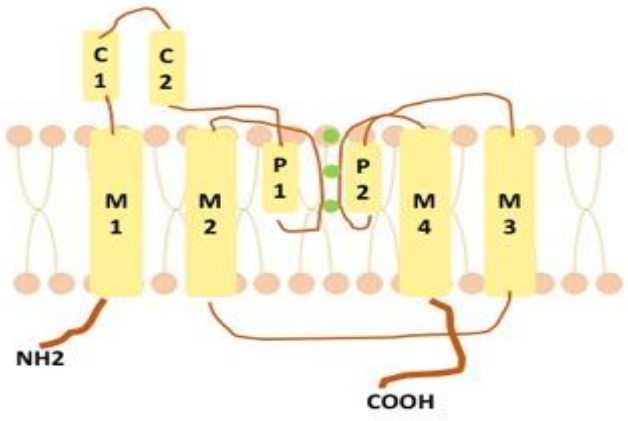

Figure 1.1: General structure of K_2P channel. This channel comprises of four transmembrane domains (M1-4), two pore-forming domains (P1 and P2) and two extracellular cap helices (C1 and C2). Picture based on (Renigunta et al., 2015).

The existence of this cap above the selectivity filter of the channel may explain why the channel is resistant to some classical K^+ channel inhibitors such as tetraethylammonium (TEA) and 4-aminopyridine (4-AP) (Steinberg et al., 2014). The two subunits appear to assemble in an anti-parallel manner. Interestingly, later research done at higher resolution confirmed that 'domain swapping' takes place between the two channel subunits. As a consequence, the C1 and M1 domain are able to swap to the opposite side of the channel and so changing in position by 180° (Brohawn et al., 2013).

This swapping has also been confirmed in a recent paper describing the structure of TREK-2 (Dong et al., 2015). This study provided further insight into the structure and gating of K_2P channels and described that gating occurs primarily within the selectivity filter and that close to this selectivity filter, there are intra-membrane side fenestrations (where norfluoxetine has

been found to bind). The authors further show that the channel can be in an up or down state, which is caused by movement of the M2, 3 and 4 domains. The down state is thought to represent a lower activity state. In the down state the lateral fenestrations are open, whereas in the up state where the channel is presumably more active, these side fenestrations are closed.

In most other K+ channels there are two different established gating mechanisms. There is an activation gate at the intracellular entrance and a distant slow activation at the selectivity filter close to the extra cellular site (Mathie et al., 2010). The most recent insights show that gating in K_2P channels occurs close to the selectivity filter, and that the inner gate of TREK-1 channels (at the helix bundle crossing) is constitutively open (Piechotta et al., 2011, Rapedius et al., 2012, Dong et al., 2015). It cannot be excluded that other types of gating within TREK and other K_2P channels are important.

1.4.2 Properties of TASK channels

The members of the K_2P channel group that are expressed in the carotid body and hence the channels of interest in this thesis, are the TASK channels. The TASK channel (TASK-1) was first described and cloned in 1997 by Duprat et al. (1997) who named the channel TASK for 'TWIK-related Acid-Sensitive K^+ channel'. The channel was identified by looking for TREK-1 and TWIK-1 related sequences in the Gen-Bank. Northern blot analysis then revealed expression in a variety of tissues such as the brain, kidney, lung, and heart.

In their conclusion, the authors compared the characteristics of these channels with some of the currents previously described in other tissues. Among them, was the current reported earlier that year in 1997 by Buckler, who described a novel O_2 sensitive current in rat carotid bodies (Buckler, 1997). Further characterization of this current revealed it to be insensitive to the classical K^+ channel blockers TEA and 4-AP. There was a decrease in membrane conductance in response to hypoxia (PO_2< 40mmHg) suggesting that hypoxia depolarizes the cell through inhibition of small voltage insensitive K^+ conductance and not voltage gated channels. In follow up work, this oxygen sensitive current was found to be increased by halothane (Buckler et al., 2000). In addition, single channel analysis of this channel revealed halothane sensitivity (increase in activity) and hypoxia sensitivity (decrease in activity), and upon the further investigation the authors concluded this to be a TASK-like channel.

In 2000 the TASK-3 channel was first cloned by Rajan et al. (2000). The authors reported that TASK-3 was especially highly expressed in the brain and that TASK-3, just like TASK-1 was pH sensitive. The TASK-3 sequence homology with TASK-1 is 62%. The pH sensitivity of the channel altered when a histidine residue on the extracellular side was mutated indicating that these residues may be important for the pH sensing, which is potentially also the case in the TASK-1 channel as these residues are conserved.

In 2002, Czirjak and Enyedi found that co-expression of both TASK-1 and TASK-3 in Xenopus oocytes resulted in a current with intermediate features to those seen with either channel expressed alone. The authors also showed that pH inhibition of a TASK-1/3 concatemer was intermediate, which further highlighted the possibility of TASK heterodimerisation (Czirjak and Enyedi, 2002).

Williams and Buckler (2004) continued further investigation on the TASK-like channel and current in the carotid body and found that the properties do not closely match either TASK-1 or TASK-3, raising the possibility that hetero dimerization may take place between TASK-1 and -3. Furthermore, the authors reported the ATP sensitivity of the TASK channel and reported how ATP can partially rescue the run-down of TASK channel activity in inside-out patches (where the channels are detached from the intracellular side).

In the same year, Kim further researched the question of hetero-dimerization (Kang et al., 2004). The authors chose cerebellar granule neurones because this tissue was known to express both TASK-1 and -3 mRNA and as such they could compare sensitivities to pH and inhibitors by comparing cloned and native channels. The authors identified a channel with nearly identical single channel kinetics to that of TASK-3. However, when ruthenium red was applied (which blocks TASK-3 more than TASK-1), this resulted in intermediate inhibition and not to the same degree of inhibition as if the current was wholly a product of TASK-3 alone. Similar research was performed by Kim et al. (2009a) in carotid body cells, in which the predominant channel has a conductance very similar to TASK-3 channels but is ruthenium red insensitive, thus suggesting the existence of another but similar channel. The final proof of hetero-dimerization in the carotid body that did not involve the application of inhibitors was provided in this lab by Turner and Buckler (2013b). Single channel recordings were made from both TASK-1 and TASK-3 knock out mice and when the channel activity in single channel patches from both mice were combined, the total activity was still less than that in wild-type mice. In the double knock out neither of the three channels were found, indicating that heterodimers must represent the most predominant expressed background channel in the carotid body.

To summarize, for the carotid bodies in rats and mice, it is currently accepted that TASK-1, TASK-3 and TASK-1/3 heterodimer are expressed and have a predominant role in the oxygen sensing cascade. In particular the heterodimer TASK-1/3 is thought to be most abundant compared to TASK-1 and TASK-3 (Yamamoto et al., 2008, Kim et al., 2009a, Turner and Buckler, 2013a). For humans however, TASK-1 is the only confirmed channel (Fagerlund et al., 2010, Mkrtchian et al., 2012). Mkrtchian et al. (2012) performed microarray and PCR analyses on five surgically removed human carotid bodies and demonstrated the presence of TASK-1 but the absence of TASK-3.

In general, cloned and native TASK channels appear to be inhibited by barium, quinidine, anandamide and methanandamide, (Buckler et al., 2000, Veale et al., 2007, Kim et al., 2009a, Enyedi and Czirjak, 2010). TASK-3 is inhibited by ruthenium and Zn^{2+} red whereas TASK-1 is not (Czirjak and Enyedi, 2003, Kim et al., 2009a, Enyedi and Czirjak, 2010). In native carotid body patches it is thought that TASK-1 has a smaller conductance than TASK-3. Kim suggests that as TASK-3 has a conductance approximately twice as large as that of TASK-1, and hence the channels are easily distinguishable from each other. The views in this lab are slightly different as we believe it is hard to classify each channel due to the diversity seen in open amplitudes. Channel activity in carotid body patches is generally high. Few and possibly no patches seem to contain a single channel and transition between conductance levels during an open event is not uncommon. Thus the extent to which there may be multiple conductance states of TASK-1/3 or just simultaneous openings of different channel types is unclear. To illustrate this, an example of native carotid body TASK channel activity can be seen in Figure 3.2. The green line is set at 1.2 pA, which is thought to be the average open amplitude of the TASK-1 channel. The blue line is set at 2.8 pA which is the believed to be

the average open amplitude for the TASK-1/3 heterodimer (Turner and Buckler, 2013b). Note the diversity of the open amplitude of each channel and how several channels in this figure cannot be clearly marked as either TASK-1 or heterodimer.

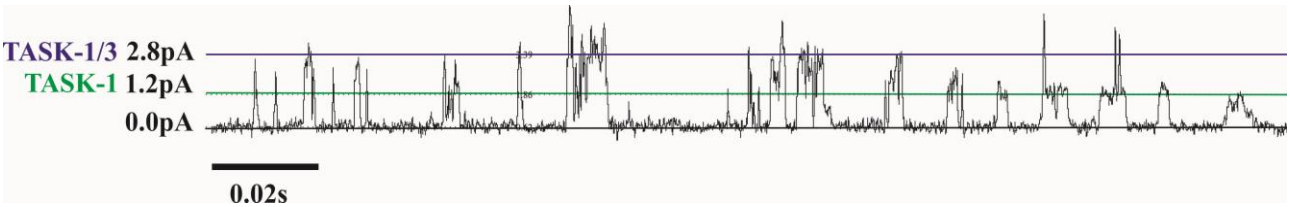

Figure 1.2: Cell-attached single channel low noise trace revealing the typical TASK channel activity in the carotid body. Bath Tyrode 100mM K^+ Pipette potential 140mM K^+.

Despite the difficulty in identifying each channel subtype in native carotid body TASK channel patches, some kinetic analyses has been performed on the TASK channel as they occur in the rat carotid body. The carotid body TASK channels have fast flickery kinetics, with short bursts of rapid openings with an estimated mean open time of approximately 0.3ms and a short closed time of constant of 0.1ms. The average burst duration is approximately 1.7ms. The long closed state is variable, the closed state varies between 2 and 30ms (Williams and Buckler, 2004). An example trace illustrating the long closed state (indicated by the purple line) and a burst (red line) can be seen in Figure 1.4.

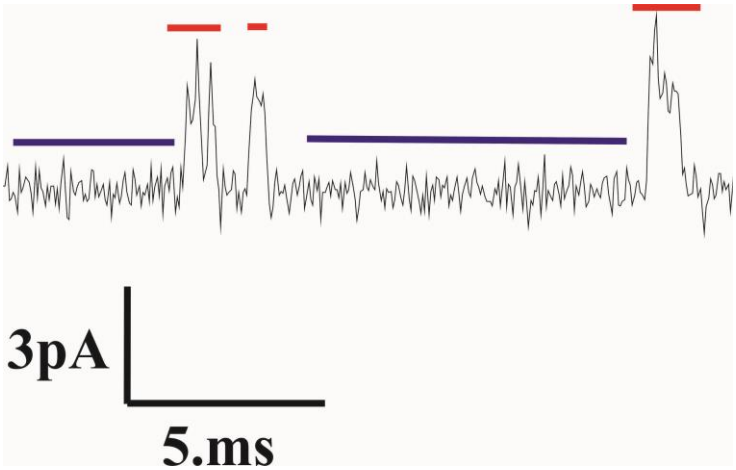

Figure 1.3: Single channel kinetics of ratTASK-1 transiently expressed in HEK293 cell. The purple line indicates the long closed states and the red line indicates the burst duration of the channel opening. Recording filtered at 5KHz

As discussed in this section, notwithstanding the remote possibility of other undiscovered channels, there is good evidence provided by different groups that the carotid body's oxygen sensitive background K^+ current that closes in response to hypoxia, comprises of TASK-1 TASK-3 and TASK-1/3. In the experimental chapters in this thesis therefore it will be referred to as carotid body TASK channels (see chapter 2 section 2.10 for further elaboration).

1.4.3 TASK channels and anaesthesia

TASK channels and volatile anaesthetics have been studied before. In general, this anaesthetic TASK channel research can be categorized in either the channel specific interaction or in a wider relevance for its hypnotic or respiratory effects. Our group, and others, have established that TASK channels can be modulated by volatile anaesthetics (Buckler et al., 2000, Berg et al., 2004, Putzke et al., 2007, Pandit et al., 2010) and that halothane is markedly able to increase TASK channel open probability in rat carotid body

cells. Our lab has also previously found that both isoflurane and halothane lead to a decreased influx of Ca^{2+} in response to hypoxia in rat carotid body cells (Pandit et al., 2010) with halothane having the more potent effect. Other groups have studied heterologously expressed K_2P channels in mammalian cell lines. Patel et al. (1999) showed that anaesthetics such as isoflurane and halothane are able to activate K_2P channels (TASK and TREK-1) in transfected COS-cells. Putzke et al. (2007) studied Xenopus oocytes expressing human TASK-1 channels and showed that isoflurane and halothane activate TASK-1. In contrast, Berg et al. (2004) used a heterologous expression system (HEK-293 with either rat TASK-1 , TASK-3 or TASK 1-3) to demonstrate that isoflurane activates TASK-3 and TASK 1-3 but inhibits TASK-1. Most literature agrees on the fact that halothane appears to be a stronger agonist and isoflurane appears to be a weaker agonist. This difference between agents in their stimulation of TASK channels is in accordance with the human and rat ventilatory studies (as mentioned in section 1.1.3).

Linden et al. (2006) found that TASK-1 knockout mice (KO) showed a reduced hypnotic sensitivity to halothane and isoflurane, reflected as a rightward shift (reduced potency) in the concentration-response curves. Linden et al. (2007) also studied TASK-3 knockout mice and reported that TASK-3 KO mice needed a higher halothane concentration for loss of withdrawal reflex than the wild-types. There was also a small difference in sensitivity observed in these animals for isoflurane, but this was not significant. Other groups who also investigated the anaesthetic sensitivity found that TASK-$3^{-/-}$ mice needed more halothane to reach loss of consciousness and immobility, and appeared less sensitive to halothane, whereas in TASK-1-knockout mice there was only a very small insignificant change detected in halothane sensitivity (Pang et al., 2009). Lazarenko et al. (2010) reported a reduced halothane

evoked membrane hyperpolarization in moto-neurones in both TASK-$1^{-/-}$ and TASK-$3^{-/-}$ mice and reported similar loss of isoflurane and halothane sensitivity. Furthermore, the authors reported that a significantly higher concentration of halothane or isoflurane was required to render mice unresponsive to a tail pinch, by comparison to wild type mice. These findings with regards to the hypnotic effects of anaesthesia may or may not translate to respiratory studies regarding the relevance of TASK channels and AHVR.

Although it is clear that some K_2P channels interact with anaesthetics, the nature and the place of this interaction is less clear. For anaesthetic binding with TASK channels, there are several regions that are thought to be important for the binding and or gating. Patel et al. (1999) identified that the VLRFMT region between amino acid 242 and 248, which is the M4 and C terminus of the TASK channel, is essential for halothane activation. Talley and Bayliss (2002) then established that this region was also important for halothane activation in TASK-3. Andres-Enguix et al. (2007) identified another important site for anaesthetic interaction by using site-directed mutagenesis in a TASK channel cloned from Lymnaea stagnalis (Ly). Mutating amino acid 159 (methionine in human TASK), located in the region between the end of M2 and the middle of M3, to alanine (a neutrally charged amino acid) greatly reduces volatile anaesthetic activation in LyTASK and human TASK. Conway and Cotten et al., (2011) used cysteine modification to see if occupancy of amino acid 159 in both LyTASK and human TASK-3 increases TASK-3 channel activity and found that covalent modification markedly increased channel activity.

1.5 Questions addressed in thesis

Linked to the intriguing question of how the carotid body responds to oxygen is the question of how this response is impaired in the presence of clinically relevant concentrations of volatile anaesthetics; and what can be done to overcome this impairment and restore a functional response. The objective of this thesis is to study to what extent volatile anaesthetics interfere with the hypoxia transduction cascade, their interaction with TASK channels and whether or not there is an interaction between the different volatile anaesthetics.

Thus, in this thesis, I will examine the effects of three common agents (halothane, isoflurane and sevoflurane) on glomus cell response to hypoxia, as well as the effects of these agents on TASK channels (native and those transiently expressed in human embryonic kidney (HEK) cells). I will also investigate in another chapter the effects of anaesthetics on mitochondrial function. Finally I present data on exploring the effects of TASK-channel blocking drugs (as potential stimulants of breathing) on glomus cell function.

Chapter 2. Materials and Methods

2.1 General molecular biology methods

The first two subsections (2.1 and 2.2) explain the molecular biology methods. Section 2.1 explains the general methods, provides recipes of media and explains the frequently used protocols such as polymerase chain reaction (PCR) protocols and the generation of a vector with DNA insert. Section 2.2 then reveals how the constructs used for experiments in this thesis are generated, by referring to the protocols explained in section 2.1.

2.1.1 LB medium and plates for culture of bacteria

Luria Bertani broth with Ampicillin (LB-AMP) was made by dissolving 20g LB Broth powder (both Sigma-Aldrich, Dorset, UK) in 1L purified H_2O. The solution was autoclaved and, once cooled down below 30ºC, AMP was added at a final concentration of 100mg/L.

Agar-AMP (100mg/L) plates were made of imMedia Amp Agar sachets (Invitrogen, Paisley, UK), which were added to 200mL of purified H_2O in a glass bottle. The solution was microwaved according to the manufacturer's instructions until bubbles started to appear. Thereafter the bottle was gently swirled to mix and reheated. Once the solution had cooled down it was poured into media plates.

2.1.2 Bacteria transformation protocol

All transformations were performed with Subconing Efficiency D-Hanahan-5-Alpha (DH5α) competent Escherichia (E) Coli cells (Invitrogen, Paisley, UK). An aliquot of cells stored at -

80ºC was thawed on wet ice for approximately 15 minutes. 50 µL of DH5α was pipetted in a microcentrifuge tube (Eppendorf, Stevenage, UK). The vial with remaining cells was immediately put in an ethanol bath in dry ice before it was returned to the -80ºC freezer. 5 to 10 ng of DNA was pipetted into the DH5α cell suspension, which was gently mixed by tapping. The suspension was incubated for 30 minutes on wet ice. The Eppendorf tube containing the cells was placed for 20 seconds in a 42ºC water bath, which resulted in a heat shock and uptake of DNA by the bacteria. Following the heat-shock the cells were placed on wet ice for an additional 2 minutes. 500-950 µL of LB-AMP was added to the cell suspension, which was then incubated for an hour at 37ºC and shaken at 225 rpm. 20-200µL of each transformation reaction was streaked on selective Agar-AMP plates and incubated overnight at 37ºC.

2.1.3 Miniprep protocol

Minipreps for isolation of up to 20µg DNA were performed with the Qiaprep spin miniprep kit according to the manufacturer's instructions. A colony was picked up from a LB-Amp plate with a small sterile stick, which was placed in 3 mL LB-AMP (100mg/L) and grown overnight. In short: cultures were pelleted by a 3 minutes centrifugation of 10000rpm in a table-top centrifuge at room temperature. The pellet was redissolved in buffer P1, P2 and N3 (all Qiagen) and then centrifuged for an additional 10 minutes at 13000 rpm at room temperature. The supernatant was then applied to the QIAprep spin column and the flow through discarded. The column was then washed by buffer PE and the DNA was eluted in a 50µl Qiagen elution buffer.

2.1.4 Midiprep protocol

The midiprep protocol for isolation of up to 100-200µg DNA was performed with the HiSpeed Plasmid Midi Kit (Qiagen, Manchester, UK). As a preparation, a single colony was picked up and inoculated in 3 mL LB AMP for 8 hours in the incubator and shaken at 220 rpm. 100 µl of this 'starter culture' was added to 50mL LB AMP medium, which was incubated and shaken overnight for 12-16 hours. The following day the bacteria were pelleted in the centrifuge at 6000xg for 15 min at 4ºC. The pellet was resuspended according to the protocol in buffer P1, P2 and P3. The lysate was then added to the barrel of the Qiafilter cartridge and incubated for 10 minutes at room temperature. The lysate was filtered through the cartridge using a plunger after which it was poured into the HiSpeed Tip and allowed to run through by gravity. When the lysate had cleared, the tip was washed with 20mL buffer QC and the DNA was eluted with 5mL buffer QF. Instead of following the rest of the protocol and precipitating the DNA with the Qiaprecipitator, the protocol was completed manually without the Qiaprecipitator, as it was found after several attempts that most of the DNA got lost during the Qiaprecipitator steps. Instead, the DNA in 5 mL QF was precipitated by adding 3.5 mL room temperature isopropanol (Sigma, Dorset, UK) and mixed. The mixture was centrifuged at 15000 xg for 30 mins at 4ºC and the supernatant was carefully decanted. 2mL of 70% ethanol was added and centrifuged for another 15 minutes at 15000 x g, 4ºC. The supernatant was carefully decanted and the pellet was air-dried for about 5-10 minutes. Care was taken to not over dry the pellet. The pellet was resuspended in 50-100 µl TE buffer (Qiagen) and warmed at 37ºC to enhance dissolving of the DNA for 1-2 hours. Concentrations of DNA in TE buffer were verified with the Nanodrop (Lite Spectrophotometer, Nanodrop products, Wilmington, Delaware, USA).

2.1.5 PCR and Colony PCR

The following standard polymerase chain reaction (PCR) was performed to check for presence of TASK-1 or TASK-3 in DNA samples, for example prior to submitting the samples for sequencing. All primers used in this thesis (unless otherwise indicated) were synthesized by Eurofins MWG Operon (Ebersberg, Germany). For the standard PCR the following primers were used:

For TASK 1:

TASK1_cDNA_Forward: gcaaggtgttctgcatgttc

TASK1_cDNA_Reverse: gtactgaggctgcgtttgc

For TASK3:

TASK3_cDNA_Forward: acaaagtcgccgaaccctat

TASK3_cDNA_Reverse: acaaagtcgccgaaccc

The PCR reaction contained the components indicated in table 2.1:

Component	Final concentration per 25μL sample
dNTP	200 µM
Primer Forward	0.2 µM
Primer Reverse	0.2 µM
Thermopol reaction buffer (NEB)	2.5 µL
NEB Taq polymerase (NEB)	0.5 units
DNA	10 ng
H_2O	To 25 µL

Table 2.1: Components of standard PCR

The annealing temperature was based on adding the following formula:

Temperature = ((melting temperatures of primers 1+ 2) / 2) -5

This resulted in an annealing temperature of 53ºC for the standard PCR

The following cycle was run:

Step	Time (Sec)	Temperature (ºC)
Initial denaturation	30	95
35 cycles of:		
Denaturation	30	95
Annealing	30	53
Elongation	60	68
Followed by		
Final extension	300	68

Table 2.2: Reaction cycle standard PCR

All samples were pipetted on ice to prevent enzyme activation.

This protocol was also run as part of a colony PCR to check for TASK containing colonies following transformation. For a colony PCR the same reaction mixture was used as indicated in Table 2.1, but instead of pipetting DNA in a buffer, a small amount from individual bacteria colonies was stirred into the PCR reaction tube with a sterile tooth-pick. As for the PCR cycle protocol, the initial denaturation step from the standard reaction cycle was extended from 30 seconds to 15 minutes at 94ºC (Table 2.2) to enhance release of DNA from the bacteria.

2.1.6 Restriction Digest

Following the PCR, the samples were mixed with 6x Blue Gel Loading Dye (New England Biolabs, Hitchin, UK) and pipetted into the wells of a 1-1.5% agarose gel (TopVision Agarose, Thermo Scientific, Paisly, UK) in 1x Tris-Borate-EDTA buffer (Sigma, Dorset, UK) containing 1x SYBR® Safe (Invitrogen, Paisley, UK) to visualize the bands.

2.1.7 PCR clean-up protocol

The PCR clean-up reactions were performed with a QIAquick® PCR purification kit (Qiagen, Manchester, UK) to wash away enzymes from previous reactions. Five volumes of buffer PB was mixed with 1 volume of the total PCR reaction and added on top of a QIAquick column. The flow-through was discarded and 750µL of buffer PE was added to wash the DNA in the column. The DNA was then eluted in 50µL Elution buffer in an Eppendorf tube (Stevenage, UK).

2.1.8 Sequencing of DNA samples

Sequencing was performed by Source-Bioscience Life Sciences (Nottingham, UK), who provided a read out in base-pairs. For crucial samples the DNA was sequenced three times to ensure accurate base-pair insertion. Plasmid DNA was delivered at a concentration of 100ng/µl. When the Bioscience stock primers were not used, custom primers were delivered at 3.2pmol/µl with a melting temperature between 55°C and 60°C and a GC content between 40% and 60%.

2.1.9 Insertion of DNA into Vector

TASK DNA was transferred to different DNA constructs (vectors), for example to vectors containing a fluorescent tag, to allow for easy identification of transfected cells in a later stage. The steps for transfer of DNA from the mother vector to a new vector consisted of amplification, digestion, antartic phosphatase treatment and ligation.

Step 1: Amplification

The DNA that was to be transferred in a vector was amplified with a PCR reaction. Custom designed primers allowed an insertion of desired restriction sites on the 5' and 3' end of the chosen DNA. Restriction sites were added and chosen, so that it was compatible with an easy insertion into a new insertion vector. The custom made primers were designed as explained below:

AAAAAA – 5 to 8 bases coding for restriction site insertion – 18-25 complementary target DNA base-pairs**.**

The -AA- sequence did not end up being inserted. This was followed by the base-pairs coding for the desired restriction site (for example EcoRV) and followed by the first few base pairs of the DNA sequence that was to be amplified. The amplification reaction mixture contained the following:

Component	Final concentration per 25μL sample
dNTP	200 μM
Primer Forward	0.5 μM
Primer Reverse	0.5 μM
Phusion buffer (NEB)	1X
Phusion Polymerase (High-Fidelity Polymerase M0530, NEB)	0.5 units
DNA (still inserted in vector of origin)	10 ng

Table 2.3: Components for the 'DNA transfer' PCR

The DNA was amplified with a PCR cycle as shown in table Table 2.4:

Step	Time (Sec)	Temperature (ºC)
Initial denaturation	30	98
35 cycles of		
Denaturation	10	98
Annealing	30	58
Elongation	45	72
Completed by		
Final extension	600	68

Table 2.4: PCR cycle for vector transfer

Following the ligation, a PCR clean up reaction was performed and the concentration of DNA was eluted in EB buffer (Qiagen) and measured with a Nanodrop to determine the DNA yield.

Step 2: Restriction digest

A digest was performed for both the amplified DNA of choice and the desired insertion vector. The reaction components can be found in Table 2.5:

Components for Insert	Per 50 μL
Vector DNA or insert DNA	1 µg
Restriction enzyme 5' end	1 µL
Restriction enzyme 3, end	1 µL
NEBuffer Cutsmart™	5 µL
H2O	To 50 µL

Table 2.5: Components for restriction digest

The reactions were incubated for 15 minutes at 37ºC (unless the NEB buffer specified otherwise). The insert was kept on ice afterwards, while the vector was treated with antartic phosphatase.

Step 3: Antartic phosphatase treatment

Directly following the restriction digest, the insertion vector was treated with antartic phosphatase (M0289S New England Biolabs, Hitchin, UK). This step was performed to dephosphorylyse, i.e. remove 5' phosphate groups, and prevent recircularization of the insertion vector. Therefore 5µL antartic phosphatase buffer (NEB) and 2µL antartic phosphatase was added to the digest reaction of the insertion vector and incubated for 1 hour at 37ºC.

A PCR clean-up was performed again with both the untreated insert and the phosphatase treated vector. Afterwards the DNA was eluted in EB buffer (Qiagen) and measured with a nanodrop to determine DNA concentration.

Step 4: Ligation

For the ligation reaction the insert and vector were combined in a 'vector to insert' ratio of 100ng vector to 66ng insert. This was based on the following formula, obtained from New England Biolabs' website.

$$\text{Total ng needed for Insert} = \frac{\text{Ng vector x Kb insert}}{\text{Kb insert}}$$

The ligation reaction contained:

Components for ligation	**Per 20 μL**
Insert	66ng
Vector	100ng
Ligase (NEB)	2µL
Ligase buffer (NEB)	5µL
H2O	To 20µL

Table 2.6: Components for ligation reaction

The ligation reaction was incubated overnight at 16ºC, or over the weekend at 4 ºC, after which it was ready for transformation in DH5α cells.

2.1.10 Storage of competent bacteria in glycerol

For long term storage of DNA in competent bacteria, a colony from an Agar-AMP plate was picked up and grown in LB-AMP overnight. 800µL of the LB containing bacteria was added to a 2mL cryovial (Corning, High Wycombe, UK) together with 200µL sterile glycerol (Sigma, Dorset, UK), which was vortexed before being placed in the -80ºC freezer.

2.2 Generation of transfection ready ratTASK constructs

2.2.1 ratTASK-1

Before the start of the experiments ratTASK-1 was present in pcDNA3 (in E Coli glycerol stock in -80ºC freezer). A sample from glycerol plates was streaked out on LB-AMP, which resulted in colonies the following day. A small number of colonies was transferred to 3mL L-AMP medium and grown overnight. The next day a miniprep was performed. The DNA was eluted in AE buffer and submitted for sequencing.

The TASK-1 sequence results (Source Bioscience) showed a single base pair mutation in the 915th base of the TASK-1 sequence.

Point mutation repair of ratTASK-1 DNA

Mutagenesis with the Q5 Site-directed Mutagenesis kit (New England Biolabs, Hitchin, UK) was performed to correct the base pair mutation to its original sequence. First, the DNA and the construct were amplified with PCR. The following primers were designed with the help of software on the New England Biolabs website:

T1SDM_A915C_F: 5'-TGGGCGTGGGcGTGGGCGTCG

T1SDM_A915C_R: 5'-TGCCGCCTGCAGCCGCTG

The following components were used for the exponential amplification (PCR):

Component	Final concentration in 25μL
Primer Forward	0.5 µM
Primer Reverse	0.5 µM
Q5 Hot start high fidelity 2x mastermix (NEB)	1X
Template DNA	25 ng
H_2O	To 25 µL

Table 2.7: components of 'point mutation' PCR

The following PCR protocol was run:

Step	Time (Sec)	Temperature (ºC)
Initial denaturation	30	98
25X		
Denaturation	10	98
Annealing	20	72
Elongation	210	72
Final extension	160	72

Table 2.8: PCR cycle for point mutation amplification

Following the PCR amplification, a Kinase-Ligase-Dpnl (KLD) treatment was carried out. This enzyme mixture facilitates rapid circularization of the PCR product and removal of the template DNA. The following components were needed for the KLD treatment:

Component	Final concentration in 25μL
PCR product	5 µL
2x KLD reaction buffer	5 µL (1X)
KLD enzyme mix	1 µL (1X)
Nuclease free H_2O	3 µL

Table 2.9: Components for KLD treatment reaction

The components were incubated at room temperature for 5 minutes.

The final step consisted of a high-efficiency transformation of the KLD treatment product into 50µl chemically competent cells, provided with the site directed mutagenesis kit, which

followed the procedure as described in section 2.1.2 of this chapter. Following transformation 40 µl of the transformation solution was plated on a agar-AMP plate and incubated overnight at 37ºC. The following day five colonies were picked up and further grown overnight in LB-AMP medium. DNA was extracted the following day with a Miniprep kit (Qiagen) resulting in good yields. The samples were then sent off for sequencing. By repeating this protocol a number of times, a colony was identified that was correctly repaired.

2.2.2 ratTASK-3

At the start of the project ratTASK-3 in Vector pCI was available freeze-dried in the -20 freezer. RatTASK-3 in pCI was redissolved from a dried DNA pellet in 20µl AE buffer (Qiagen) leading to 2.4µg/µl stock. This was transformed into competent E. Coli bacteria (section 2.1.2) and then plated on agar-AMP plates.

First, ratTASK-3 was transferred from pCI to pcDNA3 (a kind gift from Dr. Norma Masson). This was done according to the protocol described in section 2.1.9.

A PCR was performed to generate sufficient TASK-3 DNA with BAMHI (5 end) and Not1 (3 end) restriction sites inserted to generate restriction sites for ligation into the BAMHI and Not1 restriction sites in pcDNA3. A PCR clean-up was performed, followed by a digestion of both the PCR product and pcDNA3 with BAMHI-HF (new England Biolabs) and NOTI-HF. This was followed by antartic phosphatase treatment of the insertion vector and completed with a ligation with T4 DNA ligase (New England Biolabs) in a 66ng-100ng ‘insert to construct’ ratio. This was left for 48 hours in the fridge to ligate. The ligation solution was

then transformed into competent bacteria as described in section 2.1.2. A colony PCR and extensive sequencing of the miniprep DNA confirmed correct insertion and orientation. Aliquots were saved in the -80ºC freezer in glycerol stocks.

2.2.3 TASK-1 and -3 insertion into pIRES-EGFP

pIRES-EGFP was chosen as the designated transfection vector as the fluorescent tag allows easy identification of transfected HEK cells. The primers were designed with the same principle as explained in section 2.1.9 and consisted of an AAA site, restriction site and complimentary DNA.

The following primers were used for this:

TASK-1_EcoRV_F AAAAAA GATATC ATGAAGCGGCAGAATGTGCGCAC

TASK-1_EcoRI_R AAAAAA GAATTC TCACACTGAGCTCCTGCGCTTC

TASK-3_NotI_F AAAAAA GCGGCCGC ATGAAGCGGCAGAACGTGCGTAC

TASK-3_EcoRI_R AAAAAA GAATTC TTAGATGGACTTGCGACGGATGTG

The DNA was amplified with PCR, which was followed by a PCR clean-up. The TASK-1 was then digested with EcoRV and EcoRI and similarly a pIRES-EGFP vector was digested with the same enzymes. TASK-3 was digested with NotI and EcoRI as was the pIRES-EGFP vector. pIRES-EGFP was then treated with antartic phosphatase. Both the TASK DNA and the pIRES vector underwent another PCR clean-up and were eluted in EB buffer. DNA concentrations were measured with a nanodrop. The DNA was then ligated into pIRES, which was incubated at 4ºC for 48 hours.

Following the ligation, the DNA was transformed in DH5-α and plated overnight. A colony PCR was performed and, based on the obtained results, colonies containing TASK-1 or TASK-3, were picked up and grown in 3mL LB medium with AMP 100mg/L overnight at 37ºC 225 rpm. The following day a miniprep was performed and the samples were submitted for sequencing to confirm correct sequence and insertion. The colonies with a correct orientation and insertion were grown again in LB-AMP medium, from which a midiprep was performed that yielded transfection ready DNA.

2.2.4 Transient expression of TASK channels in HEK cells

Human Embryo Kidney (HEK) HEK-293t and HEK-293 cells were transfected with TASK channels. Although experiments with both cells have been performed, I found that the channel expression in the -293t cells was even higher than the regular -293 cells. Ultimately, the goal was to get low enough channel expression for single channel studies and hence I opted to perform the majority of my experiments with -293 cells.

2.2.5 Sub-Culture of HEK-293t and HEK-293 cells

HEK cells (both -293 and -293t cells) were kept in a T25 culture flask (Corning, High Wycombe, UK) at 37ºC and with 5% CO_2 in culture medium. HEK-293 cells were obtained from Sigma (Dorset, UK) (European Collection of Cell Culture Lot 13F007 P65).

1 litre of culture medium contained the following ingredients:

- 870 mL Minimum Essential Medium Eagle + Sodium Pyruvate (110mg/L) (Sigma, Dorset, UK)

- 100 mL Fetal Bovine serum 10% final concentration (Gibco, Paisley, UK)
- 10 mL L-glutamine with final concentration of 2mM (Sigma, Dorset, UK)
- 10 mL Penicillin/Streptomycin with a final concentration of 100U/mL 100 µl/mL (Fisher Scientific)

Approximately every three days the cells were split in a 1:10 ratio and plated in a new T25 flask (Corning) with fresh medium. For splitting, the culture medium was gently removed with a serological pipet and the cells were rinsed in 3mL of Phosphate Buffered Saline (PBS) (Sigma, Dorset, UK). Then 1.5 mL of trypsin EDTA was added (Sigma, Dorset, UK) and the cells were incubated for approximately three minutes at 37ºC. The flask was gently shaken to enhance detachment of the cells from the wall. 8mL of fresh medium was added to the trypsinated cells and 1mL of this suspension was then added to 10 mL of culture medium in a new flask.

2.2.6 Cell counting

For cell counting the cells were detached as described in section 2.2.5 and mixed with fresh culture medium. 100µL of the detached cell suspension was added to an Eppendorf tube, which was mixed with a 100µL of Trypan Blue (0.4%: Sigma, Dorset, UK) to produce a 1:2 dilution. A few microliters of the solution was pipetted carefully between the space of the hemacytometer (Assistant, Sondheim, Germany) and the glass coverslip.

Both the blue cells (which were alive) and non-blue cells (dead cells) were counted. Expressing the blue cells as a percentage of total cells resulted in a % cell viability, which provided useful insight for transfecting cells. The cells were counted in the five squares

indicated in Figure 2.5. The total cells were divided by 5 to get an average of cells per square and this average was multiplied by 2 (because of the Trypan blue dilution). The volume per square was 0.1µL. The amount of cells per square was then used to calculate how much cell suspension needed to be added per well to seed the correct numbers of cells for transfection.

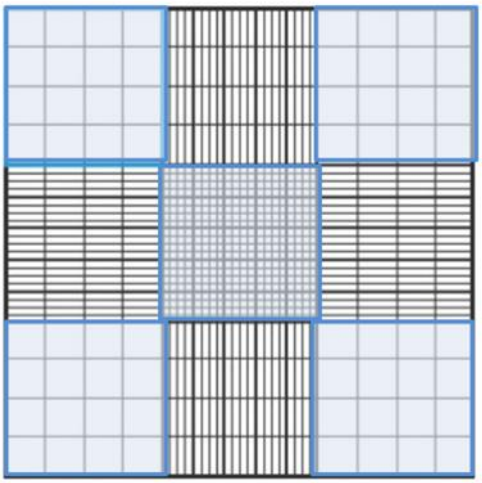

Figure 2.1: Schematic graph of cell counting Chamber. Blue squares indicate the squares used for counting. Picture modified and adapted from: **http://www.abcam.com/protocols/counting-cells-using-a-haemocytometer**

2.2.7 Transfection of HEK cells with TASK

For optimal transfection two different transfection kits were trialled. The first kit to be tried was the Qiagen polyfect kit from Qiagen and the second one was a lipofectamine 2000 kit from invitrogen. Ultimately the lipofectamine kit generated the highest percentage of transfected cells.

Qiagen polyfect protocol

The day before transfection 6 $*10^5$ HEK cells were plated in a well of a 6-well plate with three mL HEK culture medium at 37°C and 5% CO_2. The next day this resulted in a confluency of 40–80%. 2 µg of DNA dissolved in TE buffer, was diluted in Opti-MEM® Reduced Serum (Life Technologies, Paisley, UK) to a total volume of 100 µL. 20 µL of PolyFect Transfection Reagent was added and vortexed for 10s. This was incubated for 5–10 min at room temperature (20–25°C) to allow complex formation. 600µL of normal cell growth medium (as seen in section 2.2.5) was added to the reaction mixture, which was gently mixed and was immediately transferred to the well containing cells in fresh standard culture medium. Cells were harvested, plated and studied 24-48 hours post transfection.

Lipofectamine® 2000 transfection protocol

The day before transfection approximately 6 $*10^5$ HEK cells were plated in a well of a 6-well plate with 3 mL HEK culture medium at 37°C and 5% CO_2, which resulted in 70-90% confluency on the day of transfection. Depending on the DNA and experimental requirements, 800-2500ng of DNA was used for the transfection.

For the transfection 100µL of Opti-MEM® Reduced Serum (Life Technologies) medium was added to each of two Eppendorf tubes. In the first Eppendorf tube the DNA (in TE buffer) was added and gently mixed together with 5µL PLUS reagent (Life Technologies, Paisley, UK), which was used to enhance transfection efficiency. In the second Eppendorf tube between 8-12µL of Lipofectamine 2000 (Life Technologies) was added.

Both solutions were incubated for 15 minutes. The solutions were then added together and gently mixed to allow for DNA-lipid complex formation for another 15 minutes. The total solution was added to the well containing the HEK cells.

2.3 Glomus cell dissociation from rat carotid body

2.3.1 Surgical procedure and sub-dissection

Sprague Dawley rat pups P10-P15 (Harlan and Charles River) were terminally anaesthetized with 3-5% isoflurane in an induction chamber. Following a loss of righting reflex, the pup was transferred to a surgical table placed on a mouthpiece to which isoflurane was applied at a flow of approximately 500mL/minute. All procedures involving animals were approved by the University of Oxford's Local Ethical Review Process and were conducted in accordance with project and personal licences issued under the UK Animals (Scientific Procedures) Act 1986.

When a lack of pedal withdrawal reflex was observed in response to a pinch, the surgical procedure was started with an incision from clavicle to just below jaw line. During this first incision, extra care was taken to check for movement from the rat pup, which never occurred in any of the procedures. From the first incision, a triangle cut was made to expose the salivary glands. The glands were parted with forceps to expose the musculature underneath. The muscle running from clavicle to trachea and the muscle running alongside the trachea, were parted, which revealed the carotid artery. Removing the third large muscle located under the jaw line ensured completed exposure of the bifurcation.

Following exposure of the carotid artery and bifurcation, the remaining fat and tissue was removed. A ligature was tied around the caudal end of the common carotid artery. The common carotid artery was cut rostral to ligature, which was followed by two more cuts on the internal and external carotid artery. These cuts allowed the superior cervical ganglion (SCG) to stay attached and the cut out tissue was then transferred to ice cold PBS in a dissecting dish. In Figure 2.2 an image of the surgery can be seen in which the bifurcation is highlighted.

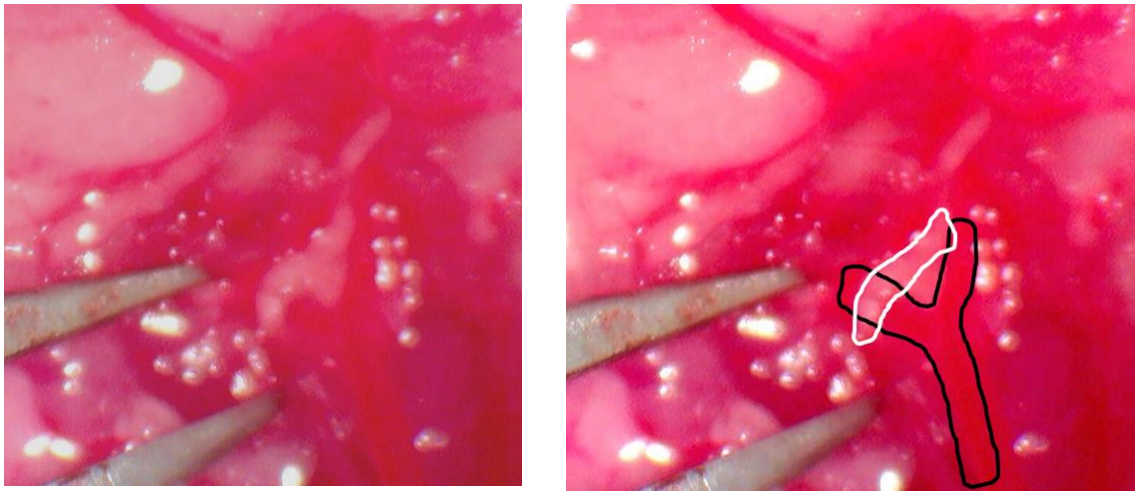

Figure 2.2: Carotid bifurcation. (A) picture showing the carotid bifurcation B: Same picture but the bifurcation highlighted in black and the glossopharyngeal nerve in white.

The bifurcation was pinned ventral side down with small insect pins in a petri dish with the common carotid artery pointing to the top of the dish and the internal and external to the bottom with the SCG lying on top of the bifurcation. Fat and other tissue was removed, which allowed for better exposure of the bifurcation with the SCG and vagus nerve. The SCG was carefully removed exposing the carotid body, which was located close to the internal carotid artery wall closest to the Vagus nerve, see Figure 2.3. The carotid body was then cut out and

put in a small dish containing PBS. During a typical day of experiments four carotid bodies were removed from two rat pups.

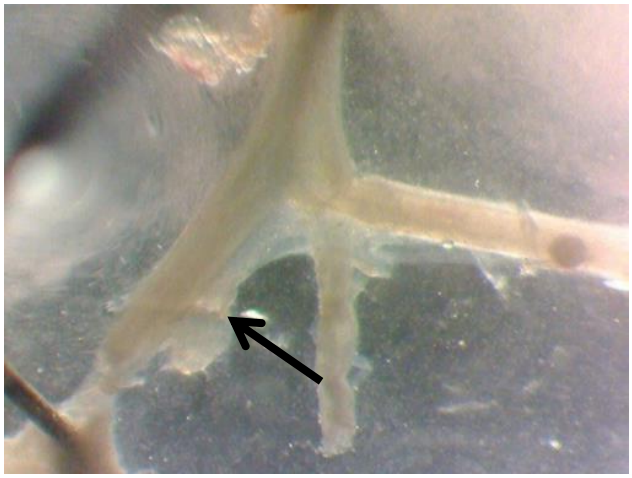

Figure 2.3 Rat carotid bifurcation. On the left, the carotid body indicated with the arrow.

Once all carotid bodies had been isolated, they were transferred to a dish containing HAMS-F12 (Sigma, Dorset, UK) with trypsin 0.4mg/mL (sigma, Dorset, UK) and Collagenase 0.6mg/mL (Worthington, Lakewood, NJ, USA), which was pre-equilibrated at 37ºC with 11% oxygen and 5% CO_2 to simulate arterial oxygen tensions. The enzymes were weighed and mixed with the medium and before application to the carotid bodies they were sterile filtered with a filter (0.22µm Merck Millipore ltd. Carrigtwohill, Ireland). The total incubation time was 21-23 minutes. After the initial 15 minutes of incubation, the carotid bodies were teased apart with forceps to increase the surface area exposed to the digestive enzymes for the second part of the incubation.

Once the enzymatic incubation time was completed, the carotid bodies were transferred to F12+ medium enriched with insulin (Sigma, Dorset, UK), fetal bovine serum (10% Gibco) and L-Glutamine (Sigma, Dorset, UK). In this solution, the carotid bodies were gently

agitated for 30 seconds to wash off enzyme solution. The carotid bodies were then transferred to a dish with similar culture medium, but with the addition of trypsin inhibitor (Sigma Dorset, UK). From this medium, 250-500μL was transferred to a clear 10mL tube in which the carotid bodies were triturated with fire polished glass pasture pipettes using a tip opening between 100 and 400 um for the larger pipette and between 30 and 100 um for the smaller pipette. The carotid bodies were triturated between 1-5 minutes, until no large pieces of tissues were visible from underneath the microscope.

The tissue containing medium was then transferred onto poly-L-lysine coated coverslips with approximately 30μL on each 6mm coverslip (VWR international). The coverslips with medium were incubated for two hours at 37ºC with 11% oxygen and 5% CO_2. Two hours later the cells were topped up with F12+ medium containing 2 uL/mL rhodamine conjugated peanut agglutinin (PNA) (Vector laboratories, Burlingame, CA, USA) to label type-1 cells. On a typical day, when two pups were used, 8-16 healthy stained type-1 cells were identified.

2.3.2 Explanation for choice of rat-pups

Rat pups were chosen over mice because isolating carotid bodies from mice remains extremely challenging, which results in a lower success rate in isolating the carotid body and also a lower total amount of cells. In mice, instead of a single cluster of cells, the carotid body appears to be spread amongst several islands of cells (Slingo, 2013). In rats the carotid body can be identified as a clearly visible discrete structure.

By using rat pups instead of adult rats, it becomes easier for the carotid body to be dissected, as there is less connective and fat tissue present. A faster identification and removal of the carotid bifurcations leads to a shorter procedure and a better chance to obtain healthy cells. Similarly, a milder and shorter enzymatic digestion and trituration improves the cell quality. The use of the relatively young pups is justified as resetting of the peripheral arterial chemoreceptors happens already in the first few days (Eden and Hanson, 1987, Carroll et al., 1993, Wang and Bisgard, 2005).

2.3.3 Staining of glomus cells

To distinguish the type-1 cells from the other cells that could end up in the carotid body cell prep, such as type-2 (sustentacular) cells, a rhodamine conjugated peanut agglutin (PNA) staining was performed. Kim et al. (2009b) established that PNA exclusively stains tyrosine hydroxylase positive cells (another marker for type-1 cells) in rat carotid bodies and that the PNA staining does not compromise cell health (i.e. a hypoxic response). For a rhodamine conjugated PNA staining, 2 mL of medium was added to the dish containing the carotid body coverslips and 4µL PNA was added, so a final concentration of 2 µL/mL was reached. Cells were incubated for at least an hour. This resulted in a bright orange staining for glomus cells once excited at 485nm.

2.4 Normoxic and anoxic solutions in perfusion rig

2.4.1 Solutions and gas mixtures used for experiments

The solution of choice was the CO_2-HCO_3^- buffered standard Tyrode solution containing the following ingredients:

Ingredient	Concentration (mM)
NaCl	117
KCl	4.5
$MgCl_2$	1
$NaHCO_3$	23
Glucose	11
$CaCl_2$	2.5

Table 2.10: Standard Tyrode ingredients

This Tyrode solution was equilibrated with 95% air/5% CO_2, pH 7.4. A few variations were made to the Tyrode solution when the experiments required, which is clearly indicated in the relevant chapters. The two most common modifications are:

- High K+ Tyrode, 100mM KCl added and NaCl reduced to 21.5mM
- Ca^{2+} free Tyrode, instead 0.1mM EGTA is added to chelate the remaining Ca^{2+}

2.4.2 Hypoxia Tyrode solutions

Hypoxic Tyrode solutions were equilibrated with

- 0% hypoxia (5% CO_2 in 95% N_2 , without sodium dithionide)
- 1% hypoxia (1% O_2, 5% CO_2, 94% N_2).

Air-tightness of the perfusion rig was assessed by measuring O_2 levels in the experimental bath. The O_2 levels were measured with an optical O_2 sensor (Presence, Regensburg, Germany) equilibrated with a normoxic and anoxic gas resulting in a two-point calibration. The normoxic gas used was 5% CO_2 in 95% air and the anoxic equilibration gas used was 5% CO_2 in 95% N_2, with the addition of 250μM $Na_2S_2O_2$ (sodium dithionide), which reacts with the remaining O_2 in the solution, so an oxygen-free solution is ensured for calibration. When 1% hypoxia (predicted pO_2 in experimental bath 7.6 mmHg) was delivered, the electrode placed in the experimental bath measured 10.6 mmHg. When 0% hypoxia (5% CO_2 in 95% N_2) was delivered the electrode measured 3 mmHg.

These results confirmed that the perfusion rig was air-tight with negligible ingress of O_2 from the atmosphere. Furthermore, since the measurements were taken directly from the experimental bath, this also indicated that the flow rates were appropriate and maintained the hypoxia. Additionally, switches into and out of anoxia/hypoxia were rapid, with the equilibrium achieved within 3 seconds.

2.4.3 The experimental 1% oxygen stimulus

The main hypoxic stimulus used in this thesis to study the effects of anaesthetics in combination with hypoxia is 1% oxygen equilibrated Tyrode solution, which, as described in the previous section, results in a PO_2 between 7.6 and 10.6 mmHg. In normoxia, the consensus regarding the PO_2 of microvascular blood in the carotid body is approximately 30-40mmHg (Acker et al., 1971) (Lahiri et al., 1993). In hypoxia the oxygen tension will consequently be lower. Furthermore, as the cells in the carotid body are clustered, the oxygen tension in the inner most cells in the centre is likely lower than the PO_2 in the supplying capillaries. Although it remains difficult to exactly determine what the most relevant hypoxic stimulus is, I reasoned that a PO_2 between 7-10mm Hg will most likely represent a relevant hypoxic stimulus, as it is not the strongest stimulus (0% O_2 and anoxia) but strong enough to evoke a robust response to hypoxia.

2.5 Anaesthetic delivery and verification

2.5.1 Description of perfusion system

The cell perfusion system is shown in Figure 2.4. Gas is delivered from compressed gas cylinders connected through air flow regulators and rotameters via narrow-bore plastic tubing to vaporizers containing anaesthetic (halothane, isoflurane and sevoflurane). The gas cylinders (British Oxygen Company, Surrey, UK) can contain air, N_2, O_2, and CO_2 in various concentrations of hypoxic mixtures. The typical flow rate of gas delivery to the vaporizers is

200-700mL/min, measured via rotameters. From the vaporizer outlet the anaesthetic-gas mixture passes through narrow-bore flexible nylon tubing (BS5409) to a plastic costar pipet gas dispersion tube (Corning, High Wycombe, UK) immersed in a glass bottle (volumes of 0.2-2 L are used, as needed) containing Tyrode solution.

The bottles (Schott Duran, Wertheim, Mainz, Germany) are capped with a plastic lid into which are punched two holes: one large hole to allow passage of the gas dispersion tube and one small hole to allow passage of the narrow bore metal aspiration tube (see below) that aspirates the solution into the delivery system for perfusion to the experimental bath. This small hole also allows passage of a fine plastic connector tube leading to the infrared gas analyser (Capnomac Ultima, Helsinki, Finland) for continuous anaesthetic vapour analysis of the headspace above the solution in the bottle. This analyser was checked and calibrated with readings from a mass spectrometer (Airspec 3000, Airspec Ltd, Biggin Hill, UK;), which was calibrated with standard agents as calibration gases.

The bottles are placed in a water bath heated to ~38ºC to achieve a temperature of 37ºC in the experimental bath. The gas from the vaporizer bubbles continuously into the bottle throughout the experimental period with sufficient time for equilibration before the start of any experimental recordings, as confirmed by attainment of the desired, stable value on infrared capnography. Both Millman and Young (1992) and Becker et al., (2012) have shown that equilibration is reliably achieved after ~10 min across a range of anaesthetic concentrations.

To deliver the solution from the bottle to the experimental bath a stainless steel (medical grade) aspiration tube is placed into the solution of the glass bottle via a small hole in the cap (see above). The delivery to the experimental bath is by gravity through stainless steel tubing and short sections of Pharmed (Akron, USA) tubing (flow 6-7mL/min). The solution is then aspirated from the bath using a peristaltic pump as a vacuum source. It is possible to make a switch from one experimental solution (eg air) to another (eg air with anaesthetic) using a two-way tap (constructed of PTFE and nylon) connected to the bath entry, which is operated by a lever. Switching the tap results in rapid change of solution within <1 second. The solution exits the experimental bath and passes through the compressors of a peristaltic pump. This perfusion system is 'closed' in the sense of being air-tight, as one particular aim is to maintain conditions that enable administration of near-anoxic stimuli to the cells of interest, so that it is suitable for work with cells like carotid body glomus cells that are oxygen sensitive.

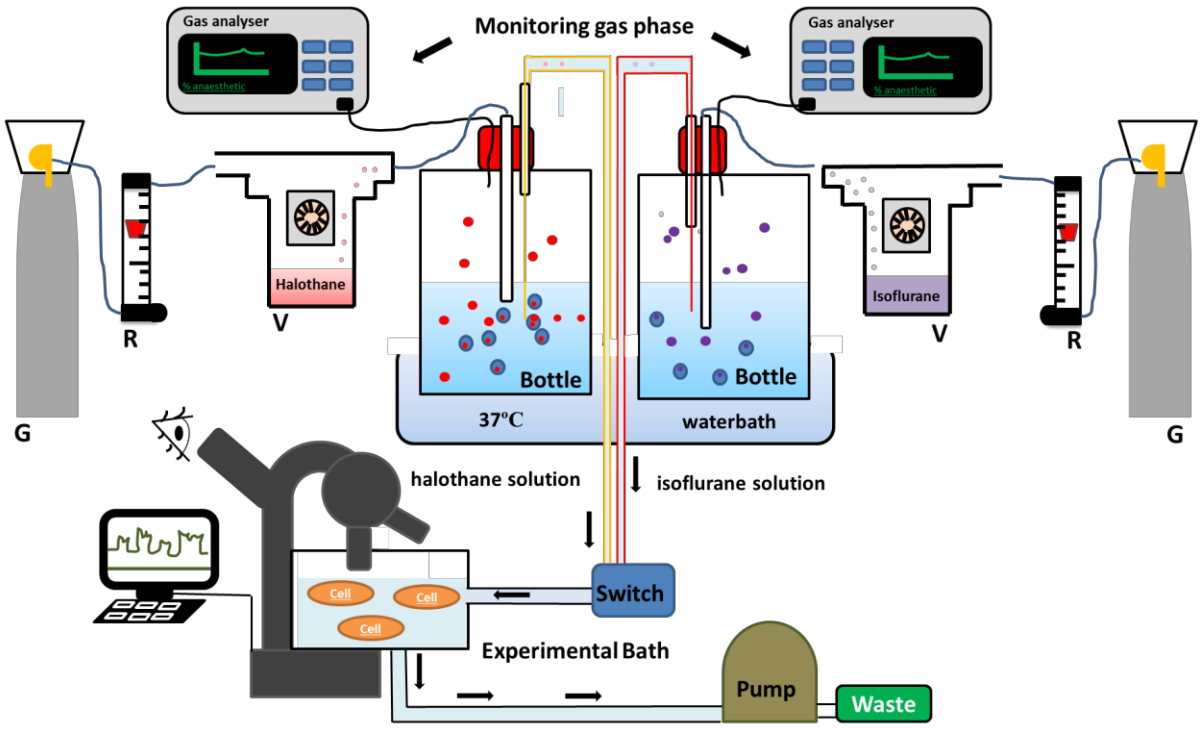

Figure 2.4: Perfusion system: From cylinders (G) carrier gas passes through rotameters (R) into vaporizers (V); which can be on or off (halothane and isoflurane shown as examples). When the vaporizer is off, all gas bypasses the anaesthetic. From the vaporizer outlet the anaesthetic-gas mixture passes through narrow-bore plastic tubing to a gas dispersion tube immersed in a glass bottle. A second, narrow bore metal aspiration tube aspirates the solution for delivery to the experimental bath. The flow of solution in the system from the bottle to the waste is driven by gravity and a peristaltic pump.

2.5.2 Challenges of accurate anaesthetic delivery

Handling volatile agents in standard perfusion rigs poses several challenges. Their very volatility (boiling points ~23-59ºC) means that these gases have a tendency to be lost from solution. Even if it is air-tight, the delivery system needs to ensure sustained equilibrium between anaesthetic gases in solution with the gas phase above the solution. However air-tight the delivery system, experimental baths into which the tissue or cells are placed are impossible to shield completely from the atmosphere and rapid evaporation can occur if this is not well controlled. Furthermore, the carotid bodies I study need to be constantly perfused

with O_2 to maintain constancy of their environment and flexibility to change the O_2 gas tensions. A review of published studies working with volatile anaesthesia revealed that to date it has been proved difficult to design a system that meets all these requirements in delivering anaesthetics to in vitro preparations. Many groups pre-equilibrate their solutions by bubbling and then storing it in bottles or air tight syringes from between a couple of minutes to several hours. How this equilibrated agent is stored and delivered to the biological preparation then differs across published studies. For example by keeping the solutions in Erlenmeyer flasks covered tightly with parafilm (Sirois et al., 1998). Generally, these methods might be described as 'closed' since their aim is to keep the anaesthetic in solution closed to the atmosphere until the time of exposure to experimental tissue.

However, despite being 'closed', chromatographic measurements of the samples from the experimental baths using these methods have revealed a loss of 20% - 50% compared with what was expected from calculations based on the dialled concentrations on the vaporizers (Miu and Puil, 1989, McDougall et al., 2008). Furthermore, because the experimental bath is inevitably exposed to the atmosphere, McDougall et al., (2008) demonstrated that a very variable loss of agent can arise unless there is a system for continuous perfusion with equilibrated solution. The option of frequent sampling from the experimental bath solution on a daily basis to confirm system performance is not only very time consuming, but also expensive. In order to verify the set-up as described in section 2.5.1 (and in order to anticipate reviewer enquiries), a gas chromatography–mass spectrometry (GC-MS) verification of the anaesthetic perfusion system has been designed with the aim of answering the following five questions:

1. Is the vaporizer output stable over time?
2. Is there a loss of anaesthetic between the bottle in which the bubbling takes place and the experimental bath in which the volatile anaesthetics are applied to the cells?
3. Is there a linear relationship when increasing the % of anaesthetic applied?
4. Is it possible to mix two different anaesthetics?
5. Is there thymol present in the Tyrode bottle?

2.5.3 GC-MS measurements of anaesthetics in solution

Samples were taken from two sites in the apparatus (Figure 2.4). The solution from (a) the bottle into which anaesthetic was bubbled and (b) from the experimental bath was carefully but rapidly drawn up using a 2 mL syringe and then swiftly placed into 2 mL autosampler vials (Finneran Associates, Vineland, USA) until a convex meniscus was formed. The cap was attached immediately excluding any air contamination. The vials were then analysed in batches. It was separately confirmed using repeated measurements of the same sample over 24 hours that there was no loss of anaesthetic from the autosampler vials, verifying that measurement in batches was appropriate.

GC-MS analysis was performed using an Agilent 7200 Quadrupole Time-of-Flight mass spectrometer, coupled directly to an Agilent 7890B Gas chromatograph and an Agilent GC Sampler 120 autosampler (Agilent, Stockport, UK). Standards were prepared in a non-polar solvent so as to exploit the high oil:gas partition coefficients of halothane and isoflurane (224 and 98 respectively). Toluene (analytical grade, Fisher, Loughborough, UK) was chosen as it has a higher boiling point (111 °C) than either halothane or isoflurane (50 and 48 °C respectively) and would elute after the analytes when using standard gas chromatography techniques. The autosampler was equipped with a 10 μL syringe and its operation was carefully designed to minimise outgassing of analytes. Prior to injection the syringe was

flushed once with toluene then three times with water. The syringe was then cleaned with the sample twice (10µL of sample was withdrawn and dispensed to waste). The syringe filling speed was set to 0.5µL/s and sample was drawn up and ejected three times before injecting 10µL of the sample. Following injection, the syringe was flushed three times with toluene and three times with water.

The gas chromatograph was equipped with an HP-5 column (30m, 0.25mm ID, 0.25µm film thickness, Agilent, Stockport, UK), the carrier gas was helium (BOC, Slough, UK) and the flow rate was 1.2mL/min. The inlet was set to 300°C with a split ratio of 100:1. The oven was held at 40°C for three minutes then ramped at 100°C/min to 240°C and held for 2 minutes. The transfer line was maintained at 300°C. The mass spectrometer was operated in electron ionisation (EI) mode with a source temperature of 230°C and electron energy of 70eV. Mass spectra were collected between 50-500 m/z and ionisation was disabled after 3.7 minutes (after all analytes had eluted but before the toluene eluted). MassHunter software (Agilent, Stockport, UK) was used for instrument control and data analysis. Responses for each analyte were determined using the area of peaks seen in the total ion count (TIC) mass chromatograms. Identities of analyte peaks were confirmed using comparison to the NIST mass spectral library (National Institute of Standards and Technology, Gaithersburg, MD, USA)[1].

[1] The GC-MS read out of the samples I delivered and prepared has been kindly performed by James Wickens, who also designed the protocol for GC-MS analysis and provided me with the textual description of the protocol as described in section 2.5.3.

2.5.4 Vaporizer output remains stable over time

To confirm that the vaporizer output remained stable over a longer time, head space gas measurements were taken every 10 seconds and then every minute to assess concentrations of anaesthetics in the head space above the Tyrode solution. As depicted in Figure 2.5 both vaporizers generate a stable output of both halothane and isoflurane in the headspace gas.

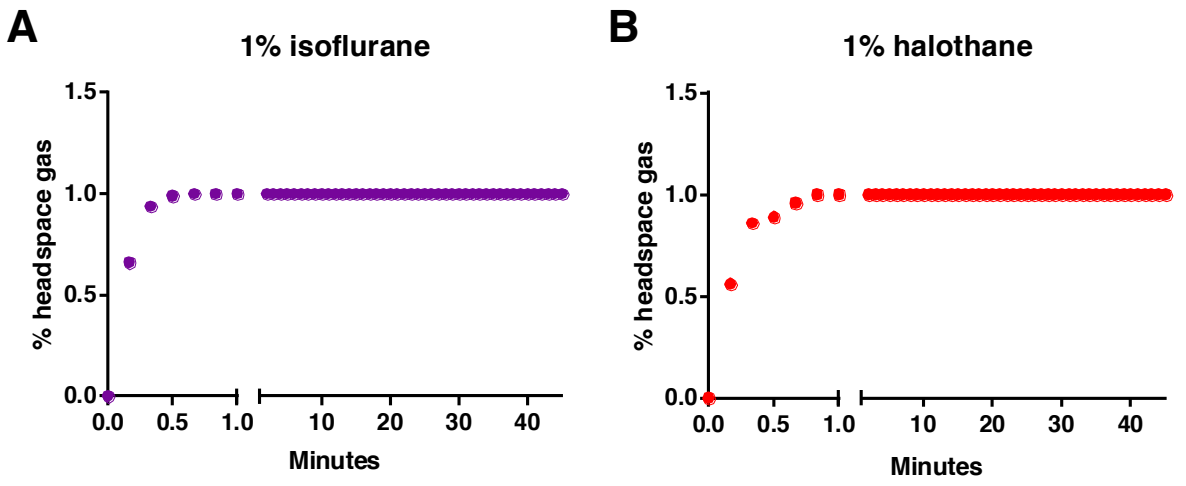

Figure 2.5: Measurement of headspace gas after opening of vaporizor dial. Measurements performed in headspace gas above 200mL Tyrode at ~37/38ºC in bottle. Within 1 minute the measurement of headspace % was stable. Measurements were performed for 45 minutes. The same experiment performed at higher concentrations of isoflurane (2% and 4%) showed similar calibration curves.

2.5.5 Linear relationship of anaesthetic concentrations bottle and bath

GC-MS samples were taken from both the bottle and the bath for the following headspace gas concentrations as measured with the infrared analyser: 0.5%, 1%, 2%, 3% and 5%. No samples were taken of concentrations higher than 5% as this is outside of what the infrared analyser has been calibrated for and can reliably measure, according to its manual. Figure 2.6

shows the results of sampling for the two anaesthetic agents from the bottle, and Figure 2.7 shows the results for sampling from the experimental bath.

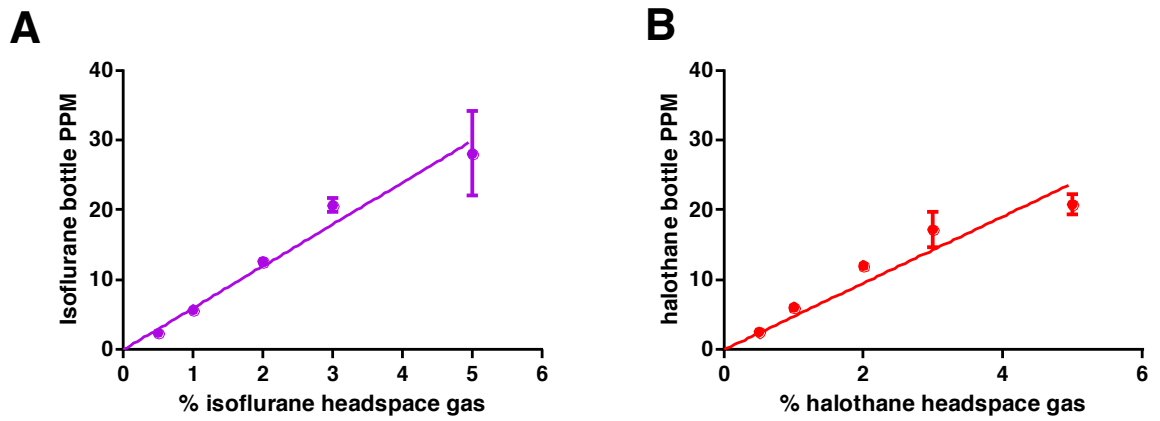

Figure 2.6: Sampling from bottles for anaesthetics. Panel A: isoflurane; panel B, halothane. Each panel is a plot of anaesthetic concentration measured by GC-MS (ppm) versus % anaesthetic in headspace gas. Each point is the mean of 5-8 samples ± SEM and line fitted by least squares linear regression. For isoflurane, the equation is: PPM = 6.0 x % headspace gas (r^2 = 0.98). For halothane, the equation is: PPM = 4.8 x % headspace gas (r^2= 0. 93)

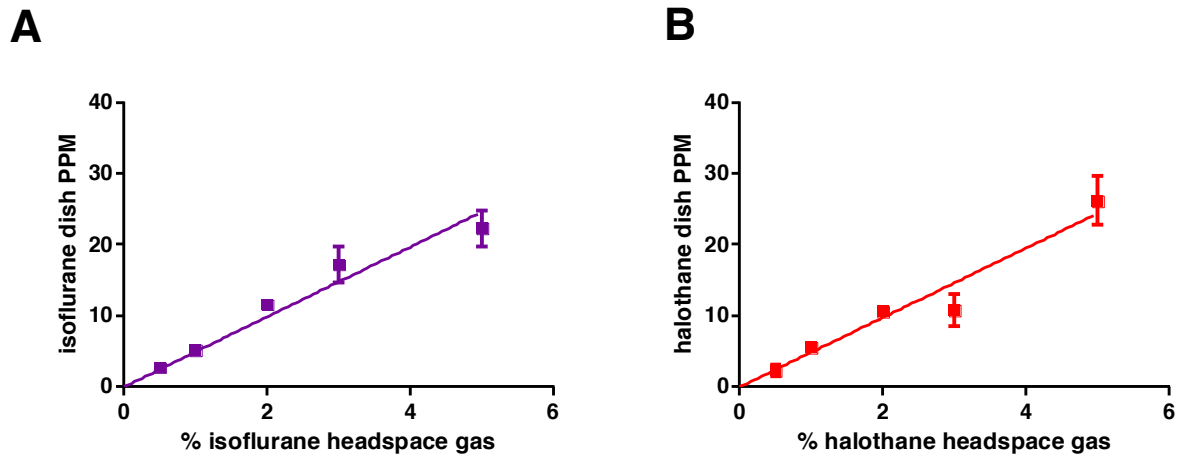

Figure 2.7: Sampling from experimental bath for anaesthetics. Panel A: isoflurane; panel B: halothane. Each panel is a plot of anaesthetic concentration measured by LGC (ppm) versus % anaesthetic in headspace gas. Each point is the mean of 5-8 samples ± SEM and line fitted by least squares linear regression. For isoflurane, the equation is: PPM = 4.9 x % headspace gas (r^2 = 0.96). For halothane, the equation is: PPM = 4.8 x % headspace gas (r^2= 0.96).

It is clear that for both agents there is a strong linear relationship between the vaporisation rate on the vaporiser and the concentration parts per million (PPM) obtained in solution across a wide range of concentrations (r^2 range 0.93-0.98). These relationships were found both in samples from the bottle and the experimental bath. Exact equations were calculated (see Figure legends), but approximately the relationship for anaesthetic concentration in the experimental bath at point of presentation to the tissue is ~5 ppm per % vapour, regardless of agent. The variation in results was highest at the higher concentrations, perhaps indicating the influence of sampling error at these higher doses.

2.5.6 No significant loss between bottle and bath

Figure 2.8 shows that there was no consistent loss of agent across a wide range of concentrations between bottle and perfusion bath for both agents (ANOVA $p = 0.127$).

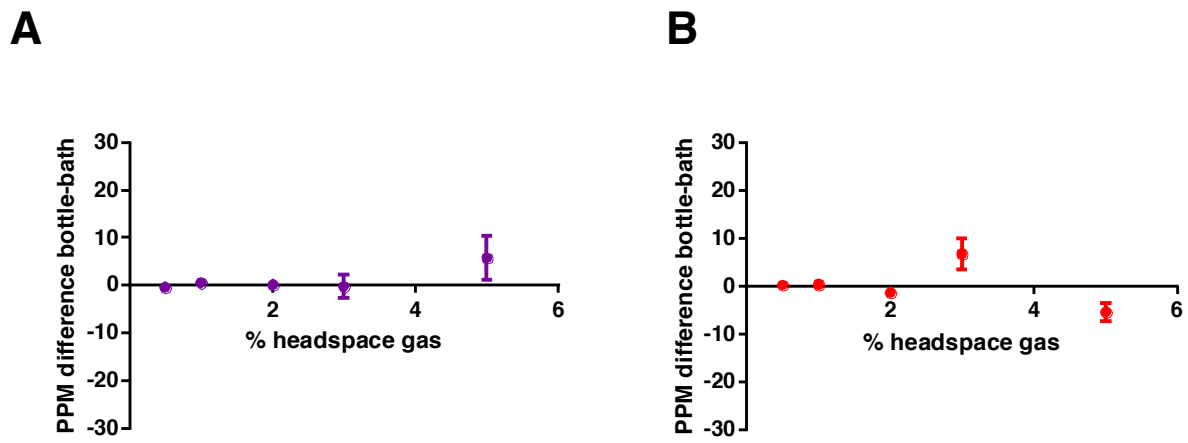

Figure 2.8: **Plot of the absolute difference in measured concentration of anaesthetic between bottle and experimental bath.** Panel A: isoflurane; panel B: halothane. Each panel is a plot of the difference in concentration (same scale as Figs 2 and 3) measured by GC-MS for bottle minus bath vs % anaesthetic in headspace gas. A positive value indicates the bottle measurement is higher than the bath (and thus potential loss of agent); a negative value indicates the bath measurement is higher than the bottle (and since anaesthetic cannot have been 'gained', is an index of inherent experimental sampling or measurement error). Each point is the mean of 5-8 samples ± SEM. There was no consistent loss of agent across a wide range of concentrations between bottle and perfusion bath for both agents (ANOVA ($p = 0.127$).

2.5.7 Concentration response curve for sevoflurane

As the halothane and isoflurane studies have shown that there is no consistent loss of agent, a few sevoflurane concentrations have been measured in the Tyrode bottle to also generate sevoflurane PPM measurements (studied in chapter 4). The data-points are an average of n=3, the equation for sevoflurane is 3.8 x % headspace gas with an R^2 of 0.98.

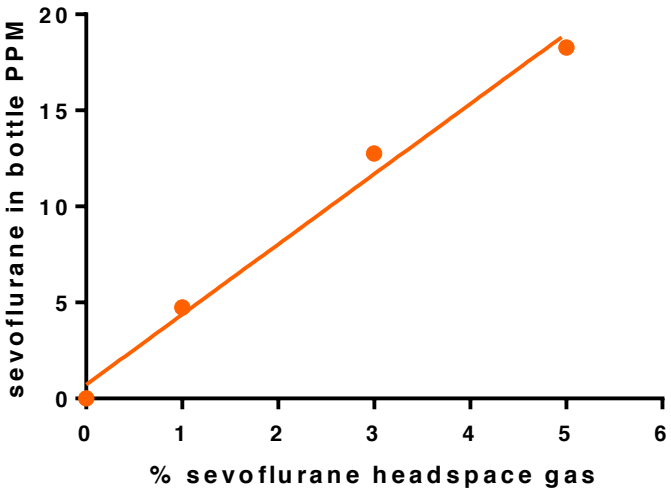

Figure 2.9: Sampling from bottles for Sevoflurane. The figure is a plot of anaesthetic concentration measured by GC-MS (PPM) versus % anaesthetic in headspace gas. Each point is the mean of 3 samples ± SEM and line fitted by least squares linear regression. The sevoflurane equation is: PPM = 3.8 x % headspace gas (r^2 = 0.98).

2.5.8 Mixes of halothane and isoflurane yield expected PPM concentrations in the bottle

A number of experiments in this thesis are performed with mixes of concentrations of halothane and isoflurane. This is more challenging than single agents, as the infrared analyser can not measure two agents simultaneously. For this set up vaporizers were put in series, so that the output of the isoflurane vaporizer was connected to the rotameter upstream of the halothane vaporizer and the isoflurane output therefore entered the halothane vaporizer. The ouput of the halothane vaporizer, containing both isoflurane and halothane, then went through the gas dispersion tube to bubble the Tyrode solution in the bottle. A schematic illustration of this is shown in Figure 2.10. This method was preferred to equilibrating the Tyrode solution with two different gas dispersion tubes, as the concern was that the high amount of bubbles generated from two dispersion tubes would prevent accurate mixing.

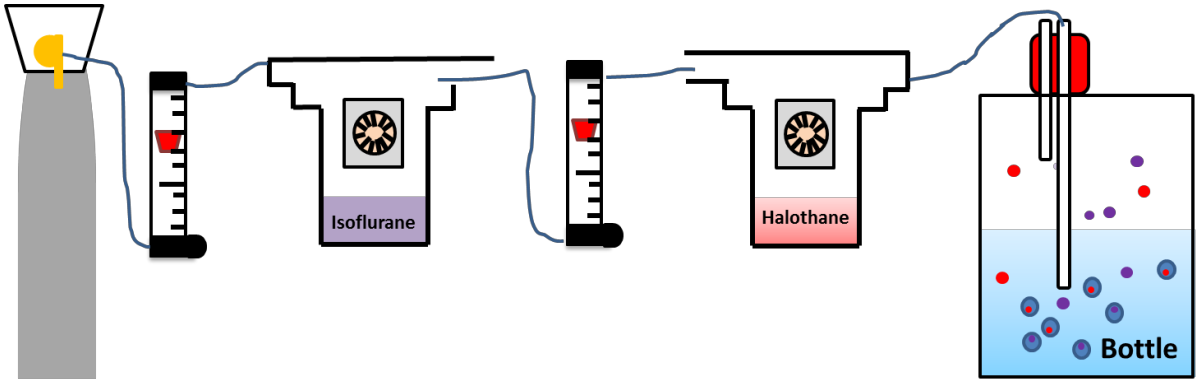

Figure 2.10: In series set up for mixes of isoflurane and halothane.

To ensure the highest possible accuracy without real time infra-red analysing, the headspace gas was measured before the start of each experiment. The vaporizers were connected in series and then individually calibrated, which meant that notes were taken as to how far the

dial needed to be opened to achieved the desired concentration in the head space. Once this was done, both vaporizers were opened.

To verify the presence of both anaesthetics in the solution, mixes of isoflurane and halothane were measured in the bottle to minimize sampling error. The PPM concentrations from the mixes were compared with the equation generated for PPM concentrations in the bottle for single agents. The equation in the bottle for halothane was PPM = 4.8 * % vaporized. For the isoflurane bottle, the formula was PPM = 6.0 * % vaporized. The concentrations represent an average of N=5 for all data-points. Table 2.11 shows combinations of mixtures that have been used for experiments in chapter 3 and reveals that there was no loss detected of agents compared to the concentrations predicted from the ppm equations.

A	**Halothane 2.5% (PPM)**	**Isoflurane 1.5% (PPM)**
Expected	**12.0**	**9**
Measured	**17.5** (0.6)	**9.9** (0.6)

B	**Halothane 2.5% (PPM)**	**Isoflurane 2.5% (PPM)**
Expected	**12.0**	**15**
Measured	**18.5** (0.2)	**16.3** (0.2)

C	**Halothane 2.5% (PPM)**	**Isoflurane 4% (PPM)**
Expected	**12.0**	**24**
Measured	**18.4** (0.3)	**26.2** (0.5)

D	**Halothane 2.5% (PPM)**	**Isoflurane 5% (PPM)**
Expected	**12.0**	**30**
Measured	**16.4** (0.9)	**29.7** (1.6)

Table 2.11: PPM for different concentrations of isoflurane mixed with 2.5% halothane. Relevant for mixes in chapter 3. Table A to D represent the mixes as indicated in table heading.

In all cases, the measured concentrations were slightly higher than predicted by the equations. This probably reflects a minor sampling error in one of the experiments. Some experiments in this thesis have been performed with 1.5% (instead of 2.5%) halothane with a variety of isoflurane mixes (not higher than 4% isoflurane). Because the higher concentrations were

bubbled successfully in the bottle, I assumed that lower concentrations should also be accurately mixed. The 4% halothane and 4% isoflurane mixture has also been measured for PPM concentrations and this also resulted in accurate bottle concentrations as can be seen in Table 2.12.

A	**Halothane 4% (PPM)**	**Isoflurane 4% (PPM)**
Expected	**19.2**	**24**
Measured	**22.5** (2.62)	**22.2** (2.83)

Table 2.12: PPM measurements for the mixture of 4% halothane and 4% isoflurane

2.5.9 Absence of Thymol in Tyrode solution

Thymol is added to commercial supplies of halothane at a concentration of 0.01% as a stabiliser and preservative. When the vaporizers are not drained as advised every week, thymol can accumulate (Rosenberg and Alila, 1984). It has been suggested that thymol may be an active ingredient since it was found to influence GABA receptor activity in mouse cortical neurons (Garcia et al., 2006) and decreases the L-type Ca^{2+} and K+ current in canine cardiomyocytes (Magyar et al., 2002). Therefore, while analysing the halothane Tyrode samples, they were also tested for the presence of Thymol, but none was detected (with an accuracy of <1parts per billion; ppb). Therefore, it is excluded that the results in this thesis are in any way influenced by the Thymol acting on the carotid body or HEK cells.

2.5.10 Comparison of our PPM values with other studies

In terms of the absolute value (in ppm or μM) of anaesthetic concentration in solution for a given percentage vaporizer concentration, a very wide range has been reported in the

literature. When converting the PPM measurements to μM for the experiments in section 2.5.5, a ~50 – 150 μM in solution for ~1-3% anaesthetic in the headspace gas was obtained. This is a slightly wider range than that reported by (McDougall et al., 2008) who reported ~100-180 μM for similar vapour concentrations and close to the ranges reported by (Miu and Puil, 1989). However, all these values are approximately half as much again as those reported by (Becker et al., 2012) and a factor of nine times less than found by (Roch et al., 2006) and by (Pancrazio, 1996). These large disparities that are reported in the literature may be related to the precise composition of solutions used in the respective studies and their solubility for anaesthetics, or sampling error, or vapour loss, or a combination of all of these. However, due to the linear relationship and consistency of PPM measurements over different days and the minimal loss of agency between bottle and bath it seems fair to conclude that measurements in this chapter represent the true solubility of the specific Tyrode solution composition.

It is also important to keep in mind that the biological action of volatile anaesthetics is regarded as driven by their partial pressure (so % measured in headspace) and not their dissolved content (Eger et al., 1986).

2.5.11 Summary of GC-MS testing of anaesthetic perfusion rig

The above experiments show that this anaesthetic perfusion system achieves reliable and stable concentration of anaesthetics in the experimental bath at point of presentation to the tissue, with minimal loss of vapour. This is confirmed for halothane, isoflurane and sevoflurane, which are the agents used in this thesis. The agents are linearly related to vaporiser dialled concentrations and with very little variation across a wide range of

concentrations. The GC-MS measurements confirmed that continuous monitoring of the concentrations of anaesthetic vapour from the headspace gas above the solution in the bottle, should be a generally sufficient method of monitoring the input vapour concentrations. In the experimental chapter in this thesis (chapter 3-6) I will however refer to % instead of PPM.

The perfusion system and experiments performed in this section were the basis of a publication in the Journal of Neuroscience Methods (Huskens et al., 2016) see appendix I.

2.6 Chemicals and drugs

The details of the chemicals used and their suppliers will be elaborated upon in the relevant chapters. This includes, where necessary, details about the solvents they were kept in and the exact way of application to the cells.

2.7 Measurements of intracellular Ca^{2+} using Indo-1-AM

2.7.1 Dye loading for glomus cell experiments

The rat glomus cells were loaded with Indo-1-AM (Molecular Probes, Leiden, The Netherlands) (dissolved in dimethyl sulfoxide) in 2mL F12+ medium at room temperature and incubated for exactly 1 hour in a final concentration of 1.5µM Indo-1-AM . Following the initial incubation, the cells were transferred to Indo-1-AM free medium to prevent the cell from overloading. By using the acetoxymethyl (AM) ester derivative of Indo, the cellular

esterases cleaved the attached methyl group once the Indo was taken up by the cell. As a result of this, the Indo became negatively charged and was then trapped in the cell.

2.7.2 Instrument settings

The fluorescence-excitation light source for Indo-1 was provided by a 100-W xenon lamp (Nikon, Tokyo, Japan) and filtered at 340 ± 5 nm. Indo-1 fluorescence was collected through an inverted microscope (Nikon Diaphot 200, Tokyo, Japan) and split by a dichroic mirror of 450nm, then fluorescence was detected at 405 and 495nm by a pair of tri-alkali photomultiplier tubes (PMT) cooled to between -20^{o}C and –28^{o}C. The output from each PMT was fed through a current-to-voltage converter and then digitized (250 Hz; CED 1401). Signals were averaged over 0.5 second intervals to give a final sampling rate of 2Hz.

2.7.3 Calibration of INDO-1-AM in type-1 cells

The concept of ratiometric measurements means that any change in fluorescence leads to a fluorescent intensity increase at one wavelength, and a decrease at the other wavelength. This increases the accuracy of the measurements. INDO-1-AM (ratiometric dye) measurements were calibrated with a two point calibration, which allowed for the fluorescence output (R) to be converted to a [Ca^{2+}]i. This was calculated with the following equation:

$$[Ca^{2+}] = \text{Kd}\ x\ \frac{\text{F495 free}}{F495\ \text{bound}}\ x\ \frac{\text{R-Rmin}}{R\text{max-R}}$$

R = observed fluorescence ratio 405 nm/ 495 nm in experiment

$\mathbf{R_{min}}$ = fluorescence ratio of the [Ca_{2+}] free form of indo-1

$\mathbf{R_{max}}$= fluorescence ratio of the saturated [Ca_{2+}] bound form of indo-1

F495 free = the fluorescence intensity in [Ca_{2+}] free solution in 495 wavelength

F495 bound = the fluorescence intensity in [Ca_{2+}] max solution at 495 wavelength

F495,free/bound ratio = ratio fluorescence of free form at 495nm/bound form at 495 nm

Kd = dissociation constant for indo-1, 230nM (Jackson et al., 1987)

The calibration constants marked with an * were obtained from the ionomycin calibration protocol using ionomycin on carotid body cells. The typical results can be seen in Table 2.13.

R min*	R max*	F495 Free*	F495 bound*	F495/495free-bound ratio
0.28	1.95	0.18	0.07	2.6

Table 2.13: Results of the ionomycin calibration.

The calibration solutions consisted of (in mM: 150 KCl 5 NaCl 1$MgCl_2$ 10 HEPES pH 7.4 at 37°C). The carotid body cells were incubated in the standard F12+ DMEM medium, stained with PNA and loaded with Indo-1-AM. After one hour of incubation, the dishes were put in the Ca2+-free 10μM ionomycin calibration solution for 20 minutes. Following the incubation, cells were put in the experimental bath in a Ca2+ and ionomycin-free solution and a peanut agglutin positive cell was quickly identified. Once identified, the background emission was corrected and the solution was switched to 10μM ionomycin containing Ca2+-free solution for 90 seconds allowing for the Rmin and F495 free values to be determined. Next the solution was switched to one containing 10mM Ca2+ wherein the values for Rmax and F495 bound were determined. Measurements were performed after background correction.

2.7.4 Analysis of $[Ca^{2+}]i$ recordings

Figure 2.12 shows a schematic representative recording. Each recording starts with an application of hypoxia and after that the normoxic solution is switched back on. Next the agent of interest is applied (A) in normoxic conditions, which allows for measurement of changes in baseline if any occurs (not in this example). Next, the same hypoxic stimulus is applied, which allows for measurement of agents (A) combined with hypoxia. In the recording the hypoxia stimulus without agent (A) represents the max response and is set to 100%. The magnitude of the hypoxic stimulus is then compared to the magnitude of the hypoxic stimulus in combination with agent (A) which is for example a 25% increase (orange arrow). The green arrow represents the depression, which is then 75%.

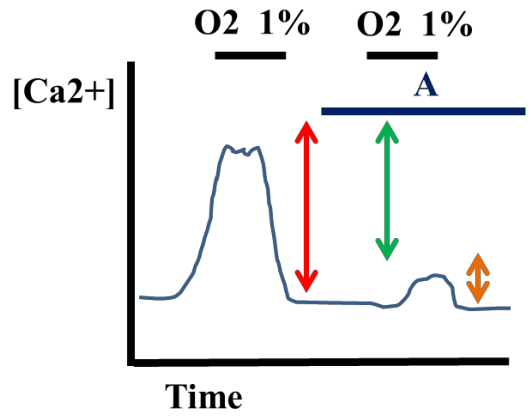

Figure 2.11: Schematic representation of a Ca2+ recording. The red arrow indicates the max increase in $[Ca^{2+}]$ in response to 1% oxygen. The orange arrow indicates the increase in $[Ca^{2+}]$ in response to 1% oxygen in combination with agent A. The green arrow indicates the magnitude of the % depression when agent A is compared to the hypoxia control response.

The agent effect is calculated as:

$$\text{Agent effect} = \frac{[Ca^{2+}]i \text{ hypoxia 1\% with agent} - [Ca^{2+}]i \text{ baseline}}{[Ca^{2+}]i \text{ hypoxia 1\%} - [Ca^{2+}]i \text{ baseline}} \cdot x\ 100$$

And consequently the agent depression is:
% depression = 100 - agent effect

In this thesis, most of the graphs will show the calibrated Ca^{2+} concentrations on the y-axis. However, a few graphs will show the unconverted raw output from the IV converter and thus the output will be displayed on the Y-axis in volts.

2.8 Measurements of mitochondrial NADH auto-fluorescence

2.8.1 Instrument settings

Single wavelength fluorescence measurements of Nicotinamide adenine dinucleotide (NADH) were performed using a microspectrofluorimeter based on a Nikon Diaphot 200 (Tokyo, Japan) equipped with a xenon lamp to provide excitation. NADH was excited at 340 nm and fluorescence was measured at 450±15 nm. A photomultiplier tube (Thorn EMI, London, UK) was cooled (−20◦C) and used to detect emitted fluorescence; this ran through an IV converter which resulted to an output in Volts. Data was collected using a CED Analog to Digital converter (1401) and Spike 2 software (Cambridge Electronic Design, Cambridge, UK). Signals were averaged over 0.5 second intervals to give a final sampling rate of 2Hz.

2.8.2 Analysis of [NADH] recordings

Figure 2.13 shows a schematic representation of an NADH recording. Before the start of each recording the cell is moved out of the field and the background is adjusted to 0 volts. The cell is moved back into the field, which results in the measurement of baseline fluorescence as indicated by the grey dotted line. Upon application of the specific complex 1 inhibitor rotenone (1μM; Sigma, Dorset, UK),] or upon application of anoxia, the mitochondrial NAD+/NADH redox couple is assumed to be maximally reduced (i.e. all in the form of NADH). Upon application of carbonyl cyanide 4-(trifluoromethoxy) phenylhydrazone (FCCP), on the other hand, the redox couple is assumed to be maximally oxidised, i.e. in the form of NAD+, which is non-fluorescent. Therefore, the total mitochondrial NADH concentration range can be defined by the application of rotenone/anoxia and FCCP, which is indicated by the green arrow. Any remaining fluorescence signal under these conditions comes from other sources including non-mitochondrial NAD+/NADH. For each individual recoding, the anoxia stimulus was used to determine the maximal increase in signal and set at 100% related to the baseline (represented by the red arrow). For every agent tested, the difference between the baseline and the agent effect was measured and expressed in percentages compared to anoxia. So in Figure 2.12 agent A evokes an increase of 25% whereas agent B evokes an increase of 50%.

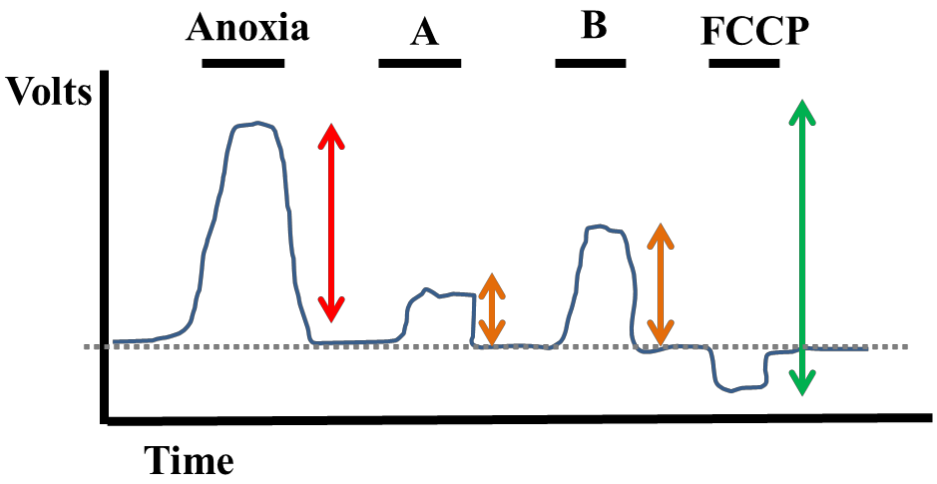

Figure 2.12: schematic representation of an NADH recording. The grey dotted line represents the steady state auto-fluorescence of the cell in 21% oxygen. The green arrow represents the total NADH range. The red arrow represents the max increase of NADH compared with baseline, The orange arrows represent the increase from baseline to max for agent A and B. The increase is then expressed as a % of the maximal possible increase.

The formula for the agent effect on NADH auto-fluorescence is:

$$\% \text{ increase} = \frac{V_{agent} - V_{baseline}}{V_{anoxia} - V_{baseline}} \times 100$$

And consequently the agent depression is:

% depression = 100 - agent effect

2.9 Measurements of mitochondrial membrane potential using rhodamine-123

2.9.1 Dye Loading for type-1 cell experiments

Rhodamine-123 (Rh123) (Sigma, Dorset, UK) was dissolved at a concentration of 6mg/mL in ethanol. For each culture dish containing 2 mL of culture medium, 5μL of stock solution was added. Carotid body cells were incubated in the rhodamine-123 dish, one coverslip at a time for 15 minutes. Following this the coverslip was immediately placed in the experimental bath to start a recording swiftly.

2.9.2 Instrument settings

Fluorescence measurements were performed using a microspectrofluorimeter based on a Nikon Diaphot 200 (Tokyo, Japan) equipped with a xenon lamp to provide excitation. A photomultiplier tube (Thorn EMI, London, UK) was cooled (−20°C) and used to detect emitted fluorescence; this ran through an IV converter, which resulted in an output in Volts. Rhodamine-123 was excited at 485 nm and fluorescence was measured at 535±15 nm, which meant it was a single wavelength measurement. Data was collected using a CED Analog to Digital converter (1401) and Spike 2 software (Cambridge Electronic Design, Cambridge, UK). Signals were averaged over 0.5 second intervals to give a final sampling rate of 2Hz.

2.9.3 Analysis of Rhodamine-123 recordings

Rh123 is a membrane permeant cation that distributes across the mitochondrial membrane according to the mitochondrial membrane potential. Accumulation of rhodamine in the mitochondria (negative membrane potential) leads to partial quenching of the dyes' fluorescence. Mitochondrial depolarisation causes the dye to diffuse back into the cytosol, causing an increase in fluorescence (Emaus et al., 1986).

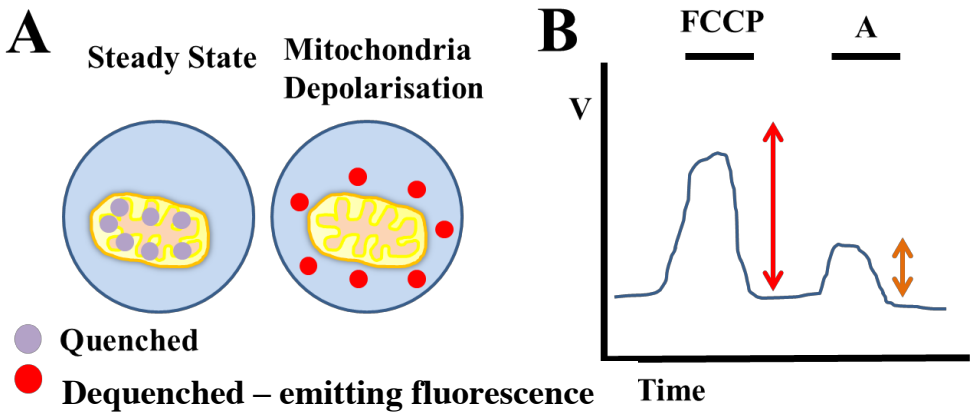

Figure 2.13: Principles of Rhodamine-123 fluorescence recordings. (A) Showing rhodamine dyes in the quenched mode inside the mitochondria and following mitochondrial depolarisation in the dequenced mode. **(B)** showing the maximal depolarisation as evoked by FCCP and revealing the depolarisation caused by agent (A).

The formula for the agent effect on Rh123 auto-fluorescence is:

$$\% \text{ increase} = \frac{V \text{ agent} - V \text{ baseline}}{V \text{ anoxia} - V \text{ baseline}} \times 100$$

And consequently the agent depression is:

% depression = 100 - agent effect

The uncoupling evoked by FCCP application leads to a complete depolarisation and thus a maximal increase in Rh123 fluorescence. This response was set at 100% (indicated by the red

arrow). The increase of fluorescence evoked by the application of agent A (orange arrow) is expressed as a percentage from the max increase in fluorescence evoked by FCCP.

On all Rh123 recordings a correction was applied for the inevitable run down of signal. This was done by entering the peak response evoked by the FCCP application at the beginning and the end of each recording and, similarly, the baseline at the beginning and end of each recording. The script was then used to interpolate values between baseline (0%) or 100% (FCCP) at all points in between. This allowed the recording to be converted to a % scale.

2.10 Cell attached single channel recordings

2.10.1 Pipette and pipette filling solution

The borosilicate glass pipettes (Harvard Apparatus Ltd, Kent, UK) used for patch clamping were pulled on a two-stage vertical puller (Narishige, Tokyo, Japan). The pipettes were coated in a thin layer of Sylgard 184 (Dow Corming, Wiesbaden, Germany) to decrease the pipette capacitance. Immediately prior to use, the pipettes were briefly fire-polished and filled with a high K^+ solution containing (mM: 140 KCl, 1 MgCl2, 1 EGTA, 10 HEPES, 10 TEA, 5 4-AP pH 7.4 at 37ºC). The addition of 4-AP and TEA resulted in the blockade of other K^+ channels.

2.10.2 Instrument settings and data acquisition

Cell-attached patch clamp recordings were performed using an Axopatch 200B (Molecular Devices LLC, Sunnyvale, US). Single-channel recordings were filtered at 2–5 kHz and current was recorded and digitalized at 20 kHz. Voltage clamp control, data acquisition and analysis were performed using Spike2 (Cambridge Electronic Design, Cambridge, UK).

2.10.3 Voltage clamp protocol

Carotid body cells were placed in the recording chamber in standard Tyrode at 37ºC in which seal formation was attempted with a borosilicate pipette. In the solution the pipette had a resistance between 10-18 MΩ. When a Giga-ohm seal was formed (>5 GΩ), the Tyrode solution was switched to 100mM K^+ and a positive pipette potential was applied of +80mV. The + 80mV pipette potential, with 100mM K+ outside and 140mM K+ in pipette, resulted in TASK channels to be shown as inward currents. The rationale for preferring to record inward currents instead of outward currents was because channel openings are much more clearly defined as an inward current, which consequently leads to more accurate measurements of channel activity. The very negative membrane potential (estimated to be -89 mV) was also chosen because of the low likelihood of other channels to be active.

2.10.4 Data analysis of nPopen

Single-channel activity was defined by nPopen in which n represents the number of channels in the patch and Popen the open probability of the channel. The main conductance state for channel activity was established manually using an all-points histogram. Most all-points histograms contained 1 main (but poorly and broadly defined) peak. This all points histogram was then used to set a 75% open threshold for nPopen definition analysis, so to best capture the TASK-1/3 heterodimer peak. Current levels that exceeded 175% of the main conductance state were classed as double openings and 275% as triple openings. In other words, the script used to determine nPopen measures each point and assigns it either a 0 (baseline), 1 (single opening), 2 (double opening) or 3 (triple opening). This is then added together and divided by the number of measurements taken. The average value of this is then the nPopen.

In Figure 2.15, an example all points histogram can be seen with a main conductance state of 2.2pA. The 75% threshold crossing is then set at 1.5. In figure 2.16 channel activity of a different patch can be seen. In this example the main conductance state was 2.8pA. The 75% threshold (threshold 1) is thus set at 2.1.

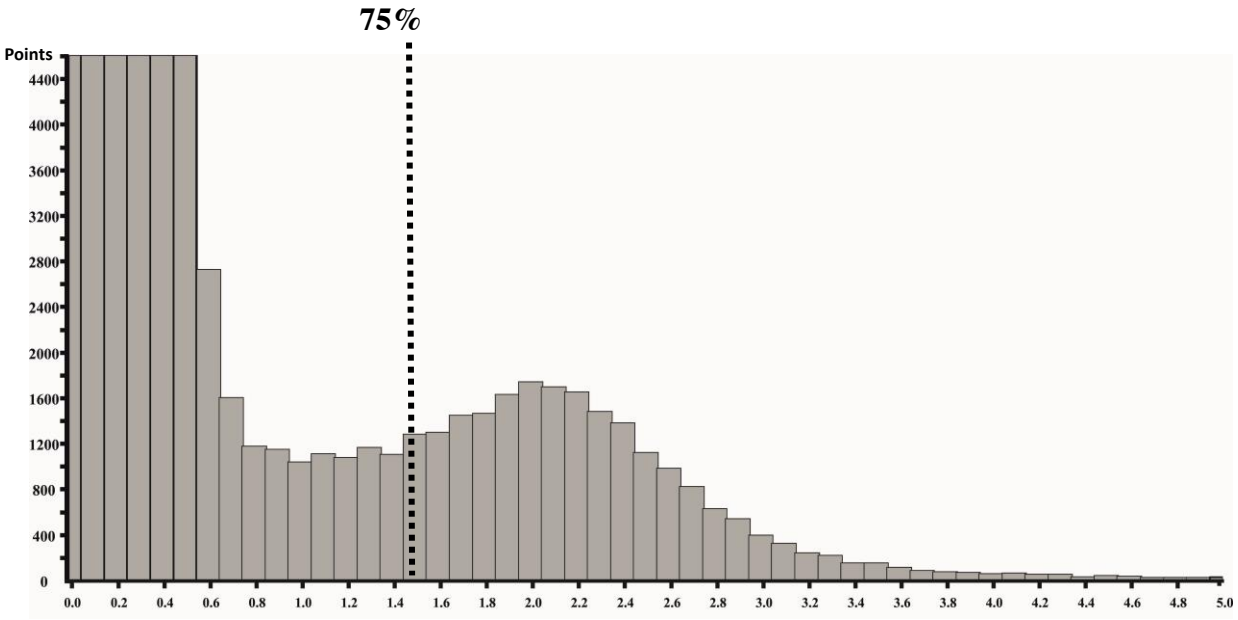

Figure 2.14: All points histogram of carotid body TASK channel activity. 75% threshold indicated in graph to best capture the presumed heterodimer peak.

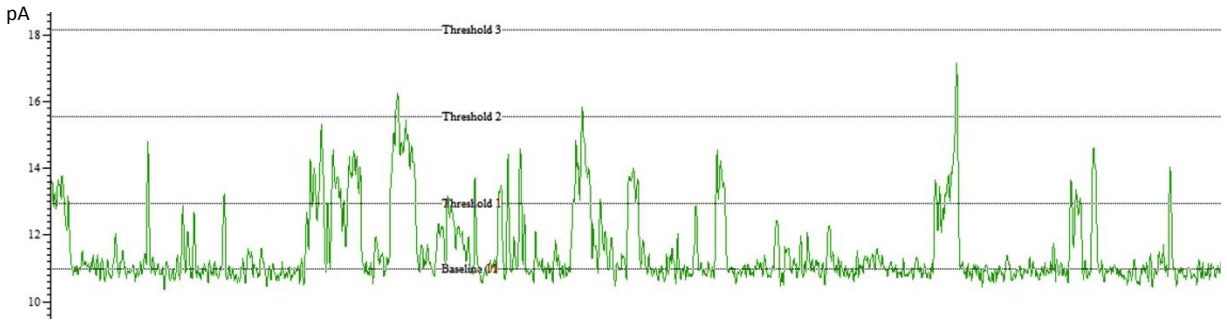

Figure 2.15: Example of nPopen analysis of type-1 TASK channel activity. Screen capture of nPopen analysis. The modal amplitude is 2.8pA (determined with all-points histogram). The first threshold is set at 75% so to best capture the channel openings with an amplitude greater than ~2.1pA. Openings greater than 4.9pA (175%) were counted as double openings (note the baseline in this patch is 11pA).

Cell attached recording of HEK-293 cells

For the recording of TASK channel in HEK cells it was decided to use the exact same recording conditions as described above with the same Tyrode solution, pipette filling solution and pipette potential. The rationale behind doing this is that because the membrane rest potential would be more negative due to the expression of a high amount of K+ channels, bringing the potential closer to the K^+ EK. Also by choosing the same recording conditions the channel amplitudes should be similar to those observed in type-1 cell patches.

2.11 Statistics

Average values are expressed as means (standard error of the mean). Although more detailed information about statistics can be found in the relevant chapters, in general, on each dataset, a normality test was run to confirm whether or not the data was normally distributed. Where possible, when two different agents or concentrations were applied within the same recording, a paired t-test was performed. For most other comparisons an analysis of variance test (ANOVA) was performed to compare different agents and concentrations. Further significant effects where then explored with a Bonferroni Post-Hoc test. Statistics were done with SPSS for Windows version 20, (SPSS Inc, Chicago, IL, USA) (Lazarenko et al., 2010). Specific statistics will be discussed in more detail in each chapter.

Chapter 3. Actions and interactions of halothane and isoflurane on the rat carotid body type I cell hypoxic response and TASK-1 channels

3.1 Introduction

Volatile anaesthetic agents are known to interfere with the body's physiological response to hypoxia and can prevent an adequate increase in ventilation in response to hypoxia (Gelb and Knill, 1978, Knill et al., 1983, Lockwood, 2010). Even at sub-anaesthetic doses (1/20th – 1/10th of that required for anaesthesia) volatile anaesthetics depress the ventilatory response (Pandit, 2002). The depression of the ventilatory response by volatile anaesthetics in humans and rats exhibits a specific order of potency which is halothane > isoflurane > sevoflurane (Pandit, 2002, Karanovic et al., 2010).

As discussed in chapter 1, the key processes occurring in the glomus cell during an acute response to hypoxia are decreased channel activity of carotid body TASK channels, a membrane depolarization and consequently Ca^{2+} entry evoking the release of neurotransmitters. In glomus cells in rats and mice it is currently accepted that TASK-1, TASK-3 and TASK-1/3 heterodimer are expressed and have a predominant role in the oxygen sensing cascade. In particular the heterodimer TASK-1/3 is thought to be most abundant compared to TASK-1 and TASK-3 homomers (Yamamoto et al., 2008, Kim et al., 2009a, Turner and Buckler, 2013a). Our group, and others, have established that TASK channels can be modulated by volatile anaesthetics (Buckler et al., 2000, Berg et al., 2004, Putzke et al., 2007, Pandit et al., 2010). In general, volatile anaesthetics activate these channels and increase their open probability and this therefore partially impedes the hypoxia evoked decrease in open probability of TASK channels, and Ca2+ influx in response to low oxygen.

To further research the carotid body mediated depression of ventilation in response to anaesthesia, this chapter sought to clarify a number of questions. The first part of this chapter aims to clarify in detail the effect of halothane and isoflurane on the carotid body (the Ca^{2+} entry and native TASK channel activity). Preliminary studies in the carotid body in this lab have highlighted that halothane appears to have a more potent effect on depressing the hypoxia evoked Ca^{2+} entry in the carotid body compared to isoflurane, which appeared to be a less potent depressor (Pandit et al., 2010). To further confirm this observation, a variety of concentrations of isoflurane and halothane were applied to the rat glomus cell in combination with hypoxia to assess the hypoxia evoked Ca^{2+} entry. Secondly, the effect of isoflurane and halothane was assessed on the TASK channel activity in the carotid body. Glomus cells were challenged with a variety of concentrations of halothane and isoflurane to look for saturation kinetics of the activity and assess the difference in potency between agents. Lastly, as many studies have shown that TASK channels cells are strongly regulated by mediators in the carotid body, the effect of halothane and isoflurane was also examined in HEK cells transiently transfected with cDNA encoding ratTASK-1.

The first part of this chapter focusses on investigating the action of halothane and isoflurane independently, the second part focusses on studying the effects of mixtures of both halothane and isoflurane. Mixes were studied at three 'levels' (Ca^{2+} signalling, native single channel activity and expressed TASK-1 activity). Franks and Lieb (1982) hypothesized that anaesthetics may compete with endogenous ligands for channel occupation. Eger et al published a number of papers (both experimental and theoretical) in 2008 studying the interaction between anaesthetics and concluded that anaesthetics act additively, which is the current accepted theory in the field (Eger et al., 2008, Hendrickx et al., 2008).

Being aware of the important role of anaesthetics acting on TASK channels and so interfering with the AHVR, and upon the preliminary observation that halothane is a stronger agonist than isoflurane (and thus may have different saturation kinetics), both agents were mixed together in an attempt to determine whether these agents act independently and are additive (in accordance with some previous literature), or act at a common binding site and are thus competitive (in accordance to classical receptor pharmacology). According to classical receptor pharmacology, a weak agonist can act as a competitive antagonist: meaning that in the presence of a strong agonist, a weak agonist can occupy the binding sites and so prevent occupancy by stronger agonists and reduce the level of channel activation (Evers et al., 2011).

Combinations of halothane and isoflurane were applied to glomus cells and the hypoxia evoked Ca^{2+} entry was measured. The specific question addressed was whether a combination of both agents, (for example 2.5% halothane mixed with 2.5% isoflurane) act additively (so more depression on Ca^{2+} entry than 2.5% halothane alone) or 'infra'-additive (less than one of the individual agents). Mixes of isoflurane and halothane were also performed on native channel activity and ultimately, also on HEK cells expressing TASK-1.

In this chapter the results will be structured by each system, starting with Ca^{2+} entry, followed by native TASK channel activity and completed with TASK-1 activity in HEK cells. Within each system the first section will focus on a detailed concentration response and finish with the mix results for that system.

3.2 Methods

3.2.1 Glomus cell isolation

The method of carotid body removal has been described in chapter 2 section 2.3. Briefly, carotid bifurcations were surgically removed from isoflurane anesthetized rat pups P10-P15. Carotid bodies were sub-dissected and digested both enzymatically and mechanically, leading to a single cell suspension that was plated onto poly-L-lysine coated glass coverslips. Cells were stained with rhodamine-PNA, which resulted in a bright orange stain for type-1 cells. Cells were recorded on the same day as the surgery took place.

3.2.2 Transient expression of TASK-1 in HEK-293

Cells from the human embryonic kidney cell line HEK 293 were transiently transfected with ratTASK-1 inserted in pIRES-EGFP using lipofectamine (Life technologies, Paisley, UK) and PLUS reagent (Life Technologies, Paisley, UK). 24-48 hours following transfection, cells were re-plated onto poly L-lysine-coated glass coverslips and used for recordings. Transfected cells expressing TASK-1 were identified by their green fluorescence.

3.2.3 Measurements of $[Ca^{2+}]i$ using Indo-1-AM

Rat glomus cells were loaded with Indo-1-AM (2.5 μM in dimethyl sulfoxide) at room temperature and incubated for exactly 1 hour. Indo-1 was excited at 340 ± 5 nm and detected at 405 and 495nm by a pair of tri-alkali photomultiplier tubes (PMT) cooled to -20 ^{o}C. The output from each PMT was fed through a current-to-voltage converter and digitized (250 Hz; CED 1401).

Anaesthetics were vaporized using calibrated vaporizers at a range of concentrations in Tyrode solution (mM: 117 NaCl, 4.5 KCl, 1 $MgCl_2$, 23 $NaHCO_3$, 11 glucose, 2.5 $CaCl_2$) to measure the effect of anaesthetic on the hypoxia-evoked rise in $[Ca^{2+}]i$. At the start of each recording, type-1 cells were identified and exposed to a hypoxic stimulus (1% O_2 in 5% CO_2 and N_2) to confirm the cell was hypoxia sensitive. Next, the cell was exposed to halothane and/or isoflurane for ~ 1 minute in normoxia (21% O_2 5% CO_2), followed by a second exposure to hypoxia (1% O_2 and equilibrated with the same halothane and/or isoflurane concentration as used in the normoxia 'pre-exposure'), which was followed by a recovery period in normoxia (no anaesthetic) of ~1 minute. Within each recording, up to three different anaesthetic stimuli were applied, which could be either a mix or a single agent. At the very end of the recording, a control ~30 sec exposure to hypoxia was performed without anaesthetic to ensure appropriate recovery of the original hypoxic response. Only cells that demonstrated this recovery were included in the analysis.

For each control hypoxic exposure the magnitude of the Ca^{2+} -transient was calculated as the absolute difference between the mean $[Ca^{2+}]i$ in the period before hypoxic exposure and the mean $[Ca^{2+}]i$ during the hypoxia. This was also done for the anaesthetic hypoxia exposure in which the absolute difference between baseline and hypoxia was calculated. The anaesthetic hypoxia exposure was then compared with the magnitude change of hypoxia control, which was set at 100%.

The statistical significance of the differences between the means of the response was assessed using factorial analysis of variance (ANOVA, SPSS for Windows version 10.0, SPSS Inc, Chicago, IL, USA). The increase of the Ca^{2+} -transient was the 'response' and there were two repeated measures factors: 'anaesthetic' (three levels, one for each anaesthetic) and 'concentration' (a level for each concentration). The locations of any significant effects were explored using post hoc Student t-tests, with the Bonferroni correction applied at the appropriate level if necessary. A p-value <0.05 was taken as statistically significant.

3.2.4 Cell attached patch clamping of CAROTID BODY and HEK cells expressing TASK-1

Detailed information can be found in section 2.11 but in short, cell-attached patch clamp recordings were performed using an Axopatch 200B (Molecular Devices LLC, Sunnyvale, US). Recordings were made with borosilicate pipettes (Harvard Apparatus Ltd, Kent, UK) which were sylgard-coated and fire-polished before use. The pipette filling solution contained (140mM K^+ and 10mM TEA and 5mM 4-AP to block other K^+ channels). Single-channel recordings were filtered at 2–5 kHz and current was recorded and digitalized at 20 kHz. Voltage clamp control, data acquisition and analysis were performed using Spike2 (Cambridge Electronic Design, Cambridge, UK). Cells were placed in the recording chamber in standard Tyrode in which seal formation was attempted with a borosilicate pipette. When a giga-ohm seal was formed (> 5GΩ), the Tyrode solution was switched to one containing 100 mM K^+ and a positive pipette potential was applied of +80mV.

The protocol for anaesthetic application was, (1) control (2) anaesthetic (3) control (all in normoxic solutions and in 100mM high K^+ Tyrode for ~30-90 sec). A maximum of up to

three different concentrations of the anaesthetic were applied within each recording in random order.

Analysis of channel activity was performed on 20s sections of recording obtained at least 10s after any solution exchange (to allow full equilibration of oxygen and anaesthetic levels within the recording chamber). From each recording, an all points histogram was constructed using a 20s section of data to determine the modal value for the main conductance state. This value was then used to set thresholds to analyse channel activity as nPopen over a 20s time period using a 75% threshold crossing method to ensure capture of the heterodimer peak. For TASK-1 recordings a 75% threshold was also used, because the average peak amplitude was smaller (~1.4pA) and this was done to exclude baseline noise as much as possible (often up to ~1pA). For each cell/patch, measurements of nPopen were then normalised to nPopen during the control period. So that if a stimulus resulted in unchanged channel activity, the increase in channel activity compared to control would be 0%.

Statistical analysis was conducted on the mean normalised nPopen values (obtained from a number of patches/cells) using factorial analysis of variance (SPSS for Windows version 10.0, SPSS Inc, Chicago, IL, USA), where normalised nPopen was the 'response' and there were two repeated measures factors: 'anaesthetic' (one level for each anaesthetic and one for no anaesthetic), and the locations of any significant effects were explored using post hoc nonparametric test (Friedman one-way ANOVA by ranks) and $p<0.05$ (two tailed) was considered significant.

Because the mixes were applied in the same recording as the halothane and isoflurane, a paired non parametric test was also performed for each mix concentration alongside the ANOVA's.

Where concentration-response relationships were plotted, lines of best fit were constructed using non-linear least squares regression (GraphPad PRISM version 6.00) fit to a simple ligand binding equation:

$$y = \frac{BMax \; x \; [X]}{Kd + [X]}$$

3.2.5 Anaesthetic delivery

For all experiments involving anaesthetics (including patch clamping and Ca^{2+}), the gas phase above the bubbled solutions was constantly monitored by an infrared analyzer to assure accuracy and equilibration of concentrations. The concentrations of anaesthetic in solution at presentation to the tissue, and an appropriately linear relationship to the dialed vapour concentrations, were confirmed by gas chromatography-mass spectrometry in the Department of Chemistry, University of Oxford (as specified in section 2.6).

3.3 Results

3.3.1 Concentration response curve of halothane and isoflurane on $[Ca^{2+}]i$

The effect of volatile anaesthetics on the hypoxia (1% O_2) evoked Ca^{2+} entry was measured in PNA selected rat carotid body type-1 cells. Baseline levels of Ca^{2+} were measured in standard Tyrode equilibrated with 21% oxygen. The hypoxia control exposure without anaesthetics induced a rapid and reversible rise in $[Ca^{2+}]i$. Exposure to different concentrations of halothane and isoflurane in standard Tyrode (21% oxygen) did not lead to a detectable change of baseline Ca^{2+} levels, which was confirmed with an ANOVA for agent and concentration, values being 0.517 and 0.796 respectively (data not shown).

Figure 3.1 shows the effects of hypoxia alone and in the presence of halothane (A) and isoflurane (B). Both anaesthetics reduced the response to hypoxia in a concentration dependent manner. It was apparent from the studies that halothane was able to almost abolish the response to hypoxia at 3% whereas a robust response to hypoxia remained in the presence of isoflurane even at 5%.

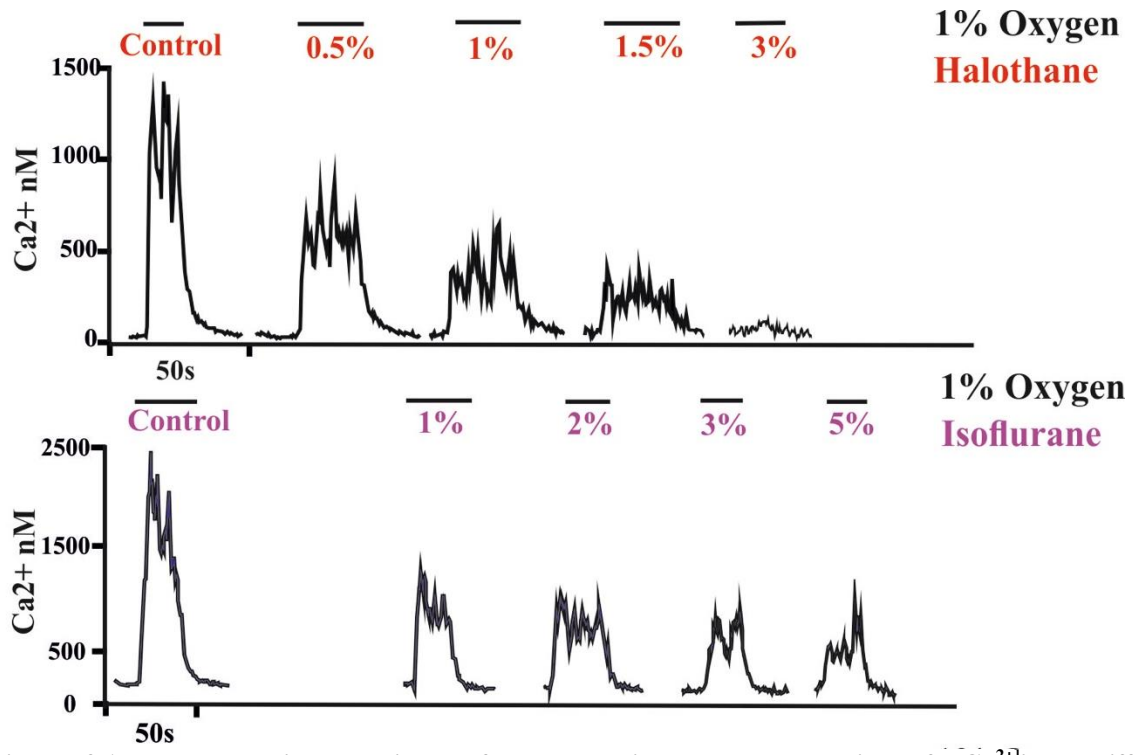

Figure 3.1: Representative transients of the hypoxia evoked depression of $[Ca^{2+}]i$ by different concentrations of halothane and isoflurane. Hypoxia stimulus consisted of 1% oxygen 5% CO_2 and the average exposure to hypoxia was 30s. Top panel: Halothane representative traces, at high enough concentrations, halothane completely abolishes the Ca^{2+} influx. Bottom panel: isoflurane representative traces, isoflurane does not completely abolish the Ca^{2+} influx even at supra clinical concentrations

In order to explore these effects further, the 'response' to anaesthetic was quantified as the % depression/inhibition of the $[Ca^{2+}]i$ signal generated in hypoxia. This 'response' was then plotted as a function of anaesthetic concentration (expressed as % anaesthetic in headspace gas). Figure 3.2 reveals the concentration-depression curve for both isoflurane and halothane. For the halothane curve n = 4-13 for each point on the curve 36 data points in total. For isoflurane the n= 3-9 for each point on the curve, 39 recordings in total. Curve fitting yielded values for Kd of 0.49% for halothane and 1.1% for isoflurane. BMax value was 100% for halothane but only 64% for isoflurane. Thus the effects of halothane on the hypoxic response were concentration-dependent but with clear evidence of saturation. These agents thus show

classical drug-receptor kinetics with halothane acting as a 'full' agonist and isoflurane as a 'partial' agonist.

The difference between halothane and isoflurane was significant (ANOVA p=0.021) and also when taking the concentration into account (ANOVA p = 0.002) confirming that the agent difference was also concentration dependent.

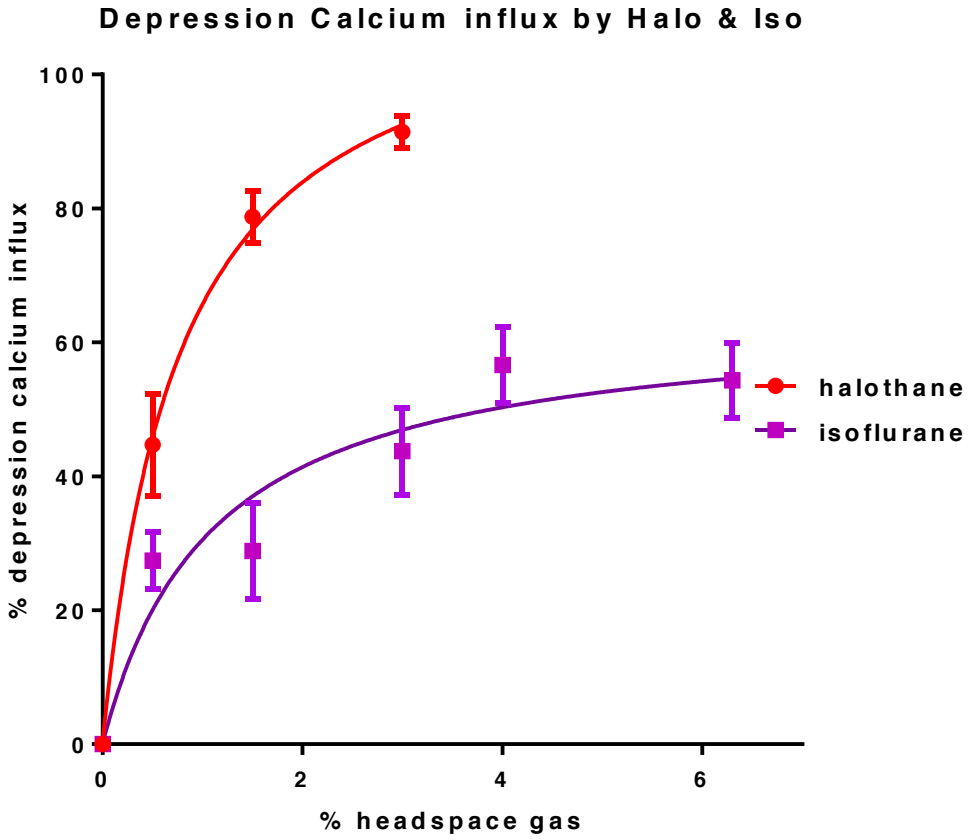

Figure 3.2: Depression of halothane and isoflurane on the hypoxia evoked Ca^{2+} entry. Values are normalized against the hypoxia control exposure in each recording and displayed as mean +/- SEM. The difference between halothane and isoflurane was significant, also when taking the dose into account (ANOVA p= 0.02). Curve fitting formula were: depression halothane = (100*[X])/(0.49 + [X]) depression isoflurane = (64*[X])/(1.1 + [X]).

3.3.2 The effect of halothane and isoflurane on voltage gated Ca^{2+} entry

In order for Ca^{2+} to enter the cell in response to low oxygen, two events need to happen. First, the TASK channels need to decrease in activity, which results in cell membrane depolarisation. Secondly, as a result of the change in membrane potential, voltage sensitive Ca^{2+} channels open and Ca^{2+} is able to enter the cell. Therefore, the observed depression of the hypoxic Ca^{2+}-response in the presence of anaesthetic can be mediated either through changing membrane potential, or through inhibition of Ca^{2+} channels or both. To tease out if this depression is mediated through Ca^{2+} channels, the effect of halothane and isoflurane on Ca^{2+} entry during high K^+ evoked membrane depolarisation was measured. This was done by superfusing the cell in a high K^+ (50mM) Tyrode solution. Figure 3.3 and 3.4 reveal that the depression of the high K^+ induced Ca^{2+} entry by both halothane and isoflurane was smaller compared to their effect on the depression of hypoxia-induced Ca^{2+} transients, but the small effect was significant ($p < 0.01$ one sample t-test). Thus 1% halothane depressed K^+ induced Ca^{2+} transient by 13.8% ± 6.3 (n=5), 3% halothane depressed 19.4% ± 4.8 (n=6). Similar effects were seen for isoflurane: 1% isoflurane depressed K^+ induced Ca^{2+} transient by 12.9% ± 4.13 (n=6) and 3% isoflurane by 24% ± 6 (n=5). There was no significant difference in effect between agents, nor was there a concentration-related effect within an agent ($p = 0.785$, ANOVA).

In summary, these data suggest that there is indeed a minor inhibitory effect of both agents on Ca^{2+} channels, but this effect is unlikely to be able to fully account for the inhibition of the Ca^{2+} response to hypoxia. Nor was there a marked difference in the efficacy of the two agents in inhibiting the Ca^{2+}-response to High K^+ induced depolarisation.

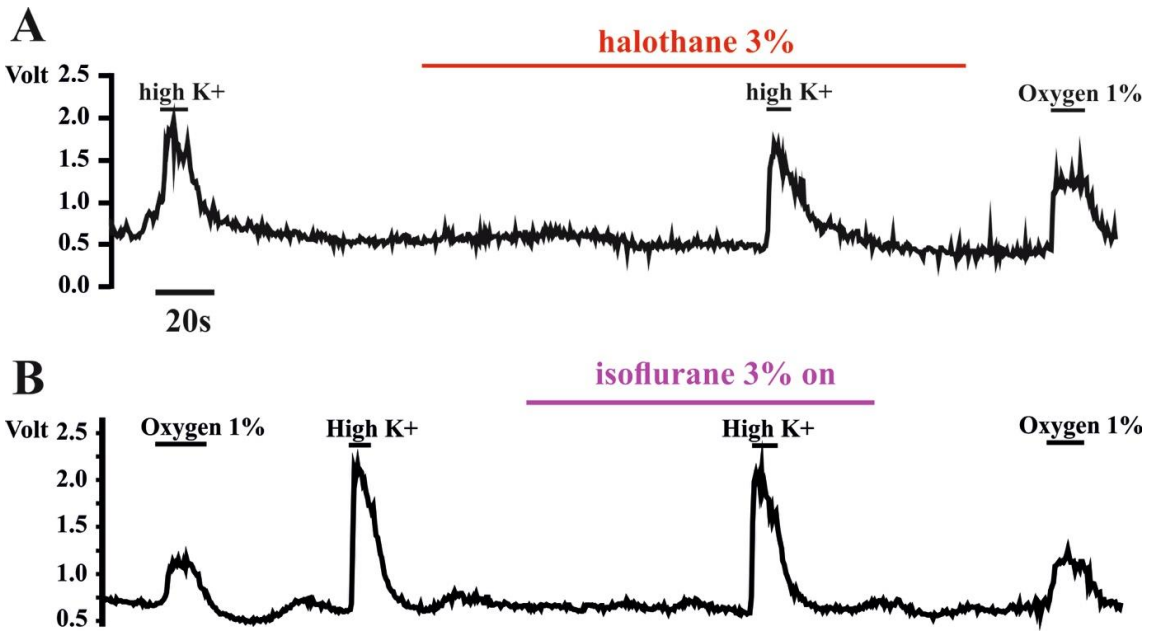

Figure 3.3: Representative recording of the high K^+ evoked Ca^{2+} entry in the presence of 3% halothane and 3% isoflurane. Recording represents the raw trace in volts prior to Ca^{2+} conversion. High K^+ stimulus consisted of 50mM K^+.

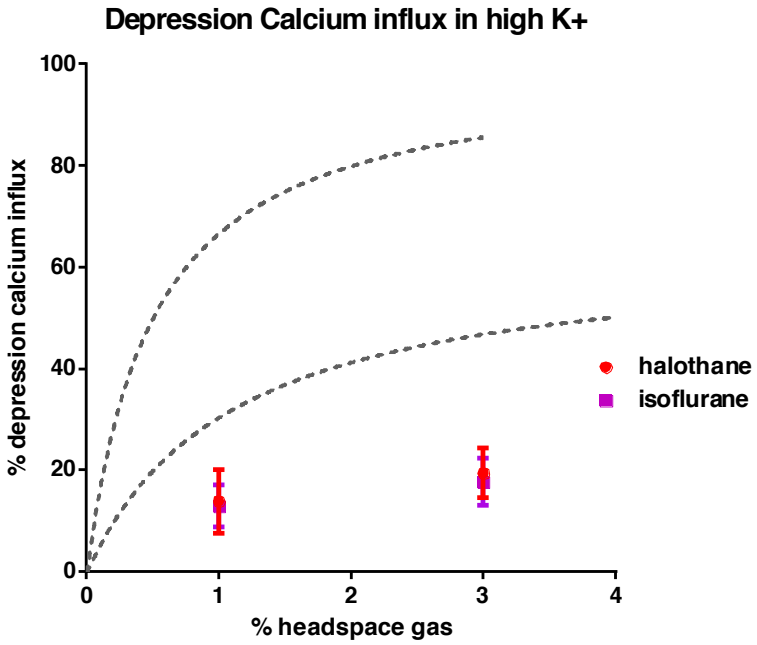

Figure 3.4: depression of Ca^{2+} influx in high K^+ medium. Depression of K^+ induced Ca^{2+} entry in glomus cells. Points are mean +/- SEM. No statistical difference between the agents compared to control (ANOVA p= 0.785) or for dose (ANOVA p=0.390) (n=5-6 for each data point). Although the agent effect is small, it is highly significant (one sample t-test $p < 0.01$). The hypoxia induced depression of Ca^{2+} influx (Figure 3.2), is indicated by the grey dotted lines.

3.3.3 Mixes of halothane and Isoflurane on $[Ca^{2+}]i$

The observed difference in efficacy between halothane and isoflurane in depressing the hypoxia evoked $[Ca^{2+}]i$, as observed in Figure 3.2, prompted me to investigate what would happen when a combination of agents was applied. Therefore, 1.5% halothane was mixed with a variety of concentrations of isoflurane: 1%, 1.5% and 3%. Halothane 1.5% was chosen because it lead to a strong, but not saturating depression of the $[Ca^{2+}]i$ response to hypoxia.

It was observed that combinations of 1.5% halothane with varying concentrations of isoflurane were less effective in depressing the hypoxia evoked $[Ca^{2+}]i$ than halothane alone. This effect was concentration dependent as high levels of isoflurane caused a greater reduction in the depressive effect of anaesthetic on the hypoxic Ca^{2+} response. These studies show that when combining the two anaesthetics rather than an additive effect, an 'antagonistic' or 'infra-additive' effect was observed, such that the depression of the Ca^{2+} response to hypoxia by halothane, was partially reversed by isoflurane. The more isoflurane was added, the more the effect of halothane was reversed (ANOVA $p < 0.001$). Figure 3.5A displays the bar charts for the individual mixes revealing a decreased depression, when more isoflurane is added (n= 8-9 for each mix data point 25 in total). Fig 3.5B reveals the normalized concentration-response relationship of isoflurane and halothane (from Figure 3.2) with curve fitted hyperbolas and the 3 mix data points for the halothane and isoflurane mix from Figure 3.5A. The concentration response curves as shown below thus demonstrate that at the cellular level Ca^{2+} entry is depressed by halothane > combination of both > isoflurane.

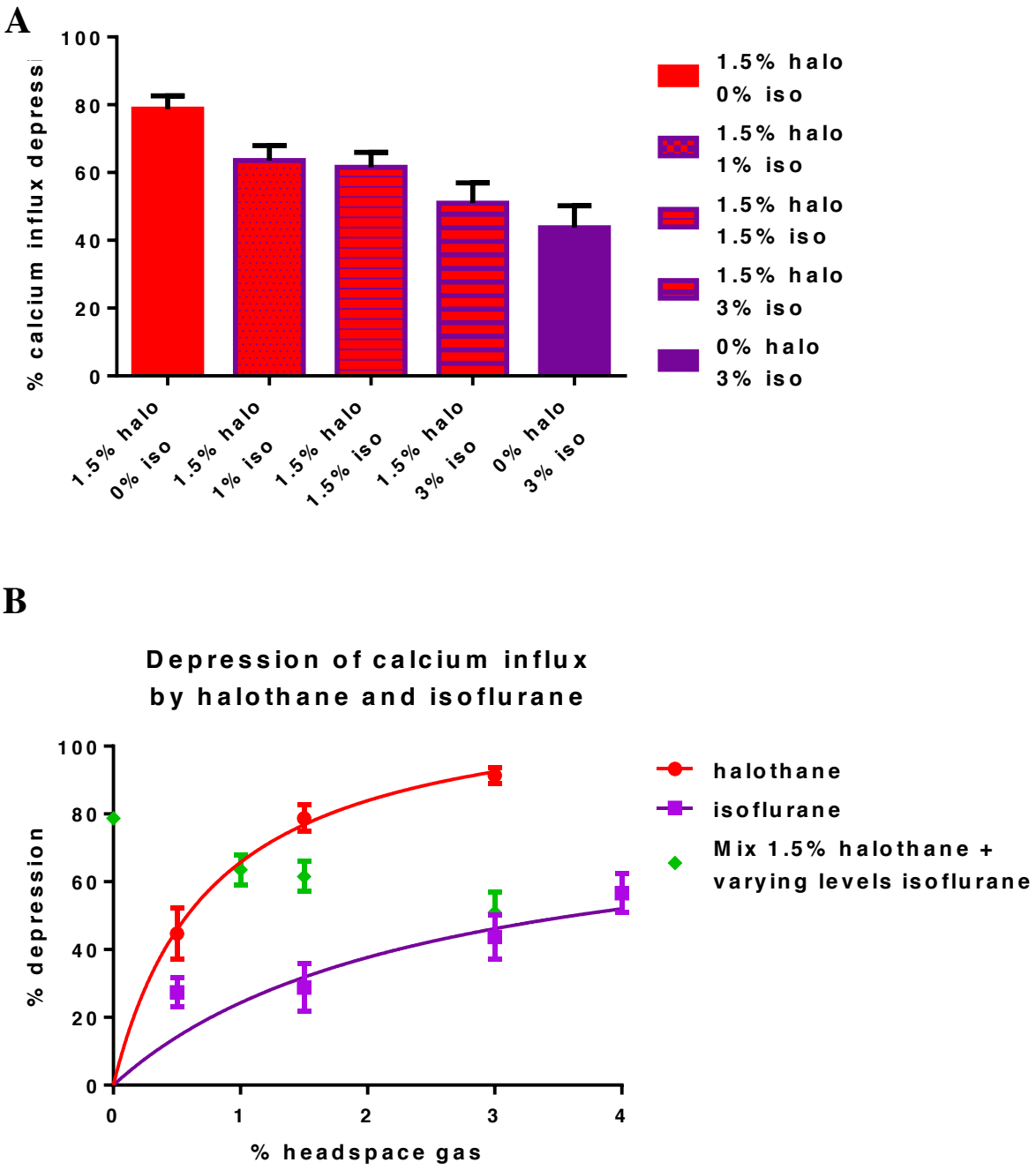

Figure 3.5: Depression of Ca^{2+} response in presence of 1.5% halothane + increasing amounts of isoflurane. (A). N = between 8-13 for each data point. There is a trend for partially reversing the halothane evoked depression caused by isoflurane. Adding any dose of isoflurane will significantly reduce the depressive effect of halothane. **(B)** The concentration response curves for isoflurane and halothane with the mix line. The green line represents 1.5% halothane throughout with the data points representing the isoflurane concentration. Therefore at 0% on the X-axis the 1.5% data point represent 1.5% halothane without isoflurane and the 1%, 1.5% and 3% represent 1.5% halothane mixed with the aforementioned isoflurane mixes. Halothane 1.5% is indicated with the red dotted line.

Concentration response curve of halothane and isoflurane on TASK channel activity

The next question studied in detail was how isoflurane and halothane affect the native TASK channel activity. It was hypothesized that the interesting observed infra-additivity could be due to differential interactions of halothane and isoflurane on the TASK channels expressed in the glomus cell. This was based on (a) the experiment in high K^+ Tyrode that showed that anaesthetics had little influence over voltage gated Ca^{2+}-entry, which turned the attention to TASK channels (responsible for depolarizing the cell membrane in response to low oxygen and so activating Ca^{2+} channels) and (b) because previous studies show that volatile anaesthesics increase cloned TASK channel activity. Thus the effect of low oxygen (which decreases open probability) could be opposed by anaesthetics. I therefore sought to investigate and compare the effects of halothane and isoflurane on native TASK channel activity.

The TASK channel activity observed under the recording conditions as described in the methods section (pipette +80mV and 140mM K+ and in Tyrode 100mM K+) resulted in short flickery openings, which were seen as inward currents. In the control condition most all-points amplitude histograms typically displayed, as expected, a single but broad peak at around ~2.6 pA suggesting one main open state, which previous research has indicted represents the heterodimeric TASK-1/3 channel predominant in rat glomus cells (Kim et al., 2009a, Turner and Buckler, 2013a). A representative single channel trace and two representative all points histograms from the same recording can be seen in Figure 3.6.

It was evident that both halothane and isoflurane increased the frequency of channel openings; halothane more so than isoflurane (Figure 3.6). Upon application of isoflurane or

halothane, the channel activity increased, so that more double openings and more frequent channel bursts were observed and the long closed state appeared to be decreased. Overall, halothane increased the channel open probability more than isoflurane did.

Figure 3.7 reveals the concentration-response curve of halothane and isoflurane with an average of 6-10 recording per concentration and a total of 147 datapoints. Curve-fitting isoflurane data suggests a Bmax of 128% and a Kd of 1.4%. For halothane, curve-fitting suggests a Bmax was 350% and Kd was 1.44%. The ~10% halothane was reached by putting the two halothane vaporizers in series. However, as discussed in the methods section, the infrared analyser can only reliably detect anaesthetics in the 0-5% range, whereas outside this range, the analyser can measure but not as accurately.

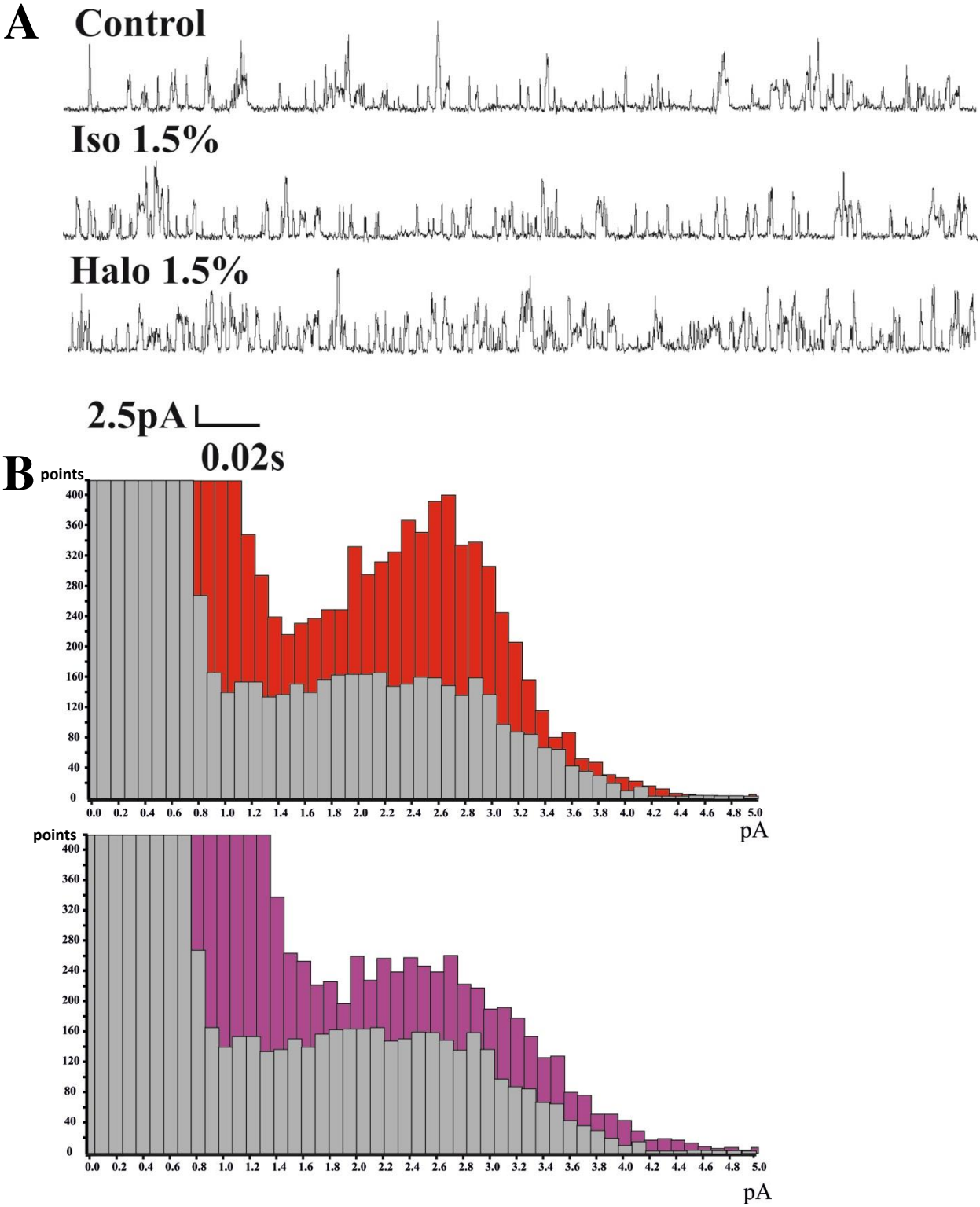

Figure 3.6: The effect of 1.5% halothane and isoflurane on channel activity in rat glomus cell. (A) three representative single channels traces showing control and 1.5% isoflurane and halothane. **(B)** two representative all points histograms from the same recording revealing the average open ampliture peak of ~2.6pA. Halothane 1.5% in red and isoflurane 1.5% in purple. Pipette potential +80mV 150mM K+ in Tyrode 200mM K+.

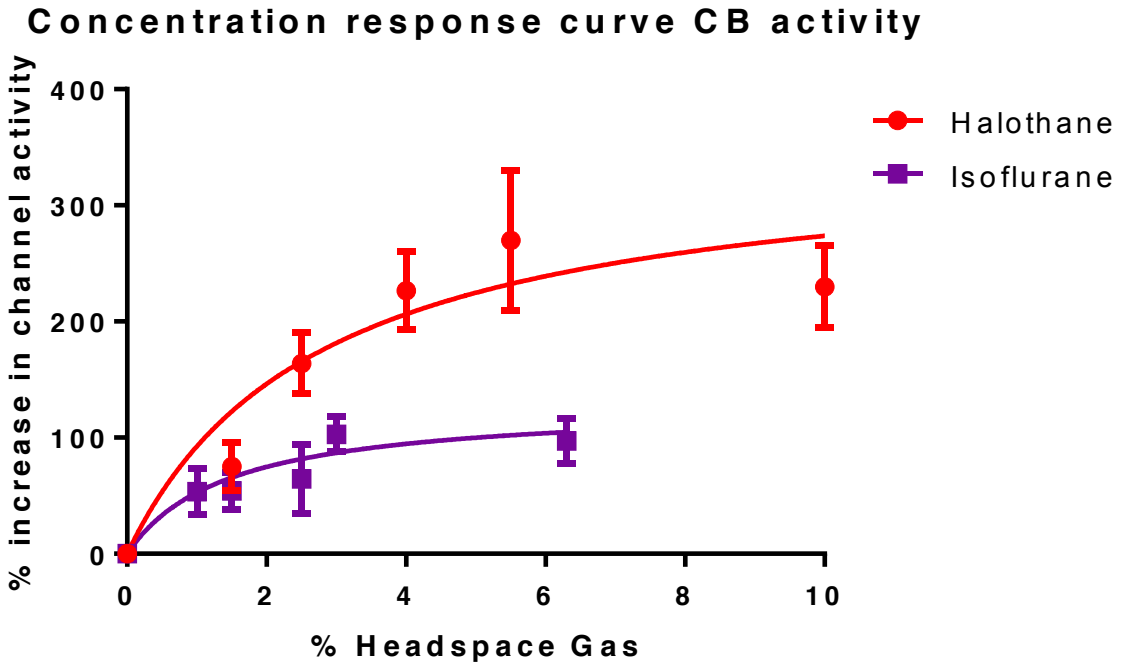

Figure 3.7: Concentration response curve of halothane and isoflurane on increase in TASK channel activity in rat carotid body. Data-points are normalised against control channel activity. Halothane: BMax = 350% and Kd = 2.88%. Isoflurane: BMax = 128% and Kd = 1.44%.

3.3.4 The effect of mixes on native TASK channel activity

After the difference in efficiency of halothane and isoflurane were established on native channel level, mixes were attempted. Due to the difficult nature of patching native carotid body cells, fewer recordings were done. The first mix was 2.5% halothane and 2.5% isoflurane (n=10). This was chosen because 2.5% halothane evokes a strong but submaximal increase of channel activity and isoflurane has nearly reached its maximal effect. The second concentration was 4% halothane with 4% isoflurane (n=15). At 4% halothane the stimulus was near maximal, which was matched by a similar concentration of isoflurane. A third mix with a smaller number of patches (n=6) was performed with 1.5% halothane and 1.5% isoflurane, which did not reach statistical significance. In channel studies no hypoxia was applied, hence the anaesthetic protocol was simply 'anaesthetic on' 'anaesthetic off'. Therefore all three anaesthetics could be applied within the same recording, allowing for paired statistics. Both mixes revealed an infra additive effect of the mix, in that isoflurane again partially reverses the depressive effect of halothane, suggesting an antagonistic effect of isoflurane. The representative traces for the 2.5% mix can be seen in Figure 3.8 with a pipette potential of +80mV, 140mM K^+ in pipette solution and 100mM K+ in Tyrode solution with nPopen increased to 152.7% ± 20.2 on average. Exposure to 2.5% isoflurane led to an increase of 54.3% ±14.4. The mix led to an increase of 90.6% ± 21.1, which was less than halothane alone. Similar results were observed for the 4% halothane and isoflurane mix as can be seen in figure 3.9B. 4% Halothane caused an increase in nPopen of 226.7% ± 33.4, isoflurane 4% caused 98.4% ± 19.9 and the mix of 4% and 4% evoked a 126.5% ± 28.6 increase in nPopen. The difference between mix and halothane alone was significant for both

the 2.5% and 4% mixes (P = 0.043 and 0.015 respectively with a non parametric paired test. In Figure3.9C the three equi-concentration mixes were plotted on the graph.

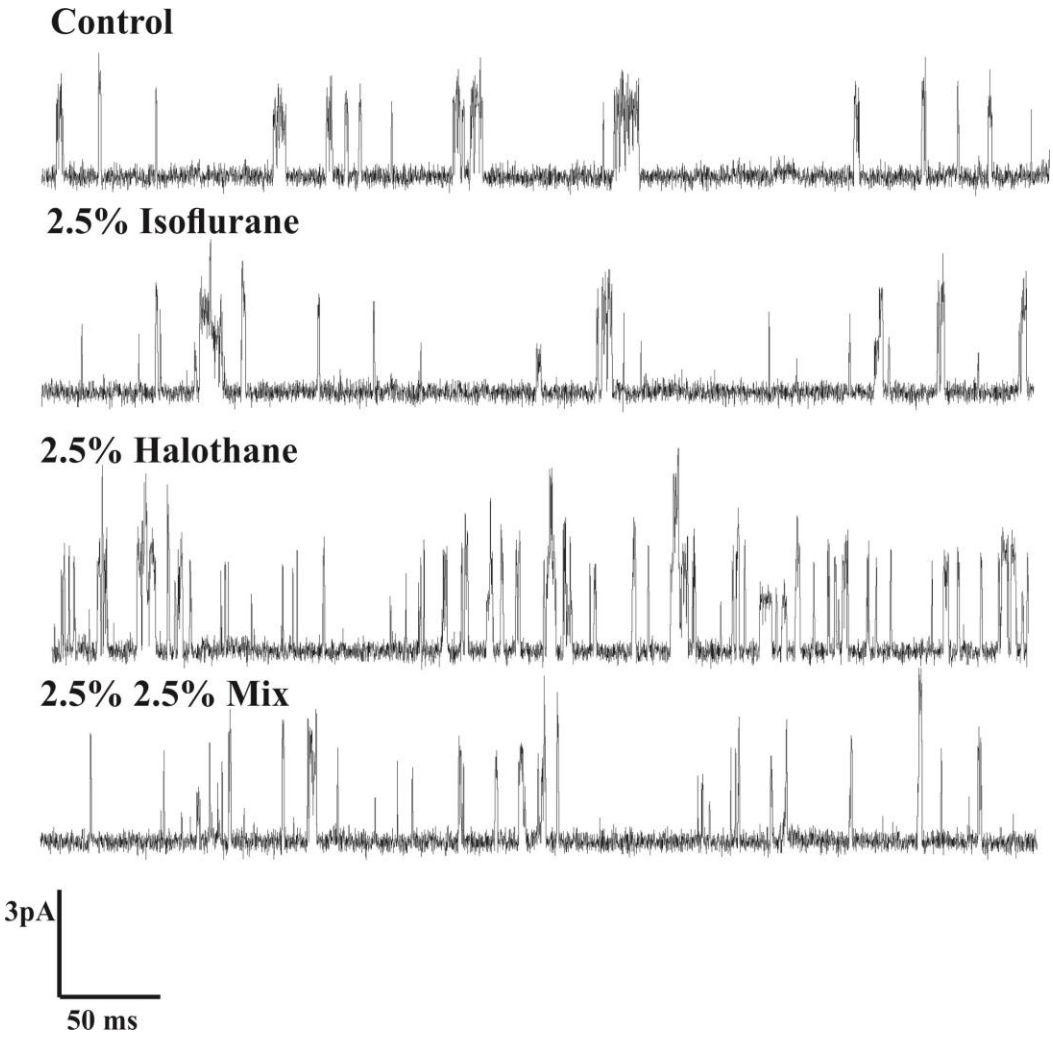

Figure 3.8: Representative single channel traces of TASK channel activity in rat carotid body. Cell-attached recording each showing four 500 ms sections of recording for control 2.5% isoflurane, 2.5%/2.5% halothane/ isoflurane mix and 2.5% halothane alone. The traces are recorded with a pipette potential of +80mV, 140mM K+ in pipette solution and 100mM K+ in Tyrode solution.

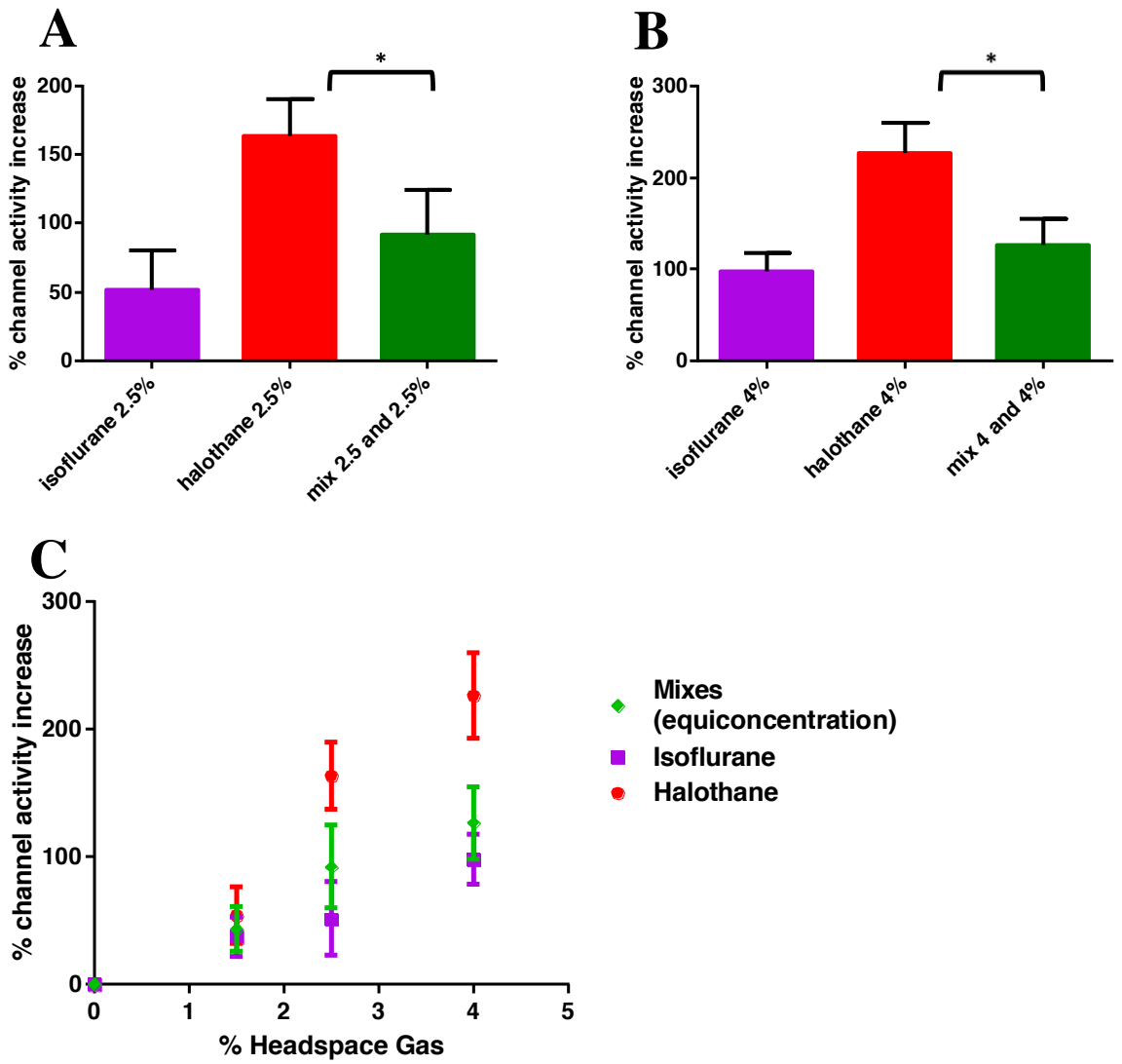

Figure 3.9: 2.5% and 4% mixes in cell attached single channel recordings of rat carotid body. Isoflurane and halothane are antagonistic at channel level. TASK1/3 channel activity expressed as % increase in nPopen compared to control. Note that in both bar charts halothane activates the TASK-1/3 channel more than isoflurane. **(A)** Bar chart of 2.5% isoflurane (purple) 2.5% halothane (red) mix of 2.5% halothane and 2.5% isoflurane. A combination of halothane and isoflurane is less effective than halothane alone (n=10) ($p = 0.034$ Mann–Whitney U test). **(B)** Bar chart of 4% isoflurane (purple) 4% halothane (red) mix of 4% halothane and 4% isoflurane. A combination of halothane and isoflurane is less effective than halothane alone (n=15) ($p = 0.015$) Mann-Whitney U test). (N=15) **(C)** Plot representing the 3 mix points with the corresponding single agents concentration of halothane and isoflurane above and below (Mix = 1.5%, 2.5% and 4% halothane and isoflurane).

Aside from the paired non-parametric tests of the 2.5 and 4% mix concentrations versus halothane, an ANOVA was performed across all three groups and concentrations (halothane mix and isoflurane). The effect of 'anaesthetic' was highly significant across the three groups (ANOVA, $p<0.001$) and post-hoc testing confirmed that whereas the effects of mix and isoflurane were significantly different from halothane ($p<0.001$, with Bonferroni correction for multiple testing) the influence of mix and iso were similar ($p= 0.586$).

Whilst the majority of patches revealed only a single peak in all-points histograms corresponding to TASK-1/3 channel (Figure 3.10A), one particular low noise recording, (Figure 3.9B) revealed a second peak around 1.2 pA, corresponding to what is believed to be a TASK-1 channel (Turner and Buckler, 2013a). The action of the anaesthetics resemble similar actions as seen in diagram A, with similar effects on both the TASK-1 and heterodimer peak. Note that the use of a 75% threshold crossing method for quantifying TASK-1/3 channel activity does indeed exclude single opening of the TASK-1 channel.

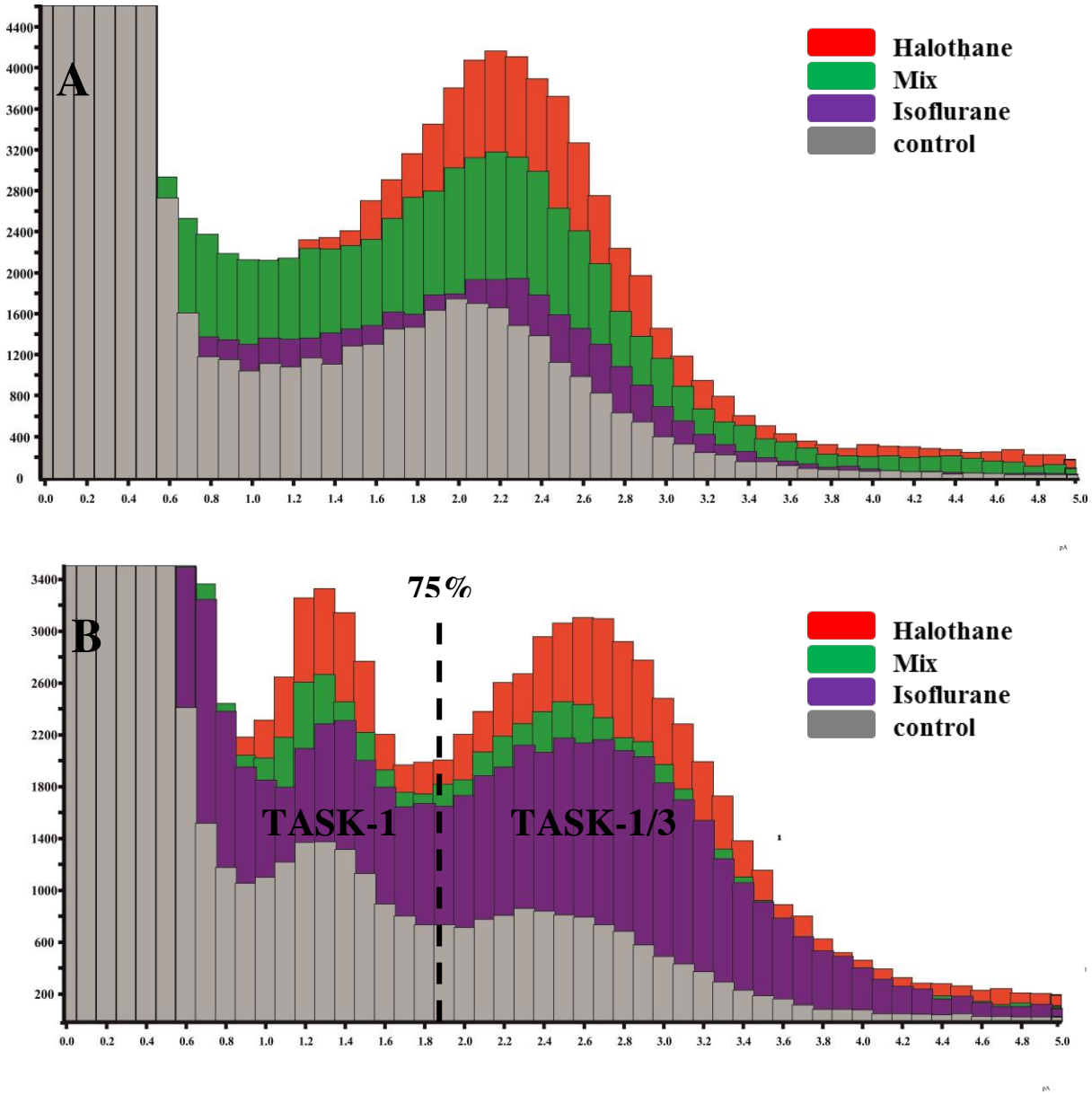

Figure 3.10: All points histogram A and B from a cell attached patch recording. The y-axis represents the number of points. The x-axis represents the amplitude (pA). **(A)** The control (grey) histogram shows the characteristic peak representing the TASK-1/3 heterodimer (~2.6 pA). Isoflurane 2.5% (purple) modestly increases the activity of the heterodimer, whereas halothane 2.5% (red) markedly increases the activity. A mix (green) of 2.5% halothane and 2.5% isoflurane results in reduced (not increased) channel openings as compared with 2.5% halothane alone. **(B)** The Control (grey) histogram shows the characteristic peaks representing the presumed TASK-1 (~1.2 pA) and heterodimer (~2.5 pA) activities. Isoflurane 2.5% (purple) increases the activity of the heterodimer, and also the TASK-1 channel. Halothane 2.5% markedly increases activity in both channels. A mix (green) of 2.5% halothane and 2.5% isoflurane results in reduced (not increased) channel openings as compared with 2.5% halothane alone. Bin-width was 0.1pA

These results demonstrated that at the level of native TASK-channel activity, isoflurane is able to partially reverse the effect of halothane with both equi-concentrations of mixes (2.5% and 4%). These experiments therefore show that this sub-additivity/antagonism takes place at the TASK channel level in the carotid body. The native TASK channel is strongly regulated within the carotid body. To find out if the infra additivity is due to direct action on the channel, or due to an action on something carotid body specific, effects of anaesthetics were also studied in TASK-1 in a heterologous expression system.

3.3.5 TASK-1 channel activity in HEK cells

TASK-1 channels were transiently expressed in HEK cells and single channel cell attached recordings were made under identical recording conditions as described for carotid body. Short flickery inward currents were observed. Figure 3.11 displays a representative single channel trace of TASK-1 transiently expressed in HEK cells. Both halothane and isoflurane increased the channel activity, as did the mixture of both. In the all points histograms (Figure 3.12) the peak open state was less clearly defined than those in native patches. Most histograms typically revealed a broad peak spanning from 1-2 pA. The concentration response curves for halothane and isoflurane reveal again a contrast between both agents. The increase in channel activity in response to anaesthetics is less compared to that observed in native carotid body channel activity. Curve fitting shows that halothane has a Bmax of 172% and a Kd of 1.46%. Isoflurane has a Bmax of 56% and a Kd of 0.46%.

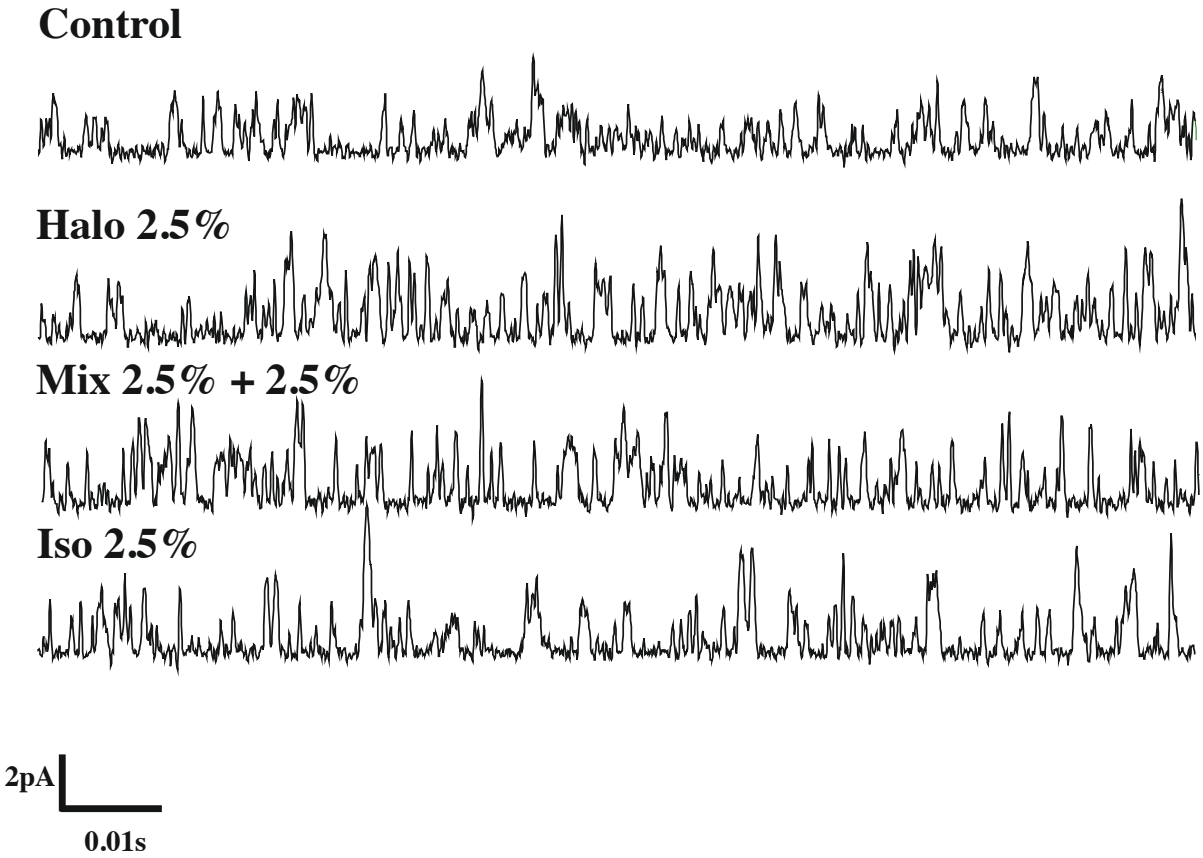

Figure 3.11: Representative traces of TASK-1 channel activity in HEK cell. Cell-attached recording each showing a 0.1s section of recording for control (no anaesthetic), 2.5% halothane, 2.5% + 2.5%mix and 2.5% isoflurane. The traces are recorded with a pipette potential of +80mV, 140mM K+ in pipette solution and 100mM K+ in Tyrode solution.

For the mixes 2.5% halothane was mixed with isoflurane 1.5% (N=10) 2.5% (n=10) 4% (n=7) 5% (n=6). The curve fitting in in Figure 3.12 reveals mixes of halothane and isoflurane appears to be infra-additive with the data-points lying between the isoflurane data and 2.5% halothane (dotted red line). Statistical comparison of channel activity in 2.5% halothane vs isoflurane (all concentrations) generated a significant infra-additive effect (P= 0.011).

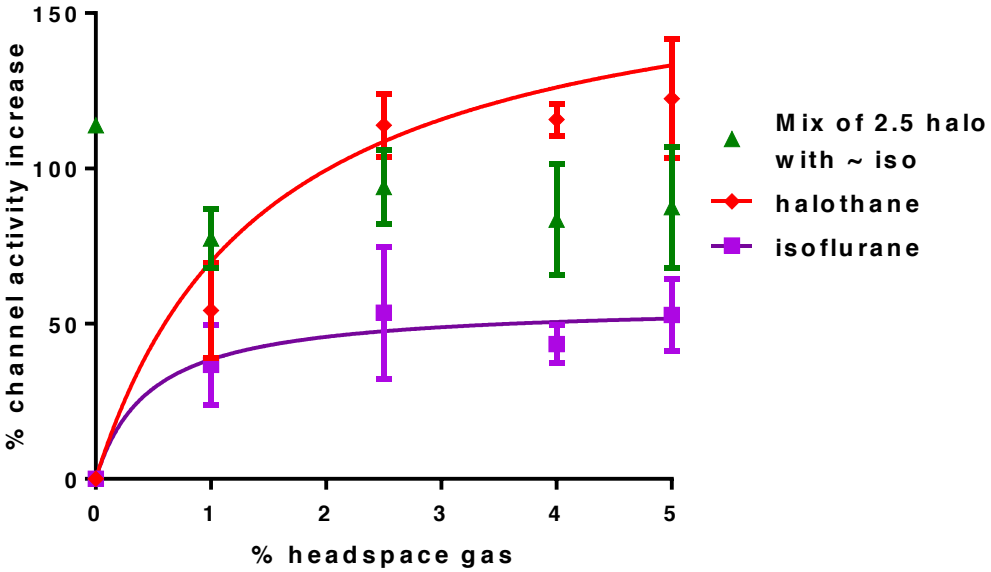

Figure 3.12: Concentration response curve of halothane and isoflurane and mix on TASK-1 channel activity transiently expressed in HEK cells. Data-points are normalised against control channel activity. Non-parametric ANOVA revealed a significant difference between the mix points and the halothane 2.5% (dotted red line) (p=0.011). The green line represents 2.5% halothane with the amount of added isoflurane plotted on the x-axis curve.

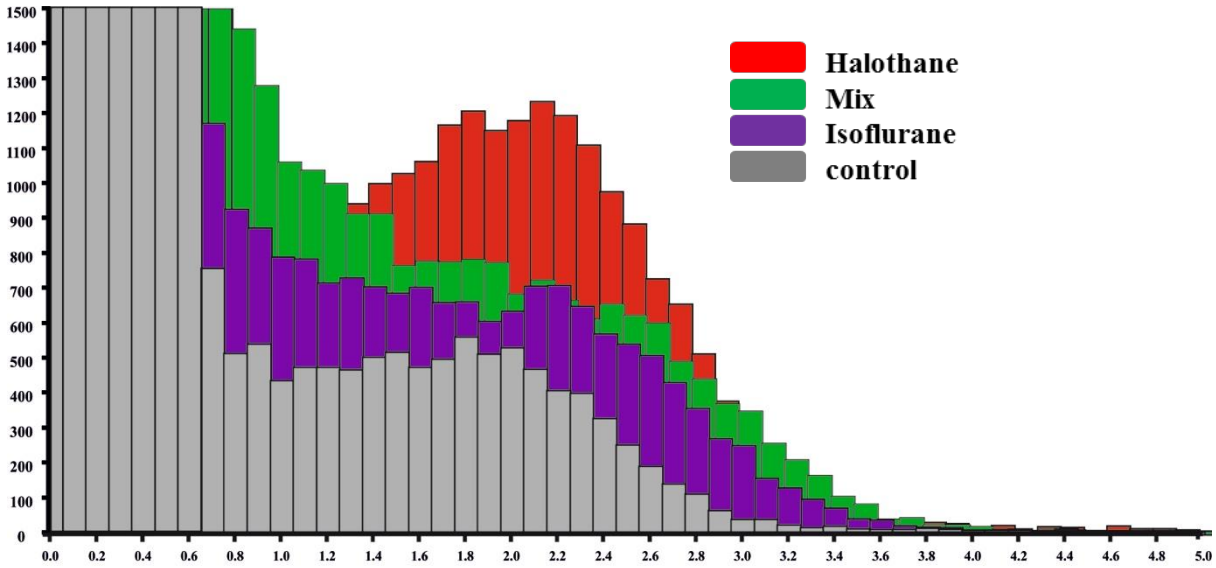

Figure 3.13: Representative all points histogram from a TASK-1 recording with 2.5% halothane and 5% isoflurane. Pipette potential +80mV 140mM K^+ and Tyrode solution 100mM K^+.

Lastly, a number of un-transfected and empty pIRES-EGFP transfected HEK cells (n=10) were patched under identical recording condition as used for TASK-1 recordings. All patches were empty but one, which contained a channel with a 6pA opening approximately twice per second(Figure 3.14). This channel therefore looks different from the TASK-1 channels and its open probability is very low. It seems unlikely that this channel will have interfered significantly with the recordings taken.

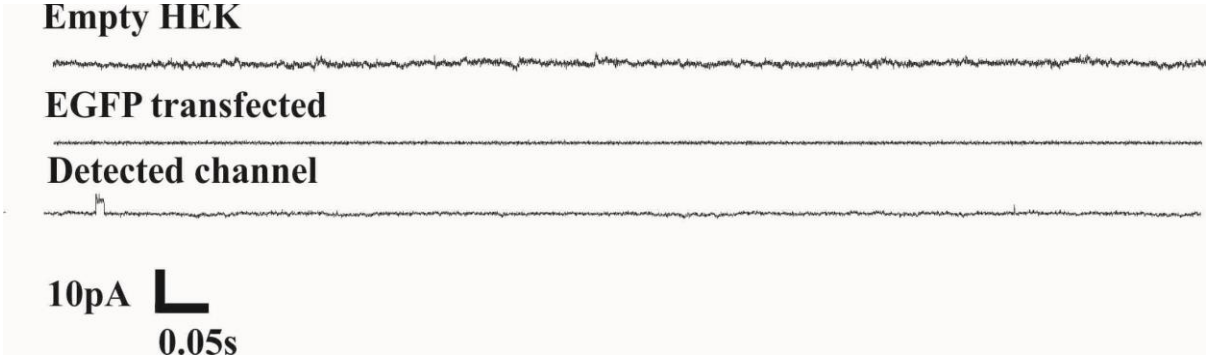

Figure 3.14: Baseline of HEK cell and EGFP transfected HEK cell. Recorded at a pipette potential of +80mV 140mm K^+ in pipette and 100mM K in Tyrode solution. The third trace shows a 6pA endogenous channel with very low activity.

3.4 Discussion

The experiments in this chapter demonstrate novel actions and interactions of halothane and isoflurane on the carotid body's response to hypoxia and TASK channels. First, the seven key findings will be discussed. This is followed by a discussion of this research compared to other studies, its implications and clinical relevance, its limitations and technical challenges and concludes with suggested future studies.

The first finding is that, consistent with whole-body ventilation studies in humans and rats (Pandit, 2002, Karanovic et al., 2010), the experiments showed that isoflurane is less effective than halothane in depressing hypoxia-stimulated Ca^{2+} entry into rat carotid body cells. This lends a cellular explanation for the whole-body effects observed on ventilation. Concentration-response relationship suggests that whereas halothane is a full agonist for this effect on Ca^{2+} entry (because of the ability to fully depress), isoflurane appears to be only a partial agonist.

The second finding is that, when studying $[Ca^{2+}]i$ in a high K^+ solution, only a small concentration independent effect of anaesthetics was observed on the voltage gated Ca^{2+} entry, suggesting that these channels do not play a major role in contributing to the effects of anaesthetics on the Ca^{2+} entry in response to hypoxia.

The third finding is that, at single channel level, halothane increases type-1 cell TASK channel activity more than isoflurane does. Halothane appears to act as a strong agonist and isoflurane as a partial agonist of channel activity.

The fourth finding is that single channel recordings of ratTASK-1 in HEK cells revealed that both halothane and isoflurane are able to activate the channel, but halothane again appeared to be a stronger agonist compared with isoflurane. This result differs from a TASK-1 study performed by Berg et al. (2004) who used a heterologous expression system (HEK-293 with either rat TASK-1 , TASK-3 or TASK 1-3) to demonstrate that isoflurane activates TASK-3 and TASK 1-3 but inhibits TASK-1. However, this result is in line with Putzke et al. (2007) who noted a small increase in human TASK-1 channel activity in Xenopus oocytes upon isoflurane application.

The fifth finding is that the addition of isoflurane to 1.5% halothane in different proportions (1%, 1.5% and 3% isoflurane) depresses hypoxia evoked Ca^{2+} entry to a lesser extent than with 1.5% halothane alone showing an antagonistic interaction between both agents.

The sixth finding is that at the single channel level in type-1 cells the addition of 2.5% isoflurane to 2.5% halothane resulted in channel activity (TASK-1/3 heterodimer) that was less than observed with 2.5% halothane alone consistent with an antagonistic interaction between isoflurane and halothane as noted for the Ca^{2+} entry data. The same 'infra-additive' result was also observed when mixing 4% halothane and 4% isoflurane.

The seventh finding is that isoflurane in different proportions (1.5%, 2.5% 4% and 5%) also decreases the effect of 2.5% halothane, on ratTASK-1 activity in HEK cells. The infra-additivity between the mix of both agents and halothane alone, was of a lesser magnitude than observed in the native channel and Ca^{2+} experiments, which was reflected into the fact that no significance was reached in the individual paired test, but that the overall effect (non-parametric ANOVA) was significant, showing that mixes act infra-additively at TASK-1.

3.4.1 Comparison with previous studies

The findings, with respect to the different efficacy of halothane and isoflurane at cellular and molecular level, are consistent with whole-body human and animal findings, with regards to ventilation, as these studies also identified halothane as a more powerful depressant of the AHVR and isoflurane a less powerful (but still significant) depressant (Pandit, 2002, Karanovic et al., 2010).

The observed antagonism represents a novel perspective on the mechanism of action of these agents, which differs from the current accepted theory that predicts that volatile anaesthetics should act additively. Analysing how anaesthetics act when they are mixed together has been little considered and tested before. It is however important to keep in mind that agent interactions can occur and be studied at a number of different levels. At whole animal and human level, immobility in response to a noxious stimulus (as a defined end point of anaesthesia), is thought to result from a combination of effects of anaesthetics on different channels and other proteins that in turn are differentially expressed in a variety of tissues contributing to anaesthetic effects (such as brain, spinal cord and moto-neurons). Studies at

the single channel level, on the other hand, may provide key insight as to how these agents act directly on the channel on one or more binding sites.

For inhaled anaesthetics at whole animal levels, the actions are reportedly additive (Eger et al., 2003, Hendrickx et al., 2008). Eger et al. (2003). This was confirmed in a follow up study in which mixes of halothane, isoflurane, sevoflurane and desflurane were all found to be additive. For mixes of anaesthetics in humans, such as halothane and xenon (Cullen et al., 1969) and ethylene and halothane (Miller et al., 1969) also produced additivity (Hendrickx et al., 2008). At the channel level, Jenkins et al. (2008) researched different combinations of volatile anaesthetics on GABA, NMDA and Glycine receptors and found that halothane and isoflurane do not show infra additive behaviour. On glycine receptors the effect of the mix was stronger than each of the agents by itself and the same result was seen on GABAa receptors.

3.4.2 Physiological antagonism or classical receptor pharmacology?

In my study, infra-additivity is shown both at a system level (hypoxia evoked Ca2+ entry) but also specifically at the level of channel activity that two agents with a similar effect but different efficacy can antagonize each other partially. In this section, different hypotheses leading to the observed infra-additivity will be discussed with evidence for and against each theory.

Firstly, when studying hypoxia evoked Ca^{2+} entry, one should take into account that the TASK channel is not the only channel involved in triggering the Ca^{2+} influx and therefore it was considered if other channels contribute to the infra-additivity. Voltage gated Ca^{2+} channels themselves appear to be little affected by the anaesthetics. Other K^+ channels, however, may contribute to the duration and magnitude of the Ca^{2+} entry. Kv channels (voltage gated K^+ channels) are thought not to be active at resting membrane potentials, but they are involved in repolarisation following action potential involved in hypoxia. HERG channels (human ether-a-go-go K^+ channels) activate upon depolarisation and may also contribute to the magnitude and duration of response to hypoxia (Kim, 2013, Kang et al., 2014). BKCa channels also contribute to the outward K^+ current and could thus influence depolarisation. The effects of volatile anaesthesics on these channels are unknown and therefore it is possible that these channels are in some ways affected. Another way in which the effect of other K^+ channels were attempted to be minimized, was by using a pipette filling solution with 4-AP and TEA, which block BKCa channels and most Kv channels. Moreover, the cells are patched at a very negative potential in a further attempt to exclude the contribution of these channels to the current observed in the patches. Taking all this into account, the parsimonious explanation regarding the infra additivity is due to anaesthetic effects on TASK channels.

It remains possible however that the infra additivity observed at the level of TASK channel activity in native cell attached single channel recordings could be due to physiological antagonism evoked by other regulatory proteins or signalling pathways. Prime candidates for these could be the mitochondria. Inhibitors of mitochondrial respiration leads to decrease in TASK channel activity and Ca^{2+} influx, thus evoking similar effects on type-1 cells as

hypoxia does. Mitochondria in type-1 cells also appear to be more oxygen sensitive compared to other cells. (Duchen and Biscoe, 1992a, b, Buckler and Turner, 2013, Turner and Buckler, 2013b). If mitochondria can indeed regulate TASK channel activity, it is important to clarify if anaesthetics have a mitochondrial effect as well, which has not been previously studied in type-1 cells. This research question will therefore be addressed in chapter 5.

The final explanation to consider for the observed infra-additivity is that halothane and isoflurane act on the TASK channel directly, and compete for binding sites in TASK channels and so obey the rules of classical receptor pharmacology. This hypothesis is supported at least in part by the infra-additive mix results on TASK-1 expressed in HEK cells.

Implications of our study

Due to 'infra-additive' actions on TASK channel activity, Ca^{2+} influx can be partially restored. Because TASK channels play a key role in the hypoxic response, the demonstrated antagonistic behaviour could be exploited to minimise the undesired side effects on ventilatory depression of general anaesthesia. This model can perhaps be used to study novel agents that can partially reverse the increase in TASK activity, or can even decrease TASK channel activity in the presence of volatile anaesthesia. These types of drugs could be useful for peri-operative management of the ventilation. Therefore such drugs will be studied in chapter 6.

3.4.3 Limitations of the experiments

There are two limitations in this study that will be addressed and discussed. Firstly, the experiments were limited by the vaporizers ability to deliver high levels of anaesthetic for the output of anaesthetics and the limited range of accuracy from the infrared analyser, therefore it was not possible to apply a more extensive range of concentrations. The highest concentration that could be reliably applied and measured was 5% of either isoflurane or halothane. However, the concentration range actually studied is fairly close to the clinically relevant range.

A second limitation of this study is that type-1 cell patches may contain a mixture of TASK-1, TASK-3 and TASK-1/3 with the latter being the most predominant channel. There is very good evidence showing that the main form of channel activity, which is measured and analysed represents the TASK-1/3 heterodimer, but it is possible that some patches may also contain TASK-3 channels and perhaps double openings of TASK-1. Chapter 6 will discuss two TASK blockers that may potentially block TASK-1 or -3 in the patches to address this limitation and attempt to get more selective channel activity. One way of trying to tease out where the infra-additivity derives from is by transfecting the channels separately in HEK cells. I accomplished this for TASK-1, but failed to do so for TASK-3, where it was not possible to get recordings with sufficiently low channel numbers that would allow the study of single channel activity clearly. However, some measurements on total current in HEK cells expressing TASK-3 are presented in chapter 4.

3.4.4 Technical challenges of the experiments in this chapter

I found that working with HEK cells that transiently express TASK channels was challenging. For both TASK-1 and TASK-3, the transfected cells appeared slightly unhealthy. The transfected 'green' cells often contained one or more blobs on their cell surface and appeared less evenly shaped than the untransfected cells. The biggest difference was that the transfected cells were always less well attached to the poly-L-lysine coated coverslips than the untransfected cells. The best cells to patch were those partly attached to other cells as this appeared to lead to a higher chance of completing the experimental procedure. The TASK-1 cells looked the unhealthiest (compared with TASK-3), however I believe that the upside of this was, that channel activity was therefore low enough to record clean single channel activity. A good seal was established in approximately 1 in 15 green TASK-1 transfected cells. A higher chance of a successful and complete recording was reached by learning to identify the most 'promising' green cells. The biggest difference between transfected HEK cells and type-1 cells was their number. There was always a limited number of type-1 cells suitable for patching available each day, whereas there were unlimited transfected green fluorescent cells expressing TASK-1 available. Patching of type-1 cells was more successful, with 50% of the cells patched (compared with perhaps 5-10% of HEK cells tried) yielding a good seal and usable recordings.

Numerous times I have tried to obtain clear single channel recordings from HEK cells expressing TASK-3. However, the channel expression was incredibly high. In an attempt to reach less channel activity, a shorter incubation time post transfection was tried, but attempts to record less than 24 hours post transfection still resulted in cells with too high channel

activity. Similarly, when decreasing the amount of TASK-3 DNA, although a decrease in total green cells was observed, activity was still too high. For future projects therefore it is worth considering creating a stable cell line in which the activity can perhaps be regulated with use of an inducible promoter system in a stably transfected mammalian cell line (Trapani and Korn, 2003). Because of the high channel activity of TASK-3, whole cell recordings were attempted. Although this initially worked, in all cases the cells would de-attach before the end of the recording and the seal would be broken.

3.4.5 Suggested follow up experiments

Logical follow up experiments would be to study mixtures on TASK-3 expressed in HEK cells. Secondly, it would be interesting to study the TASK-1/3 concatemer in HEK. In this concatemer the C terminus of TASK-1 is fused with the N-terminus of TASK-3, or the other way around in the TASK-3/1 concatemer. However, a limitation with using this construct is that it remains unclear if both subunits are assembled in a way that allows for the anaesthetic binding sites to remain intact and for potential domain swapping to take place (Brohawn et al., 2013). Therefore, although studying the infra-additivity in the TASK-1/3 concatemer would be useful, some caution will need to be taken regarding the interpretation of the results.

To conclude, the results in this chapter show interesting and novel interactions between anaesthetics. However, before the true cause of the infra-additivity can be established, more studies are needed to further clarify the possible binding site on the channels. Furthermore, regulation of the channel by other proteins and molecules needs to be excluded. Despite that the exact cause of infra-additivity was not established in this chapter, this interesting observation of partial reversal of the undesired anaesthetic interference with the hypoxia transduction cascade could be further exploited clinically, by searching for potential agonists or antagonists.

Chapter 4. Influence of sevoflurane on TASK channels and the hypoxic response in glomus cells.

4.1 Introduction

The ventilatory response to hypoxia is an important protective mechanism that normally mitigates against severe hypoxaemia. However, it is well established that volatile anaesthetics have a potent depressive effect even at very low doses that pertain long after surgery. This exacerbates the risks of post-operative hypoxaemia, (as discussed in chapter 1).

However, not all agents are equally depressive to the hypoxic chemoreflex, and there appears to be a specific order of potency with halothane being generally the most depressive (Dahan et al., 1994a, Dahan et al., 1994b, Pandit et al., 2004) and sevoflurane being the least (van den Elsen et al., 1998, Pandit et al., 1999). The overall order for depression in humans appears to be: halothane > enflurane > isoflurane > sevoflurane (Pandit, 2002).

As established in chapter 3, the effects of hypoxia on the TASK channel and hypoxia evoked $[Ca^{2+}]i$ is opposed by halothane and isoflurane. Furthermore, in intact rat preparations (Karanovic et al., 2010), it has been shown that halothane, sevoflurane and isoflurane blunt the nervous activity initiated by hypoxia. There appears to be a similar order of potency for these effects at carotid body and glomus cell level, with halothane the most potent and sevoflurane and isoflurane much less so (Pandit and Buckler, 2009, Karanovic et al., 2010).

In whole body human and rat studies the agent sevoflurane is found to be the least depressive in its effects. At cellular and single channel level, however, sevoflurane has been relatively little studied. Sirois et al. (1998) studied hypoglossal moto-neurones and found that sevoflurane caused an outward current and increased membrane conductance in a manner approximately equally effective as isoflurane and halothane. In a follow up study in the same tissue, Sirois et al. (2000) found that the specific pH sensitive K^+ current (most likely mediated by TASK-1) was increased upon sevoflurane application. (Putzke et al., 2007) examined the effect of sevoflurane on human TASK-1 expressed in oocytes at clinically relevant concentrations and also found that sevoflurane increases the TASK-1 current.

The latest hospital survey in the United Kingdom indicated that sevoflurane is the most commonly used volatile maintenance agent; used in 58.5% of all cases (Sury et al., 2014). Sevoflurane is also particularly used for pediatric anaesthesia, where it also serves as an induction agent in 40% of all cases (Sury et al., 2014). Despite its widespread use in the UK sevoflurane is not as extensively studied as halothane and isoflurane on the hypoxic response and TASK channels. As such, the main aim of this chapter is to examine the effect of sevoflurane on the glomus cell response to hypoxia and, specifically, compare it with the effects of halothane and isoflurane.

In common with the effects of these agents at whole-body (human and rat) level, the overall question to be addressed is whether sevoflurane is less potent a depressant than halothane, and somewhat less potent than isoflurane. Effects of sevoflurane will be studied on hypoxia evoked Ca^{2+} entry and compared with isoflurane and halothane. The next question to be addressed is whether sevoflurane (like halothane and isoflurane) increases the open

probability of native TASK channels within the rat carotid body, in a manner similar to its effects on TASK channels in other (on O_2 sensing) tissues. Finally, the effect of sevoflurane is examined in TASK channels (rat TASK-1 and -3 subunits) expressed in HEK293 cells to confirm whether or not these agents have a direct effect on channel function, or if they require the machinery of the glomus cell in an obligatory way. The data presented in this chapter will be novel recordings, in which sevoflurane was compared within the same recording to another anaesthetic, with the paired statistics shown in the graphs. However, at the end of each section an overview graph will be shown, repeating also some results from the previous chapter, to offer the full perspective on sevoflurane versus halothane and isoflurane.

4.2 Methods

4.2.1 Glomus cell isolation

The detailed method of carotid body removal has been described in chapter 2 section 2.3. Briefly, carotid bifurcations were surgically removed from isoflurane anesthetized rat pups P10-P14. Carotid bodies were digested both enzymatically and mechanically, leading to a single cell suspension that was plated onto poly-L-lysine coated glass coverslips. Cells were stained with rhodamine-peanut-agglutin, which resulted in a bright orange stain for type-1 cells. All recordings took place within the same day as the surgery was performed.

4.2.2 Transient expression of TASK-1 and TASK-3 in HEK-293 and HEK-293t cells

Cells from the human embryonic kidney cell line HEK 293 and HEK-293t were grown in DMEM High glucose + sodium pyruvate (110mg/L) supplemented with 10% fetal calf serum, 100 units/mL penicillin/streptomycin and 6mM L-glutamine. RatTASK-1 and RatTASK-3 were inserted in pIRES-EGFP (Clontech: containing enhanced green fluorescent protein), which was transiently transfected using lipofectamine and PLUS reagent in HEK 293 cells. The pIRES-EGFP constructs were sequenced (Source Bioscience, Oxford, UK) to confirm correct insertion of either TASK-1 or TASK-3. For one experiment, TASK-3 in PcDNA3 (also sequenced for correct insertion) was co-transfected with empty pIRES EGFP into HEK-293t cells. 24-48 hours following transfection, cells were re-plated onto poly L-

lysine-coated glass coverslips and used for recordings. Transfected cells expressing TASK-1 or TASK-3 were identified by their green fluorescence.

4.2.3 Measurements of $[Ca^{2+}]i$ using Indo-1-AM

Rat glomus cells were loaded with Indo-1-AM at room temperature and incubated for exactly 1 hour.

Recording Protocol

Sevoflurane was vaporized using calibrated vaporizers at a range of concentrations in Tyrode solution (mM: 117 NaCl, 4.5 KCl, 1 $MgCl_2$, 23 $NaHCO_3$, 11 glucose, 2.5 $CaCl_2$) to measure the effect of sevoflurane on the hypoxia-evoked rise in $[Ca^{2+}]i$. At the start of each recording type-1 cells (bright orange cells, as described in glomus cell isolation) were identified and exposed to a hypoxic stimulus (1% O_2 in 5% CO_2 and N_2) to confirm a robustly hypoxic sensitive cell. Next, the cell was exposed to sevoflurane for ~ 1 minute in normoxia (21% O_2 5% CO_2), followed by a second exposure to hypoxia (equilibrated with halothane and/or isoflurane), which was followed by a recovery period in normoxia (no sevoflurane) of ~1 minute. Within each recording up to three different anaesthetic stimuli were applied. At the very end of the recording a control ~30 sec exposure to hypoxia was performed without anaesthetic to ensure appropriate recovery of the original hypoxic response. Only cells that demonstrated this recovery were included in analysis.

Statistical analysis of [Ca2+]i recordings in glomus cells

The statistical significance of the differences between the means of the agent response was assessed using factorial analysis of variance (ANOVA, SPSS for Windows version 10.0, SPSS Inc, Chicago, IL, USA). The ratio of the Ca^{2+} -transient was the 'response', the ANOVA tested for 'agent' (three levels, one for each agent) and 'concentration' (a level for each concentration). The locations of any significant effects were explored using post hoc student t-tests with the Bonferroni correction applied at the appropriate level if necessary. A p-value <0.05 was taken as statistically significant.

4.2.4 Cell attached patch clamping of glomus and HEK cells expressing TASK-1 and TASK-3

Cell attached patching recording conditions for glomus and HEK cells

Cell-attached patch clamp recordings were performed using an Axopatch 200B (Molecular Devices LLC, Sunnyvale, US). Recordings were made with borosilicate pipettes (Harvard Apparatus Ltd, Kent, UK) and were sylguard-coated and fire-polished before use. Single-channel recordings were filtered at 2–5 kHz and current was recorded and digitalized at 20 kHz. Voltage clamp control, data acquisition and analysis were performed using Spike2 (Cambridge Electronic Design, Cambridge, UK).

Cells were placed in the recording chamber in standard Tyrode in which seal formation was attempted with a borosilicate pipette. When a giga-ohm a seal was formed, the Tyrode solution was switched to one with 100 mM K^+ and a positive pipette potential was applied of +80mV. The pipette filling solution contained 140mM K+ 10mM and TEA and 5mM 4-AP (to block other K^+ channels). Under the recording conditions used in this study the type-1 cell background K^+ channel conducts inward currents exhibiting short, flickering openings. The protocol for anaesthetic application was (all in normoxic solutions and in high K^+ Tyrode for ~30-90 sec), (1) control (2) sevoflurane (3) control. A maximum of up to three different concentrations of the anaesthetic were applied within each recording in random order.

Data-analyses for glomus and HEK cells expressing TASK-1

For glomus cells and HEK cells expressing ratTASK-1, analysis of channel activity was performed on 20s sections of recording obtained at least 10s after any solution exchange (to allow full equilibration of oxygen and anaesthetic levels within the recording chamber). For each cell an all points histogram was constructed using a 20s section of data to determine the modal single channel current. This modal current was then used to analyse channel nPopen over a 20s time period using a 75% threshold crossing method.

Data analysis for HEK cells expressing TASK-3

For HEK cells expressing TASK-3, no single channel analysis was performed due to extremely high channel activity. Instead, the average current was measured for the control channel activity and channel activity during sevoflurane activity following baseline

substraction. The increase in channel activity evoked by an anaesthetic was expressed as a percentage increase of total current compared to control channel activity before.

Statistical analysis for glomus cell single channel recordings

Statistical analysis was conducted on the mean normalised nPopen values (obtained from a number of patches/cells) using factorial analysis of variance (SPSS for Windows version 10.0, SPSS Inc, Chicago, IL, USA), where normalised nPopen was the 'response' and there were two repeated measures factors: 'agent' (one level for each anaesthetic and one for no anaesthetic) and the locations of any significant effects were explored using post hoc Student t-tests and $p<0.05$ considered significant.

Statistical analysis for HEK cells expressing TASK-1 and TASK-3

The application of sevoflurane and isoflurane, or halothane and sevoflurane, were done within the same recording. Therefore, a paired t-test was conducted on the increase in current or channel activity evoked by the three anaesthetics.

4.2.5 Anaesthetic delivery

For all experiments involving anaesthetics (both patch clamping and Ca^{2+}), the gas phase above the bubbled solutions was constantly monitored by an infrared analyzer to assure accuracy and equilibration of concentrations as described in detail in methods chapter 2 section 2.5.

4.3 Results

4.3.1 Effect of sevoflurane on hypoxia evoked $[Ca^{2+}]i$ in glomus cell

Like halothane and isoflurane, sevoflurane did not change baseline levels of $[Ca^{2+}]i$ in normoxic conditions. Figure 4.1 shows the depression of the hypoxia evoked Ca^{2+} entry by halothane and isoflurane from chapter 3, with the sevoflurane representative traces added. Generally, $[Ca^{2+}]i$ increased rapidly on induction of hypoxia with this response being depressed by increasing doses of sevoflurane. The depression on $[Ca^{2+}]i$ was least with sevoflurane. There was good recovery of the Ca^{2+} response to hypoxia after anaesthetic washout.

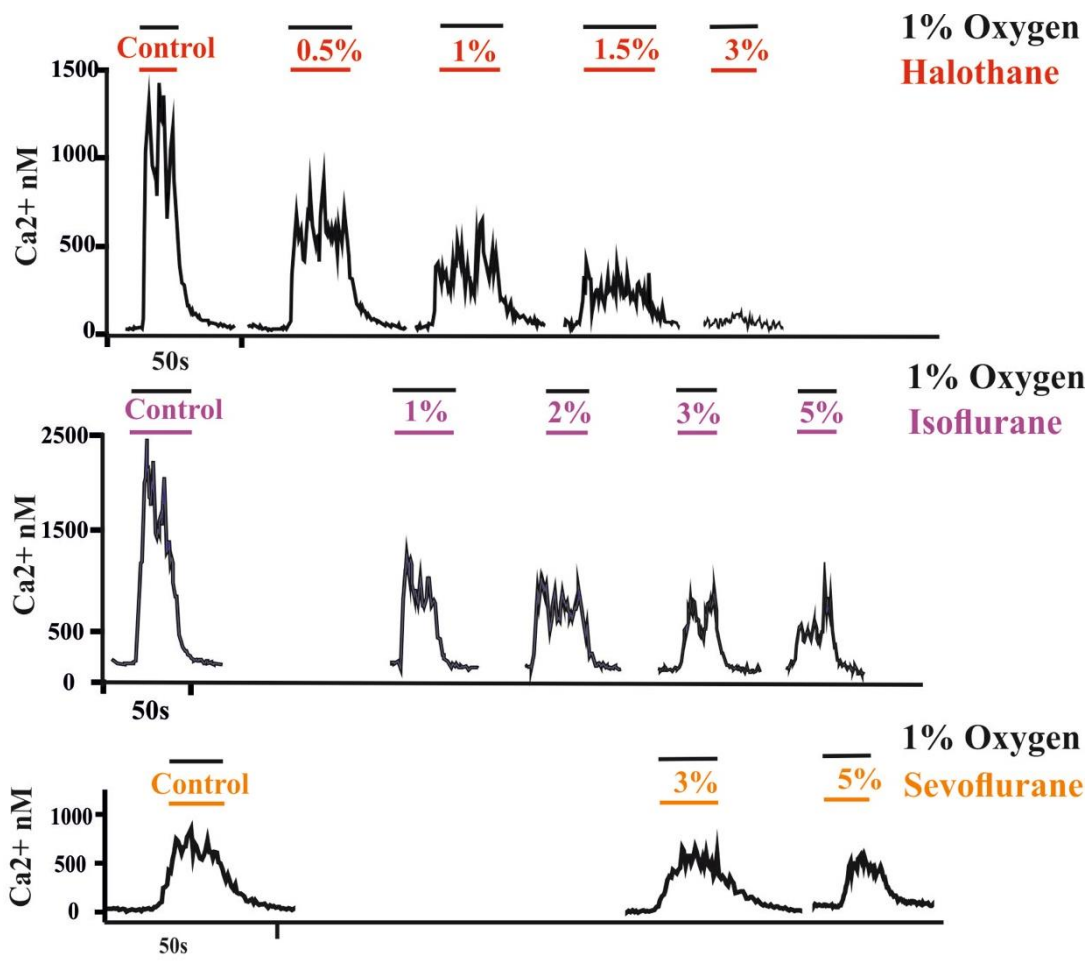

Figure 4.1: Representative traces of anaesthetics depressing the hypoxia evoked $[Ca^{2+}]i$. Within each panel the traces are: hypoxia (far left), then up to 4 concentrations of anaesthetic. Hypoxia stimulus consisted of 1% oxygen 5% CO_2 and the average exposure to hypoxia was 30s. **(A)** Halothane representative traces: at high enough concentrations halothane completely abolishes the Ca2+ influx. **(B)** Isoflurane representative traces: isoflurane does not completely abolish the Ca^{2+} influx even at supra clinical concentrations. **(C)** Sevoflurane representative traces: sevoflurane does not completely abolish the Ca^{2+} influx. The halothane and isoflurane data presented in this graph are a repeat from chapter 3.

Figure 4.2 shows the effect of the anaesthetics on the response to hypoxia, plotted as a 'concentration-response' relationship in absolute % concentration of anaesthetic in the gas-phase. Concentrations of 0.5%, 3% and 5% sevoflurane were applied, which led to a depression of 20.9%, 23.4%, and 21.0% respectively on the hypoxia evoked $[Ca^{2+}]i$. Consistent with the initial impression from the raw traces (Figure 1), quantitative analysis makes clear that sevoflurane is least depressive. ANOVA confirmed significant effects for 'anaesthetic' ($p<0.001$) when comparing halothane and isoflurane with sevoflurane. Post-hoc tests revealed that, when comparing sevoflurane and halothane, there was an agent difference between halothane and isoflurane ($p<0.001$) and also between isoflurane and sevoflurane ($p<0.005$), indicating that all agents depressed the response to hypoxia. The overall order of potency appeared to be halothane > isoflurane > sevoflurane.

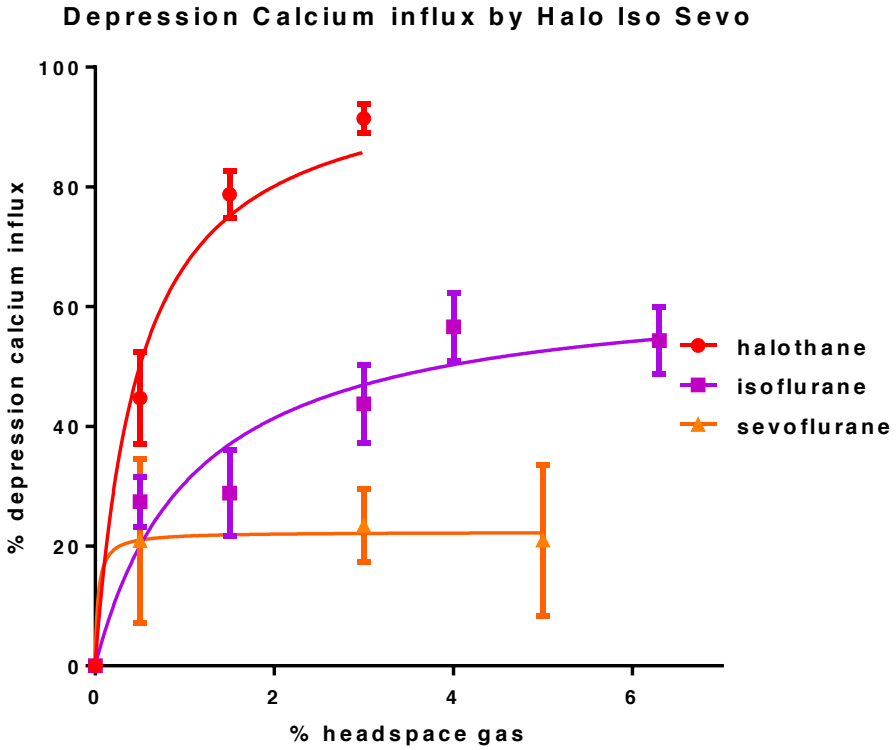

Figure 4.2: Depression of hypoxia evoked Ca^{2+} influx into glomus cells by anaesthetics. Points are mean +/- SEM, with N=3-13 recordings per point (total 88 data-points). Depression is plotted by normalising to the hypoxic response for that recording in absence of anaesthetic. The halothane and isoflurane data presented in this graph are a repeat from chapter 3.

The sevoflurane effect on single channel TASK activity was assessed at a range of concentrations. Figure 4.3 shows an example trace of single channel recordings from rat glomus cells, demonstrating the characteristic opening of TASK channels. Upon application of 5% sevoflurane, the TASK channel activity increases, leading to more frequent openings, an increase of double openings and a decreased long closed state. However, as can be seen in the halothane trace of a similar recording, the increase in activity evoked by sevoflurane was less than that by 5% halothane.

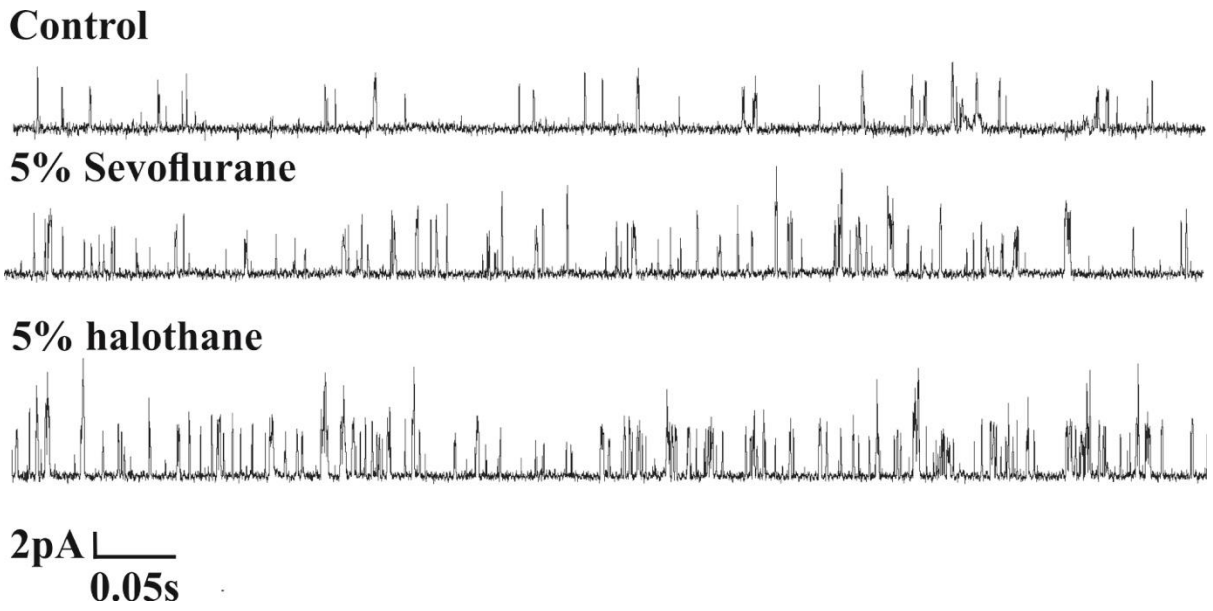

Figure 4.3: Representative trace of 5% sevoflurane increasing TASK channel activity in rat glomus cell. Representative single channel trace over ~1 second. Cells were superfused with 100 mM K^+ Tyrode, with 140 mM K+ in the pipette solution. Pipette potential was +80 mV.

Figure 4.4 shows a typical all points histogram for the channel activity upon sevoflurane exposure (in orange). Although the increase is clear, it is of a lesser magnitude than that of halothane.

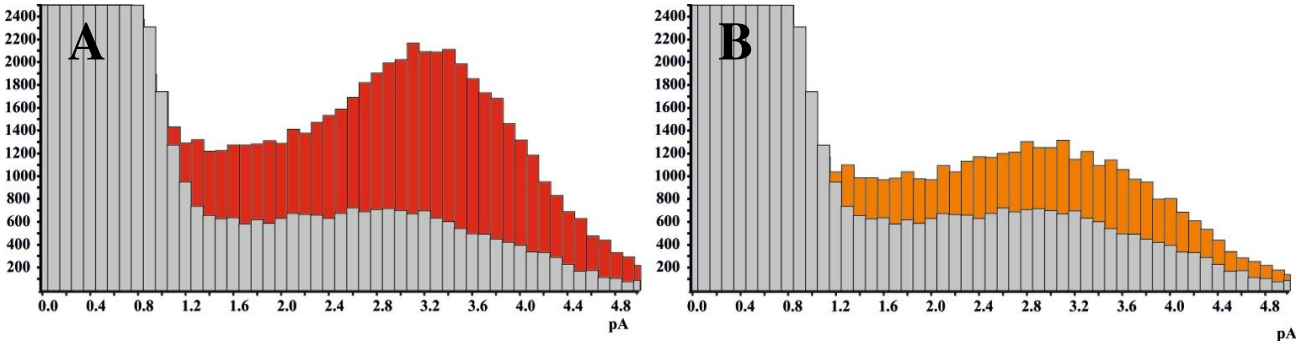

Figure 4.4: All-points histograms showing the effect of halothane and sevoflurane 5%. (10 fA bin widths) generated from 20 s segments of cell-attached recordings under standard recording conditions (+80mV pipette potential, 140mm K^+ and 100mM K^+ in Tyrode. **(A)** Halothane all-points histogram. **(B)** Sevoflurane all-points histogram from the same recording. Binwidth was 0.1pA

Figure 4.5 shows the quantitative analysis of the increase in channel activity as defined by nPopen for the three anaesthetics at the measured concentrations. ANOVA confirmed that the effect of 'agent' was highly significant ($P < 0.027$), suggesting that the three agents did differentially influence TASK channel opening. In post hoc tests the differences between halothane and sevoflurane were significant ($P = 0.004$), but there was no difference between isoflurane and sevoflurane ($P = 1.000$).

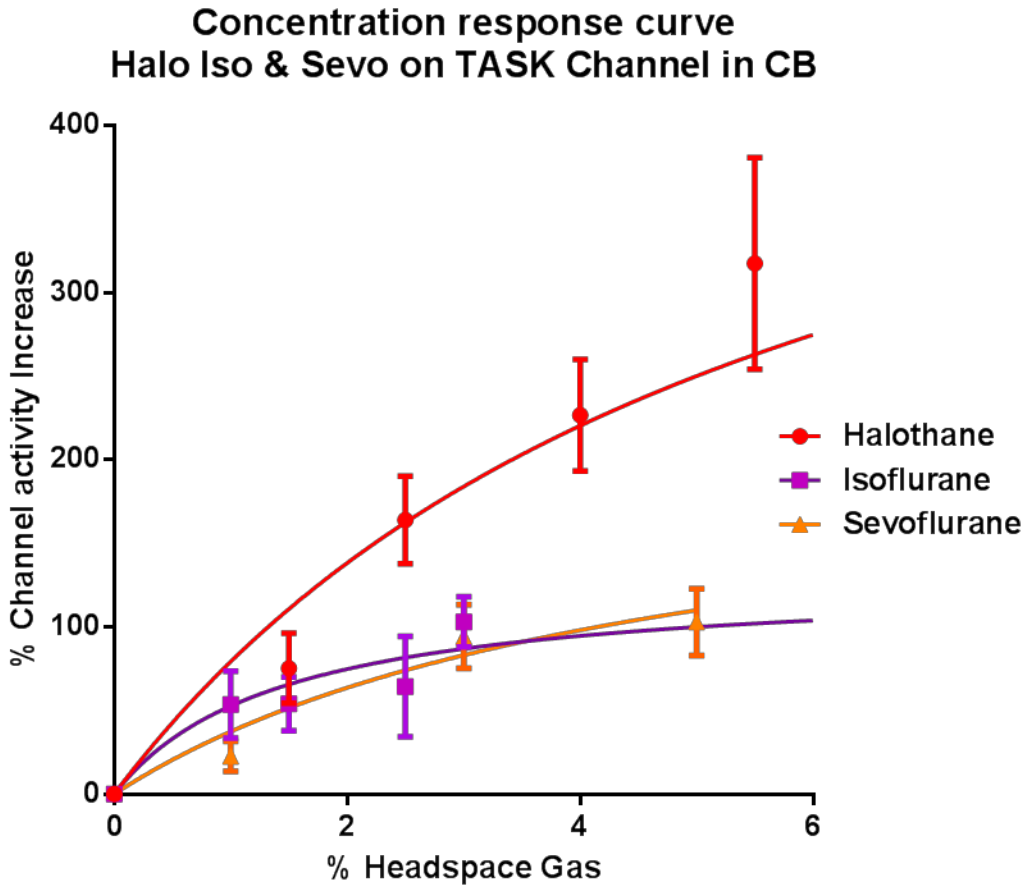

Figure 4.5: Influence of volatile anaesthetics on TASK channel activity. Displayed is the increase in nPopen, expressed as % increase from control value. Data are mean ± SEM. Cells were superfused with 100 mM K^+ Tyrode, with 140 mM K^+ in the pipette solution. Pipette potential was +80 mV. The halothane and isoflurane data presented in this graph are a repeat from chapter 3.

4.3.2 Effect of sevoflurane on HEK cells expressing TASK-3 and TASK-1 channels

HEK-293 cells were transiently expressed with either TASK-1 or TASK-3 and exposed to sevoflurane. This was done for two reasons: firstly, in order to assess if I could replicate activation of TASK-1 by sevoflurane and secondly, because unlike TASK-1, sevoflurane had to my knowledge not been studied on TASK-3 yet.

Electrophysiology on HEK cells expressing TASK-3

Sevoflurane 2.5% and halothane 2.5% was applied to five HEK cells expressing TASK-3. The TASK channel activity increase was small but considerable upon sevoflurane application, as seen in the exemplar trace in Figure 4.6A. Sevoflurane evoked an increase in average current of 23.5% (SEM 5.5%), which was less compared to halothane that evoked an increase in channel activity of 122% (SEM 32.4%). A paired t-test revealed that compared to halothane 2.5%, the magnitude of the effect evoked by sevoflurane was smaller (P= 0.026, Figure 4.6B).

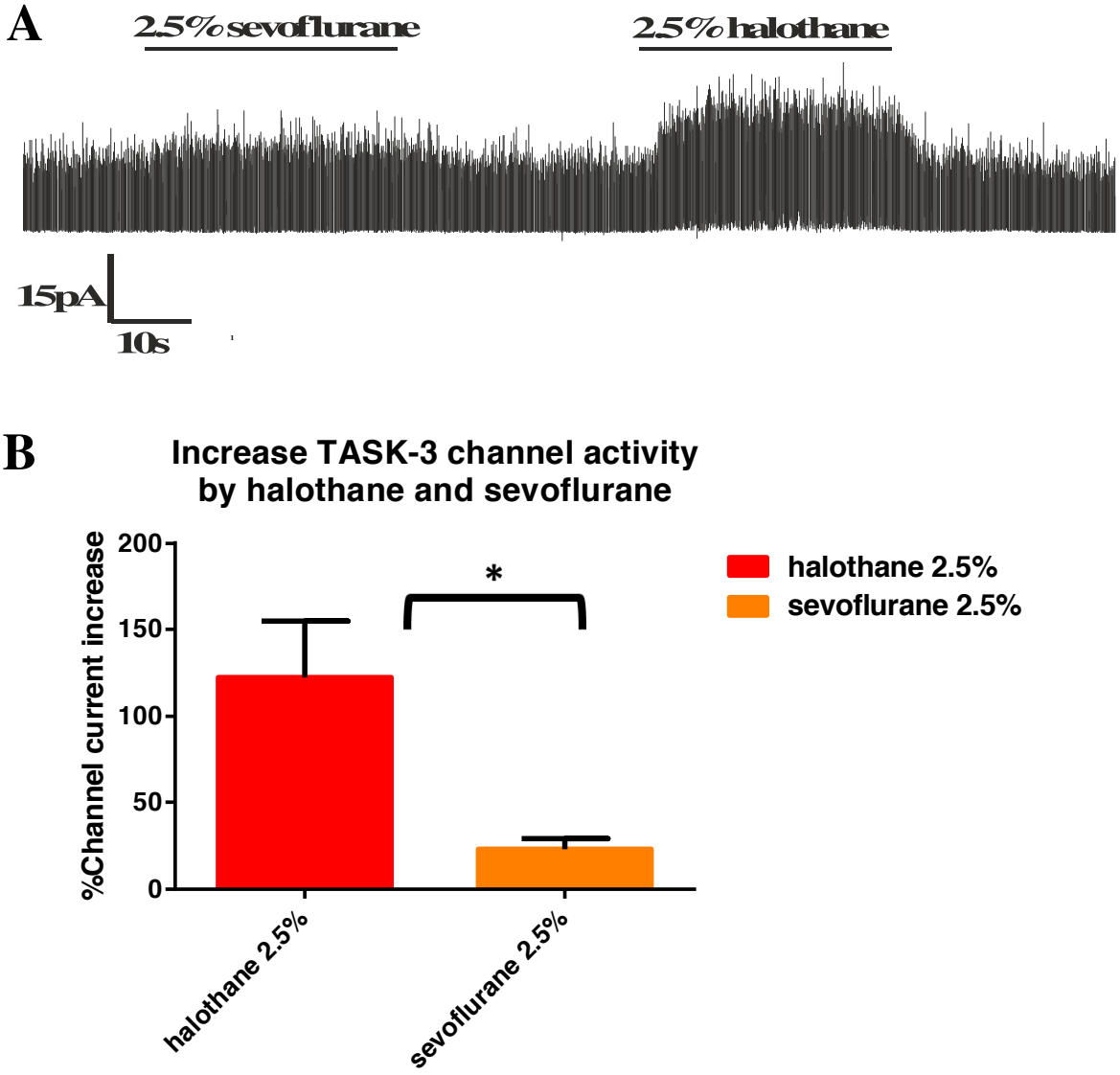

Figure 4.6: Increase in TASK-3 channel activity by 2.5% sevoflurane and 2.5% halothane in HEK-293 cells. (A) Representative trace of TASK-3 channel activity over approximately 2 minutes. **(B)** Sevoflurane and halothane (n=5) significantly differ in the increase in channel activity: paired t-test p= 0.026. Cells were superfused with 100 mM K^+ Tyrode, with 140 mM K^+ in the pipette solution. Pipette potential was +80 mV.

Four HEK cells expressing TASK-3 were exposed to sevoflurane 2.5% and isoflurane 2.5%. A representative trace in Figure 4.7A, reveals that isoflurane increases the channel activity more so than sevoflurane. Sevoflurane evoked an increase in average current of 20.9% (SEM 4.2%), whereas isoflurane evoked an increase of 54.8% (SEM 5.9%). A paired t-test revealed that compared to isoflurane 2.5%, the magnitude of the effect evoked by sevoflurane was smaller (P= 0.043, Figure 4.7B).

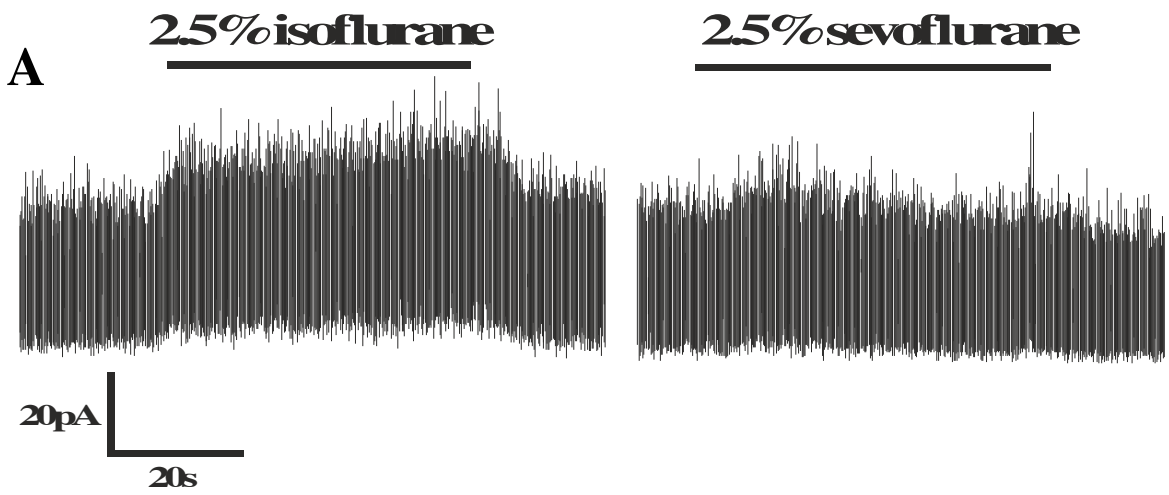

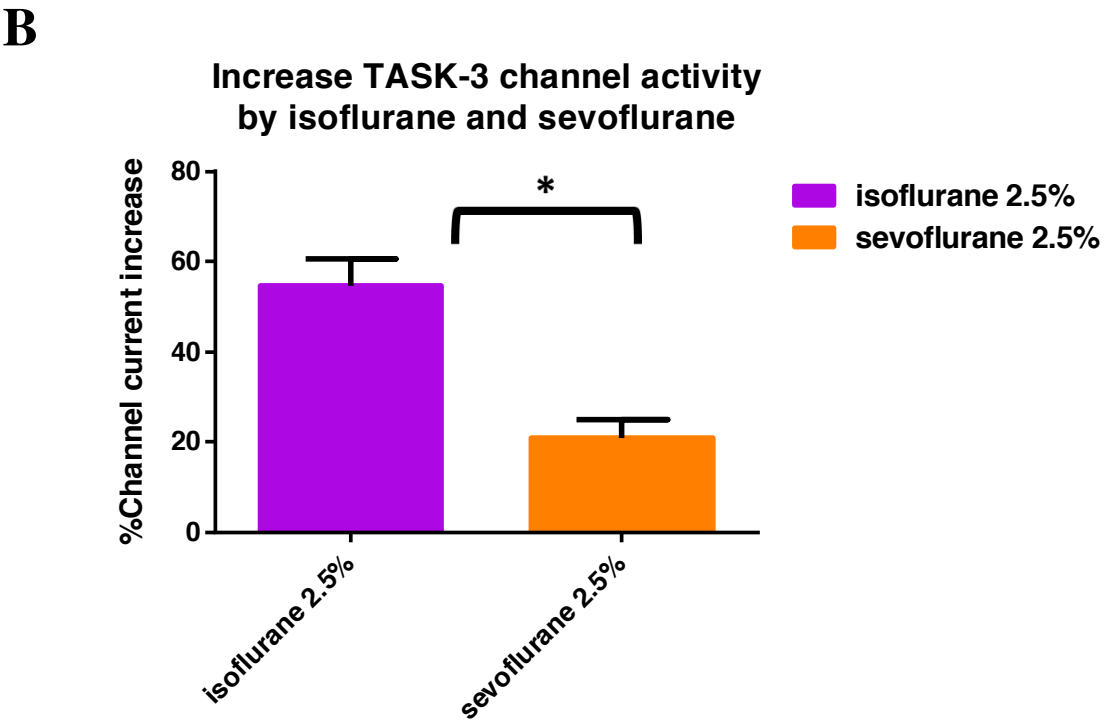

Figure 4.7: Increase in TASK-3 channel activity by 2.5% sevoflurane and 2.5% isoflurane in HEK-293t cells. (A) Representative trace of TASK-3 channel activity over approximately 2 minutes. **(B)** Sevoflurane and isoflurane (n=5) significantly differ in the increase in channel activity, paired t-test p= 0.026. Cells were superfused with 100 mM K^+ Tyrode, with 140 mM K^+ in the pipette solution. Pipette potential was +80 mV.

Electrophysiology on HEK cells expressing TASK-1

The overall level of channel activity seen in HEK cells expressing TASK-1 was low enough to allow for standard single channel analysis. Sevoflurane 3% and halothane 2.5% was applied to five HEK cells expressing TASK-1. The channel activity increase was small but considerable upon sevoflurane application, as seen in the exemplar trace in Figure 4.6A. Sevoflurane evoked an increase in average current of 33.1% (SEM 5.6%), which was less compared to halothane that evoked an increase in channel activity of 88.3% (SEM 14.8%). A paired t-test revealed that compared to halothane 2.5%, the magnitude of the effect evoked by sevoflurane was smaller (P= 0.04, Figure 4.8B).

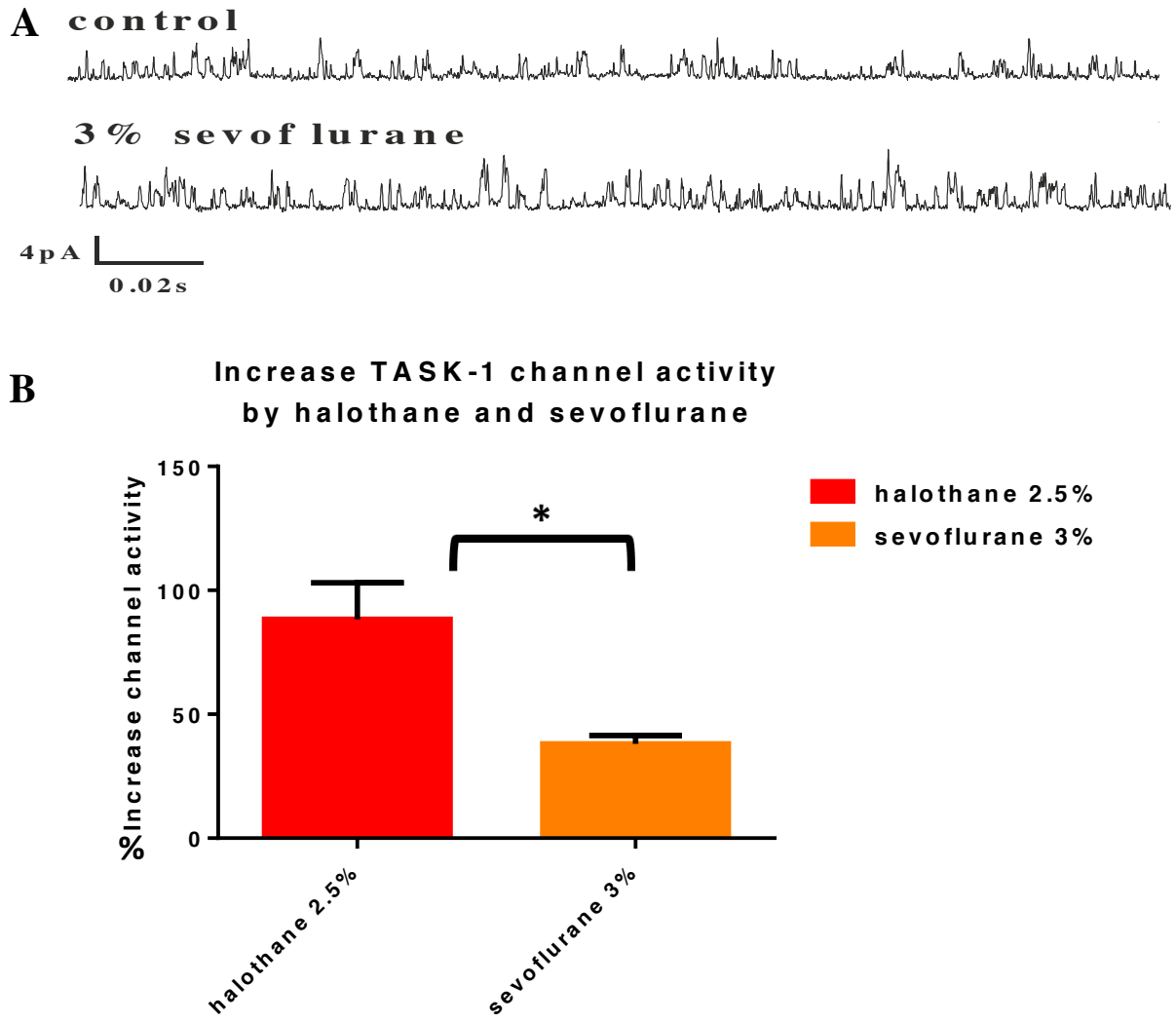

Figure 4.8: Increase in TASK-1 channel activity by 3% sevoflurane and 2.5% halothane in HEK-293 cells. (A) Representative trace of TASK-1 channel activity over approximately 0.3s. **(B)** Sevoflurane and isoflurane (n=5) significantly differ in the increase in channel activity, paired t-test p= 0.04. Cells were superfused with 100 mM K^+ Tyrode, with 140 mM K^+ in the pipette solution. Pipette potential was +80 mV.

Summary of the comparative study of sevoflurane on TASK-1 and TASK-3

In Figure 4.9 an overview bar chart can be seen for both TASK-1 and TASK-3 in which all the data-points are collected for the 2.5% concentration (except for TASK-1 sevoflurane 3%), which were 63 data-points in total. Remarkably, even in these expressed channels the same order of potency is reflected as that observed in the depression of the AHVR in humans.

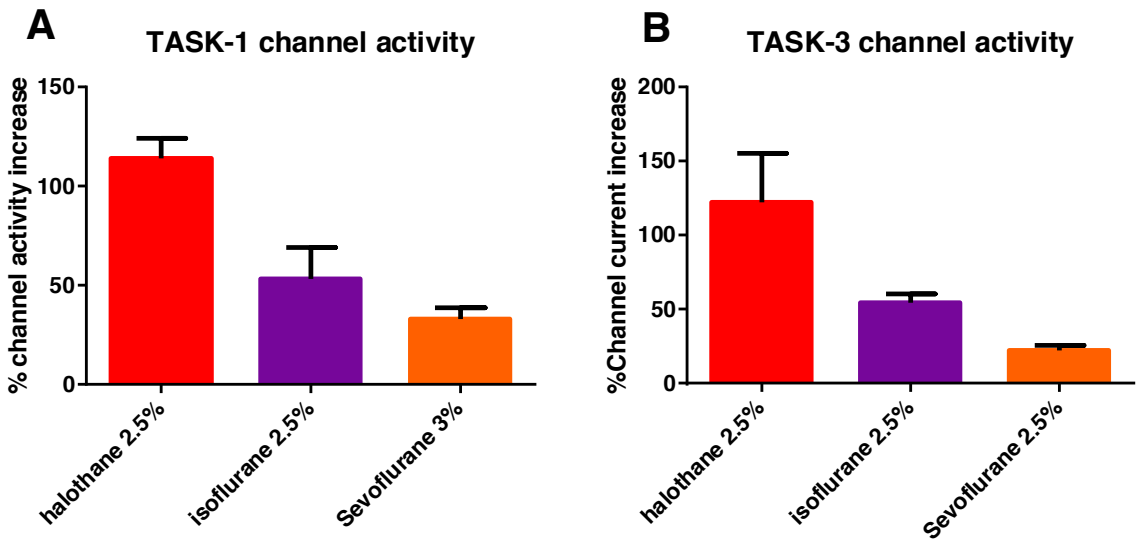

Figure 4.9: Channel activity of halothane, isoflurane and sevoflurane in HEK cells transiently expressed with TASK-1 or TASK-3. Table summarizes all the data-points obtained for the 2.5% data-points (except for 3% sevoflurane in TASK-1). (A) Average Increase in channel activity halothane 2.5% (n=33) isoflurane 2.5% (n=10) sevoflurane 3% (n=5). (B) Average increase in channel current halothane 2.5% (n=5) isoflurane 2.5% (n=5) sevoflurane 3% (n=5).

4.4 Discussion

The novel results in this chapter are that sevoflurane very modestly depresses the hypoxia-evoked rise in $[Ca^{2+}]i$ in glomus cells; that it increases channel opening of the native heterodimeric TASK channel in glomus cells; and that it acts to increase channel opening of both TASK-1 and TASK-3 in HEK293 cells transiently expressed with these channels. At all levels studied, sevoflurane is less effective than halothane in depressing the hypoxia evoked Ca2+ entry and in increasing the activity of both native and expressed TASK channels. Compared to isoflurane, sevoflurane is also less effective in depressing the hypoxia evoked Ca2+ entry and in increasing the expressed TASK-1 and TASK-3 channel activity. Only at native channel level in the glomus cell, there is no significant difference between isoflurane and sevoflurane in its effect.

Sevoflurane's relatively modest effect on each of these processes is not only in keeping with the observation from humans and rats, in that it is a weak depressant of the hypoxic chemoreflex, but also in mice, as recently established in our lab by fellow DPhil student P O'Donohoe (2015). In that regard, these results reflect the previous finding that there is a specific order of potency for the depressive effects of these agents: halothane > isoflurane > sevoflurane. This order seems to be conserved across the organisational hierarchies from whole organism, to glomus cell and to TASK channels. As the experiments in this chapter are performed on rat glomus cells, they are extending the work of Karanovic et al., who carefully observed in intact rats that halothane was the most potent depressant of the hypoxic chemoreflex, while sevoflurane was the least. Since TASK channels are believed to play a

key role in O_2-sensing, the experiments in this chapter provide a plausible explanation (at least in part) as to why sevoflurane is the least depressive volatile agent.

The sevoflurane results are also consistent with the results of Sirois et al. (1998) who found halothane, isoflurane and sevoflurane to activate a Ba^{2+} and voltage-sensitive current in motoneurones (likely a TASK or TASK-like channel). Sirois et al. (2000) reported that halothane activated TASK-1 channels heterologously expressed in HEK-293 cells (as confirmed in this chapter), but did not extend that work to analysing possible effects of isoflurane or sevoflurane. They did, however, confirm that these latter two agents activated pH-sensitive K+ current (presumably TASK) in hypoglossal motoneurones. Putzke et al. (2007) showed that sevoflurane activated whole cell current in oocytes expressing human TASK-1, but did not perform a specific comparative studies not studied TASK-3. Therefore, my results both confirm and further refine the knowledge regarding sevoflurane and cloned and carotid body TASK channels to date.

The predominant native TASK channel found in glomus cells is now thought to be a TASK-1/3 heterodimer but it remained unclear which subunit (or both) sevoflurane might influence. The results provide compelling evidence that in fact, sevoflurane can influence both subunits.

The concentrations of sevoflurane were clinically relevant. Where higher concentrations were used, this was for a concentration-response effect to look for a ‘max’ effect, rather than mimic clinical conditions at cell level. While concentrations like 5% sevoflurane are unlikely used for maintenance anaesthesia, they are commonly employed for inhalational induction.

In summary, the experiments in this chapter demonstrate a small effect of sevoflurane on the hypoxic response (hypoxia evoked Ca2+ entry and TASK channel activity) and a direct effect on both TASK-1 and TASK-3 channels in a transiently expressed system. It remains interesting and intriguing that the effect of these anaesthetics on TASK channels resemble (and therefore might at least in part explain) their behaviour on whole-body hypoxic ventilatory response. Furthermore, the relative small effect of sevoflurane on the systems studied is reassuring, as it is the most commonly used maintenance volatile anaesthetic in the UK.

Chapter 5. The influence of volatile anaesthetics on mitochondria in rat glomus cells

5.1 Introduction

How exactly oxygen sensing occurs in the type-1 cell of the carotid body has not been completely elucidated, but as discussed in chapter 1, a number of candidate mechanisms and components have been proposed based on the distinct features that make the type-1 cell specifically oxygen sensitive compared with most other cells in the body. One feature is the closing of carotid body TASK channels in response to low oxygen. However, the TASK channel itself is probably not directly oxygen-sensitive as, unlike native TASK channels in type-1 cells, TASK channels expressed in HEK cells, or those studied in excised patches, do not appear to be oxygen responsive (Buckler et al., 2000, Buckler and Honore, 2004). These observations raise the possibility that the TASK channel is regulated by factors further upstream, which are themselves sensitive to oxygen.

Leading candidates for this oxygen sensing function are the mitochondria. Mills and Jobsis (1972) reported that the respiratory chain in the carotid body has an unusual sensitivity for oxygen. Duchen and Biscoe (1992a) showed that mitochondrial NADH levels change below a PO_2 of 60mmHg in type-1 cells, whereas in other tissues (such as chromaffin cells) this did not happen until the PO_2 fell below 5mmHg. The authors suggest that mitochondria in type-1 cells can alter their respiratory function over the physiologically relevant PO_2 range. In the accompanying paper (Duchen and Biscoe, 1992b) the authors explored the link between hypoxia and mitochondria further and reported that the mitochondrial membrane potential depolarize in response to hypoxia and that this depolarisation is graded (just like the increase of [NADH]) to graded levels of hypoxia. Wyatt and Buckler (2004) have provided further

evidence for the key role of mitochondria in oxygen sensing, by demonstrating that inhibitors of the mitochondrial transport chain significantly inhibited background K^+ currents in type-1 cells.

Although this research provides compelling evidence that mitochondria are involved in oxygen sensing and TASK channel regulation, it remains unclear how exactly the slowdown of electron transport in mitochondria leads to a decrease in TASK channel open probability. One possibility is that this link may consist of altered levels of mitochondrial metabolites, such as ATP, Mg-ATP or AMP-Kinase and that these metabolites directly or indirectly influence TASK channel opening (Varas et al., 2007, Peers et al., 2010, Buckler, 2015). The activity of TASK channels in inside-out patches is influenced by solutions containing Mg-ATP (Varas et al., 2007).

In normoxic conditions in the electron transport chain complexes I to IV pump, or aid in pumping, protons across the mitochondrial membrane, which maintains a negative mitochondrial membrane potential. The pumped protons in turn diffuse back into the inner membrane through ATP-synthase and so generate ATP (Sazanov et al., 2013). In hypoxic conditions the electron transport chain function is impaired, such that the mitochondrial membrane potential diminishes (ie, depolarises). Due to the slower electron transport, less NADH is converted to NAD^+ to release its electrons and protons and, as a consequence, fewer electron and protons will be pumped across the membrane. As a result, ATP levels decline (Varas et al., 2007). Hypoxia thus evokes an increase in [NADH] and depolarizes the mitochondrial membrane and decreases ATP production.

The increase of NADH as a result of impaired electron transport can be measured, because NADH is auto-fluorescent when excited at the right wavelength, but NAD is not (Mayevsky and Rogatsky, 2007). Separately, mitochondrial membrane potential can be measured using a voltage sensitive dye that will change in fluorescence intensity as the membrane potential changes (Skarka and Ostadal, 2002). Using such measurements, Buckler and Turner (2013) have recently confirmed that changes in mitochondrial membrane potential and [NADH] are more sensitive in type-1 cells compared to other cells.

Volatile anaesthetics have also been reported to inhibit mitochondrial function and this has been proposed to be a mechanism for anaesthetic-induced depression of cellular function, especially in the heart (Hall et al., 1973, Merin, 1973, Rusy and Komai, 1987), or as a possible mechanism for 'anaesthetic preconditioning' (Riess et al., 2002). This is the observation that a brief period of exposure to volatile anaesthetic protects the myocardium from later hypoxic- (or anaesthetic-) induced depression of function or cell damage. Hanley et al. (2002) reported that volatile anaesthetics (halothane, isoflurane and sevoflurane) reversibly and dose dependently increase NADH auto-fluorescence in ventricular myocytes. In sub-mitochondrial particles the authors furthermore show that the rate of ubiquinone oxidoreductase (complex I) activity with an artificial electron-acceptor (decylubiquinone) was slowed down in the presence of anaesthetics, attributing the effect of increased NADH to partial inhibition complex I activity. An additional modification to this experiment also showed some effect of halothane (but not isoflurane or sevoflurane) on complex II activity.

Hanley and Ray's observation is also interesting, because it demonstrates that, in cardiac tissue, anaesthetics can act in a manner similar to the effect of hypoxia (i.e., increasing

NADH levels). Yet, in relation to carotid body function it is well established that anaesthetics act antagonistically to hypoxia (as described in chapter 3 and 4). In contrast to almost all other tissues, the carotid body is excited by hypoxia. Anaesthetics partly oppose the effect of hypoxia on type-1 cells, which is manifested in several levels: on type-1 cell depolarisation, on hypoxia evoked [Ca^{2+}] entry (Buckler et al., 2000) and on the opening of TASK channels (Pandit and Buckler, 2010).

The aim of this chapter is thus to assess if volatile anaesthetics act like hypoxia to increase [NADH] (as Hanley and Ray (2002) observed in cardiac myocytes) and also depolarise the mitochondrial membrane potential. Or whether, given well-established observations on anaesthetics on type I cell hypoxic response, anaesthetics would act to oppose the effect of hypoxia and thus reduce [NADH] (in contrast to Hanley and Ray's results) and hyperpolarise the mitochondrial membrane potential.

5.2 Methods

The extended methods for both NADH measurements and Rh123 can be found in the methods section 2.9 and 2.10. A brief summary will be given below, including the detailed information regarding the recording protocols.

5.2.1 Single cell isolation

The method of carotid body removal has been described in chapter 2 section 2.4. Briefly, carotid bifurcations were surgically removed from isoflurane anesthetized rat pups P10-P14. Carotid bodies were sub-dissected and a single cell suspension was generated and plated onto poly-L-lysine coated glass coverslips. Cells were recorded on the same day as that surgery took place.

In the recording chamber, cells are constantly perfused with Tyrode (in mM: 117 NaCl, 4.5 KCl, 1 $MgCl_2$, 23 $NaHCO_3$, 11 glucose, 0.1 EGTA) equilibrated with either normoxic (21% O_2) or anoxic (0% O_2) gas with or without volatile anaesthetic, as described below. EGTA was added to chelate any contaminating Ca^{2+} to maintain a zero Ca^{2+} extracellular environment. The reason for choosing Ca^{2+}-free Tyrode instead of normal Tyrode, is because in normal Tyrode Ca^{2+} would enter the cell in response to anoxia. This is undesired, because elevation of $[Ca^{2+}]i$ promotes mitochondrial Ca^{2+} uptake, which can activate NADH producing dehydrogenases and depolarize the mitochondrial membrane (McCormack and Denton, 1989, Werth and Thayer, 1994). This Ca^{2+} evoked NADH increase and change in potential is therefore a confounder of the research.

5.2.2 Protocols and measurements of NADH

Type-1 cells incubated with rhodamine-PNA were identified by their bright orange staining. NADH was excited at 340nm and fluorescence was measured at 450±15nm. The output of the PMT was connected to an IV converter that generated an output in volts. Before the start of each recording, the cell was moved out of the field, which allowed the background to be set at 0 volts, corresponding to the background emission. After this the cell was moved back into the field leading to a value in volts corresponding with the cell in steady state 21% oxygen in standard Tyrode. The traces generated in this chapter show raw data (in volts) on the y-axis. Other graphs show the increase in fluorescence for each volatile anaesthetic as a % of the maximal fluorescence increase obtained in response to an anoxic stimulus (5% CO_2 95%N_2 + 100μM $Na_2S_2O_2$).

Cells were exposed to the following protocol for NADH measurements. An anoxic stimulus (5% CO_2 and 95% N_2 + 250μM $Na_2S_2O_2$) was applied for 30 sec (to calibrate the NADH response as described above). Then, cells were exposed to a range of anaesthetic concentrations. For halothane and isoflurane these were zero, 0.5%, 1%, 1.5%, 2.5% or 3% and for sevoflurane these were zero, 2%, 3% or 5%.

As a control experiment, a complex I inhibitor, rotenone was applied with and without 1.5% isoflurane. Mitochondrial NADH fluorescence in the presence of rotenone will be maximal and therefore if isoflurane evokes any additional changes in fluorescence in the presence of rotenone, it would indicate a non-specific effect of isoflurane.

5.2.3 Measurements of mitochondrial membrane potential

Carotid body cells were incubated with rhodamine-123, which results in an increase in fluorescence following mitochondrial membrane depolarisation (See section 2.10). Each recording of mitochondrial membrane potential started and ended with an application of I μM FCCP. In between there were up to two 30-60 sec exposures to anaesthetic, followed by an anoxic stimulus of 30-60 sec. Anaesthetic exposure consisted of halothane (1% or 3%), isoflurane (0.5%, 1.5% or 3%) or sevoflurane (2% or 5%). It was assumed that FCCP elicited a near total mitochondrial depolarisation and so the peak of this response was set at 100%. The reference 0% baseline was set to the initial amount of fluorescence within the cell, measured in standard Tyrode (normoxia). Responses to volatile anaesthesia and anoxia were then measured on this 0-100% scale. FCCP was applied with and without isoflurane 3%, to check for non-specific effects of anaesthetics on Rh123 fluorescence.

5.2.4 Statistical analysis

Comparisons of concentration-response relationships were assessed with factorial analysis of variance (ANOVA), with the factors being ‘agent’ (three levels, one for each agent) and ‘dose’ (three levels, one for each dose). Any significant effects were explored with post hoc paired t-tests.

5.3 Results

5.3.1 Measurements of the anaesthetic effect on [NADH] in type-1 cells

Figure 1 shows a representative trace of the [NADH] increase evoked by anaesthetics. Anoxia rapidly increases [NADH], followed by a rapid recovery upon reoxygenation, followed by a rebound with a slower recovery. All three anaesthetic agents also, but to a lesser extent sevoflurane, increase [NADH] with a return to baseline on washout. Compared to anoxia, the onset of both the increase and decrease in NADH is more gradual than that of anoxia. FCCP is expected to maximally oxidise mitochondrial NADH to NAD^+ and represent the lowest range of fluorescence for each recording. The remaining fluorescence in the presence of FCCP is assumed to represent non mitochondrial NADH and background fluorescence.

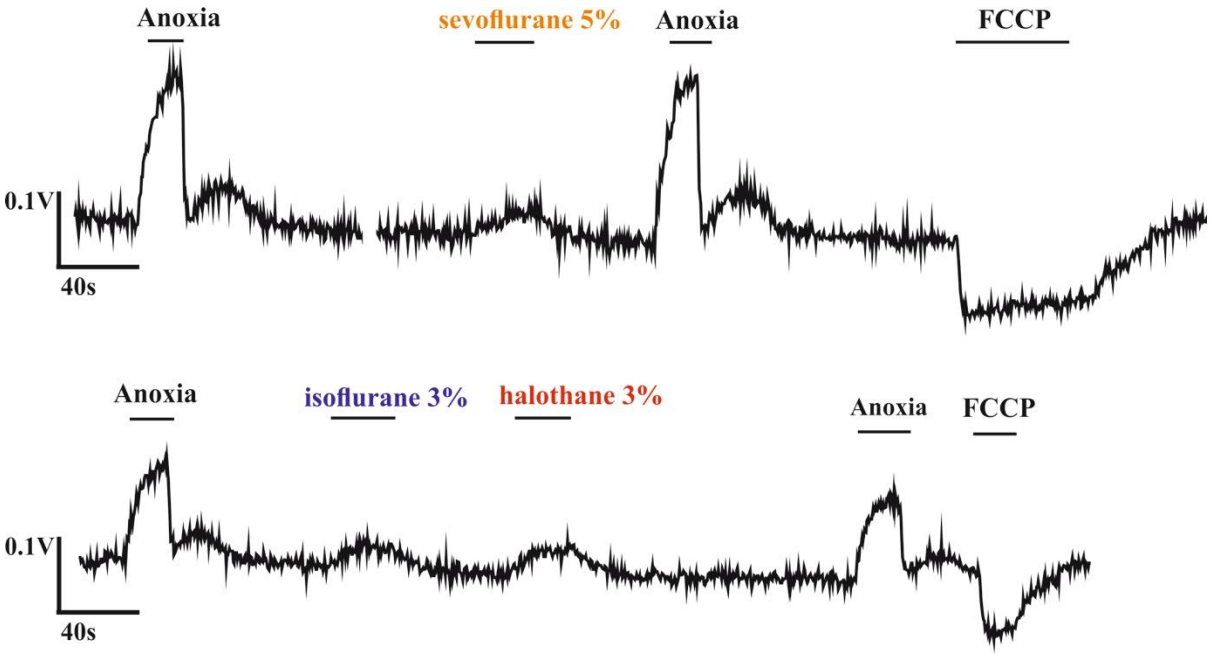

Figure 5.1: Representative traces of NADH auto-fluorescence. The increase in NADH fluorescence in volts, evoked by **(A)** sevoflurane 5% and **(B)** isoflurane 3% and halothane 3%.

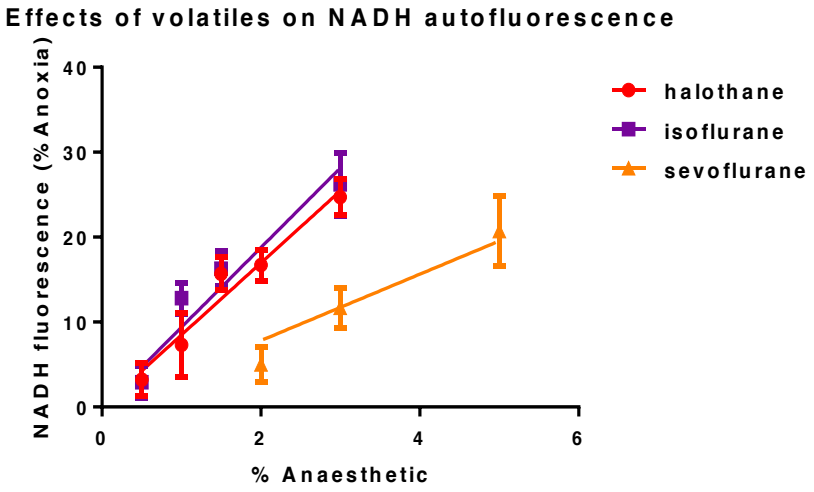

Figure 5.2: Concentration-response curve of halothane isoflurane and sevoflurane on NADH auto-fluorescence in rat glomus cells. Data represented as mean ± SEM. The y-axis is normalised to the fluorescence obtained with anoxia, and the x-axis is the concentration of anaesthetic delivered in percentages. Total of 77 data-points.

Figure 5.2 shows the concentration dependence of NADH increase for each agent. Over the range of concentrations assessed (which are in the clinically relevant range) NADH fluorescence increases linearly with anaesthetic concentration. Analysis of covariance (ANOVA) was used to assess the significance of differences between agents and dosing. The response sensitivity to halothane and isoflurane are similar ($p = 0.370$; NS) but sevoflurane clearly has a much weaker effect ($p>0.001$).

No evidence of saturation of the NADH response was observed in the concentration response relationships for any agent, so the potential for additive effects between any two agents, if administered simultaneously was assessed. Figure 5.3A shows a representative trace, which indicates that the effect of halothane and isoflurane in combination is greater than each alone. Figure 5.3B shows the quantitative analysis, indicating a precisely additive effect on NADH, when two agents are combined (fluorescence of 18% and 17% with halothane and isoflurane respectively, and 39% with the mix; $p<0.001$, $n=7$).

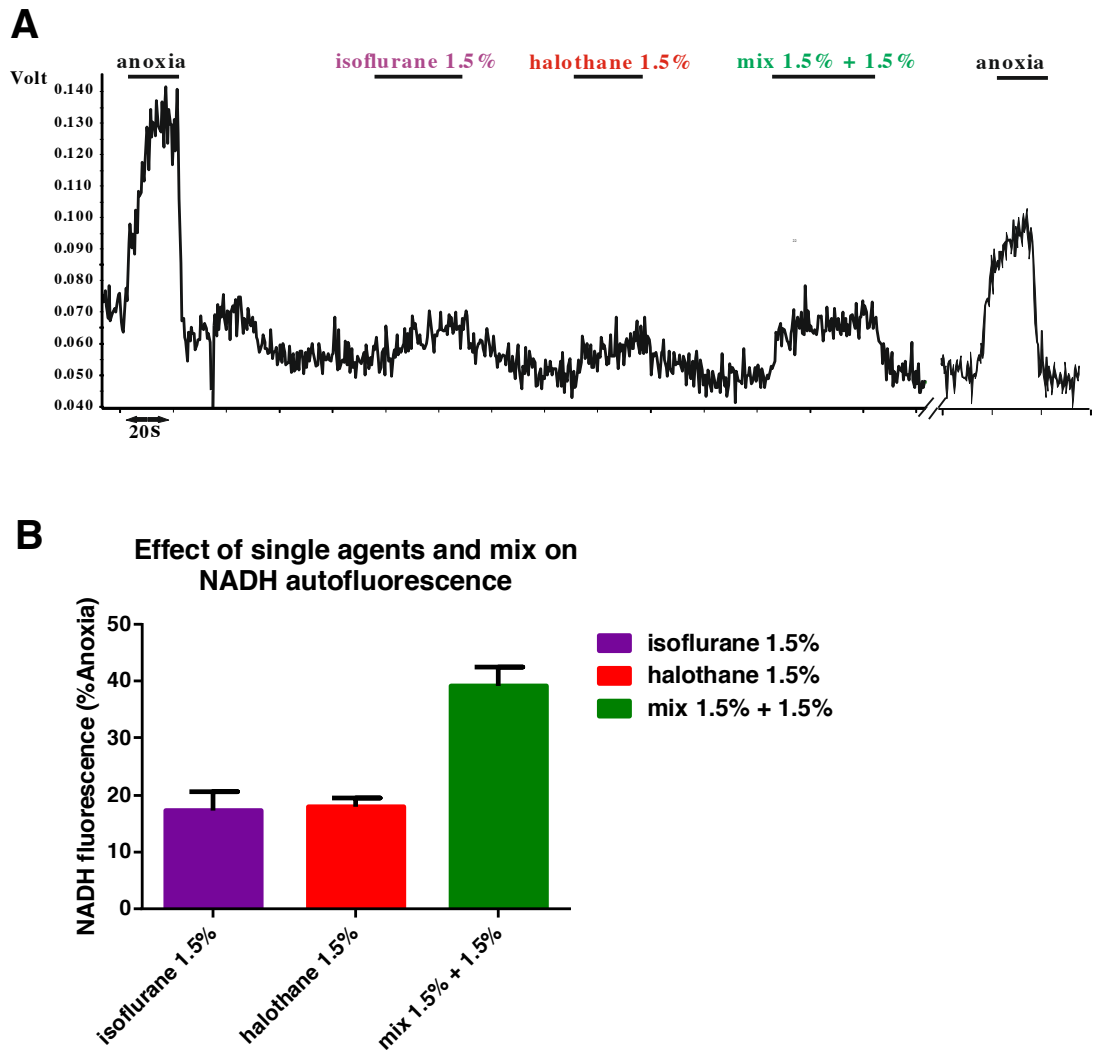

Figure 5.3: Increase of NADH fluorescence by single agent volatile anaesthesia and mixes. (A) Representative trace of NADH auto-fluorescence evoked by 1.5% halothane, 1.5% isoflurane and a mix of 1.5%/1.5% halothane/isoflurane. **(B)** Quantitative analysis of the effect of mixtures of halothane and isoflurane (mean ± SEM; n = 7, paired t-test). NADH fluorescence is expressed as the % of value of the first anoxic response.

5.3.2 Control for non-specific effects of anaesthetic on NADH auto-fluorescence

Since it was found that anaesthetics increase [NADH], a subsidiary question that arose was whether anaesthetics solely targeted complex I and not any other possible, but undefined,

sources of auto-fluorescence. Therefore, it was assessed whether the most potent agent for this effect, isoflurane (Figure 5.4) was additive to the effect of rotenone (complex I inhibitor). There was no significant effect of the addition of isoflurane in the presence of rotenone (Figure 4; p = 0.599, paired t-test).

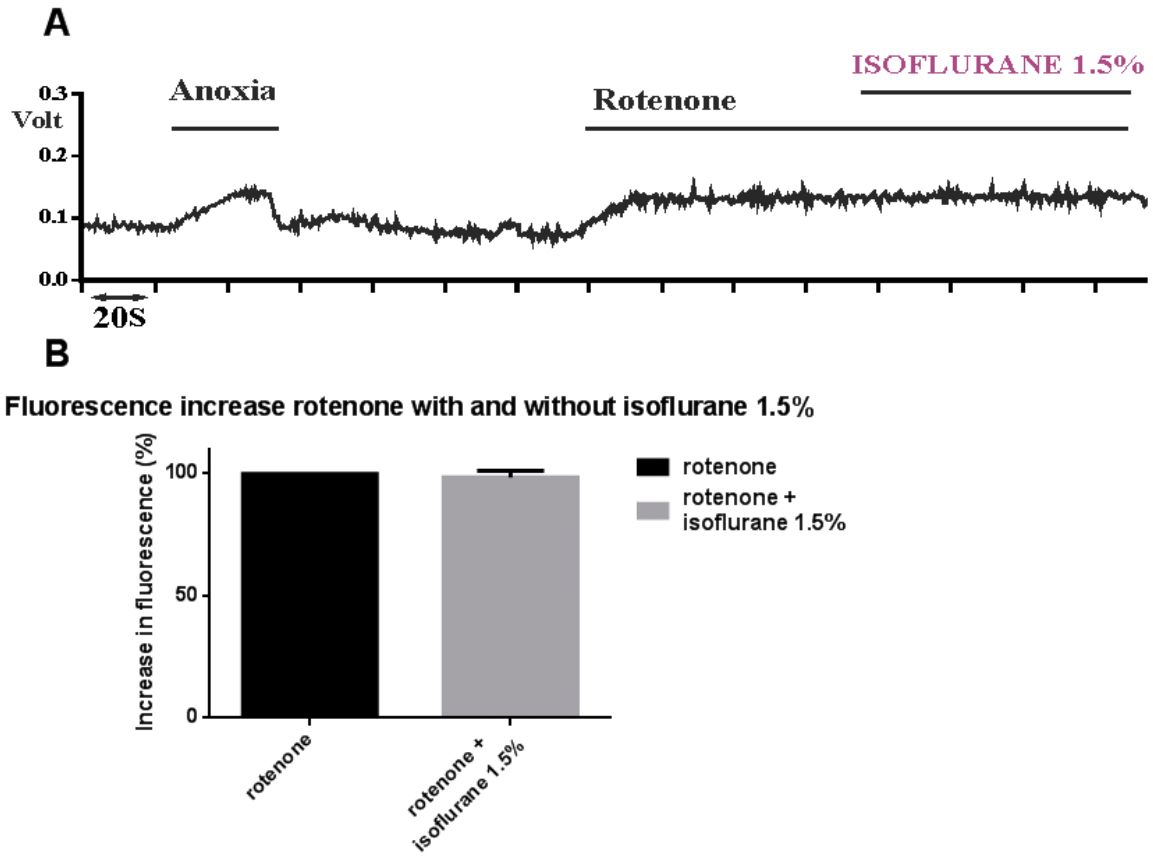

Figure 5.4: Effects of rotenone in combination with isoflurane on NADH auto-fluorescence in type-1 cells. **(A)** representative trace **of** NADH auto-fluorescence evoked by rotenone with and without 1.5% isoflurane. **(B)** Change in fluorescence of isoflurane 1.5% + rotenone compared to rotenone alone (mean ± SEM; n = 5). The y-axis is the % increase in fluorescence from baseline; the comparison of isoflurane effect is NS (p = 0.599).

In summary, the increase of NADH auto-fluorescence evoked by the application of isoflurane, halothane and sevoflurane suggests that these agents possibly inhibit the electron

transport in type-1 cells. To further explore this, changes in membrane potential were measured during application of anaesthetics.

5.3.3 Measurements of anaesthetics on mitochondrial membrane potential in type-1 cell

All anaesthetic agents evoked a small depolarisation in mitochondrial membrane potential to varying degrees (Figure 5.5). From the raw traces it appears that anaesthetics exhibited a similar order of potency as they did on [NADH] of isoflurane ≥ halothane > sevoflurane.

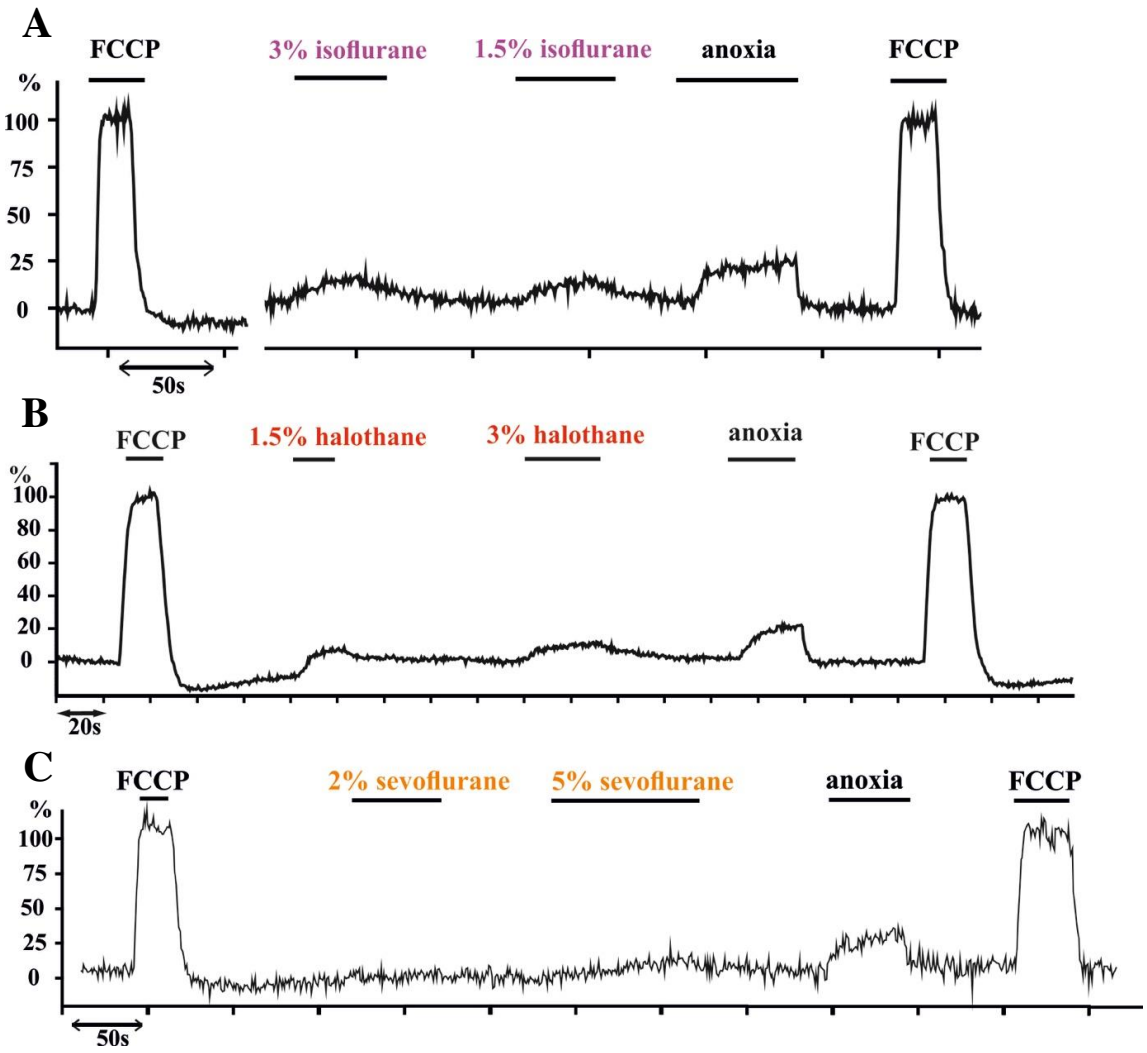

Figure 5.5: Representative traces of the effect of volatile agents on mitochondrial membrane potential. Note the initial and last exposures to FCCP used in calibration and the control anoxic response. The order of potency appears to be isoflurane > halothane > sevoflurane. **(A)** Isoflurane **(B)** Halothane **(C)** Sevoflurane

Figure 5.6 shows the results of quantitative analysis. The order of potency was the same as for anaesthetic effects on [NADH] (Figure 5.2). Differences between agents were significant (ANOVA; p =0.033) with post hoc tests confirming that the effect of sevoflurane was different from that of either halothane or isoflurane ($p < 0.001$).

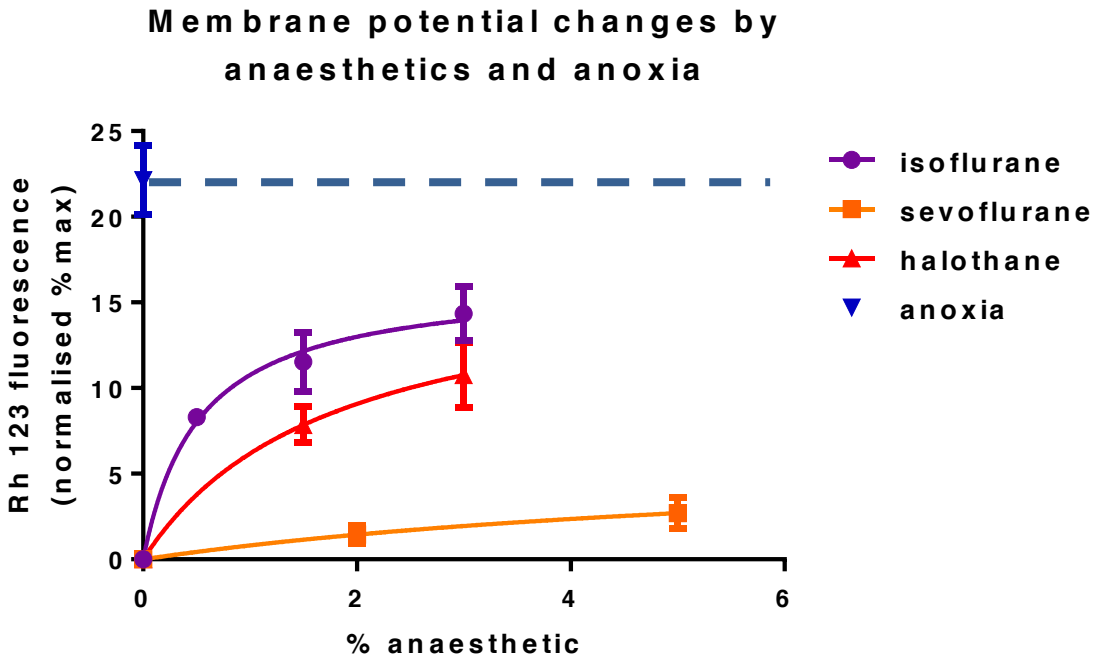

Figure 5.6: Effects of volatile anaesthetics on mitochondrial membrane potential. Data is (mean +/- SEM) plotted against absolute concentration of agent. The membrane potential was calibrated and normalised to the FCCP response for each experimental period. As a reference the response evoked by anoxia is indicated by the blue dotted line (and displayed in blue with error bars on the 0 point): The x axis shows absolute percentages as measured from vaporizer output. Data was curve fitted by nonlinear regression with a hyperbola with r^2 0.995 for isoflurane and 1.0 for sevoflurane and halothane using PRISM software.

To account for the possibility that application of anaesthesia increased fluorescence unrelated to a change in membrane potential, FCCP was applied both with and without 3% isoflurane (n=3) to detect if an additional increase in fluorescence was detected (Figure 5.7). Isoflurane did not alter the fluorescence response to FCCP indicating that the isoflurane does not affect

other sources of cellular fluorescence and that the increase in auto-fluorescence during isoflurane application is due to a change in mitochondrial membrane depolarisation.

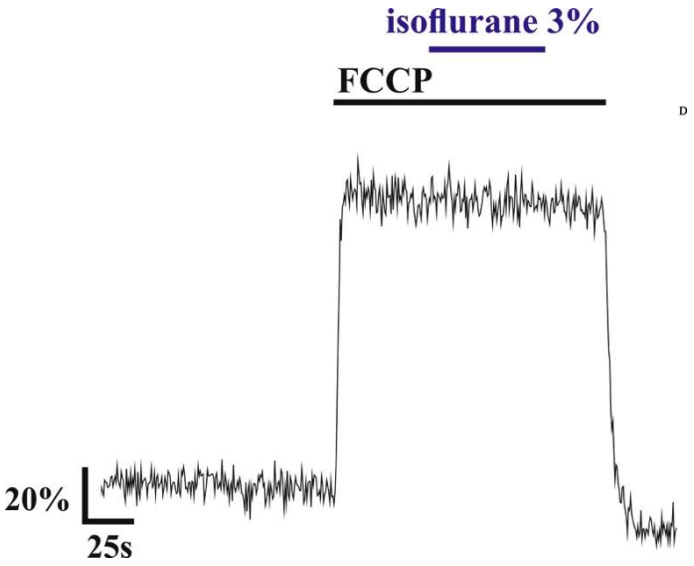

Figure 5.7: Rho123 trace showing the application of FCCP with and without isoflurane in type-1 cell. (n=3).

In summary, isoflurane, halothane, and to a lesser extent sevoflurane are all able to increase Rh123 fluorescence, indicating a mitochondrial depolarisation, suggesting that these anaesthetics may act to inhibit electron transport.

5.3.4 Measurements of anaesthetics on [NADH] in HEK cells

Intrigued by the effect and the magnitude of the effect of clinically relevant concentrations of anaesthetics on [NADH] in type-1 cells, the question arose whether this effect was also found in other cells, as suggested by some published studies. Untransfected HEK cells were chosen for this because of their availability and because HEK cells have also been used for other experiments in this thesis. One concentration of both halothane and isoflurane have been applied to six HEK cells. The application of 1.5% halothane or isoflurane resulted in an increase of NADH auto-fluorescence of a similar magnitude as seen in type-1 cells. A mix of 1.5% isoflurane and halothane also showed an additive effect in that the effect of the mix was greater than each single agent.

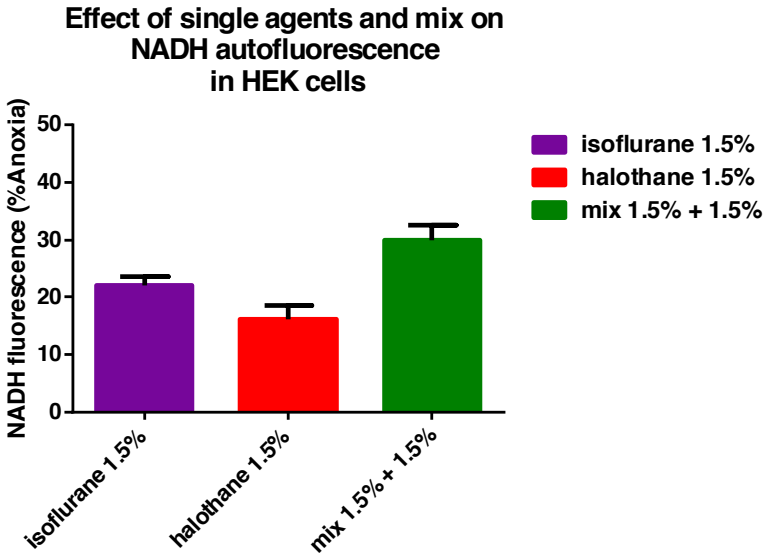

Figure 5.8: Increase of NADH fluorescence by single agent volatile anaesthesia and mixes in HEK cell. Quantitative analysis of effect of mixtures of halothane and isoflurane ((mean ± SEM; n = 6, paired t-test). NADH fluorescence is expressed as the % of value in anoxia.

5.4 Discussion

This chapter shows that volatile anaesthetics partially inhibit electron transport in type-1 cell mitochondria. Upon application of anaesthetics there is an increase in NADH auto-fluorescence and mitochondrial membrane depolarisation. Furthermore, there appears to be an order of potency for this effect, when expressed in absolute %, of isoflurane ≥ halothane > sevoflurane for both NADH and mitochondrial membrane potential effects. Finally, the effects of anaesthetics were additive with respect to the increase of NADH.

In the next section limitations of experimental technique and how I addressed them will be discussed, which will be followed by a discussion of previous literature and the potential physiological implications of the findings in this chapter.

5.4.1 Limitations of experimental technique and how they were addressed

The measurements of mitochondrial NADH and membrane potential are indirect. However, the dye methods that were used are well established (Emaus et al., 1986, Mayevsky and Rogatsky, 2007) and are able to show differences of NADH levels and membrane potential evoked by anaesthetics which then allow comparison of anoxic and FCCP stimuli. Furthermore, the administration of anaesthetics was monitored continuously in real time using infra-red spectroscopy (confirmed by GC-MS) as discussed in methods chapter section 2.6.

The interpretation that the change in fluorescence is evoked by a change in mitochondrial [NADH] is supported by a lack of additive effect on [NADH] to that of rotenone alone (Figure 5.4). The fact that this is not the case is consistent with the notion that rotenone saturates the single mechanism by which NADH is increased (i.e., inhibition of complex I). Similarly, FCCP in the presence of 3% isoflurane did not result in further membrane depolarisation, indicating that isoflurane does not have a non-specific effect.

5.4.2 Comparison with previous work: volatile anaesthesia and NADH

These results support the work of Hanley et al., (2002) who reported similar results for the same volatile agents in cardio myocytes. They expressed the NADH increase as a function of the maximum fluorescence evoked by rotenone, whereas the data in this chapter is expressed as a function on maximum fluorescence achieved with anoxia. Nevertheless, a quantitative comparison of the results is possible: they used slightly higher concentrations of anaesthetics compared to this study and consequently their measured NADH auto fluorescence in the presence of anaesthetic is understandably slightly higher, but nevertheless the results are similar. They found the same order of potency in absolute % (i.e. that sevoflurane is the least potent and halothane and isoflurane very similar), although isoflurane is perhaps slightly more potent than halothane in this chapter. Further experiments reported in this paper reveal that the increase in [NADH] may be due to an inhibition of complex I. Furthermore, the experiment in this chapter measuring the anaesthetic-evoked increase in NADH autofluorescence in HEK cells confirms that, in accordance with previous literature, the effect of anaesthetics may be ubiquitous to all tissues, likely common to all cell types.

There are a number of other studies indicating that anaesthetics act on complex I in mitochondria with examples in C. elegans, (see also discussion below of mouse models and human patients). In C. elegans, Kayser et al., (1999;2004) found that mutations that result in decreased mitochondrial complex I function also increase sensitivity to volatile anaesthetics. In a follow up study with more mutants, Falk et al., (2006) report a clear correlation between mitochondrial complex I oxidative phosphorylation capacity and volatile anaesthetic sensitivity. Other studies performed by this group also analysed complex II, III and IV, but no changes in sensitivity in response to volatile anaesthesics were reported (Falk et al., 2006, Suthammarak et al., 2009). Although the methods used in this chapter do not allow us to define the site of action within the electron transport chain, based on the above studies published inhibition of complex I could likely offer (part of) the explanation for this observation.

5.4.3 Comparison with previous work: volatile anaesthetics and mitochondrial membrane potential

Whereas the anaesthetic influence on mitochondrial membrane potential in other tissues has been previously reported, the results in glomus cells are novel. Bains et al. (2006) reported that sevoflurane and isoflurane depolarize mitochondria of presynaptic neural tissue in rats and that isoflurane is more potent than sevoflurane (in this thesis; Figure 5.5 and Figure 5.6). Similarly, Pravdic et al. (2012) reported that isoflurane slightly, but significantly, depolarized mitochondrial membrane potential in isolated rat heart mitochondria and suggested this was due to an inhibition of complex I and of ATP synthase. With this additional evidence in other

cell types, it can be concluded that the changes in membrane potentials reported in this paper are in line with other research previously published.

5.4.4 Implications of the results

There are three potentially relevant implications of the result that clinically relevant concentrations of halothane, isoflurane and sevoflurane influence mitochondrial function: first, in relation to anaesthetic effects on oxygen sensing; second, in relation to anaesthetic preconditioning; and third, in relation to hypnotic effects of anaesthetics.

5.4.5 Oxygen sensing

One theory of oxygen sensing in the carotid body is the 'metabolic theory', which argues that oxygen is sensed through changes in mitochondrial energy, which in turn can contribute to the regulation of TASK channel activity (Duchen and Biscoe, 1992a, b, Buckler and Turner, 2013). Volatile anaesthetics, so far, always appear to act in an opposite way to hypoxia. However, the observations in this chapter reveal a novel insight in the role of volatile anaesthetics within the framework of that theory. Drugs that inhibit mitochondrial metabolism or complex I (like rotenone and cyanide) reliably activate glomus cells (via *closure* of TASK channels, cell membrane depolarisation and Ca^{2+} influx) to secrete neurotransmitters to activate the hypoxic chemoreflex. If the sole actions of volatile anaesthetics were similar to this (albeit of more modest magnitude) then it would be expected that volatile anaesthetics would enhance the hypoxic chemoreflex.

Yet it is well established that volatile anaesthetics *open* TASK channels and inhibit Ca^{2+} entry into glomus cells and obtund the hypoxic chemoreflex (chapter 3 and 4). Because the net effect of anaesthetics is one of chemoreflex depression in the carotid body, anaesthetics elicit actions other than their effects of mitochondrial metabolism within the glomus cell that counteract and overcome any tendency to enhance the hypoxic chemoreflex. Therefore the apparently opposing effects of anaesthetics on the carotid body (one on mitochondria the other on TASK channels) constitute a complex form of regulation. The utility of such a mechanism remains unclear.

5.4.6 Anaesthetic preconditioning

Anaesthetic pre- or post- conditioning is the phenomenon in which the pre-exposure to volatile anaesthesia provides protection against subsequent ischemic insult in heart or brain tissue (Hu and Liu, 2009, Eckenhoff and Morgan, 2015). It is suggested that the mechanisms of anaesthetic preconditioning may be common to the phenomenon of 'hypoxic preconditioning', wherein a prior exposure to brief hypoxia protects the tissue from subsequent sustained hypoxic exposure. There are several mechanisms proposed with candidates being protein tyrosine kinases, mitogen activated protein kinases, K_{ATP} channels and especially some emerging evidence that volatile anaesthesia decrease reactive oxygen species generated by mitochondria during ischemia (Hu and Liu, 2009).

Supporting the notion that complex I inhibition may be involved in the preconditioning phenomenon, (Niatsetskaya et al., 2012) reported that preventive partial inhibition of complex I in mice resulted in decreased oxidative stress and less damage during hypoxic injury to hearts and brains. Volatile anaesthetics have been suggested to induce pharmacological preconditioning via the production of reactive oxygen species (ROS; Mullenheim et al. 2002; Novalija et al. 2002; Tanaka et al. 2002). Rotenone and other complex I inhibitors have been shown to increase the rate of production of ROS (Hasegawa et al. 1990; Ide et al. 1999) and drugs that open K^+ channels like diazoxide and pinacidil (widely used to facilitate preconditioning (Saltman et al., 2000, Schwartz et al., 2007, Han et al., 2010), also depress the respiratory chain. The results in this chapter are consistent with these interpretations, demonstrating that the effect of anaesthetics on complex I is present in a wide variety of tissues, HEK cells included.

5.4.7 Hypnotic effects of anaesthesia

A very interesting observation was made when the data obtained in this chapter were converted to MAC. Figure 5.9A shows the NADH data expressed as the minimum alveolar concentration (MAC) of each agent for rats. This was 1.1% for halothane, 1.51% for isoflurane and 2.5% for sevoflurane (Kashimoto et al., 1997, Niemann et al., 2002, Leon et al., 2004). The MAC is in many ways an arbitrary end-point, focussed on an anaesthetic's hypnotic effect (i.e., its ability to induce unconsciousness, or more accurately loss of response to a standardised surgical stimulus). At the same MAC value, the biological effect of any agent with respect to hypnotic endpoint is identical, so the scale normalises anaesthetic doses to the functional end-point of hypnosis (Aranake et al., 2013).

It appears that once converted to MAC, the agents effect is more similar, and statistically significant differences between sevoflurane and the other agents are lost ($p = 0.489$; NS). When converting the membrane potential measurements, the agent difference was retained. However, the fact that the agent discrimination disappears in the NADH MAC conversion is very interesting, and it is tempting to speculate if this mechanism therefore is important in facilitating the hypnosis in general anaesthetics.

An emerging theory proposes a role for mitochondria in the hypnotic/narcotic effects of general anaesthesia. Modelling has suggested that a direct effect of volatile anaesthesics on ion channels alone is not enough to explain the profound effects of anaesthesia on consciousness (Chance et al., 1963, Morgan et al., 2002, Eckenhoff and Morgan, 2015). A generalised mechanism, such as the reduction in overall metabolism, could contribute at least in part to immobility and unconsciousness. The mitochondria play a crucial role in supplying the cells in the body with energy. Complex I is the main entry point for electrons entering the transport chain and consequently if the function of this complex decreases due to anaesthetic interaction, the entire transport chain will be disturbed and slowed down.

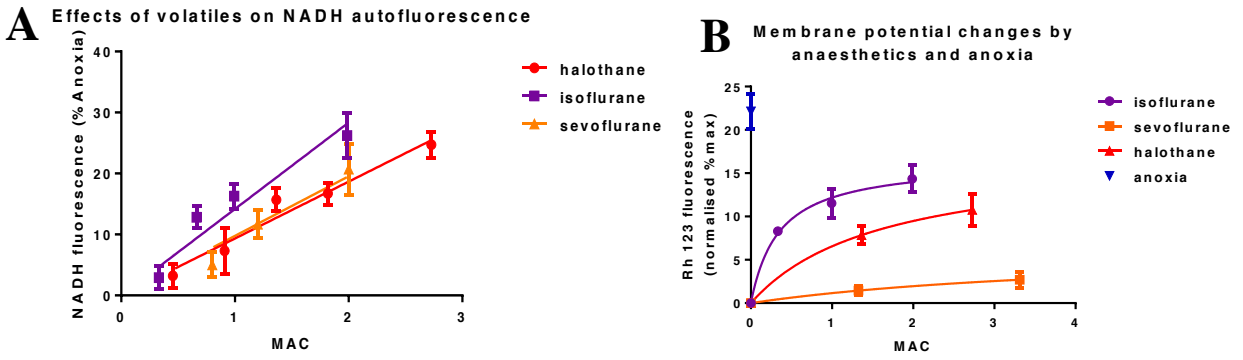

Figure 5.9: NADH and membrane potential measurements converted to MAC. Values of 1.1% for halothane, 1.51% for isoflurane and 2.5% for sevoflurane **(A)** NADH measurements converted to MAC **(B)** Membrane potential measurements converted to MAC**.**

There is no inherent expectation that the effects of different anaesthetics at identical MAC values should be the same for all biological functions. Thus with respect to say glomus cell hypoxic response it does not follow that these concentrations of the anaesthetics will have the same effect. However, if a function is part of the mechanism of hypnosis then it would be expected that the effect of different agents is identical when expressed as MAC. Therefore, the result in Figure 5.9A is consistent with the notion that complex I/partial inhibition of electron transport may be involved in the hypnotic mechanism of anaesthetic action.

Quintana et al. (2012) studied a knock out (KO) mouse model lacking the Ndufs4 gene, which is a subunit of mitochondrial complex I. The authors reported that the KO mice were extremely sensitive to isoflurane with an ED50 for hypnotic effect that was a third compared to littermate controls. For halothane the ED50 was more than half as much as controls. These observations suggest that anaesthetic effect on complex I function may go beyond oxygen sensing influences and be a target for the narcotic effect of volatile anaesthesia.

A relationship between complex I and anaesthetic sensitivity has also been identified in patients. Morgan et al. (2002) induced 16 young patients with various mitochondrial mutations using sevoflurane. Four patients, who had a specific complex I mutation, needed much lower than usual doses of sevoflurane to reach an appropriate anaesthetic depth for surgery. It is interesting that we found sevoflurane to be the least potent of the volatiles in its influence on complex I (Figure 5.9A and Figure 5.9B) It is important to stress that these mitochondrial disorders result in a severely affected phenotype and do not provide conclusive evidence of its role in hypnotic effects of general anaesthetics. Nevertheless, there is a growing body of evidence across species suggesting some interaction between anaesthetics act and complex I.

In summary, the data in this chapter show that mitochondria are a potentially important target for volatile anaesthetics in the carotid body and their effects highlight the complexity of the hypoxia transduction cascade.

Chapter 6. Effects of novel TASK blockers on glomus cell background K^+ channels

6.1 Introduction

While the focus in the other chapters has been on identifying the mechanisms of volatile anaesthetic depression on the hypoxia transduction cascade in the carotid body, this chapter will look ahead to a potential solution to volatile anaesthetic evoked depression of the chemo-reflex. In this chapter I will characterize two recently described compounds reported to block TASK channels and stimulate breathing in anaesthetized rats. The effects of these compounds will be studied on rat carotid body type-1 cells. The novel compounds are A1899, which is a cloned TASK-1 blocker and PK-THPP, a cloned TASK-3 blocker. The molecular structures are shown in Figure 6.1.

There is much incentive for developing novel TASK blockers. Recent evidence suggests that compounds decreasing TASK channel activity in the carotid body have the potential to be useful for the treatment of conditions in the perioperative environment, with examples being anaesthesia induced ventilatory depression, sleep apnoea, or hypoventilation caused by obesity (Kiper et al., 2015). One of the main reasons that new breathing stimulants are needed is because the few existing drugs have strong side effects and are therefore not used very frequently. Two existing agents, which are both thought to act as chemo-excitants on the carotid body, are almitrine and doxapram (Peers, 1991, Takahashi et al., 2005, Golder et al., 2013). Almitrine is a respiratory stimulatory drug that has been withdrawn in European Member States because of the risk of substantial weight loss and long-lasting peripheral neuropathy (European Medicines Agency, 2013). There is only a limited availability in a few other countries. Individuals without carotid bodies do not experience stimulatory breathing

effects when treated with almitrine, suggesting the almitrine effect does indeed work through carotid body activation (de Backer et al., 1983). Doxapram on the other hand, is a breathing stimulant currently approved in EU Member States. This drug is usually administered by one time infusion to stimulate respiration in the post-operative patient (Golder et al., 2013). However, due to its side effects it is not used very often, as the adverse effects include increased in blood pressure and seizures due to central nervous system stimulation (Ward, 1968, Cotten, 2013). Like almitrine, doxapram was shown to stimulate carotid bodies in cats, but failed to do so after carotid body denervation (Mitchell and Herbert, 1975). Research on Xenopus oocytes injected with rat cRNA shows that doxapram targets TASK-1, TASK-3 and the TASK-1/3 and TASK-3/1 heterodimer (Cotten et al., 2006).

PK-THPP is a propylketone (PK) derivative of tetrahydropyrido-pyrimidine (THPP) and was discovered and optimized by Merck & Co following a high throughput screening based on a 5,6,7,8-tetrahydropyrido[4,3-d]pyrimidine (Coburn et al., 2012). It was described as a TASK-3 antagonist and was promising for its ability to modulate sleep architecture in rodent models.

A1899 was initially described by Streit et al., (2011) as a potent and highly selective blocker of TASK-1, blocking both inward and outward currents to the same extent in TASK-1 expressed in Xenopus oocytes. In a high K^+ medium, 400nM of A1899 leads to a block of 60% of the channel current. Chimeric channels with different combinations of the transmembrane segments of the drug insensitive TASK-4 and drug sensitive TASK-1 were generated and expressed in oocytes. Through using different subunit combinations, the authors identified that both M2 and M4 segments of TASK-1 are crucial for the binding and block of the channel. Deletions in the halothane response element, or replacing this element

with the TASK-3 halothane response element, drastically reduce the drug affinity, suggesting that the TASK-1 halothane responsive element is involved in the binding and/or blocking of the drug and potentially also explaining the different drug affinities for TASK-1 and TASK-3 (Streit et al., 2011).

Cotten (2013) further examined both A1899 and PK-THPP in vivo in rats, suggesting further potential for these drugs as breathing stimulants. Rats were anaesthetized with isoflurane while receiving a dose of A1899, PK-THPP or doxapram. Cotton reported that PK-THPP and A1899 increased minute ventilation by increasing tidal volume and breathing rate. The stimulatory breathing effects observed in these experiments were of a greater magnitude and/ or duration compared to that of doxapram. The authors also highlight that unlike doxapram, PK-THPP and A1899 do not show an increase in blood pressure. If the drugs are indeed more potent compared to doxapram, this would suggest that there is a smaller likelihood of developing side effects, because less of the agent is needed.

Rinne et al., (2015) further studied the effect of A1899 on TASK-1, TASK-3, and the concatomers TASK-1/3 and TASK-3/1 expressed in HEK cells. The authors reported that 40nm A1899 induces a 46% block in whole cell recordings of HEK expressing TASK-1, whereas the same concentration of A1899 in HEK cells expressing TASK-3 channels lead to a modest 9% reduction. The authors also reported inhibition by A1899 on the concatemer mediated current.

The relevance of A1899 appears not to be exclusive to ventilation research. In pancreatic mouse cell lines, A1899 has been reported to reduce TASK-1 currents and as a consequence could be used to regulate α-cell excitability (Dadi et al., 2015).

The above research strongly suggests that these agents may be powerful breathing stimulants, acting through inhibition of TASK channel activity. These agents are therefore of interest to my research for two reasons. Firstly, no studies to date have been performed that examine the effect of these drugs on type-1 carotid body cells. It needs to be confirmed whether these compounds can decrease the native (heterodimer) TASK channel activity and excite the type-1 cells. So far, the effect of these drugs on the heterodimer has only been tested using concatemers and attempting spontaneous hetero dimerisation by cotransfection (Rinne et al., 2015). To date, the carotid body is the only organ in which different research groups have independently confirmed the presence of heterodimers (Czirjak and Enyedi, 2002, Kim et al., 2009a, Turner and Buckler, 2013b). The second reason for studying these inhibitors is to test whether application of these drugs could be used to selectively block subtypes of TASK channels in carotid body patch clamp recordings. TASK channel expression in the carotid body is thought to comprise a mixture of the homodimers of TASK-1, TASK-3 and the heterodimer TASK-1/3. If these compounds show differential selectivity for one of the homodimers, this would enable us to study the TASK channels in a more isolated way, which would make a very useful tool for studying the relevance of each of the subtypes.

The first aim of this chapter is thus to investigate the effects of PK-THPP and A1899 on TASK channel activity in the rat glomus cell, and to compare this with the effects of doxapram, as a drug which is currently in use. The second aim of this chapter is to investigate

the effect of PK-THPP and A1899 in the presence of a clinically relevant concentration of isoflurane. Again, this will be compared with the effect of doxapram in the presence of isoflurane. The third aim of this chapter is to establish if A1899 and PK-THPP can be used to selectively block subtypes of TASK channels in carotid body single channel recordings.

To address these three questions, both compounds will first be applied to HEK cells expressing ratTASK-1 for A1899 and ratTASK-3 for PK-THPP to examine channel activity through cell attached single channel recordings as a positive control. This will provide a first insight if the compounds added to the bath solution will reach the channel in cell attached recordings. Next, a concentration response curve will be made for the effect of both agents on the background TASK channel activity in rat type-1 carotid body cells. In the final experiment, the compounds will be combined with a clinical relevant dose of isoflurane, to see if these compounds can (partially) reverse the increase of channel activity evoked by isoflurane.

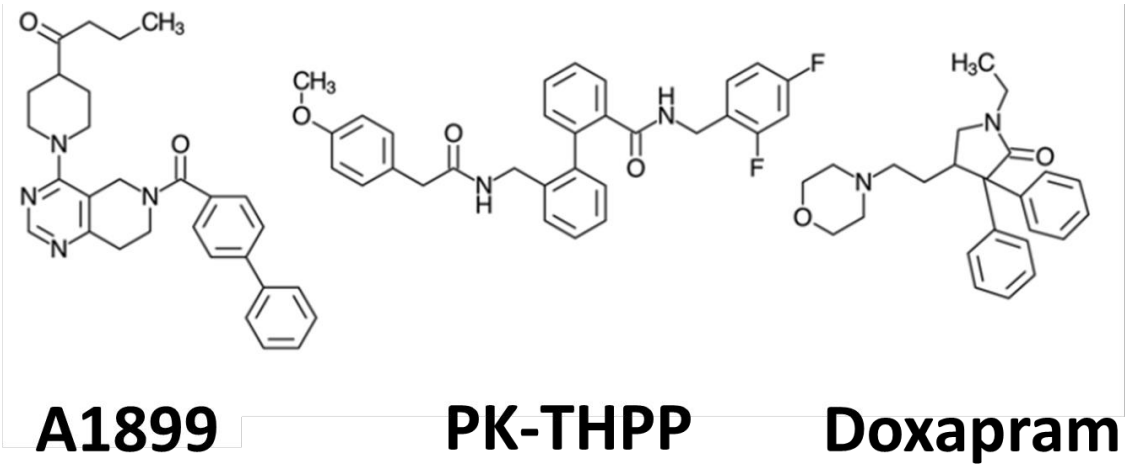

Figure 6.1: Molecular structure of A1899, PK-THPP and doxapram. Adapted from (Cotten, 2013)

6.2 Methods

6.2.1 A1899 and PK-THPP

A1899 and PK-THPP were synthesized by Aberjona Laboratories, Inc. (Woburn, USA) and delivered in 10mg aliquots. At the beginning of each week, the aliquots were dissolved in dimethylsulfoxide (DMSO) and kept at -20ºC. The DMSO solution was added to the bottle containing Tyrode solution 15 minutes prior to the start of the experiments. From experience we noted that the drug potency of the DMSO diluted aliquots rapidly declined from 1 week following dilution in DMSO, and that no effect was noticed two weeks post dissolving in DMSO. The recordings included in this chapter were therefore dissolved in DMSO no less than a week prior to the start of the experiments. The inhibitors were dissolved in such a way that 5-8µL needed to be pipetted into a bottle containing 200mL Tyrode. However, for a few A1899 experiments in which a concentration higher than 400nM was used and thus more DMSO, a control application of 80µL DMSO in 200mL Tyrode without inhibitor was applied to glomus cells to verify whether or not this concentration evoked a change in TASK channel activity, however, none was detected (result not shown, n=2).

6.2.2 HEK Cell culture and transfections

HEK cells were cultured and transfected with 1.2µg ratTASK-1 or ratTASK-3 inserted in pIRES-EGFP, using lipofectamine and PLUS reagent as previously described in methods chapter 2 section 2.2.7. 24-48 hours post transfection, cells were harvested and plated onto

poly-L-lysine coated glass coverslips. Two hours after plating, the cells were used for recordings.

6.2.3 Glomus cell isolation

For the extended procedure, refer to methods chapter 2 section 2.3. In short, carotid bifurcations were surgically removed from isoflurane anesthetized rat pups P10-P14. Carotid bodies were sub dissected and plated in medium onto poly-L-lysine coated glass coverslips. Cells were incubated with rhodamine-PNA, which resulted in a bright orange staining for glomus cells. Glomus cells were used for recordings within 8 hours of plating.

6.2.4 Recording conditions for cell attached patching of HEK and glomus cells

Cell-attached patch clamp recordings were performed using an Axopatch 200B (Molecular Devices LLC, Sunnyvale, US). Recordings were made with borosilicate pipettes (Harvard Apparatus Ltd, Kent, UK) and were sylgard-coated and fire-polished before use. Cells were placed in the recording chamber in standard tyrode in which seal formation was attempted with the borosilicate pipette containing high K^+ (140mM) as previously described in chapter 2. When a giga-ohm a seal was formed, the Tyrode solution was switched to 100mM K^+ and a positive pipette potential was applied of +80mV. Single-channel recordings were filtered at 2–5 kHz and current was recorded and digitalized at 20 kHz. Voltage clamp control, data acquisition and analysis were performed using Spike2 (Cambridge Electronic Design, Cambridge, UK).

6.2.5 Experimental protocol and data analyses for HEK expressing cells TASK-1 or -3

To verify the effect of A1899 on TASK-1 and PK-THPP on TASK-3, the compounds were applied to HEK cells expressing TASK-1 or TASK-3. Because of the large amount of channels in the average patch, these multichannel recordings are not suitable for detailed and elegant single channel analysis, instead the average current evoked by the multichannel patches was measured before and during drug application. The current during inhibitor application was expressed as a % inhibition compared to control channel activity before application. 400nM of each inhibitor was added to the bath solution, the pipettes did not contain any inhibitor. Cells were placed in the recording chamber in standard Tyrode (in mM: 117 NaCl, 4.5 KCl, 1 MgCl2, 23 NaHCO3, 11 glucose equilibrated with 5% CO_2) in which seal formation was attempted with a borosilicate pipette containing (140mM K^+). Once a giga-ohm a seal was formed, the Tyrode solution was switched to 100mM K^+ Tyrode solution. The protocol for drug application was (1) high K^+ control, (2) inhibitor application (A1899 or PK-THPP) (30-80 seconds) (3) high K^+ control.

6.2.6 Experimental protocol for the measurement of TASK channel activity in glomus cells

Single-channel activity was defined by nPopen. Main conductance states for channel activity were established in an all-points histogram and used to set a 75% open threshold for nPopen definition analysis, so to enable a the best possible capture of the TASK-1/3 heterodimer. The increase in channel activity as defined by nPopen was measured as an increase compared to control.

Single agent and concentration response curve recordings

The protocol for drug application was (1) high K^+ control on, (2) drug on (30-80 seconds) (3) high K^+ control on. Cells were challenged with doxapram, PK-THPP or A1899. A maximum of up to 3 different doses of the same drug were applied within each recording in random order.

The effects of breathing stimulants combined with isoflurane

Once a giga-ohm seal was formed, the bath solution was switched to high K^+. The protocol for drug application was: (1) High K^+ control (2) 1.5% isoflurane (3) 1.5% isoflurane + 400nm breathing stimulant (4) isoflurane 1.5% (5) high K^+ control on. For data analyses, the change in nPopen Isoflurane alone was compared to isoflurane with drug.

Statistical analysis for glomus cell recordings

A normality test was run for all the single channel data sets. Where normality was confirmed with a Shapiro-Wilk test, a paired t-test was used to compare channel activity of drug compared to control. In the data set where no normality was found, a related samples Wilcoxon signed rank test was run.

6.2.7 NADH auto-fluorescence recordings in glomus cells

A1899 and PK-THPP were tested for mitochondrial interaction by measuring a change in NADH auto-fluorescence upon application. Detailed information can be found in the NADH

auto-fluorescence methods section of chapter 2 section 2.8. In short, fluorescence measurements were performed using a microspectrofluorimeter. NADH was excited at 340 nm and fluorescence was measured at 450±15 nm. The output of the PMT was connected to an IV converter which generated an output in volts. In each recording, PK-THPP or A1899 was applied for approximately 30 seconds and a 5 seconds section of the plateau of each challenge was used to measure the value in volts. A Wilcoxon Signed Rank test was performed to test whether there was a change in baseline NADH upon application of the inhibitors.

6.3 Results

6.3.1 Breathing stimulants in HEK cells

A1899

A1899 was applied to HEK cells expressing TASK-1 as positive control to determine if the method of drug application (by dissolving the drug in the Tyrode bath solution) results in a noticeable change in TASK-1 channel activity as previously reported and thus can access the channel. Figure 6.2A and B show a representative trace revealing that 400nM A1899 strongly depresses TASK-1 channel activity. The recordings (n=4) show that A1899 significantly reduces the channel activity in a reversible fashion by 63.4% (SEM 7.7%, t-test $p = 0.045$ Figure 6.2C). It took up to 90 seconds for the cell to recover to baseline channel activity following A1899 application. Upon application, the large multichannel current reduced significantly, which resulted in a cell attached patch in which individual channels can be identified more clearly.

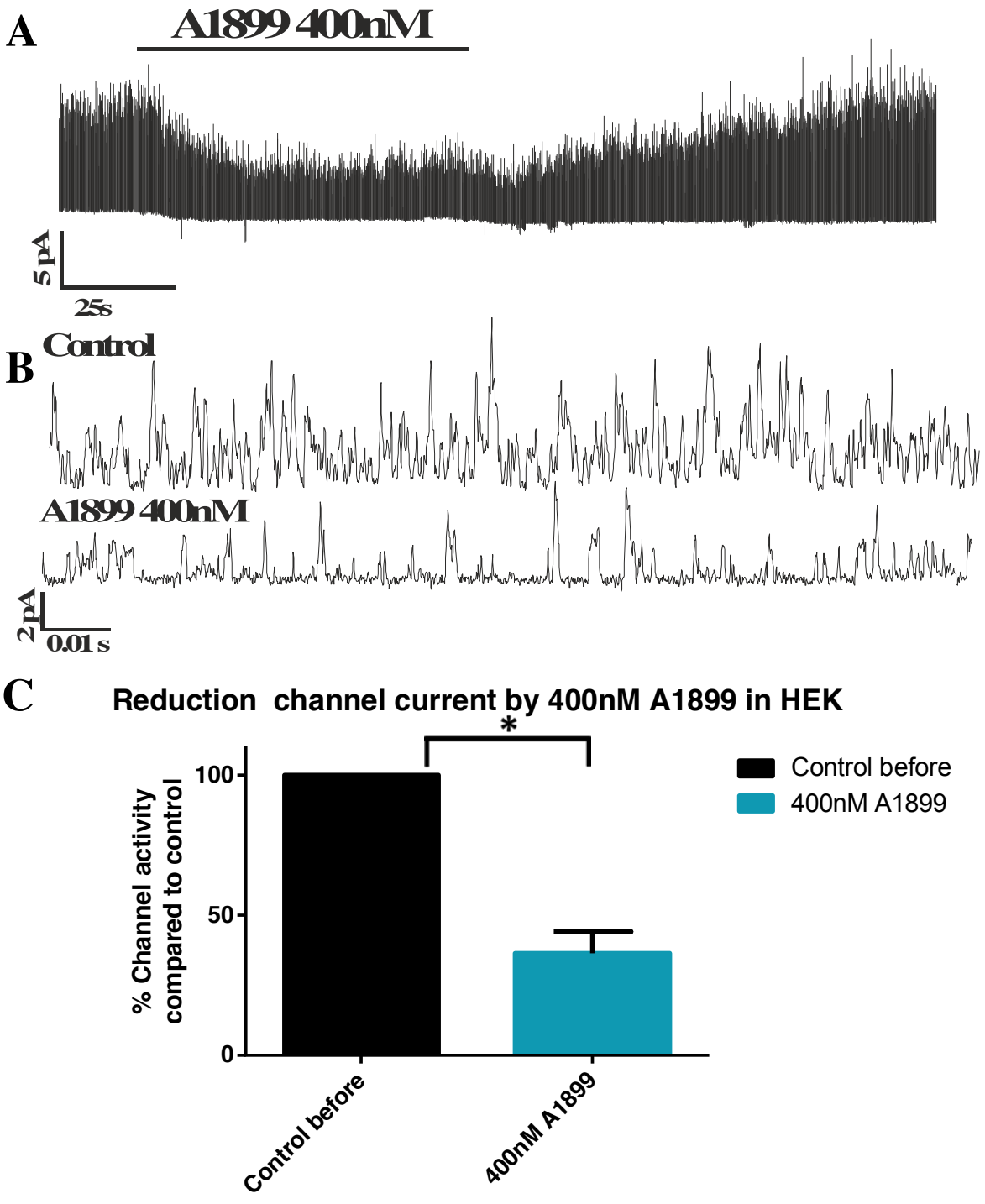

Figure 6.2: A1899 reduces TASK-1 channel activity in cell-attached patches in HEK cells. Representative trace of TASK-1 channel activity over **(A)** approximately 3 minutes and **(B)** superimposed over 0.1 seconds. **(C)** A1899 (n=4) significantly depresses the channel activity by 63.4% (SEM 7.7%, t-test p = 0.045). Cells were superfused with 100 mM K^+ Tyrode, with 140 mM K^+ in the pipette solution. Pipette potential was +80 mV.

PK-THPP

Similar results were obtained for the effect of PK-THPP on HEK cells expressing TASK-3. 400nM PK-THPP strongly depressed the TASK-3 channel activity. Figure 6.3A and B show a representative trace revealing that 400nM of PK-THPP (n=3) strongly depresses the TASK-3 activity in a reversible fashion by 85.1% (SEM 2.6%, Figure 6.3C). It took up to 90 seconds for the cell to recover to baseline channel activity following PK-THPP application. Upon application, the large multichannel current reduced significantly, which resulted in a cell attached patch in which individual channels can be identified more clearly.

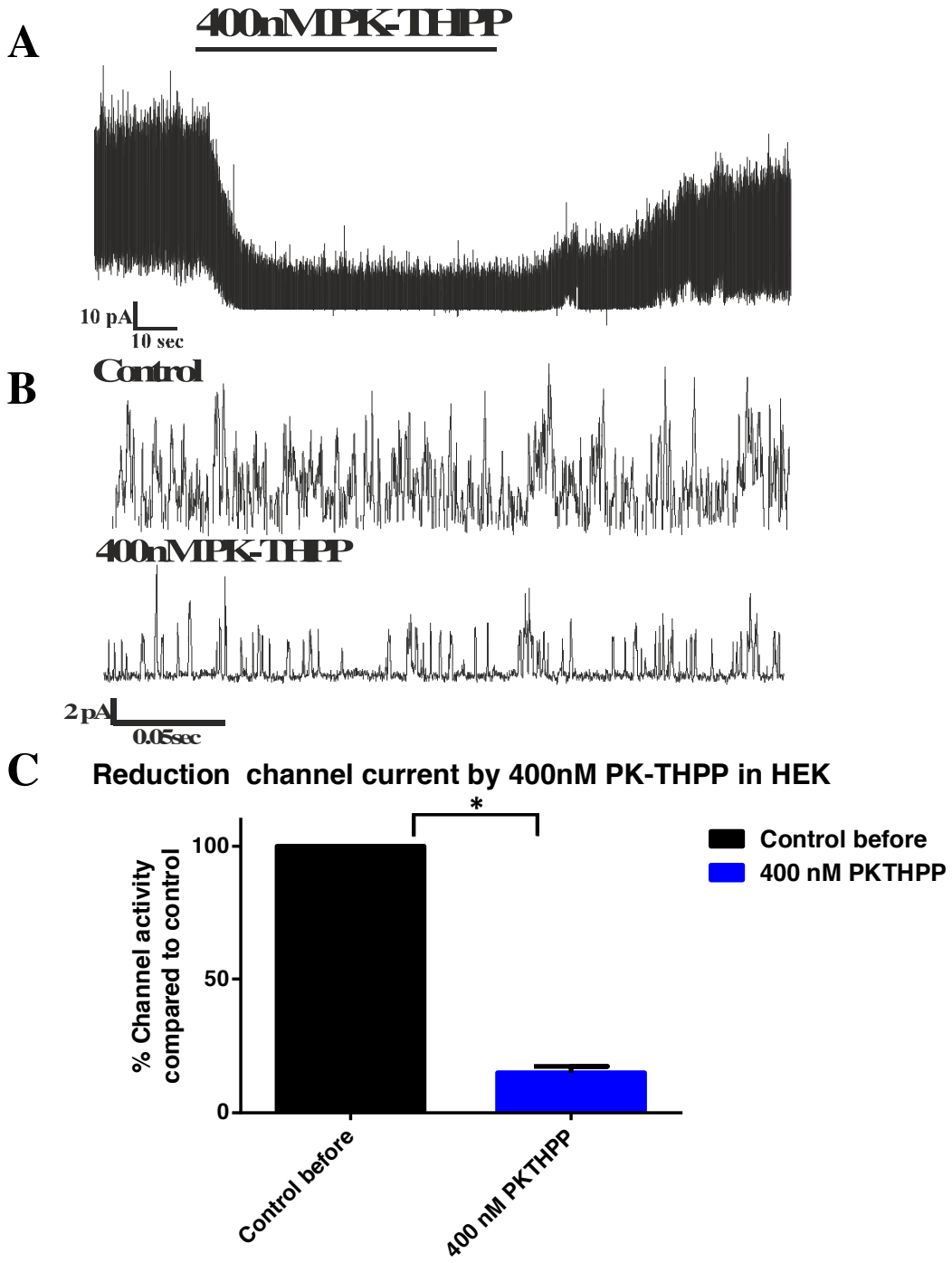

Figure 6.3: PK-THPP reduces TASK-3 channel activity in cell-attached patches in HEK cells. Representative trace of TASK-3 channel activity over **(A)** approximately 2 minutes and **(B)** 0.3 seconds. **(C)** PK-THPP (n=3) significantly depresses the channel activity by 85.1% (SEM 2.6%). Cells were superfused with 100 mM K^+ Tyrode, with 140 mM K^+ in the pipette solution. Pipette potential was +80 mV.

6.3.2 Breathing stimulants in Rat Glomus cells

Now that the drug effect and its application have been verified in HEK cells, the next question was to assess if, and by how much, PK-THPP and A1899 inhibit native TASK channel activity in the rat glomus cell. This is followed by application of doxapram, to allow for comparison of the depressive effect to an existing breathing stimulant.

A1899

Upon 400nM A1899 application, TASK channel activity in rat carotid body glomus cells was inhibited in a modest and reversible fashion. Figure 6.4A and B show an example trace of the same concentration (400nM) as also used in the HEK cells. A paired t-test between the nPopen values of a 20s period prior to and during 400nm A1899 application revealed a significant depression of 35% (SEM 6.7% N=8) with $p = 0.028$ ($df= 7$ $t = 2.759$) (Figure 6.4C).

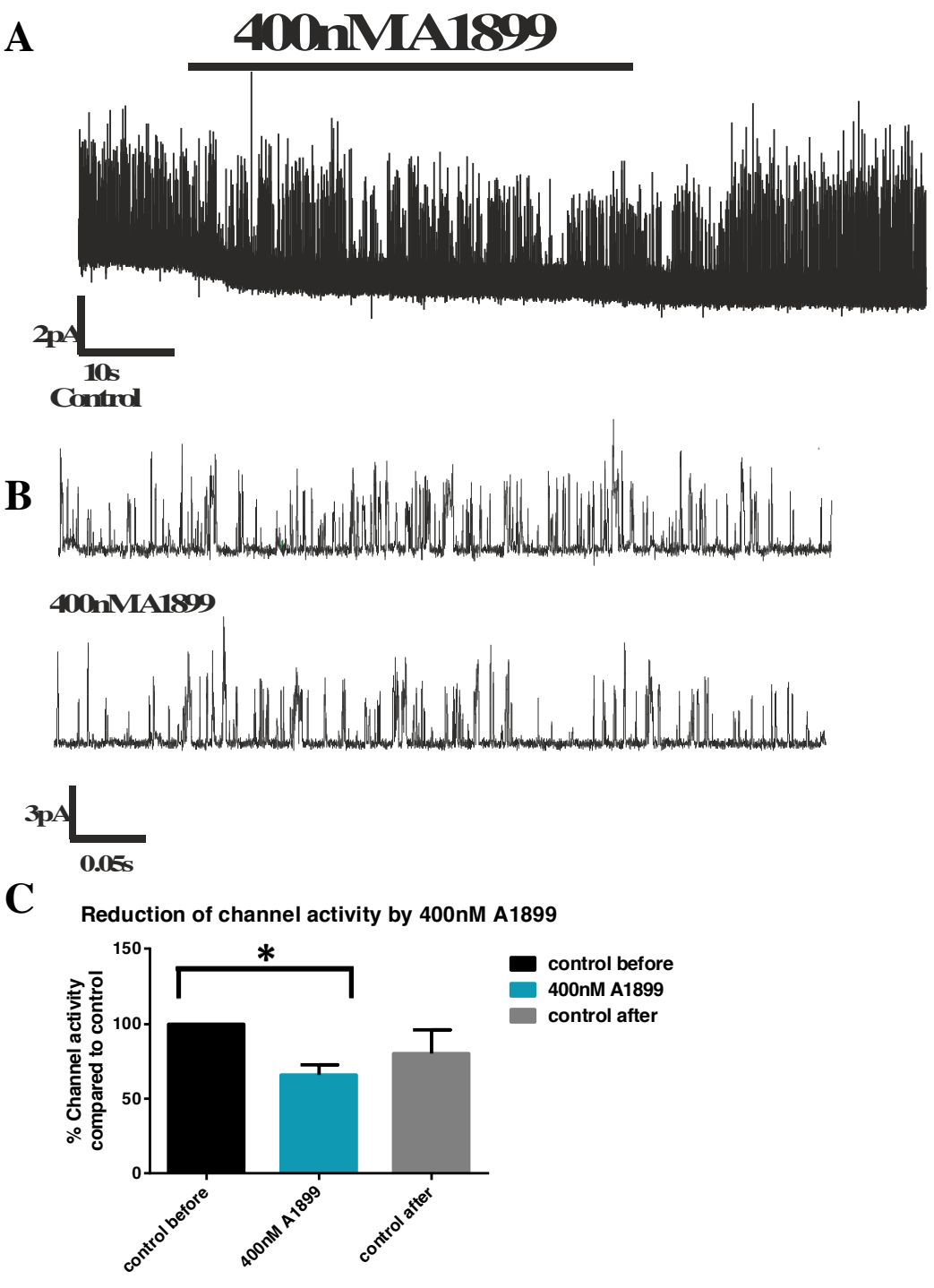

Figure 6.4: A1899 reduces background channel activity in cell-attached a rat type-1 cell patch. 400 nm A1899 (n=8) has a modest and reversible depression on the TASK channel activity. Representative trace of TASK channel activity over **(A)** approximately 1.5 minutes and **(B)** 0.4 seconds. **(C)** A1899 significantly depresses channel activity by 35% (SEM 6.7%, p = 0.028 df= 7 t = 2.759). The diagram displays % change in nPopen values compared to channel activity before A1899 application.

A representative all-points histogram in Figure 6.5 reveals that A1899 partly inhibits the peak channel activity around 2.6pA which typically represents the TASK-1/3 heterodimer. Open amplitudes around 1.2pA are also partly inhibited, which are assumed to represent some TASK-1 channel activity present in the patch.

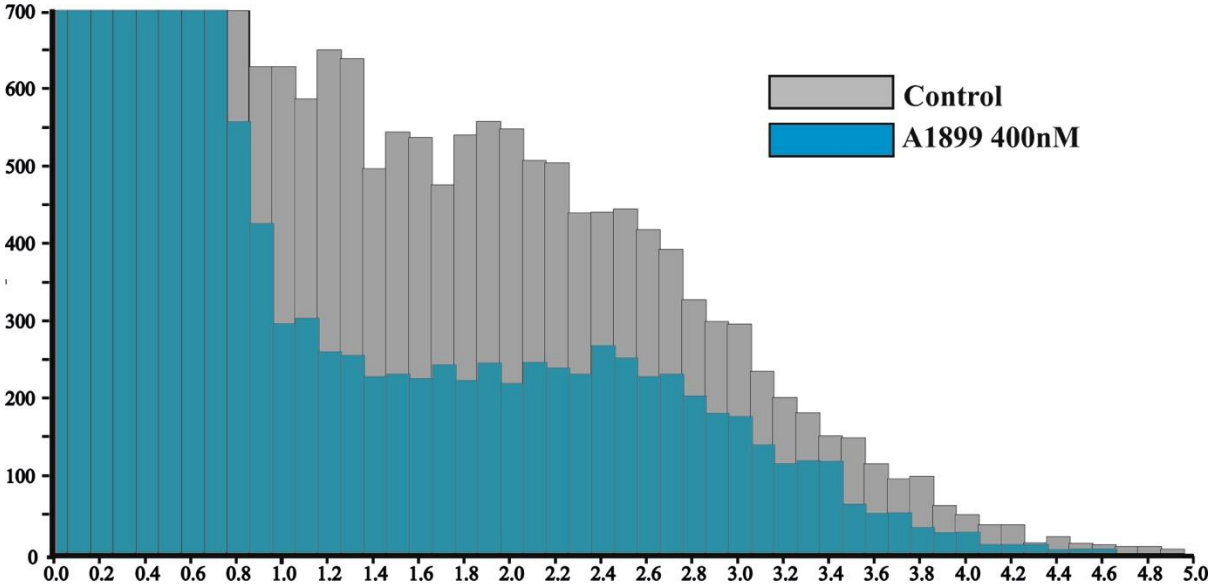

Figure 6.5: Representative all points histogram for the effect of 400nM A1899 on glomus cell TASK channel activity. Histogram was generated from a selected 20s section of both control and A1899 application. Bin-width was 0.1pA.

A concentration-response over a log scale was done to further establish the effect of A1899 on TASK channels in rat glomus cells (Figure 6.6). The graph reveals that at higher concentration, the depression evoked by 1899 increases.

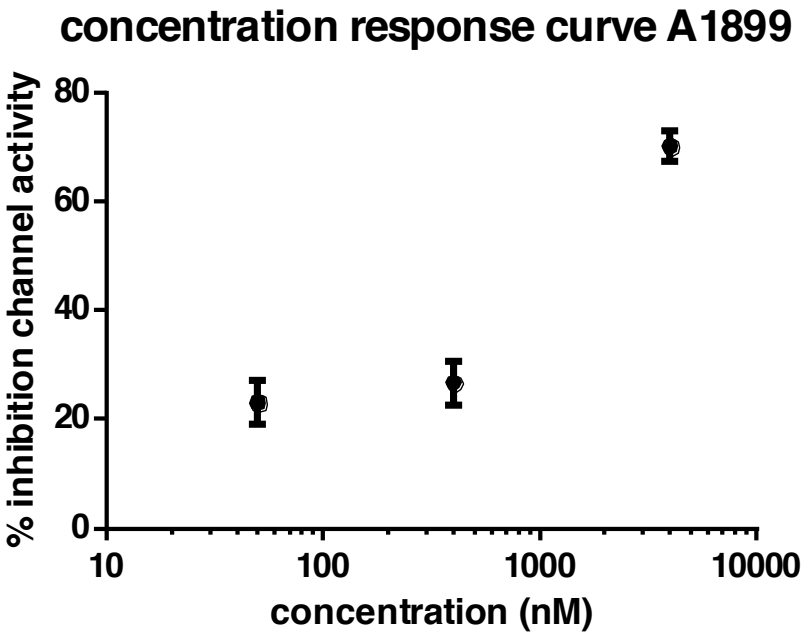

Figure 6.6: Concentration response of A1899 on background TASK channel activity in rat type-1 cell. % change in nPopen values compared to channel activity before A1899 application (50nm: n=4, 400nm: n=8 , 4000nm: n=6). Threshold 75%.

Although the reduction in channel activity was modest at 400nM, this concentration is nonetheless sufficient to stimulate the glomus cell and cause an increase in $[Ca^{2+}]i$ in rat glomus cells as observed by P. O' Donohoe in our lab (O'Donohoe, 2015). To confirm these results and to serve as a positive control for the modest reduction seen in the TASK glomus cells, I performed Ca^{2+} recordings on two type-1 cells. On one of the cells, after the Ca2+ measurements were completed, a single channel recording was also obtained. A representative trace is displayed in Figure 6.7 in which 400nM A1899 is flanked on each side with a hypoxia stimulus representing 0% oxygen.

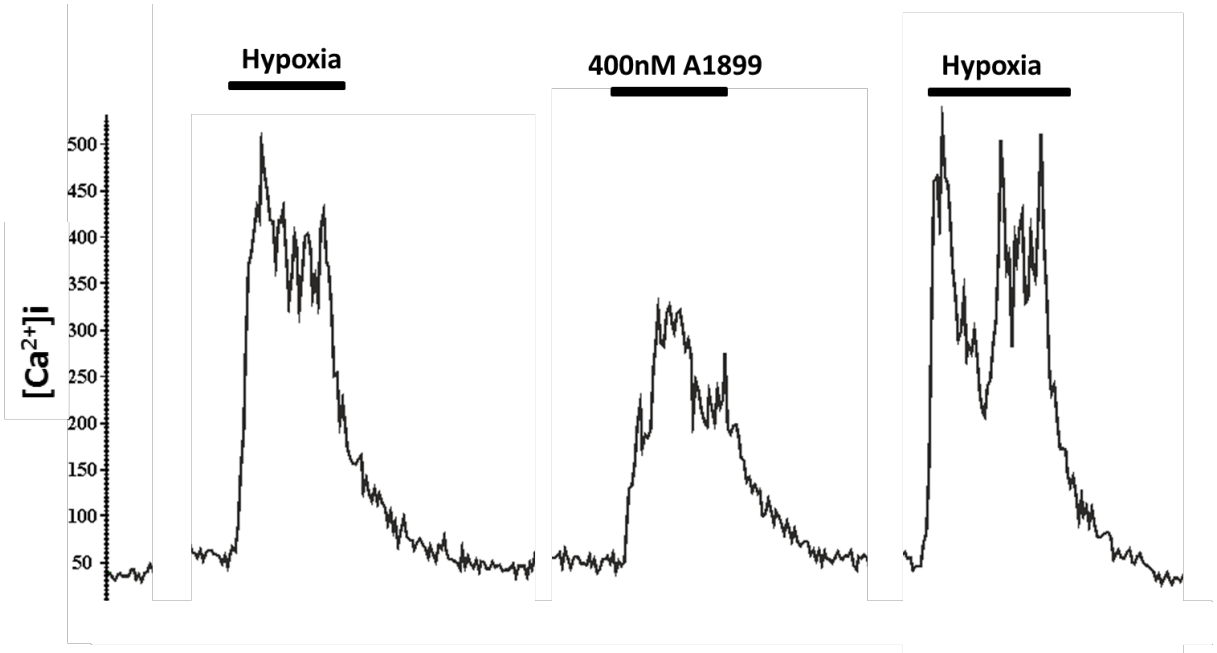

Figure 6.7: A1899 evoked Ca2+ entry in rat glomus cell. An original recording of intracellular $Ca2^{+}$ concentration measured using Indo-1 in a type-1 cell bathed in normal Tyrode. Cells are first exposed to a hypoxic stimulus of 0% oxygen and then exposed to 400nm A1899 in 21% O_2.

PK-THPP

The effect of PK-THPP was studied on carotid body glomus cells. Upon 400nM PK-THPP application, TASK channel activity in rat carotid body glomus cells was inhibited in a strong and reversible fashion. Figure 6.8A and B show an example trace of the same concentration (400nM) as also used in the HEK cells. A paired t-test of ten recordings between the nPopen values of a 20s period prior to and during 400nm PK-THPP application revealed a significant depression of 90% (SEM 2.7%, P= 0.034 df = 9 t = 2.489. Figure 6.8C).

A representative all-points histogram in Figure 6.9 reveals that PK-THPP partly inhibits the peak channel activity around 1.2pA which are assumed to represent some TASK-1 channel activity present in the patch. All other amplitudes, are strongly inhibited by PK-THPP. In particular the ~2.6pA which typically represents the TASK-1/3 heterodimer, but also the peak amplitudes around 3-3.5pA which may represent some TASK-3 channel activity present in the patch.

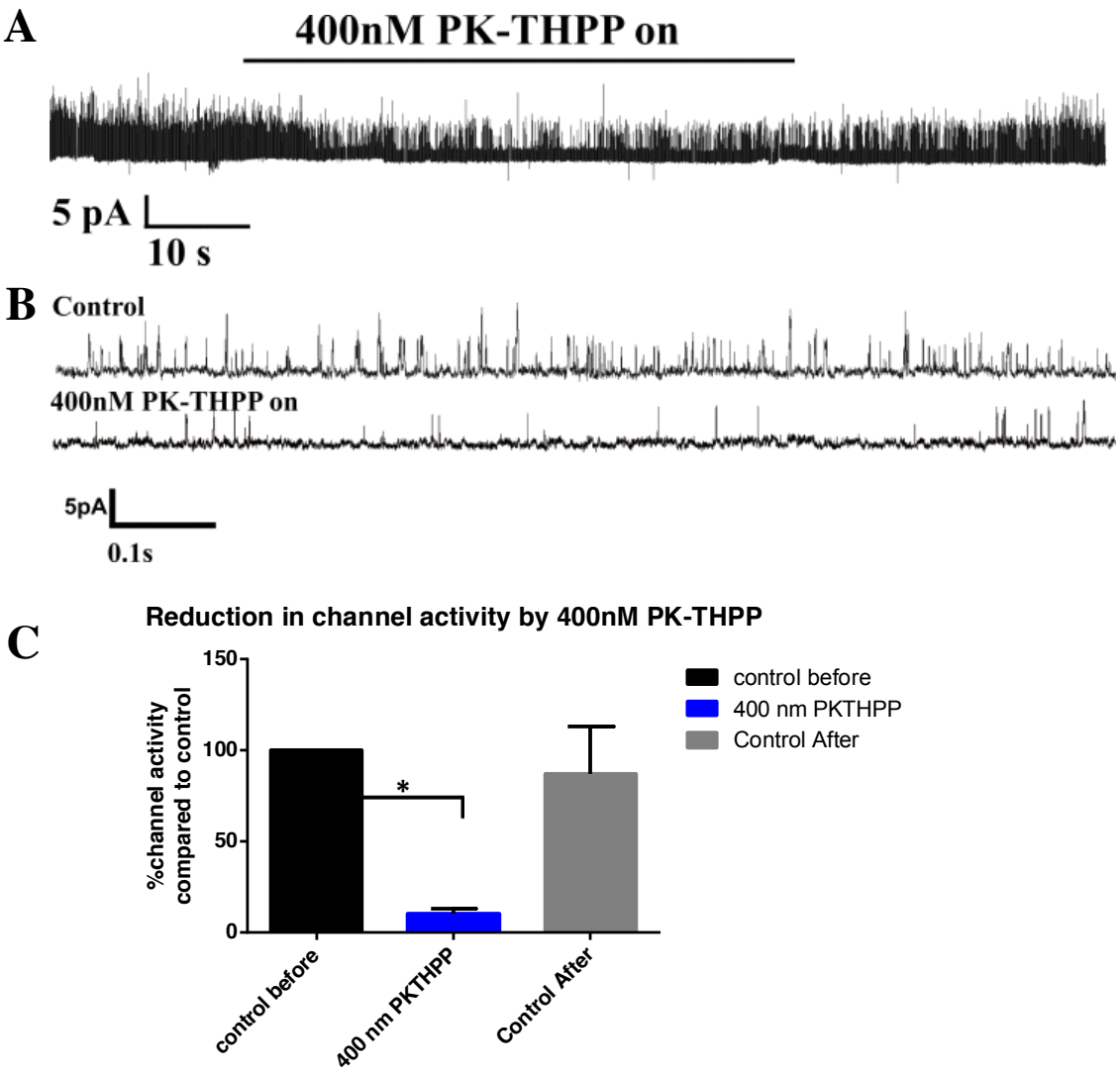

Figure 6.8: PK-THPP reduces background channel activity in cell-attached rat type-1 cell patch. 400 nm PK-THPP (n=10) evokes a strong and reversible depression of background TASK channel activity. Representative trace of TASK channel activity over **(A)** approximately 1.5 minutes and **(B)** 1 second. **(C)** PK-THPP significantly depresses channel activity by 90% (SEM 2.7% paired t-test P= 0.034 df=9 t= 2.489). The diagram displays % change in nPopen values compared to channel activity before PK-THPP application. Threshold for nPopen was 75%. Pipette potential was +80 mV. Cells were superfused with 100 mM K^+ Tyrode, with 140 mM K^+ in the pipette solution.

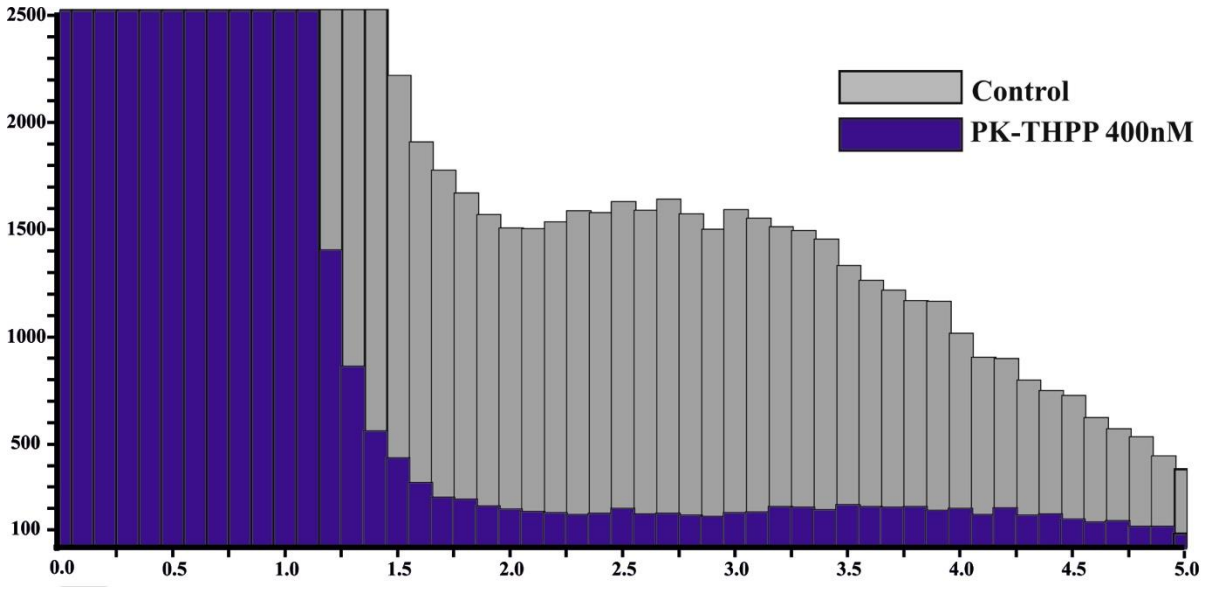

Figure 6.9: Representative all points histogram for the effect of 400nM PK-THPP on glomus cell TASK channel activity. Histogram was generated from a selected 20s section of both control and A1899 application. Bin-width was

Two lower concentrations (40nM and 120nM) were applied to glomus cells to generate a concentration response curve of the effect of PK-THPP on TASK. Curve fitting of a hyperbola suggests a Kd for the effect of PK-THPP of 66.0nM and a Bmax of 100% inhibition.

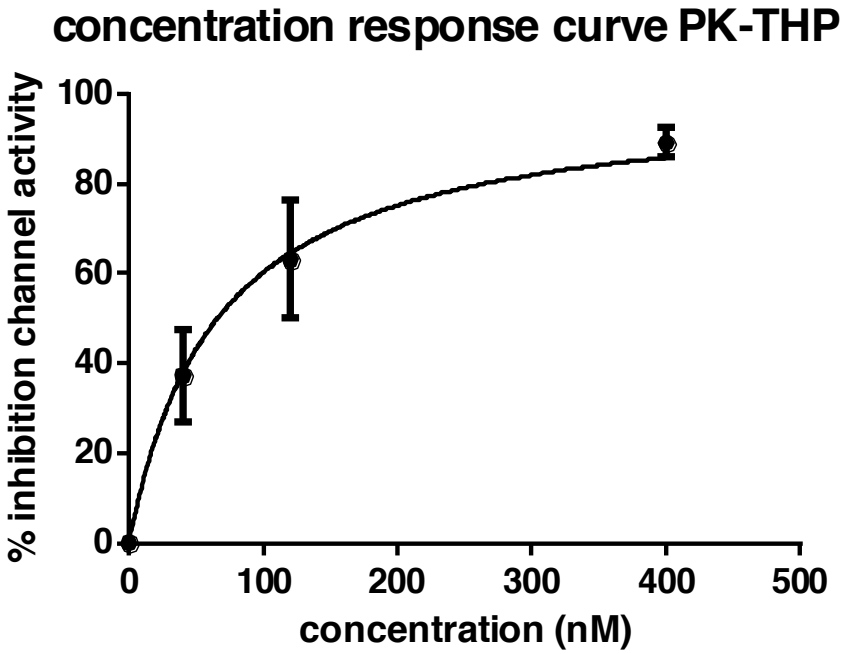

Figure 6.10: Concentration response of PK-THPP on background TASK channel activity in rat type-1 cell. % change in nPopen values compared to channel activity before PK-THPP application (40nm: n=5, 120nm: n=5 , 400nm: n=10). Hyperbola curve fitting generated a curve with R square of 0.997, BMax of 100 and a Kd of 66.02nM (SEM 9.5)

Doxapram

To compare the new breathing stimulants to an existing breathing stimulant drug, doxapram was applied to rat glomus cells while recording TASK channel activity. The effect of doxapram has not been fully studied on native TASK channels in type-1 cells before, but only in expressed systems (Cotten et al., 2006). Figure 6.11A and B show a representative trace of 50μM doxapram revealing a rapid and reversible depression of TASK channel activity. Figure 6.11C reveals the average channel activity compared to control channel activity which was set at a 100%. The 5μM concentration evoked a 6.8% depression (n=3, SEM 2.2%) and 50μM evoked a significant depression of 42.3% depression Wilcoxon Signed Rank Test (n=7, SEM 4.6%, P= 0.018).

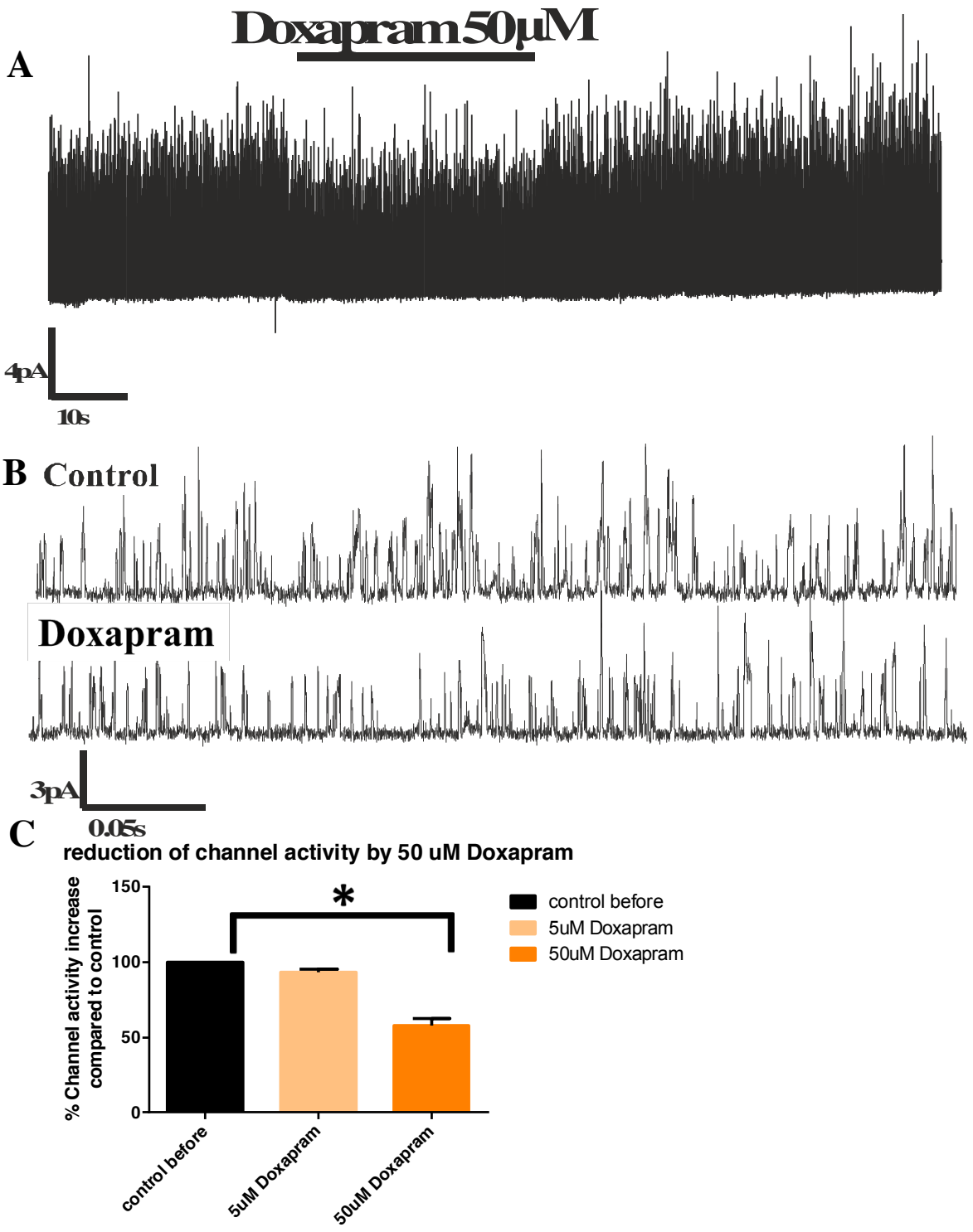

Figure 6.11: Background channel activity in cell-attached rat type-1 cell patch. 50 µM doxapram (n=7) evokes a modest and reversible depression on the TASK channel activity. Representative trace of TASK channel activity over **(A)** approximately 1.5 minutes and **(B)** superimposed over 0.3 seconds. **(C)** Doxapram 5µM N=3 slightly decreases channel activity. Doxapram 50µM significantly depresses channel activity by 42.3% (SEM 4.6% Wilcoxon Signed Rank P= 0.018).

Figure 6.12 displays an all points histogram revealing that doxapram depression is most apparent at 2.7pA representing the TASK-1/3 heterodimer, although modest inhibition is also observed all other peak amplitudes.

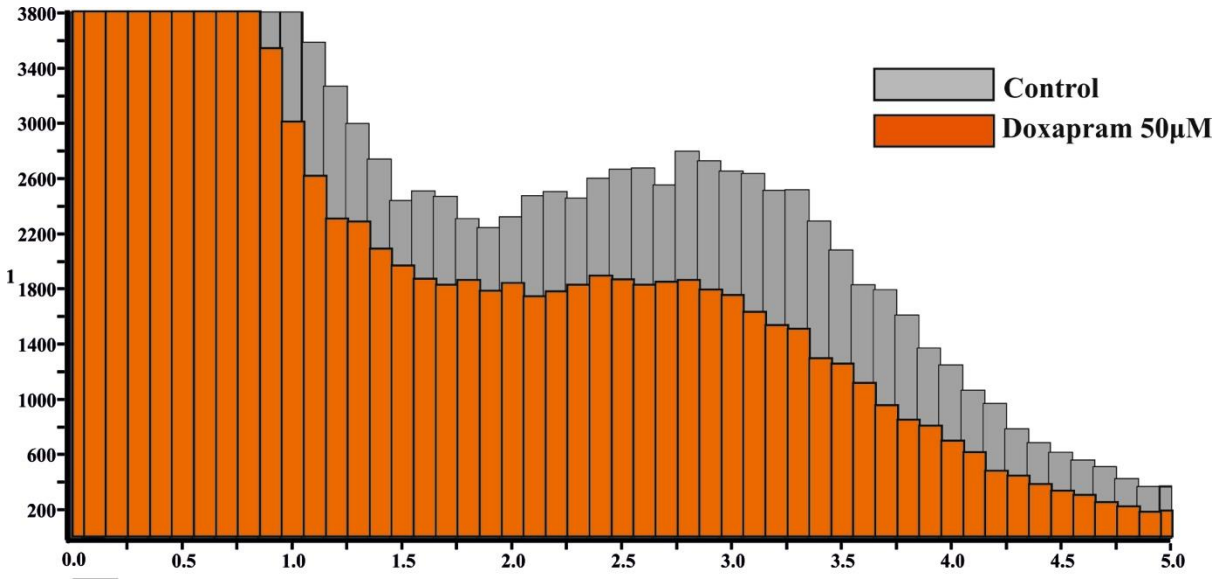

Figure 6.12: representative all-points histogram of 50 μM on rat glomus cells TASK channels. Histogram was generated from a selected 20s section of both control and doxapram application. Bin-width was 0.1pA.

6.3.3 The effects of breathing stimulants combined with isoflurane

A1899, PK-THPP and doxapram were all applied in combination with a relevant concentration of isoflurane (1.5%), to investigate if the inhibition of TASK channel was still apparent in the presence of an anaesthetic known to increase TASK channel activity.

A1899

A1899 and a clinically relevant concentration of 1.5% isoflurane, was combined and applied to glomus cells. First 1.5% isoflurane was applied to the cells followed directly by an application of 1.5% isoflurane combined with 400nM A1899. Isoflurane evoked a rapid and reversible increase of channel activity of 69% (n=8 SEM 19.6%) compared to control which can be seen in the representative traces of Figure 6.13A and B. Isoflurane 1.5% in the presence of 400nM A1899 evoked a depression of 25.5% (n=8 SEM 13.9%) compared to control. A related samples Wilcoxon signed rank test comparing nPopen of isoflurane alone and isoflurane combined with A1899 revealed a significant difference with p=0.012 (Figure 6.13C).

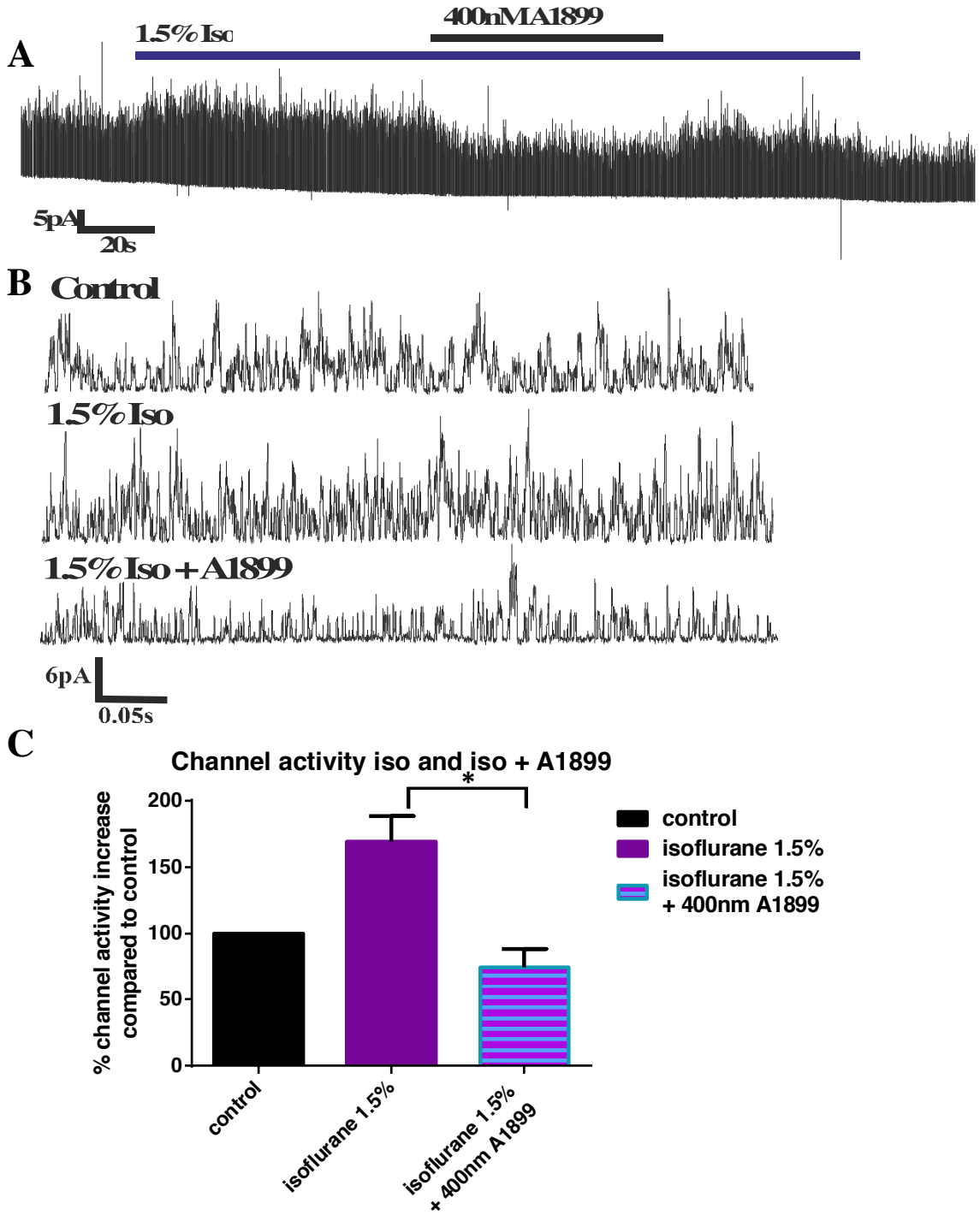

Figure 6.13: **A1899 depresses background TASK channel activity in rat type-1 cell in the presence of 1.5% isoflurane** In the presence of a clinically relevant dose of 1.5% isoflurane, 400nm A1899 is still able to depress TASK channel activity in glomus cell. Representative trace of TASK channel activity over **(A)** approximately 4 minutes and **(B)** 1 second. **(C)** % change in nPopen values compared to channel activity before isoflurane and A1899 application. Isoflurane evoked an increase of channel activity of 69% (N=8 SEM 19.6%) (N=8). Isoflurane 1.5% in the presence of 400nM A1899 evoked a depression of 25.5% (N=8 SEM 13.9%) compared to control. A related samples Wilcoxon signed rank test p=0.012

Figure 6.14 shows a representative all points histogram. Isoflurane 1.5% (purple) application results in an increase in channel activity of the heterodimer peak. The application of isoflurane 1.5% in the presence of 400 nM A1899 (light blue) leads to a depression, especially amongst the channels with the main peak amplitude of 2.8pA. Very little depression can be seen around the open amplitudes of 1-1.5pA.

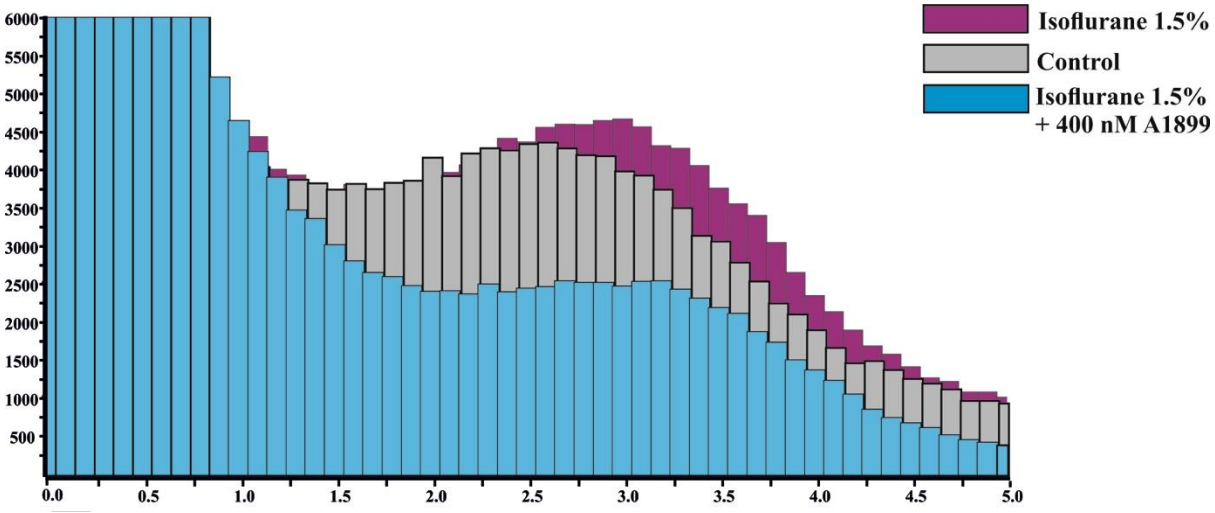

Figure 6.14: all-points histograms revealing control, 1.5% isoflurane and 1.5% isoflurane + 400nM PK-THPP. Each histogram was (0.1 pA bin widths) generated from 20 s segments of cell-attached recordings.

PK-THPP

To examine if PK-THPP is also able to depress TASK channel activity in the presence of a clinically relevant dose of isoflurane (1.5%), both agents were combined and applied to glomus cells. First 1.5% isoflurane was applied to the cells followed directly by an application of 1.5% isoflurane combined with 400nM PK-THPP. The representative traces in Figure 6.15A and B show that 400nM PK-THPP in the presence of 1.5% isoflurane leads to a rapid and strong depression. Isoflurane evoked an increase of channel activity of 51.9% (N=8 SEM 15.1%) compared to control. Isoflurane 1.5% in the presence of 400nM PK-THPP evoked a depression of 84.8% (N=8 SEM 4.4%) compared to control. A paired t-test between nPopen of isoflurane alone and isoflurane combined with PK-THPP revealed a significant difference with p=0.012 (df=7 Figure 6.15C).

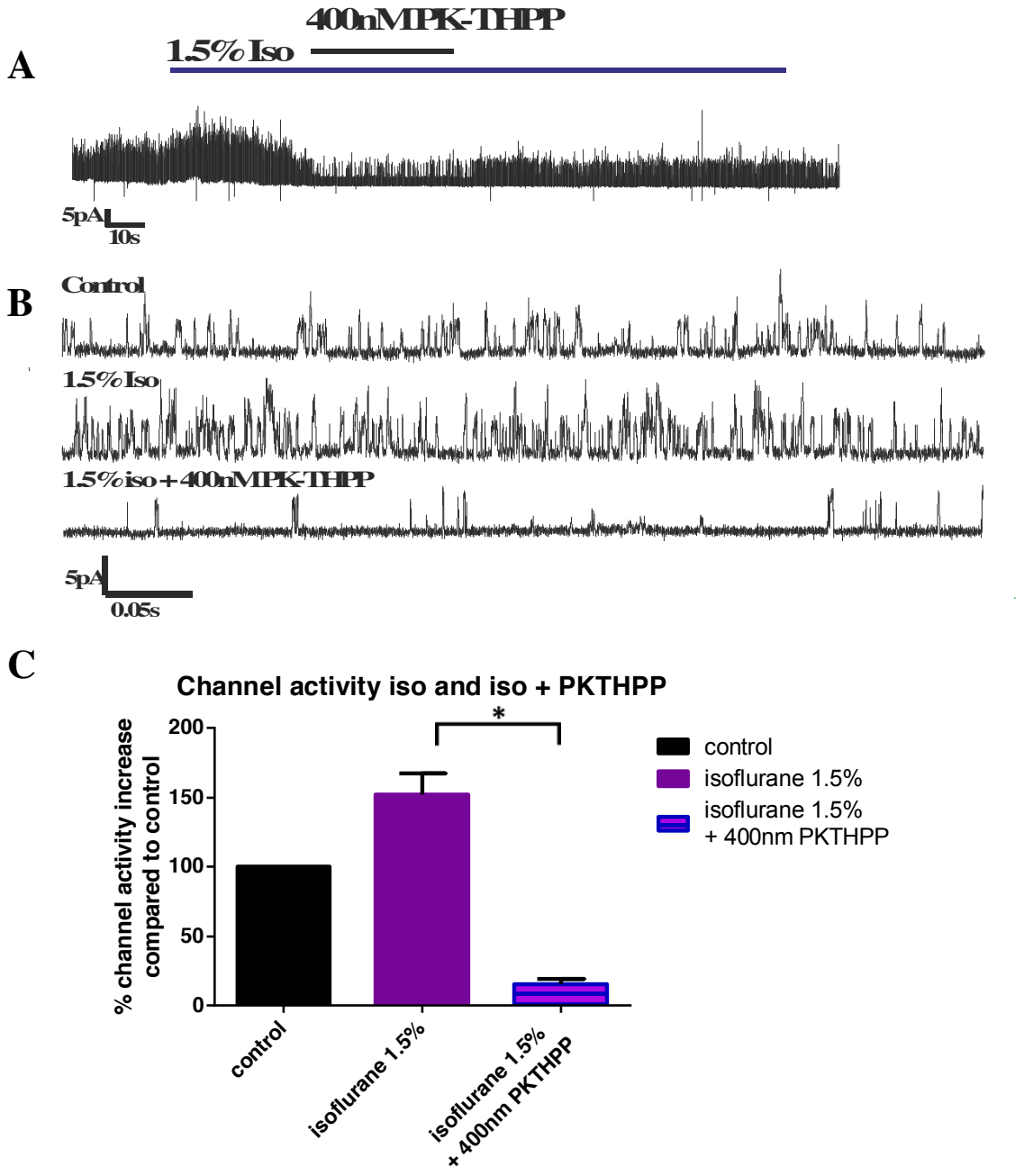

Figure 6.15: PK-THPP depresses background TASK channel activity in rat type-1 cells in the presence of 1.5% isoflurane In the presence of a clinically relevant dose of 1.5% isoflurane, 400nm PK-THPP is still able to depress TASK channel activity in glomus cell. Representative trace of TASK channel activity over **(A)** approximately 2 minutes and **(B)** 1 second. **(C)** % change in nPopen values compared to channel activity before isoflurane application (N=8). Isoflurane evoked an increase of channel activity of 51.9% (n=8 SEM 15.1%) compared to control. Isoflurane 1.5% in the presence of 400nM PKTHPP evoked a depression of 84.8% (n=8 SEM 4.4%) compared to control. A paired t-test between nPopen of isoflurane alone and isoflurane combined with PK-THPP revealed a significant different with p=0.012 (df=7). Recording filtered at 5kHZ.

Figure 6.16 shows a representative all points histogram. Isoflurane 1.5% (purple) application results in an increase in channel activity. The application of isoflurane 1.5% in the presence of 400 nM PK-THPP (dark blue) leads to a depression, especially in the channels with an amplitude of 1.7pA and larger.

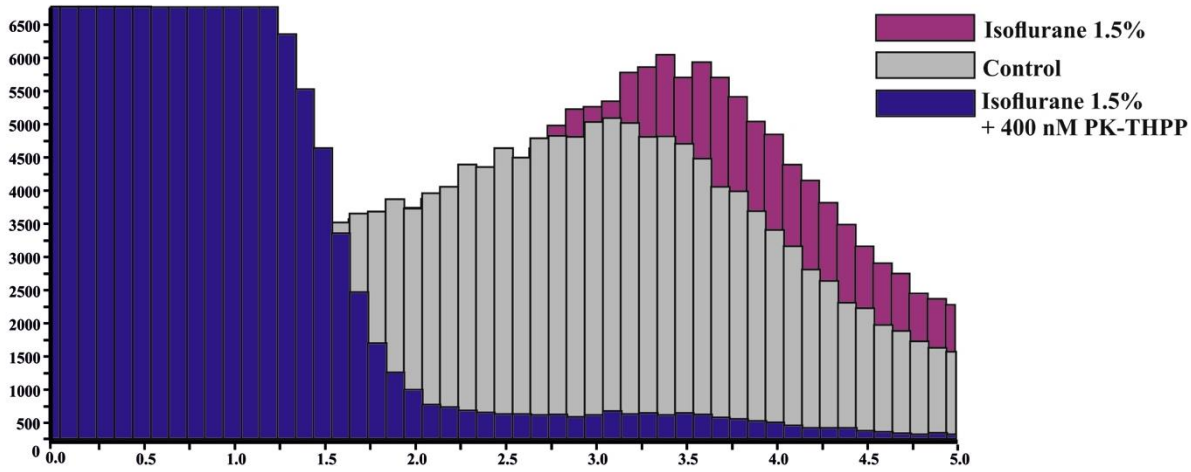

Figure 6.16: all-points histograms revealing control, 1.5% isoflurane and 1.5% isoflurane + 400nM A1899. Histogram was generated from 20 seconds segments of cell-attached recordings.

Doxapram

To examine if doxapram is able to depress TASK channel activity in the presence of a clinically relevant dose of isoflurane, both agents were combined and applied to glomus cells. First 1.5% isoflurane was applied to the cells followed directly by an application of by 1.5% isoflurane combined with 50μM Doxapram. Figure 6.17 shows that isoflurane evoked an increase of channel activity of 35% (n=8 SEM 6.6%) compared to control as seen in Figure 6.17. Isoflurane 1.5% in the presence of 50μM doxapram evoked a depression of 35.1% (n=5 SEM 10.8%) compared to control. A related samples Wilcoxon signed rank test comparing nPopen of isoflurane alone and isoflurane combined with doxapram revealed a significant difference with p= 0.043.

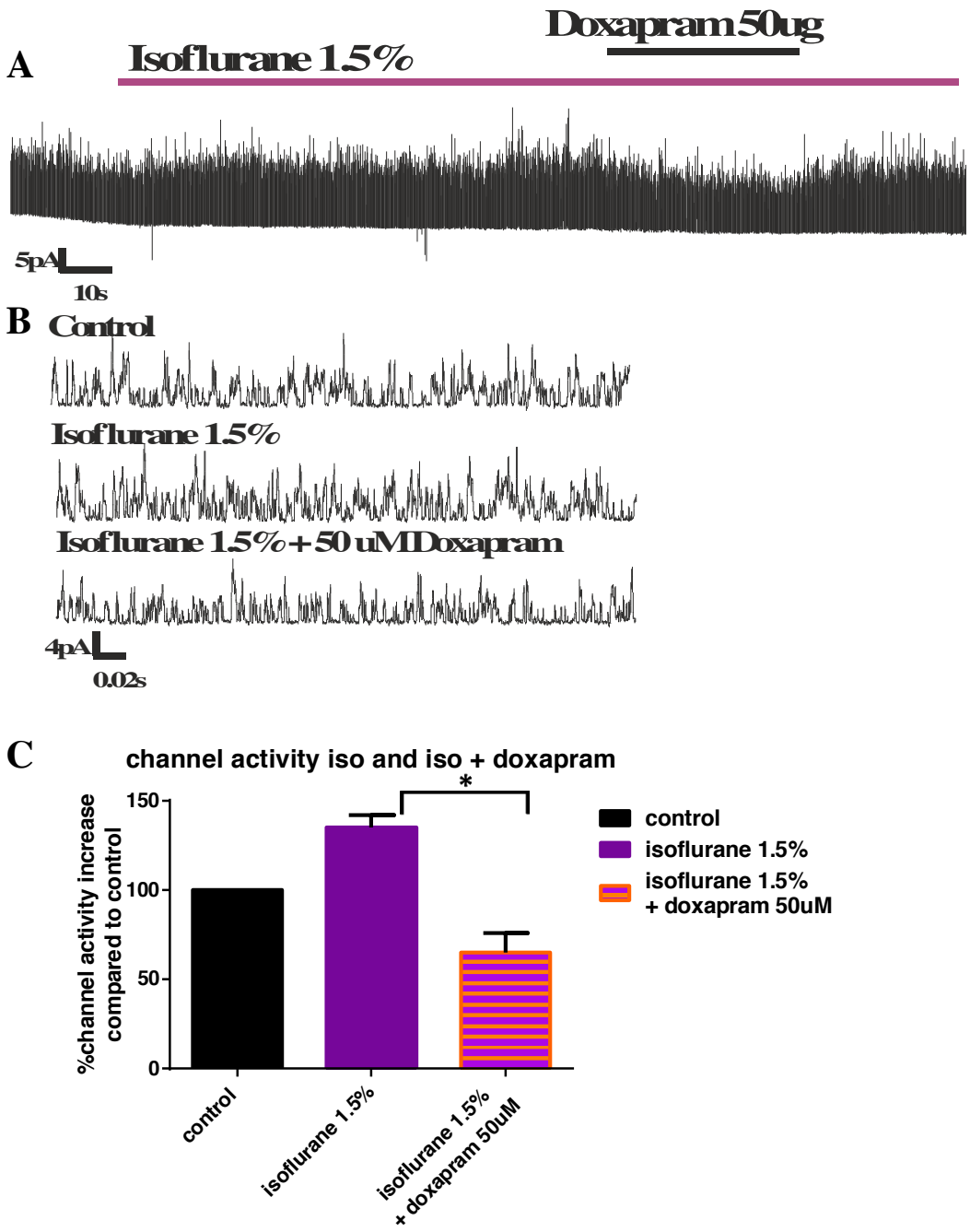

Figure 6.17: Doxapram (50µM) depresses background TASK channel activity in rat type-1 cell in the presence of 1.5% isoflurane. Representative trace of TASK channel activity over **(A)** approximately 2 minutes and **(B)** superimposed over 1 second. % change in nPopen values compared to channel activity before isoflurane application (N=8). Isoflurane evoked an increase of channel activity of 35.0% (N=8 SEM 6.6%) compared to control. Isoflurane 1.5% in the presence of 400nM A1899 evoked a depression of 35.0% (N=8 SEM 10.8% P = 0.043) compared to control. Note: in panel A, a small section of recording was removed in which a noise or disturbance occurred.

Figure 6.16 shows a representative all points histogram. Isoflurane 1.5% (purple) application results into an increase in channel activity. The application of isoflurane 1.5% in the presence of 50μM doxapram (orange) leads to a partial inhibition which is most predominant in the presumed heterodimer channels, but also to some degree in channels with smaller and larger open amplitudes.

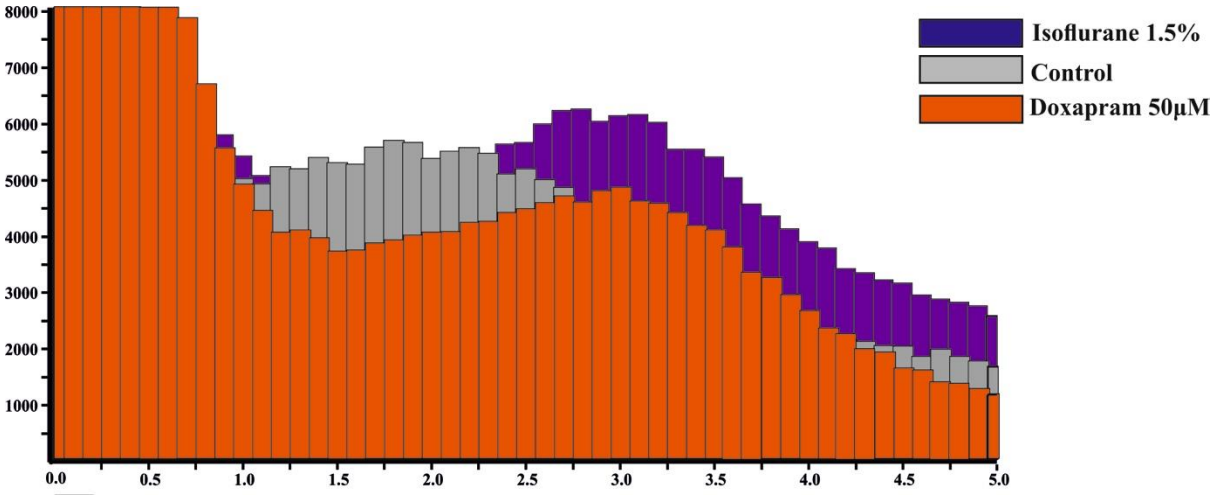

Figure 6.18: all-points histograms revealing control, 1.5% isoflurane and 1.5% isoflurane + 50M doxapram. Histogram was generated from 20 s segments of cell-attached recordings.

6.3.4 NADH auto-fluorescence measurements of A1899 and PK-THPP in glomus cell

NADH auto-fluorescence measurements were carried out to observe, if there were any interactions between either compound and mitochondrial respiration in glomus cells. Either 400nM A1899 or PK-THPP was applied in standard Tyrode (21%O_2 with 5% CO_2). No change in baseline signal was detected between the control auto-fluorescence baseline level and the baseline level during PK-THPP application (p= 1.00, n=4, Wilcoxon Signed Rank Test) indicating that these drugs do not change NADH levels within mitochondria. Similarly, for A1899, four recordings showed no difference in NADH fluorescence of control baseline level compared to 400nM A1899 application (p=0.715 Wilcoxon Signed Rank Test).

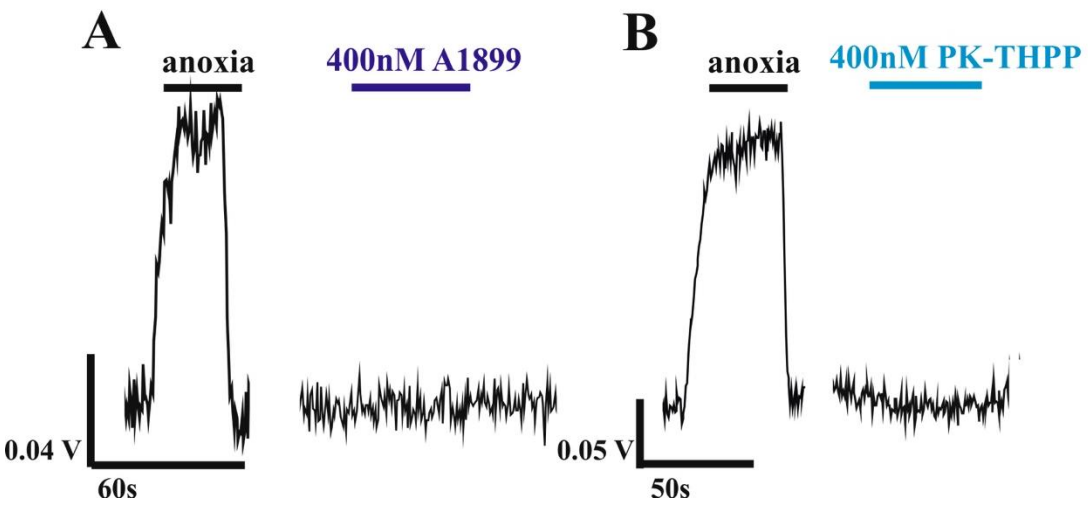

Figure 6.19: Representative traces of A1899 and PK-THPP on NADH autofluorescence. (A) Anoxia stimulus followed by the application of 400nM A1899 in normoxic conditions. **(B)** Anoxia stimulus followed by PK-THPP application in normoxic conditions.

6.4 Discussion

The experiments in this chapter demonstrate that application of PK-THPP, A1899 and doxapram decrease background TASK channel activity in native rat glomus cells and that the two novel inhibitors appear to be more efficient in doing so than doxapram. This work is in line with experiments simultaneously performed by P. O'Donohoe (O'Donohoe, 2015), who showed that application of A1899 and PK-THPP in the nanomolar range cause a Ca^{2+} influx in rat glomus cells. Taking all results together, we can conclude these two novel drugs act as chemo excitants through (partial) TASK channel inhibition. Experiments in this chapter also show that all three drugs are still able to depress TASK channel activity in the presence of a clinically relevant concentration of isoflurane. The sections below will discuss the results of this chapter in more detail and will discuss the potential clinical relevance of these drugs in the future, both the promising aspects and the possible limitations.

6.4.1 A1899 and PK-THPP on glomus cell TASK activity

The results in this chapter suggest that application of PK-THPP, A1899 and doxapram decrease background TASK channel activity in native rat glomus cells. PK-THPP is the most effective inhibitor of TASK-channel and upon application, results in a rapid and reversible decrease of channel activity across all amplitude ranges. Application of concentrations in the nanomolar range such as 400nM decrease the nPopen values for channel activity of the heterodimer by 90%. Similarly, 400nM A1899 also reduces channel activity across all amplitude ranges and 400nm decreases channel activity of the heterodimer by 35% in a

reversible fashion. doxapram decreases TASK channel activity at a much higher concentration, reaching a 35% depression of the heterodimer by applying 50μM to the bath, which is more than a 100 fold higher concentration. Therefore, it appears that the novel compounds are more effective inhibitors of the native heterodimer channel than doxapram.

In most of the single channel cell attached recordings, it is believed that we predominantly observe TASK-1/3 channel activity, which typically has an average peak amplitude of 2.7pA (Turner and Buckler, 2013b). When looking at the all points histograms of the inhibitors effects, an equal depression of all channel amplitudes can be seen with no clear discrimination of selectivity for channels with a larger or smaller average peak amplitudes. For example around 1.2pA, which is where we expect TASK-1 channels to appear or ~3.2 pA where we expect to observe TASK-3 channels, no clear discrimination in the degree of inhibition is detected. The fact that we fail to observe a discrimination of different TASK subsets can be explained in two different ways. The first possible explanation is that the patches rarely contain TASK-1 or TASK-3 homomeric channels. Thus, the only effect observed in the recorded patches, is the effect on the heterodimer. Even if the patches contain one or two homomers, these are 'hidden' behind the TASK-1/3 heterodimer, which are believed to be present at much higher frequencies. This explanation is supported by research performed by Kim et al. (2009a), who predicted that 75% of the background current comes from the heterodimer and therefore 75% of wild-type channel activity could come from heterodimer. Turner and Buckler (2013b) also concluded that the total channel activity combined of both TASK 3 KO mice and TASK-1 KO mice is still 3.6 times lower than wild type-1 cell channel activity, indicating that the heterodimer accounts for the vast majority of channels observed in the patches. A second explanation for the lack of discrimination is that

the drug affinity for the heterodimer is simply as strong as that for the individual TASK-1 or TASK-3 channels. However, with the results obtained so far, it is not possible to exclude either explanation. These results do however demonstrate for the first time, that A1899 and PK-THPP effectively depress the native heterodimer as it appears in the rat glomus cell.

The only previous study performed on a TASK-1/3 'heterodimer' was carried out by Rinne et al. (2015). The authors investigated the effect of A1899 on TASK-1/3 concatemers and discovered that the orientation of the concatemer determined the amount of block evoked by the A1899 inhibitor. The TASK-3/1 concatemer was inhibited by 34%, resembling the TASK-1 block, whereas the TASK-1/3 was inhibited by 9%, resembling the block on TASK-3. As it appeared that the pharmacology of the concatemer depended on the orientation of the construct, the authors suggested that heterodimer studies are best done by co-transfecting TASK-1 and -3 together or by performing studies on the native channel itself.

6.4.2 Clinical relevance of A1899 and PK-THPP

With promising results in this chapter regarding the drug efficacy, and taken into consideration the positive results from (Cotten, 2013) who noted an increased minute ventilation by increasing tidal volume and breathing rate, one could hypothesize about the suitability of these drugs for clinical application. The sections below will elaborate briefly on the many potential clinical targets for TASK channel blockers. Examples will be anaesthesia evoked ventilatory depression, obstructive sleep apnoea, atrial fibrillation and breast cancers.

Studying the effect of the inhibitors on human carotid body cells would be ideal. There is some evidence suggesting that the most promising drug for human use would be A1899. Immunohistochemistry studies performed by (Fagerlund et al., 2010) and microarray studies performed by (Mkrtchian et al., 2012) reveal that TASK-1, but potentially not TASK-3, is expressed in the human carotid body. Therefore TASK-1 may be the predominant background K_2P channel in human glomus cells. Because of the similarity in action compared to doxapram (they both act on TASK channel in carotid body), it would therefore be worth considering its use to stimulate breathing in patients experiencing anaesthesia evoked ventilatory depression.

Another condition that could benefit from TASK blockers is obstructive sleep apnoea. This is a disorder characterised by repetitive partial or complete upper airway occlusion during sleep, leading to reduction of airflow and a decrease in arterial oxygen saturation (Mason et al., 2015). Wirth et al., (2013) administered AVE0118 to a sleep apnoea model in anesthetized pigs. This agents has been reported to block TASK-1 (and Kv 1.5 to a lesser extend) (Kiper et al., 2015). The authors suggest that AVE0118 sensitized upper airway mechanoreceptors, by making the resting membrane potential less negative and thus enhancing depolarization, which then enhances a negative pressure reflex in the upper airways and prevents collapsing. These results indicate that A1899 and/or PK-THPP could potentially be beneficial for treatment of sleep apnoea.

Limberg et al., (2011) showed with PCR studies that TASK-1 is expressed in human atria and auricles. Their single channel recordings revealed TASK-1 currents in cardio myocytes in right human auricles. The authors suggest that TASK-1 might be a drug target for the

treatment of atrial fibrillation, because of the specific expression in atria and auricles only and because of TASK-1 proposed importance in contributing to the action potential duration. A recent study performed by (Harleton et al., 2015) also confirmed the presence of TASK-1 in human and canine atrial cardio myocytes and found that inhibition of TASK-1 currents disrupted repolarization of isolated cells. Although A1899 may potentially be promising for the treatment of certain heart conditions, the wide expression of TASK-1 in different parts of the human heart should also be carefully considered when testing A1899 for human use.

Lastly, there are a few reports indicating a role of TASK channel overexpression in certain cancer cell types. Mu et al., (2003) identified in breast cancer samples that in 10% of the cases KCNK9 (encoding TASK-3) is amplified and overexpressed and suggest this may play an important role in hypoxia tolerance of tumour cells. Innamaa et al., (2013) reported TASK-3 is expression in epithelial ovarian cancer and also Pei et al., (2003) indicated that blocking TASK-3 in certain tumours may have therapeutic potential for the treatment of cancers.

To summarize, based on the existing literature and the experiments in this chapter, there appears to be a promising future for TASK blockers, which may not only extend to the treatment of carotid body related conditions, but also to a wide variety of other potential clinical applications. The results also highlight the need for further preclinical studies to elucidate more about the role TASK channels and their inhibition in a variety of tissues.

Chapter 7. Discussion

7.1.1 Main findings

The primary aim of this thesis was to investigate how volatile anaesthetics depress the hypoxia sensitivity in the carotid body. My research started by examining hypoxia evoked Ca^{2+} entry and, following exclusion of a significant effect of anaesthetics on voltage gated Ca^{2+} channels, attention turned to TASK channels. Native TASK channels were investigated first, followed by a study of TASK channels transiently expressed in HEK cells. Next, my attention turned to the mitochondria to examine whether the anaesthetic evoked changes in mitochondrial function. The study was concluded by examining the effect of two novel TASK blocking agents on native TASK channel activity and their ability to offset the effects of anaesthetics.

This thesis has achieved its primary goal and revealed that, in carotid body cells, hypoxia evoked Ca^{2+} entry is depressed by halothane > isoflurane > sevoflurane. Similarly, the activity of native carotid body TASK channels and that of rat-TASK-1 and rat TASK-3 transiently expressed in HEK cells is increased by halothane > isoflurane > sevoflurane. This is in accordance with the variable depressive effects of anaesthetics in human and rat ventilatory studies (Pandit, 2002, Karanovic et al., 2010). The fact that this order of potency of anaesthetics is conserved even across cloned TASK channels, suggests that these channels may be key to the effects of anaesthetic in relation to respiratory control, and could even be a sufficient explanation for whole-body phenomena, notably the differential depressive sensitivity of the system to different agents.

A further interesting result was that at the level of mitochondria, anaesthetics act in the *same direction* as hypoxia. All three volatile anaesthetics have an effect on both mitochondrial potential and [NADH]. Anaesthetics increase [NADH] and depolarize the mitochondrial potential. This effect was not exclusive to carotid body cells only, but was also found in HEK cells. This effect has also been reported for cardiac myocytes (Hanley et al., 2002) but little is known regarding other cell-types. According to previous literature, mitochondria are thought to be upstream of TASK channels in the hypoxia transduction cascade (Duchen and Biscoe, 1992a, b, Buckler and Turner, 2013) and may regulate the activity of TASK channels through signalling molecules. The new hypothesis that arose from this work is that volatile anaesthetics may have, in addition to their direct *activating* effect, a second indirect *inhibiting* effect on TASK channel activity, through their effect on mitochondria. How these apparently opposing effects interact when the cell is exposed to anaesthetic is unclear although the net effect is evidently a depressive one in respect of the glomus cells response to hypoxia.

In the course of these investigations, I discovered the most intriguing finding that isoflurane behaved as a 'partial agonist' at the level of a single channel and, consistent with this, partially antagonized the effects of halothane (a strong agonist) consistent with competitive antagonism. This finding cannot be explained by the lipid perturbation theory of Meyer and Overton, but further supports the anaesthetic receptor interaction model. These results suggest that anaesthetics may compete with each other for a binding site on the TASK channel.

A promising finding in this thesis for therapeutics is the effect of PK-THPP and A1899 native TASK activity. Both agents were able to profoundly reduce the native carotid body channel

activity in the nanomolar range, even in the presence of 1.5% isoflurane. The effects of PK-THPP and A1899 on the carotid body were comparable to that of the classical respiratory stimulant doxapram, except that the concentration of both agents was over 100 fold lower than that of doxapram. These results therefore highlight the potential use of these agents for treating the anaesthetic evoked depression of the AHVR.

7.1.2 Future work

Three different research questions arise from the findings presented in this thesis:

1. How do anaesthetics interact (in detail) with TASK channels in order to increase the channel activity?
2. What are the physiological implications of the anaesthetic effects on mitochondria?
3. Is there a clinical use for the TASK channel antagonists?

1. Anaesthetic interaction with TASK

Infra-additivity: Classical receptor pharmacology?

The most parsimonious explanation for the observed infra-additivity is the explanation of halothane and isoflurane competing for a common binding sites on the channel. However, our experimental design could not exclude the possibility (however remote) of complex indirect effects of volatile anaesthetics via mitochondrial regulation (in particular in the carotid body).

One way to exclude such indirect effects, especially metabolic or mitochondrial, as contributors to an infra-additive effect of anaesthetic mixtures would be by repeating the

experiments on TASK channels transiently expressed in HEK cells, but with a mitochondrial inhibitor (eg, with FCCP). It is unlikely that such metabolic control exists. Transient transfection, resulting in the sudden introduction of vast amounts of TASK channels within a short time frame (recording between 24-48 hours post transfection), would unlikely generate a proper signalling link between mitochondria and TASK channels. Furthermore, this lab has not been able to demonstrate oxygen sensitivity of TASK channels in heterologous expression systems. One other way to further examine the infra-additivity is by repeating the mix experiment in excised TASK-1 patches. However, attempts to do so have been unsuccessful.

There is one other interesting variation of the classical receptor interaction theory as described above. Instead of competing for the same binding site on the TASK channels, isoflurane may also bind to an inhibitory binding site on the TASK channel. Chloroform for example has previously been reported to activate human TASK-3, whereas it had an inhibiting effect on human TASK-1 (Andres-Enguix et al., 2007). Although the net effect of isoflurane on TASK-1 is one of activation, it is a possibility that its partial agonist behaviour may be explained by binding to both an inhibitory and activating binding site.

Other relevant research questions worth pursuing are:

A. Do other agents (eg, sevoflurane, IV agents) also demonstrate interactive infra-additive effects on TASK channels like halothane and isoflurane?
B. What is the effect (and interaction between) these agents in HEK cells transiently transfected with TASK-3 channels or the TASK-1/3 concatemer?

C. What are the putative binding sites for volatile anaesthetics on the TASK hetero and homodimers.

2. The physiological implications of the anaesthetic effects on mitochondria

There are several general directions for future research based on the mitochondrial results obtained in this thesis. Intravenous anaesthetics like propofol are known to inhibit the hypoxic chemoreflex (Nagyova et al., 1995) but relevant studies seem sparse. One report in macrophages suggested that propofol in clinical concentrations reduced mitochondrial membrane potential but did not influence [NADH] (Wu et al., 2005). The latter finding of an absence of effect on [NADH] by propofol has been reported in context of cerebral hypoperfusion in rabbits (Wang et al., 2011). Similarly, the actions of the anaesthetic agent nitrous oxide (N_2O) have been investigated for interactions with mitochondria. N_2O has been demonstrated to decrease respiration rates in bovine sub-mitochondrial particles (Sowa et al., 1987) and also Becker et al. (1986) have shown that nitrous oxide decreases mitochondrial respiration in certain conditions in cerebral cortex mitochondria. However, recent evidence of interaction between nitrous oxide and mitochondria respiration is lacking, which warrants for further investigation to establish anaesthetic agent effects on mitochondrial respiration. It is not clear if all anaesthetics have similar effects on mitochondrial membrane potential or [NADH], but if not, then these mitochondrial processes would unlikely underlie a 'common mechanism of anaesthesia', but may nonetheless contribute to ways in which anaesthetics differ in the way they induce unconsciousness (Pandit, 2014). Furthermore, it may also be possible that the decrease in mitochondrial respiration and thus an altered metabolic state

may account for some of the side effects of anaesthesia such as the decrease in contractility or negative inotropic effects in the heart.

The suggested interaction of these mitochondrial processes with ROS is interesting, because studies performed by Teppema et al. (2002), (2005) have suggested that ROS modulation (by pre-treating human volunteers with antioxidants) can prevent or reverse the depressive effects of sub-anaesthetic doses on the hypoxic ventilatory response for both halothane and isoflurane. It would be interesting to assess if similar pre-treatment or co-treatment with agents like vitamins C or E influences the action of anaesthetics on mitochondrial membrane potential or [NADH].

In relation to theories of narcosis by anaesthetics, although it has been shown that knockouts of complex I subunits (Quintana et al., 2012) or mitochondrial diseases (Morgan et al., 2002) influence sensitivity to anaesthetic agents in the intact animals or humans, it has not been shown that cells from these sources are in fact differently sensitive to anaesthetic effects at the mitochondrial level. It would be of interest to compare the mitochondrial membrane potential measurements and [NADH] of type-1 cells of mice lacking this gene to my results obtained in rats. Similarly, it would be of interest to investigate if the effect of volatile anaesthesia on TASK channel activity and hypoxia evoked Ca^{2+} influx would be in any sense altered in type-1 cells of these mice.

3. The clinical translation regarding treating the anaesthetic evoked depression of ventilation

Regarding the novel antagonists, it would be of interest to further test the ability of these agents to stimulate breathing, for example in the treatment of anaesthetic induced depression of the AHVR and post-operative hypoxaemia in general in humans. The key future experiment regarding this would be to test the AHVR in mice with and without anaesthetics, and the stimulants.

Chapter 8. References

Acker H (1994) Oxygen sensing in the carotid body: ideas and models. Advances in Experimental Medicine and Biology 360:21-27.

Acker H, Lubbers DW, Purves MJ (1971) Local oxygen tension field in the glomus caroticum of the cat and its change at changing arterial PO_2. Pflugers Archiv : European Journal of Physiology 329:136-155.

Andres-Enguix I, Caley A, Yustos R, Schumacher MA, Spanu PD, Dickinson R, Maze M, Franks NP (2007) Determinants of the anesthetic sensitivity of two-pore domain acid-sensitive K+ channels: molecular cloning of an anesthetic-activated K+ channel from Lymnaea stagnalis. The Journal of Biological Chemistry 282:20977-20990.

Aranake A, Mashour GA, Avidan MS (2013) Minimum alveolar concentration: ongoing relevance and clinical utility. Anaesthesia 68:512-522.

Bains R, Moe MC, Larsen GA, Berg-Johnsen J, Vinje ML (2006) Volatile anaesthetics depolarize neural mitochondria by inhibiton of the electron transport chain. Acta Anaesthesiologica Scandinavica 50:572-579.

Bateman NT, Leach RM (1998) ABC of oxygen. Acute oxygen therapy. Bmj 317:798-801.

Bayliss DA, Barrett PQ (2008) Emerging roles for two-pore-domain K+ channels and their potential therapeutic impact. Trends in Pharmacological Sciences 29:566-575.

Becker GL, Pelligrino DA, Miletich DJ, Albrecht RF (1986) The effects of nitrous oxide on oxygen consumption by isolated cerebral cortex mitochondria. Anesthesia and Analgesia 65:355-359.

Becker K, Eder M, Ranft A, von Meyer L, Zieglgansberger W, Kochs E, Dodt HU (2012) Low dose isoflurane exerts opposing effects on neuronal network excitability in neocortex and hippocampus. PloS one 7:e39346.

Berg AP, Talley EM, Manger JP, Bayliss DA (2004) Motoneurons express heteromeric TWIK-related acid-sensitive K+ (TASK) channels containing TASK-1 (KCNK3) and TASK-3 (KCNK9) subunits. The Journal of Neuroscience :24:6693-6702.

Bernardini A, Brockmeier U, Metzen E, Berchner-Pfannschmidt U, Harde E, Acker-Palmer A, Papkovsky D, Acker H, Fandrey J (2015) Measurement of ROS Levels and Membrane Potential Dynamics in the Intact Carotid Body Ex Vivo. Advances in Experimental Medicine and Biology 860:55-59.

Bigelow HJ, (1846) Insensibility during surgical operations produced by inhalation. The Boston Medical and Surgical Journal 35:309-317.

Belelli D, Lambert JJ, Peters JA, Wafford K, Whiting PJ (1997) The interaction of the general anesthetic etomidate with the gamma-aminobutyric acid type A receptor is influenced by a single amino acid. Proceedings of the National Academy of Sciences of the United States of America 94:11031-11036.

Biscoe TJ (1971) Carotid body: structure and function. Physiological reviews 51:437-495.

Booth HS, Bixby EM (1932) Fluorine derivates of chloroform. Industrial and Engineering Chemistry 24:637-641.

Bovill JG, (2008) Inhalation anaesthesia: from diethyl ether to xenon. Handbook of Experimental Pharmacology 121-142.

Brohawn SG, Campbell EB, MacKinnon R (2013) Domain-swapped chain connectivity and gated membrane access in a Fab-mediated crystal of the human TRAAK K+ channel. Proceedings of the National Academy of Sciences of the United States of America 110:2129-2134.

Brohawn SG, del Marmol J, MacKinnon R (2012) Crystal structure of the human K2P TRAAK, a lipid- and mechano-sensitive K+ ion channel. Science 335:436-441.

Brunelle JK, Bell EL, Quesada NM, Vercauteren K, Tiranti V, Zeviani M, Scarpulla RC, Chandel NS (2005) Oxygen sensing requires mitochondrial ROS but not oxidative phosphorylation. Cell Metabolism 1:409-414.

Buckler K, Honore E (2004) Molecular strategies for studying oxygen-sensitive K+ channels. Methods in Enzymology 381:233-256.

Buckler KJ (1997) A novel oxygen-sensitive K+ current in rat carotid body type I cells. The Journal of Physiology 498:649-662.

Buckler KJ (2012) Effects of exogenous hydrogen sulphide on Ca2+ signalling, background (TASK) K channel activity and mitochondrial function in chemoreceptor cells. Pflugers Archiv : European Journal of Physiology 463:743-754.

Buckler KJ (2015) TASK channels in arterial chemoreceptors and their role in oxygen and acid sensing. Pflugers Archiv : European Journal of Physiology 467:1013-1025.

Buckler KJ, Turner PJ (2013) Oxygen sensitivity of mitochondrial function in rat arterial chemoreceptor cells. The Journal of Physiology 591:3549-3563.

Buckler KJ, Vaughan-Jones RD (1994) Effects of hypoxia on membrane potential and intracellular Ca2+ in rat neonatal carotid body type I cells. The Journal of Physiology 476:423-428.

Buckler KJ, Williams BA, Honore E (2000) An oxygen-, acid- and anaesthetic-sensitive TASK-like background K+ channel in rat arterial chemoreceptor cells. The Journal of Physiology 525 Pt 1:135-142.

Carroll JL, Bamford OS, Fitzgerald RS (1993) Postnatal maturation of carotid chemoreceptor responses to O2 and CO2 in the cat. Journal of Applied Physiology 75:2383-2391.

Chance B, Williams GR, Hollunger G (1963) Inhibition of electron and energy transfer in mitochondria. I. Effects of amytal, thiopental, rotenone, progesterone, and methylene glycol. The Journal of Biological Chemistry 238:418-431.

Chemin J, Girard C, Duprat F, Lesage F, Romey G, Lazdunski M (2003) Mechanisms underlying excitatory effects of group I metabotropic glutamate receptors via inhibition of 2P domain K+ channels. The EMBO journal 22:5403-5411.

Chen X, Talley EM, Patel N, Gomis A, McIntire WE, Dong B, Viana F, Garrison JC, Bayliss DA (2006) Inhibition of a background potassium channel by Gq protein alpha-subunits. Proceedings of the National Academy of Sciences of the United States of America 103:3422-3427.

Coburn CA, Luo Y, Cui M, Wang J, Soll R, Dong J, Hu B, Lyon MA, Santarelli VP, Kraus RL, Gregan Y, Wang Y, Fox SV, Binns J, Doran SM, Reiss DR, Tannenbaum PL, Gotter AL, Meinke PT, Renger JJ (2012) Discovery of a pharmacologically active antagonist of the two-pore-domain K+ channel K2P9.1 (TASK-3). ChemMedChem 7:123-133.

Cotten JF (2013) TASK-1 (KCNK3) and TASK-3 (KCNK9) tandem pore K+ channel antagonists stimulate breathing in isoflurane-anesthetized rats. Anesthesia and Analgesia 116:810-816.

Cotten JF, Keshavaprasad B, Laster MJ, Eger EI, 2nd, Yost CS (2006) The ventilatory stimulant doxapram inhibits TASK tandem pore (K2P) K+ channel function but does not affect minimum alveolar anesthetic concentration. Anesthesia and Analgesia 102:779-785.

Craig DB (1981) Postoperative recovery of pulmonary function. Anesthesia and Analgesia 60:46-52.

Cullen SC, Eger EI, 2nd, Cullen BF, Gregory P (1969) Observations on the anesthetic effect of the combination of xenon and halothane. Anesthesiology 31:305-309.

Czirjak G, Enyedi P (2002) Formation of functional heterodimers between the TASK-1 and TASK-3 two-pore domain K+ channel subunits. The Journal of Biological Chemistry 277:5426-5432.

Czirjak G, Enyedi P (2003) Ruthenium red inhibits TASK-3 K+ channel by interconnecting glutamate 70 of the two subunits. Molecular Pharmacology 63:646-652.

Dadi PK, Luo B, Vierra NC, Jacobson DA (2015) TASK-1 K+ channels limit pancreatic alpha-cell Ca2+ Influx and Glucagon Secretion. Molecular Endocrinology 29:777-787.

Dahan A, van den Elsen MJ, Berkenbosch A, DeGoede J, Olievier IC, Burm AG, van Kleef JW (1994a) Influence of a subanesthetic concentration of halothane on the ventilatory response to step changes into and out of sustained isocapnic hypoxia in healthy volunteers. Anesthesiology 81:850-859.

Dahan A, van den Elsen MJ, Berkenbosch A, DeGoede J, Olievier IC, van Kleef JW, Bovill JG (1994b) Effects of subanesthetic halothane on the ventilatory responses to hypercapnia and acute hypoxia in healthy volunteers. Anesthesiology 80:727-738.

Daniels S, Smith EB (1993) Effects of general anaesthetics on ligand-gated ion channels. British Journal of Anaesthesia 71:59-64.

Davies PA, Hanna MC, Hales TG, Kirkness EF (1997) Insensitivity to anaesthetic agents conferred by a class of GABA(A) receptor subunit. Nature 385:820-823.

De Backer W, Bogaert E, Van Maele R, Vermeire P (1983) Effect of almitrine bismesylate on arterial blood gases and ventilatory drive in patients with severe chronic airflow obstruction and bilateral carotid body resection. European Journal of Respiratory Diseases Supplement 126:239-242.

Dong YY, Pike AC, Mackenzie A, McClenaghan C, Aryal P, Dong L, Quigley A, Grieben M, Goubin S, Mukhopadhyay S, Ruda GF, Clausen MV, Cao L, Brennan PE, Burgess-Brown NA, Sansom MS, Tucker SJ, Carpenter EP (2015) K2P channel gating mechanisms revealed by structures of TREK-2 and a complex with Prozac. Science 347:1256-1259.

Duchen MR, Caddy KW, Kirby GC, Patterson DL, Ponte J, Biscoe TJ (1988) Biophysical studies of the cellular elements of the rabbit carotid body. Neuroscience 26:291-311.

Duchen MR, Biscoe TJ (1992a) Mitochondrial function in type I cells isolated from rabbit arterial chemoreceptors. The Journal of Physiology 450:13-31.

Duchen MR, Biscoe TJ (1992b) Relative mitochondrial membrane potential and [Ca2+]i in type I cells isolated from the rabbit carotid body. The Journal of Physiology 450:33-61.

Dunham CM, Hileman BM, Hutchinson AE, Chance EA, Huang GS (2014) Perioperative hypoxemia is common with horizontal positioning during general anesthesia and is associated with major adverse outcomes: a retrospective study of consecutive patients. BMC Anesthesiology 14:43.

Duprat F, Lesage F, Fink M, Reyes R, Heurteaux C, Lazdunski M (1997) TASK, a human background K+ channel to sense external pH variations near physiological pH. The EMBO Journal 16:5464-5471.

e Silva MJ, Lewis DL (1995) L- and N-type Ca2+ channels in adult rat carotid body chemoreceptor type I cells. The Journal of Physiology 489 (Pt 3):689-699.

Eckenhoff RG, Morgan PG (2015) Forward to the past. Anesthesia and Analgesia 120:259-260.

Eden GJ, Hanson MA (1987) Maturation of the respiratory response to acute hypoxia in the newborn rat. The Journal of Physiology 392:1-9.

Eger EI, 2nd, Tang M, Liao M, Laster MJ, Solt K, Flood P, Jenkins A, Raines D, Hendrickx JF, Shafer SL, Yasumasa T, Sonner JM (2008) Inhaled anesthetics do not combine to produce synergistic effects regarding minimum alveolar anesthetic concentration in rats. Anesthesia and Analgesia 107:479-485.

Eger EI, 2nd, Xing Y, Laster M, Sonner J, Antognini JF, Carstens E (2003) Halothane and isoflurane have additive minimum alveolar concentration (MAC) effects in rats. Anesthesia and Analgesia 96:1350-1353, table of contents.

Emaus RK, Grunwald R, Lemasters JJ (1986) Rhodamine 123 as a probe of transmembrane potential in isolated rat-liver mitochondria: spectral and metabolic properties. Biochimica et Biophysica Acta 850:436-448.

Enyedi P, Czirjak G (2010) Molecular background of leak K+ currents: two-pore domain K+ channels. Physiological Reviews 90:559-605.

European Medicines Agency (2013) Oral almitrine to be withdrawn by EU Member States. www.ema.europa.eu.

Evans AM, Hardie DG, Peers C, Wyatt CN, Viollet B, Kumar P, Dallas ML, Ross F, Ikematsu N, Jordan HL, Barr BL, Rafferty JN, Ogunbayo O (2009) Ion channel regulation by AMPK: the route of hypoxia-response coupling in thecarotid body and pulmonary artery. Annals of the New York Academy of Sciences 1177:89-100.

Evans AM, Mustard KJ, Wyatt CN, Peers C, Dipp M, Kumar P, Kinnear NP, Hardie DG (2005) Does AMP-activated protein kinase couple inhibition of mitochondrial oxidative phosphorylation by hypoxia to Ca2+ signaling in O_2-sensing cells? The Journal of Biological Chemistry 280:41504-41511.

Evers A.S. MM, Kharasch E.D. (2011) Anesthetic Pharmacology, Basic Principals and Clinical Practice. Cambidge: Cambridge University Press.

Fagerlund MJ, Kahlin J, Ebberyd A, Schulte G, Mkrtchian S, Eriksson LI (2010) The human carotid body: expression of oxygen sensing and signaling genes of relevance for anesthesia. Anesthesiology 113:1270-1279.

Falk MJ, Kayser EB, Morgan PG, Sedensky MM (2006) Mitochondrial complex I function modulates volatile anesthetic sensitivity in C. elegans. Current Biology :16:1641-1645.

Fandrey J (2015) Rounding up the usual suspects in O2 sensing: CO, NO, and H_2S. Science Signaling 8:fs10.

Feldman JL, Del Negro CA (2006) Looking for inspiration: new perspectives on respiratory rhythm. Nature reviews Neuroscience 7:232-242.

Franks NP, Lieb WR (1982) Molecular mechanisms of general Anaesthesia. Nature 300:487-493.

Franks NP, Lieb WR (1984) Do general anaesthetics act by competitive binding to specific receptors? Nature 310:599-601.

Franks NP, Lieb WR (1988) Volatile general anaesthetics activate a novel neuronal K+ current. Nature 333:662-664.

Franks NP, Lieb WR (1991) Stereospecific effects of inhalational general anesthetic optical isomers on nerve ion channels. Science 254:427-430.

Franks NP, Lieb WR (1994) Molecular and cellular mechanisms of general anaesthesia. Nature 367:607-614.

Frobenius (1729) An Account of a Spiritus Vini AEthereus, Together with Several Exeriments Tried Therewith. Philisophical Transactions 36.

Froese AB (2014) From the Journal archives: Be alert to the risk of unexpected prolonged postoperative hypoxemia! Canadian Journal of Anaesthesia 61:379-382.

Garcia DA, Bujons J, Vale C, Sunol C (2006) Allosteric positive interaction of thymol with the GABAA receptor in primary cultures of mouse cortical neurons. Neuropharmacology 50:25-35.

Gelb AW, Knill RL (1978) Subanaesthetic halothane: its effect on regulation of ventilation and relevance to the recovery room. Canadian Anaesthetists' Society Journal 25:488-494.

Golder FJ, Hewitt MM, McLeod JF (2013) Respiratory stimulant drugs in the post-operative setting. Respiratory Physiology & Neurobiology 189:395-402.

Goldstein SA, Bayliss DA, Kim D, Lesage F, Plant LD, Rajan S (2005) International Union of Pharmacology. LV. Nomenclature and molecular relationships of two-P K+ channels. Pharmacological reviews 57:527-540.

Goldstein SA, Bockenhauer D, O'Kelly I, Zilberberg N (2001) K+ leak channels and the KCNK family of two-P-domain subunits. Nature reviews Neuroscience 2:175-184.

Gonzalez C, Almaraz L, Obeso A, Rigual R (1994) Carotid body chemoreceptors: from natural stimuli to sensory discharges. Physiological reviews 74:829-898.

Goto T, Nakata Y, Ishiguro Y, Niimi Y, Suwa K, Morita S (2000) Minimum alveolar concentration-awake of Xenon alone and in combination with isoflurane or sevoflurane. Anesthesiology 93:1188-1193.

Hales TG, Lambert JJ (1991) The actions of propofol on inhibitory amino acid receptors of bovine adrenomedullary chromaffin cells and rodent central neurones. British journal of pharmacology 104:619-628.

Hall GM, Kirtland SJ, Baum H (1973) The inhibition of mitochondrial respiration by inhalational anaesthetic agents. British Journal of Anaesthesia 45:1005-1009.

Han JS, Wang HS, Yan DM, Wang ZW, Han HG, Zhu HY, Li XM (2010) Myocardial ischaemic and diazoxide preconditioning both increase PGC-1alpha and reduce mitochondrial damage. Acta cardiologica 65:639-644.

Hanley PJ, Ray J, Brandt U, Daut J (2002) Halothane, isoflurane and sevoflurane inhibit NADH:ubiquinone oxidoreductase (complex I) of cardiac mitochondria. The Journal of Physiology 544:687-693.

Harless E. vBE (1847) Die Ergebnisse der Versuche über die Wirkung des Schwefeläthers. Erlangen.

Harleton E, Besana A, Chandra P, Danilo P, Jr., Rosen TS, Rosen MR, Argenziano M, Robinson RB, Feinmark SJ (2015) TASK-1 current is inhibited by phosphorylation during human and canine chronic atrial fibrillation. American Journal of Physiology Heart and Circulatory Physiology 308:H126-134.

He L, Dinger B, Sanders K, Hoidal J, Obeso A, Stensaas L, Fidone S, Gonzalez C (2005) Effect of p47phox gene deletion on ROS production and oxygen sensing in mouse carotid body chemoreceptor cells. American Journal of Physiology Lung cellular and Molecular Physiology 289:L916-924.

Heath D, Edwards C, Harris P (1970) Post-mortem size and structure of the human carotid body. Thorax 25:129-140.

Hendrickx JF, Eger EI, 2nd, Sonner JM, Shafer SL (2008) Is synergy the rule? A review of anesthetic interactions producing hypnosis and immobility. Anesthesia and Analgesia 107:494-506.

Heymans C. BJ (1930) Sinus caroticus and respiratory reflexes. The Journal of Physiology 69.

Hu ZY, Liu J (2009) Mechanism of cardiac preconditioning with volatile anaesthetics. Anaesthesia and Intensive Care 37:532-538.

Huskens N, O'Donohoe P, Wickens JR, McCullagh JS, Buckler KJ, Pandit JJ (2016) A method for continuous and stable perfusion of tissue and single cell preparations with accurate concentrations of volatile anaesthetics. Journal of Neuroscience Methods 258:87-93.

Innamaa A, Jackson L, Asher V, Van Shalkwyk G, Warren A, Hay D, Bali A, Sowter H, Khan R (2013) Expression and prognostic significance of the oncogenic K2P K+ channel KCNK9 (TASK-3) in ovarian carcinoma. Anticancer Research 33:1401-1408.

Jackson AP, Timmerman MP, Bagshaw CR, Ashley CC (1987) The kinetics of Ca2+ binding to fura-2 and indo-1. FEBS Letters 216:35-39.

Jenkins A, Lobo IA, Gong D, Trudell JR, Solt K, Harris RA, Eger EI, 2nd (2008) General anesthetics have additive actions on three ligand gated ion channels. Anesthesia and Analgesia 107:486-493.

Kafer ER, Sugioka K (1981) Respiratory and cardiovascular responses to hypoxemia and the effects of anesthesia. International Anesthesiology Clinics 19:85-122.

Kahlin J, Mkrtchian S, Ebberyd A, Hammarstedt-Nordenvall L, Nordlander B, Yoshitake T, Kehr J, Prabhakar N, Poellinger L, Fagerlund MJ, Eriksson LI (2014) The human carotid body releases acetylcholine, ATP and cytokines during hypoxia. Experimental Physiology 99:1089-1098.

Kang D, Han J, Talley EM, Bayliss DA, Kim D (2004) Functional expression of TASK-1/TASK-3 heteromers in cerebellar granule cells. The Journal of Physiology 554:64-77.

Kang D, Wang J, Hogan JO, Vennekens R, Freichel M, White C, Kim D (2014) Increase in cytosolic Ca2+ produced by hypoxia and other depolarizing stimuli activates a non-selective cation channel in chemoreceptor cells of rat carotid body. The Journal of Physiology 592:1975-1992.

Karanovic N, Pecotic R, Valic M, Jeroncic A, Carev M, Karanovic S, Ujevic A, Dogas Z (2010) The acute hypoxic ventilatory response under halothane, isoflurane, and sevoflurane Anaesthesia in rats. Anaesthesia 65:227-234.

Kashimoto S, Furuya A, Nonaka A, Oguchi T, Koshimizu M, Kumazawa T (1997) The minimum alveolar concentration of sevoflurane in rats. European Journal of Anaesthesiology 14:359-361.

Katoh T, Ikeda K, Bito H (1997) Does nitrous oxide antagonize sevoflurane-induced hypnosis? British Journal of Anaesthesia 79:465-468.

Kaw R, Pasupuleti V, Walker E, Ramaswamy A, Foldvary-Schafer N (2012) Postoperative complications in patients with obstructive sleep apnea. Chest 141:436-441.

Kayser EB, Morgan PG, Sedensky MM (1999) GAS-1: a mitochondrial protein controls sensitivity to volatile anesthetics in the nematode Caenorhabditis elegans. Anesthesiology 90:545-554.

Kayser EB, Morgan PG, Sedensky MM (2004) Mitochondrial complex I function affects halothane sensitivity in Caenorhabditis elegans. Anesthesiology 101:365-372.

Kemp PJ, Telezhkin V (2014) Oxygen sensing by the carotid body: is it all just rotten eggs? Antioxidants & Redox Signaling 20:794-804.

Kim D (2013) K(+) channels in O(2) sensing and postnatal development of carotid body glomus cell response to hypoxia. Respiratory Physiology & Neurobiology 185:44-56.

Kim D, Cavanaugh EJ, Kim I, Carroll JL (2009a) Heteromeric TASK-1/TASK-3 is the major oxygen-sensitive background K+ channel in rat carotid body glomus cells. The Journal of Physiology 587:2963-2975.

Kim D, Kang D, Martin EA, Kim I, Carroll JL (2014) Effects of modulators of AMP-activated protein kinase on TASK-1/3 and intracellular Ca(2+) concentration in rat carotid body glomus cells. Respiratory Physiology & Neurobiology 195:19-26.

Kim I, Yang DJ, Donnelly DF, Carroll JL (2009b) Fluoresceinated peanut agglutinin (PNA) is a marker for live O(2) sensing glomus cells in rat carotid body. Advances in Experimental Medicine and Biology 648:185-190.

Kiper AK, Rinne S, Rolfes C, Ramirez D, Seebohm G, Netter MF, Gonzalez W, Decher N (2015) Kv1.5 blockers preferentially inhibit TASK-1 channels: TASK-1 as a target against atrial fibrillation and obstructive sleep apnea? Pflugers Archiv : European Journal of Physiology 467:1081-1090.

Knill RL, Clement JL (1984) Site of selective action of halothane on the peripheral chemoreflex pathway in humans. Anesthesiology 61:121-126.

Knill RL, Gelb AW (1978) Ventilatory responses to hypoxia and hypercapnia during halothane sedation and anesthesia in man. Anesthesiology 49:244-251.

Knill RL, Gelb AW (1982) Peripheral chemoreceptors during anesthesia: are the watchdogs sleeping? Anesthesiology 57:151-152.

Knill RL, Kieraszewicz HT, Dodgson BG, Clement JL (1983) Chemical regulation of ventilation during isoflurane sedation and Anaesthesia in humans. Canadian Anaesthetists' Society Journal 30:607-614.

Kumar P, Prabhakar NR (2012) Peripheral chemoreceptors: function and plasticity of the carotid body. Comprehensive Physiology 2:141-219.

Lahiri S, Rumsey WL, Wilson DF, Iturriaga R (1993) Contribution of in vivo microvascular PO2 in the cat carotid body chemotransduction. Journal of Applied Physiology 75:1035-1043.

Lazarenko RM, Willcox SC, Shu S, Berg AP, Jevtovic-Todorovic V, Talley EM, Chen X, Bayliss DA (2010) Motoneuronal TASK channels contribute to immobilizing effects of inhalational general anesthetics. The Journal of Neuroscience 30:7691-7704.

Leon A, Mayzler O, Benifla M, Semionov M, Fuxman Y, Eilig I, Passuga V, Doitchinova MK, Gurevich B, Artru AA, Shapira Y (2004) Determining minimum alveolar anesthetic concentration of halothane in rats: the effect of incremental change in halothane concentration and number of crossovers. Anesthesia and Analgesia 99:1822-1828.

Lewis A, Hartness ME, Chapman CG, Fearon IM, Meadows HJ, Peers C, Kemp PJ (2001) Recombinant hTASK1 is an O(2)-sensitive K(+) channel. Biochemical and Biophysical Research Communications 285:1290-1294.

Lewis A, Peers C, Ashford ML, Kemp PJ (2002) Hypoxia inhibits human recombinant large conductance, Ca(2+)-activated K(+) (maxi-K) channels by a mechanism which is membrane delimited and Ca(2+) sensitive. The Journal of Physiology 540:771-780.

Limberg SH, Netter MF, Rolfes C, Rinne S, Schlichthorl G, Zuzarte M, Vassiliou T, Moosdorf R, Wulf H, Daut J, Sachse FB, Decher N (2011) TASK-1 channels may modulate action potential duration of human atrial cardiomyocytes. Cellular Physiology and Biochemistry 28:613-624.

Linden AM, Aller MI, Leppa E, Vekovischeva O, Aitta-Aho T, Veale EL, Mathie A, Rosenberg P, Wisden W, Korpi ER (2006) The in vivo contributions of TASK-1-containing channels to the actions of inhalation anesthetics, the alpha(2) adrenergic sedative dexmedetomidine, and cannabinoid agonists. The Journal of Pharmacology and Experimental Therapeutics 317:615-626.

Linden AM, Sandu C, Aller MI, Vekovischeva OY, Rosenberg PH, Wisden W, Korpi ER (2007) TASK-3 knockout mice exhibit exaggerated nocturnal activity, impairments in cognitive functions, and reduced sensitivity to inhalation anesthetics. The Journal of Pharmacology and Experimental Therapeutics 323:924-934.

Lindner M, Leitner MG, Halaszovich CR, Hammond GR, Oliver D (2011) Probing the regulation of TASK potassium channels by PI4,5P(2) with switchable phosphoinositide phosphatases. The Journal of physiology 589:3149-3162.

Lockwood G (2010) Theoretical context-sensitive elimination times for inhalation anaesthetics. British Journal of Anaesthesia 104:648-655.

Lopes CM, Rohacs T, Czirjak G, Balla T, Enyedi P, Logothetis DE (2005) PIP2 hydrolysis underlies agonist-induced inhibition and regulates voltage gating of two-pore domain K+ channels. The Journal of physiology 564:117-129.

Lopez-Barneo J, Macias D, Platero-Luengo A, Ortega-Saenz P, Pardal R (2015) Carotid body oxygen sensing and adaptation to hypoxia. Pflugers Archiv : European Journal of Physiology.

Magyar J, Szentandrassy N, Banyasz T, Fulop L, Varro A, Nanasi PP (2002) Effects of thymol on Ca2+ and K+ currents in canine and human ventricular cardiomyocytes. British Journal of Pharmacology 136:330-338.

Mason M, Cates CJ, Smith I (2015) Effects of opioid, hypnotic and sedating medications on sleep-disordered breathing in adults with obstructive sleep apnoea. The Cochrane Database of Systematic Reviews 7:CD011090.

Mathie A, Al-Moubarak E, Veale EL (2010) Gating of two pore domain K+ channels. The Journal of Physiology 588:3149-3156.

Mayevsky A, Rogatsky GG (2007) Mitochondrial function in vivo evaluated by NADH fluorescence: from animal models to human studies. American Journal of Physiology Cell Physiology 292:C615-640.

McCormack JG, Denton RM (1989) The role of Ca2+ ions in the regulation of intramitochondrial metabolism and energy production in rat heart. Molecular and Cellular Biochemistry 89:121-125.

McDougall SJ, Peters JH, LaBrant L, Wang X, Koop DR, Andresen MC (2008) Paired assessment of volatile anesthetic concentrations with synaptic actions recorded in vitro. PloS One 3:e3372.

Merin RG (1973) Inhalation anesthetics and myocardial metabolism: possible mechanisms of functional effects. Anesthesiology 39:216-255.

Meyer H (1899) Welche eigenschaft der anasthetica bedingt inre Narkotische wirkung? Arch Experimental Pathology Pharmacology 42:109-118.

Mihic SJ, Ye Q, Wick MJ, Koltchine VV, Krasowski MD, Finn SE, Mascia MP, Valenzuela CF, Hanson KK, Greenblatt EP, Harris RA, Harrison NL (1997) Sites of alcohol and volatile anaesthetic action on GABA(A) and glycine receptors. Nature 389:385-389.

Miller AN, Long SB (2012) Crystal structure of the human two-pore domain K+ channel K2P1. Science 335:432-436.

Miller RD, Wahrenbrock EA, Schroeder CF, Knipstein TW, Eger EI, 2nd, Buechel DR (1969) Ethylene--halothane anesthesia: addition or synergism? Anesthesiology 31:301-304.

Millman MS, Young M (1992) Kinetics of dissolution of gaseous halothane in Krebs-Ringer's solution. Canadian Journal of Anaesthesia 39:980-986.

Mills E, Jobsis FF (1972) Mitochondrial respiratory chain of carotid body and chemoreceptor response to changes in oxygen tension. Journal of Neurophysiology 35:405-428.

Mitchell RA, Herbert DA (1975) Potencies of doxapram and hypoxia in stimulating carotid-body chemoreceptors and ventilation in anesthetized cats. Anesthesiology 42:559-566.

Miu P, Puil E (1989) Isoflurane-induced impairment of synaptic transmission in hippocampal neurons. Experimental Brain Research 75:354-360.

Mkrtchian S, Kahlin J, Ebberyd A, Gonzalez C, Sanchez D, Balbir A, Kostuk EW, Shirahata M, Fagerlund MJ, Eriksson LI (2012) The human carotid body transcriptome with focus on oxygen sensing and inflammation--a comparative analysis. The Journal of Physiology 590:3807-3819.

Morgan PG, Hoppel CL, Sedensky MM (2002) Mitochondrial defects and anesthetic sensitivity. Anesthesiology 96:1268-1270.

Mu D, Chen L, Zhang X, See LH, Koch CM, Yen C, Tong JJ, Spiegel L, Nguyen KC, Servoss A, Peng Y, Pei L, Marks JR, Lowe S, Hoey T, Jan LY, McCombie WR, Wigler MH, Powers S (2003) Genomic amplification and oncogenic properties of the KCNK9 K+ channel gene. Cancer Cell 3:297-302.

Nagyova B, Dorrington KL, Gill EW, Robbins PA (1995) Comparison of the effects of sub-hypnotic concentrations of propofol and halothane on the acute ventilatory response to hypoxia. British Journal of Anaesthesia 75:713-718.

Niatsetskaya ZV, Sosunov SA, Matsiukevich D, Utkina-Sosunova IV, Ratner VI, Starkov AA, Ten VS (2012) The oxygen free radicals originating from mitochondrial complex I contribute to oxidative brain injury following hypoxia-ischemia in neonatal mice. The Journal of neuroscience 32:3235-3244.

Niemann CU, Stabernack C, Serkova N, Jacobsen W, Christians U, Eger EI, 2nd (2002) Cyclosporine can increase isoflurane MAC. Anesthesia and Analgesia 95:930-934, table of contents.

O'Donohoe P (2015) D.Phil Thesis In: Deprartment of Physiology Anatomy and Genetics. Doctorate of Philosophy Oxford: University of Oxford.

Otsubo T, Yamaguchi S, Okumura M, Shirahata M (2006) Differential expression of oxygen sensitivity in voltage-dependent K channels in inbred strains of mice. Advances in Experimental Medicine and Biology 580:209-214.

Overton CE (1901) Studien über die Narkose zugleich ein Beitrag zur allgemeinen Pharmakologie.

Pancrazio JJ (1996) Halothane and isoflurane preferentially depress a slowly inactivating component of Ca^{2+} channel current in guinea-pig myocytes. The Journal of Physiology 494 (Pt 1):91-103.

Pandit JJ (2002) The variable effect of low-dose volatile anaesthetics on the acute ventilatory response to hypoxia in humans: a quantitative review. Anaesthesia 57:632-643.

Pandit JJ (2014) Monitoring (un)consciousness: the implications of a new definition of 'Anaesthesia'. Anaesthesia 69:801-807.

Pandit JJ, Buckler KJ (2009) Differential effects of halothane and sevoflurane on hypoxia-induced intracellular Ca2+ transients of neonatal rat carotid body type I cells. British Journal of Anaesthesia 103:701-710.

Pandit JJ, Buckler KJ (2010) Halothane and sevoflurane exert different degrees of inhibition on carotid body glomus cell intracellular Ca^{2+} response to hypoxia. Advances in Experimental Medicine and Biology 669:201-204.

Pandit JJ, Cook TM, Jonker WR, O'Sullivan E, (2013) A national survey of anaesthetists (NAP5 Baseline) to estimate an annual incidence of accidental awareness during general Anaesthesia in the UK. Anaesthesia 68:343-353.

Pandit JJ, Manning-Fox J, Dorrington KL, Robbins PA (1999) Effects of subanaesthetic sevoflurane on ventilation. 2: Response to acute and sustained hypoxia in humans. British Journal of Anaesthesia 83:210-216.

Pandit JJ, Moreau B, Donoghue S, Robbins PA (2004) Effect of pain and audiovisual stimulation on the depression of acute hypoxic ventilatory response by low-dose halothane in humans. Anesthesiology 101:1409-1416.

Pandit JJ, Winter V, Bayliss R, Buckler KJ (2010) Differential effects of halothane and isoflurane on carotid body glomus cell intracellular Ca^{2+} and background K^{+} channel responses to hypoxia. Advances in Experimental Medicine and Biology 669:205-208.

Pang DS, Robledo CJ, Carr DR, Gent TC, Vyssotski AL, Caley A, Zecharia AY, Wisden W, Brickley SG, Franks NP (2009) An unexpected role for TASK-3 K+ channels in network oscillations with implications for sleep mechanisms and anesthetic action. Proceedings of the National Academy of Sciences of the United States of America 106:17546-17551.

Papreck JR, Martin EA, Lazzarini P, Kang D, Kim D (2012) Modulation of K2P3.1 (TASK-1), K2P9.1 (TASK-3), and TASK-1/3 heteromer by reactive oxygen species. Pflugers Archiv : European Journal of Physiology 464:471-480.

Patel AJ, Honore E, Lesage F, Fink M, Romey G, Lazdunski M (1999) Inhalational anesthetics activate two-pore-domain background K+ channels. Nature Neuroscience 2:422-426.

Peers C (1991) Effects of doxapram on ionic currents recorded in isolated type I cells of the neonatal rat carotid body. Brain Research 568:116-122.

Peers C, Wyatt CN, Evans AM (2010) Mechanisms for acute oxygen sensing in the carotid body. Respiratory Physiology & Neurobiology 174:292-298.

Pei L, Wiser O, Slavin A, Mu D, Powers S, Jan LY, Hoey T (2003) Oncogenic potential of TASK3 (Kcnk9) depends on K+ channel function. Proceedings of the National Academy of Sciences of the United States of America 100:7803-7807.

Piechotta PL, Rapedius M, Stansfeld PJ, Bollepalli MK, Ehrlich G, Andres-Enguix I, Fritzenschaft H, Decher N, Sansom MS, Tucker SJ, Baukrowitz T (2011) The pore structure and gating mechanism of K2P channels. The EMBO Journal 30:3607-3619.

Prabhakar NR (2006) O2 sensing at the mammalian carotid body: why multiple O2 sensors and multiple transmitters? Experimental Physiology 91:17-23.

Pravdic D, Hirata N, Barber L, Sedlic F, Bosnjak ZJ, Bienengraeber M (2012) Complex I and ATP synthase mediate membrane depolarization and matrix acidification by isoflurane in mitochondria. European Journal of Pharmacology 690:149-157.

Putzke C, Hanley PJ, Schlichthorl G, Preisig-Muller R, Rinne S, Anetseder M, Eckenhoff R, Berkowitz C, Vassiliou T, Wulf H, Eberhart L (2007) Differential effects of volatile and intravenous anesthetics on the activity of human TASK-1. American Journal of Physiology Cell Physiology 293:C1319-1326.

Quintana A, Morgan PG, Kruse SE, Palmiter RD, Sedensky MM (2012) Altered anesthetic sensitivity of mice lacking Ndufs4, a subunit of mitochondrial complex I. PloS one 7:e42904.

Rajan S, Wischmeyer E, Xin Liu G, Preisig-Muller R, Daut J, Karschin A, Derst C (2000) TASK-3, a novel tandem pore domain acid-sensitive K+ channel. An extracellular histiding as pH sensor. The Journal of Biological Chemistry 275:16650-16657.

Rapedius M, Schmidt MR, Sharma C, Stansfeld PJ, Sansom MS, Baukrowitz T, Tucker SJ (2012) State-independent intracellular access of quaternary ammonium blockers to the pore of TREK-1. Channels 6:473-478.

Rebecchi MJ, Pentyala SN (2002) Anaesthetic actions on other targets: protein kinase C and guanine nucleotide-binding proteins. British Journal of Anaesthesia 89:62-78.

Renigunta V, Schlichthorl G, Daut J (2015) Much more than a leak: structure and function of K(2)p-channels. Pflugers Archiv : European Journal of Physiology 467:867-894.

Riess ML, Camara AK, Chen Q, Novalija E, Rhodes SS, Stowe DF (2002) Altered NADH and improved function by anesthetic and ischemic preconditioning in guinea pig intact hearts. American Journal of Physiology Heart and Circulatory Physiology 283:H53-60.

Rigual R, Gonzalez E, Fidone S, Gonzalez C (1984) Effects of low pH on synthesis and release of catecholamines in the cat carotid body in vitro. Brain Research 309:178-181.

Rinne S, Kiper AK, Schlichthorl G, Dittmann S, Netter MF, Limberg SH, Silbernagel N, Zuzarte M, Moosdorf R, Wulf H, Schulze-Bahr E, Rolfes C, Decher N (2015) TASK-1 and TASK-3 may form heterodimers in human atrial cardiomyocytes. Journal of Molecular and Cellular Cardiology 81:71-80.

Robbins BH (1946) Preliminary studies of the anesthetic activity of fluorinated hydrocarbons. The Journal of pharmacology and Experimental Therapeutics 86:197-204.

Roch A, Shlyonsky V, Goolaerts A, Mies F, Sariban-Sohraby S (2006) Halothane directly modifies Na+ and K+ channel activities in cultured human alveolar epithelial cells. Molecular Pharmacology 69:1755-1762.

Rong W, Gourine AV, Cockayne DA, Xiang Z, Ford AP, Spyer KM, Burnstock G (2003) Pivotal role of nucleotide P2X2 receptor subunit of the ATP-gated ion channel mediating ventilatory responses to hypoxia. The Journal of Neuroscience 23:11315-11321.

Rosenberg PH, Alila A (1984) Accumulation of thymol in halothane vaporizers. Anaesthesia 39:581-583.

Rusy BF, Komai H (1987) Anesthetic depression of myocardial contractility: a review of possible mechanisms. Anesthesiology 67:745-766.

Saltman AE, Krukenkamp IB, Gaudette GR, Horimoto H, Levitsky S (2000) Pharmacological preconditioning with the adenosine triphosphate-sensitive K+ channel opener pinacidil. The Annals of Thoracic Surgery 70:595-601.

Sanders KA, Sundar KM, He L, Dinger B, Fidone S, Hoidal JR (2002) Role of components of the phagocytic NADPH oxidase in oxygen sensing. Journal of applied Physiology 93:1357-1364.

Sazanov LA, Baradaran R, Efremov RG, Berrisford JM, Minhas G (2013) A long road towards the structure of respiratory complex I, a giant molecular proton pump. Biochemical Society Transactions 41:1265-1271.

Schmidt U, Schwinger RH, Muller-Ehmsen J, Bohm S, von Meyer L, Uberfuhr P, Reichart B, Erdmann E, Bohm M (1994) Influence of halothane on the effect of cAMP-dependent and cAMP-independent positive inotropic agents in human myocardium. British Journal of Anaesthesia 73:204-208.

Schuttler J, Schwilden H (2008) Modern Anesthetics. Heidelburg: SpringerLink.

Schwartz LM, Reimer KA, Crago MS, Jennings RB (2007) Pharmacological preconditioning with diazoxide slows energy metabolism during sustained ischemia. Experimental and Clinical Cardiology 12:139-147.

Sirois JE, Lei Q, Talley EM, Lynch C, 3rd, Bayliss DA (2000) The TASK-1 two-pore domain K+ channel is a molecular substrate for neuronal effects of inhalation anesthetics. The Journal of Neuroscience 20:6347-6354.

Sirois JE, Pancrazio JJ, Lynch C, 3rd, Bayliss DA (1998) Multiple ionic mechanisms mediate inhibition of rat motoneurones by inhalation anaesthetics. The Journal of Physiology 512 (Pt 3):851-862.

Skarka L, Ostadal B (2002) Mitochondrial membrane potential in cardiac myocytes. Physiological research / Academia Scientiarum Bohemoslovaca 51:425-434.

Slingo MD, (2013) The role of hypoxia-inducible pathway in metabolism and cardiopulmonary Physiology. In: Department of Physiology Anatomy and Genetics, DPhil Oxford: University of Oxford.

Smith I, Nathanson M, White PF (1996) Sevoflurane--a long-awaited volatile anaesthetic. British Journal of Anaesthesia 76:435-445.

Smith JC, Abdala AP, Borgmann A, Rybak IA, Paton JF (2013) Brainstem respiratory networks: building blocks and microcircuits. Trends in Neurosciences 36:152-162.

Smith RA, Porter EG, Miller KW (1981) The solubility of anesthetic gases in lipid bilayers. Biochimica et Biophysica Acta 645:327-338.

Sowa S, Dong A, Roos EE, Caughey WS (1987) The anesthetic nitrous oxide affects dioxygen utilization by bovine heart and bean seed mitochondrial particles. Biochemical and Biophysical Research Communications 144:643-648.

Steinberg EA, Wafford KA, Brickley SG, Franks NP, Wisden W (2014) The role of K channels in Anaesthesia and sleep. Pflugers Archiv : European Journal of Physiology.

Streit AK, Netter MF, Kempf F, Walecki M, Rinne S, Bollepalli MK, Preisig-Muller R, Renigunta V, Daut J, Baukrowitz T, Sansom MS, Stansfeld PJ, Decher N (2011) A specific two-pore domain K+ channel blocker defines the structure of the TASK-1 open pore. The Journal of Biological Chemistry 286:13977-13984.

Sury MR, Palmer JH, Cook TM, Pandit JJ (2014) The state of UK Anaesthesia: a survey of National Health Service activity in 2013. British Journal of Anaesthesia 113:575-584.

Suthammarak W, Yang YY, Morgan PG, Sedensky MM (2009) Complex I function is defective in complex IV-deficient Caenorhabditis elegans. The Journal of Biological Chemistry 284:6425-6435.

Takahashi T, Osanai S, Nakano H, Ohsaki Y, Kikuchi K (2005) Doxapram stimulates the carotid body via a different mechanism than hypoxic chemotransduction. Respiratory Physiology & Neurobiology 147:1-9.

Temp JA, Henson LC, Ward DS (1994) Effect of a subanesthetic minimum alveolar concentration of isoflurane on two tests of the hypoxic ventilatory response. Anesthesiology 80:739-750.

Teppema LJ, Nieuwenhuijs D, Sarton E, Romberg R, Olievier CN, Ward DS, Dahan A (2002) Antioxidants prevent depression of the acute hypoxic ventilatory response by subanaesthetic halothane in men. The Journal of Physiology 544:931-938.

Teppema LJ, Romberg RR, Dahan A (2005) Antioxidants reverse reduction of the human hypoxic ventilatory response by subanesthetic isoflurane. Anesthesiology 102:747-753.

Terrell RC (2008) The invention and development of enflurane, isoflurane, sevoflurane, and desflurane. Anesthesiology 108:531-533.

Trapani JG, Korn SJ (2003) Control of ion channel expression for patch clamp recordings using an inducible expression system in mammalian cell lines. BMC Neuroscience 4:15.

Turner PJ, Buckler KJ (2013) Oxygen and mitochondrial inhibitors modulate both monomeric and heteromeric TASK-1 and TASK-3 channels in mouse carotid body type-1 cells. The Journal of Physiology 591:5977-5998.

Urban BW (2002) Current assessment of targets and theories of Anaesthesia. British Journal of Anaesthesia 89:167-183.

Urena J, Lopez-Lopez J, Gonzalez C, Lopez-Barneo J (1989) Ionic currents in dispersed chemoreceptor cells of the mammalian carotid body. The Journal of General Physiology 93:979-999.

van den Elsen M, Sarton E, Teppema L, Berkenbosch A, Dahan A (1998) Influence of 0.1 minimum alveolar concentration of sevoflurane, desflurane and isoflurane on dynamic ventilatory response to hypercapnia in humans. British Journal of Anaesthesia 80:174-182.

Van den Elsen MJ, Dahan A, Berkenbosch A, DeGoede J, van Kleef JW, Olievier IC (1994) Does subanesthetic isoflurane affect the ventilatory response to acute isocapnic hypoxia in healthy volunteers? Anesthesiology 81:860-867; discussion 826A.

Varas R, Wyatt CN, Buckler KJ (2007) Modulation of TASK-like background K+ channels in rat arterial chemoreceptor cells by intracellular ATP and other nucleotides. The Journal of Physiology 583:521-536.

Veale EL, Buswell R, Clarke CE, Mathie A (2007) Identification of a region in the TASK3 two pore domain K+ channel that is critical for its blockade by methanandamide. British Journal of Pharmacology 152:778-786.

Verna A (1979) Ulstrastructure of the carotid body in the mammals. International review of Cytology 60:271-330.

Wallin R.F. NMD (1971) Sevoflurane (fluoro-methyl-1,1,1,3,3,3-hexafluro-2-propoyl ether): a new inhalational anesthetic agent. Federated Proceedings 30.

Wang M, Agarwal S, Mayevsky A, Joshi S (2011) Optically measured NADH concentrations are unaffected by propofol induced EEG silence during transient cerebral hypoperfusion in anesthetized rabbits. Brain Research 1396:69-76.

Wang ZY, Bisgard GE (2005) Postnatal growth of the carotid body. Respiratory Physiology & neurobiology 149:181-190.

Ward DS, Karan SB, Pandit JJ (2011) Hypoxia: developments in basic science, Physiology and clinical studies. Anaesthesia 66 Suppl 2:19-26.

Ward JWG, Donald L, Franko V, Woodard, Geoffrey T, Gilbert L, ; (1968) Toxicologic studies of doxapram hydrochloride. Toxicology and Applied Pharmacology 13:242-250

Waypa GB, Guzy R, Mungai PT, Mack MM, Marks JD, Roe MW, Schumacker PT (2006) Increases in mitochondrial reactive oxygen species trigger hypoxia-induced Ca2+ responses in pulmonary artery smooth muscle cells. Circulation Research 99:970-978.

Weir EK, Lopez-Barneo J, Buckler KJ, Archer SL (2005) Acute oxygen-sensing mechanisms. The New England Journal of Medicine 353:2042-2055.

Werth JL, Thayer SA (1994) Mitochondria buffer physiological Ca2+ loads in cultured rat dorsal root ganglion neurons. The Journal of Neuroscience 14:348-356.

West J (2012) Respiratory Physiology, The Essentials. Baltimore: Lippincott Williams and Wilkins.

Williams BA, Buckler KJ (2004) Biophysical properties and metabolic regulation of a TASK-like K+ channel in rat carotid body type 1 cells. American Journal of Physiology Lung Cellular and Molecular Physiology 286:L221-230.

Wirth KJ, Steinmeyer K, Ruetten H (2013) Sensitization of upper airway mechanoreceptors as a new pharmacologic principle to treat obstructive sleep apnea: investigations with AVE0118 in anesthetized pigs. Sleep 36:699-708.

Wu GJ, Tai YT, Chen TL, Lin LL, Ueng YF, Chen RM (2005) Propofol specifically inhibits mitochondrial membrane potential but not complex I NADH dehydrogenase activity, thus reducing cellular ATP biosynthesis and migration of macrophages. Annals of the New York Academy of Sciences 1042:168-176.

Wyatt CN, Buckler KJ (2004) The effect of mitochondrial inhibitors on membrane currents in isolated neonatal rat carotid body type I cells. The Journal of Physiology 556:175-191.

Wyatt CN, Mustard KJ, Pearson SA, Dallas ML, Atkinson L, Kumar P, Peers C, Hardie DG, Evans AM (2007) AMP-activated protein kinase mediates carotid body excitation by hypoxia. The Journal of Biological Chemistry 282:8092-8098.

Yamamoto Y, Ishikawa R, Omoe K, Taniguchi K (2008) Expression of inwardly rectifying K+ channels in the carotid body of rat. Histology and Histopathology 23:799-806.

Zhang M, Nurse CA (2004) CO2/pH chemosensory signaling in co-cultures of rat carotid body receptors and petrosal neurons: role of ATP and ACh. Journal of Neurophysiology 92:3433-3445.

Appendix I

Journal of Neuroscience Methods 258 (2016) 87–93

Contents lists available at ScienceDirect

Journal of Neuroscience Methods

journal homepage: www.elsevier.com/locate/jneumeth

Basic neuroscience

A method for continuous and stable perfusion of tissue and single cell preparations with accurate concentrations of volatile anaesthetics

Nicky Huskens[a], Peadar O'Donohoe[a,b], James R. Wickens[c], James S.O. McCullagh[c], Keith J. Buckler[a], Jaideep J. Pandit[b,*]

[a] Department of Physiology, Anatomy & Genetics, University of Oxford, Parks Road, Oxford OX1 3PT, UK
[b] Nuffield Department of Anaesthetics, Oxford University Hospitals NHS Trust, Oxford OX3 9DU, UK
[c] Mass Spectrometry Research Facility Chemistry Research Laboratory, Department of Chemistry, University of Oxford, 12 Mansfield Road, Oxford OX1 3TA, UK

HIGHLIGHTS

- Due to the volatility of some anaesthetic gases, it has been proved difficult to design a system quantitatively to deliver these agents in stable concentrations to in vitro preparations.
- We describe a reliable system for the accurate administration of volatile anaesthetics to cell and tissue samples, with minimal loss of vapour and consistency of anaesthetic stimulus.
- In contrast to previously described 'closed' systems, our 'open' system uses continuous bubbling of anaesthetics in the perfusing solution and continuous monitoring of the headspace gas of above the solution with infrared analyses. GC–MS measurements demonstrate consistent concentrations in our experimental tissue perfusion bath.

ARTICLE INFO

Article history:
Received 30 July 2015
Received in revised form 30 October 2015
Accepted 1 November 2015
Available online 10 November 2015

Keywords:
Volatile anaesthetics
Perfusion rig
Infrared analyses
Gas chromatography–mass spectrometry

ABSTRACT

Background: It is difficult to design a system to reliably deliver volatile anaesthetics such as halothane or isoflurane to in vitro preparations such as tissues or cells cultures: the very volatility of the drugs means that they can rapidly dissipate from even carefully-prepared solutions. Furthermore, many experiments require the control of other gases (such as oxygen or carbon dioxide) which requires constant perfusion.
New method: We describe a constant perfusion system that is air-tight (i.e., allows the accurate administration of hypoxic or hypercapnic gas mixtures), in which volatile anaesthetic is delivered via calibrated vaporisers by constant bubbling into the perfusing solution (and continuously monitored for stability by infrared spectroscopy in the headspace above the solution).
Results: We have confirmed the accuracy (i.e., linear relationship of dissolved concentrations with vapour dial settings) and stability (i.e., over time) of the anaesthetic concentrations in solutions in samples taken from the bottles into which anaesthetic is bubbled, and from samples taken from the tissue perfusion bath, using gas chromatrography–mass spectrometry (GC–MS).
Conclusions: It is possible to deliver volatile anaesthetics in accurate concentrations to cell/tissue preparations whilst adjusting ambient air composition rapidly, stable over sustained time periods.

1. Introduction

In a reductive approach to understanding the mechanism of action of volatile anaesthetics, it is often necessary to perfuse tissue cultures or single cell preparations with solutions equilibrated with these agents and study their responses, such as changes in intracellular calcium or membrane electrophysiology. Sometimes, it is further necessary simultaneously to change the background gas (O_2 and CO_2) tensions to study the interactions of anaesthetic with hypoxia/hypercapnia (Pandit and Buckler, 2009; Pandit et al., 2010) as relevant to many questions in clinical practice (van den Elsen et al., 1994; Pandit, 2002, 2005).

Handling volatile agents in standard delivery systems (perfusion 'rigs') poses several challenges. Their very volatility (boiling points

* Corresponding author. Tel.: +44 1865 221590; fax: +44 1865 220027.
E-mail address: jaideep.pandit@dpag.ox.ac.uk (J.J. Pandit).

http://dx.doi.org/10.1016/j.jneumeth.2015.11.002
0165-0270/

~23–59 °C) means that these gases have a tendency to be lost from solution. Even if it is air-tight, the delivery system needs to ensure sustained equilibrium between anaesthetic gases in solution with the gas phase above the solution. This is because the biological effect of anaesthetics is determined by their partial pressure rather than absolute content in solution. However air-tight the delivery system, experimental baths into which the tissue or cells are placed are impossible to shield completely from the atmosphere and rapid evaporation can occur if this is not well controlled. Furthermore, some tissue/cell preparations need to be constantly perfused with O_2 or nutrients to maintain constancy of their environment, or there is often a need to adjust the prevailing O_2 and/or CO_2 gas tensions (e.g., switches between euoxia and hypoxia and/or hyperapnia are necessary). These aims are not possible to achieve simply by immersing the preparation in a fixed volume of pre-prepared liquid.

To date, it has been proved difficult to design a system that meets all these requirements in delivering anaesthetics to in vitro preparations. In a typical set up, the anaesthetics are delivered to a physiological solution (e.g., Tyrode) with vaporisers to achieve equilibration. For such a set-up, Franks and Lieb (1993) and Smith et al. (1981) described a method for estimating the concentration in solution (in mM) of anaesthetic delivered from a calibrated vaporiser (where the delivery of agent is marked in percent, corresponding to a partial pressure), using the relevant Bunsen or Ostwald water/gas partition coefficient for the agent in question. Following the equilibration by bubbling, the solution is then stored in bottles or syringes 'air tight' from between a couple of minutes to several hours, to be delivered later to an experimental bath (which is inevitably exposed to the atmosphere). How this equilibrated agent is stored and delivered to the biological preparation differs across published studies. One convenient way of storing the pre-equilibrated solutions is in Erlenmeyer flasks covered tightly with parafilm (Sirois et al., 1998). Generally, these methods might be described as 'closed', since their aim is to keep the anaesthetic in solution closed to the atmosphere until the time of exposure to experimental tissue.

Despite being 'closed', chromatographic measurements of the samples from the experimental baths using these methods have revealed a loss of 20–50% compared with what was expected from calculations based on the dialled concentrations on the vaporisers (Miu and Puil, 1989; McDougall et al., 2008). Furthermore, because the experimental bath is inevitably exposed to the atmosphere, McDougall et al. (2008) demonstrated that a very variable loss of agent can arise unless there is a system for continuous perfusion with equilibrated solution. The option of frequent sampling from the experimental bath solution on a daily basis to confirm system performance is not only very time consuming, but also expensive.

In contrast to such 'closed' methods of delivery, Conway and Cotten (2012) described an 'open' system. They directly applied gas vaporised with anaesthetics to the solution perfusing the experimental bath, and monitored the gas phase of the anaesthetics in the head space above the bath by continuous infrared analyses. A similar set-up was also described by Jinks et al. (2005). However, these systems did not allow for control of the gas composition (O_2 and CO_2) perfusing the tissue.

In this paper we describe an extension to Conway et al.'s and Jinks et al.'s systems, which can both be described as 'open' in the sense there is continuous administration of anaesthetic to solution rather than prior storage of agent. Yet, our system is also 'closed' in the sense of being air-tight, as one additional aim is to maintain conditions that enable us to administer near-anoxic stimuli to the cells of interest, so that it is suitable for work with cells like carotid body glomus cells that are oxygen-sensing. Here we describe the new system and its performance in achieving these aims.

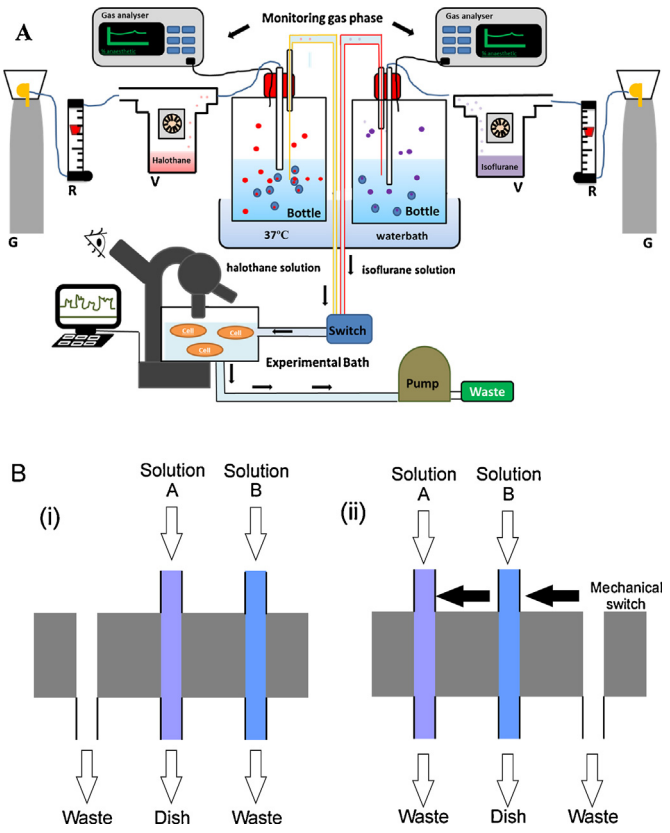

Fig. 1. (*A*) *Delivery system.* From cylinders (G) carrier gas passes through rotameters (R) into vaporisers (V); which can be on or off (halothane and isoflurane shown as examples). When the vaporiser is off, all gas bypasses the anaesthetic. From the vaporiser outlet, the anaesthetic–gas mixture passes through narrow-bore plastic tubing to a gas dispersion tube immersed in a glass bottle. A second, narrow bore metal aspiration tube aspirates solution for delivery to the experimental bath. Note also the use of an infrared gas analyser for continuous anaesthetic vapour analysis of the headspace above the solution in the bottle. The flow of solution in the system, from the bottle to the waste, is driven by a peristaltic pump. (B) Details of the rapid switching mechanism to the experimental bath. The solution of interest always runs through the central channel (to bath). In panel (i), the cells in the bath are being bathed in experimental solution, the alternative solution passed to waste. Mechanically switching the inflow, panel (ii) allows a rapid change to a different milieu with a total volume change occurring in <10 s.

2. Methods

2.1. Perfusion system

The cell perfusion system is shown in Fig. 1. Gas is delivered from compressed gas cylinders connected through air flow regulators and rotameters via narrow-bore plastic tubing to vaporisers containing anaesthetic. The gas cylinders (British Oxygen Company, Surrey, UK) can contain air, N_2, O_2, and CO_2 in various concentrations of hypoxic mixtures (we commonly use N_2 in 5% CO_2 or 1% O_2 with 5% CO_2), or hypercapnic mixtures of air with various concentrations of CO_2 (20% being common). The typical flow rate of gas delivery to the vaporisers is 200–500 ml/min, measured via calibrated rotameters. From the vaporiser outlet the anaesthetic-gas mixture passes through narrow-bore flexible nylon tubing (BS5409) tubing to a plastic costar pipet gas dispersion tube (Corning, New York, USA) immersed in a glass bottle (volumes of 0.2–2 l are used, as needed) containing the experimental salt solution (Tyrode, in mM: 117 NaCl, 4.5 KCl, 1 $MgCl_2$, 23 $NaHCO_3$, 11 glucose). The bottles are capped with a plastic lid (Schott Duran, Wertheim, Main, Germany), into which are punched two holes: one large hole to allow passage of the gas dispersion tube, and one small

hole to allow passage of the narrow bore metal aspiration tube (see below) that aspirates the solution into the delivery system for perfusion to the experimental bath. This small hole also allows passage of a fine plastic connector tube leading to the infrared gas analyser (Capnomac Ultima, Helsinki, Finland) for continuous anaesthetic vapour analysis of the headspace above the solution in the bottle. This analyser was checked and calibrated with readings from a mass spectrometer (Airspec 3000, Airspec Ltd, Biggin Hill, UK; not used continuously during this experiment), in turn calibrated with standard agents as calibration gases.

The bottles are placed in a water bath heated to ~38 °C to achieve a temperature of 37 °C in the experimental bath. The gas from the vaporiser bubbles continuously into the bottle throughout the experimental period, with sufficient time for equilibration before the start of any experimental recordings, as confirmed by attainment of the desired, stable value on infrared capnography. Both Millman and Young (1992) and Becker et al. (2012) have shown that equilibration is reliably achieved after ~10 min across a range of anaesthetic concentrations.

To deliver the solution from the bottle to the experimental bath, a stainless steel (medical grade) aspiration tube is placed into the solution of the glass bottle via a small hole in the cap (see above). The delivery to the experimental bath is by gravity through stainless steel tubing and short sections of Pharmed (Akron, USA) tubing (flow 6–7 ml/min). The solution is then aspirated from the bath using a peristaltic pump as a vacuum source. It is possible to make a switch from one experimental solution (e.g., air) to another (e.g., air with anaesthetic) using a two-way tap (constructed of PTFE and nylon) connected to the bath entry, which is operated by a lever (Fig. 1B). Switching the tap results in rapid change of solution within <1 s. The solution exits the experimental bath and passes through compressors of a peristaltic pump. The experimental batch is itself moulded from Perspex in-house, in its centre being a depression (volume 100 μl) in which sits the coverslip containing the cells or tissue sample. Its base is clear glass, allowing focussing of the cells using an inverted microscope.

2.1.1. Assessment of delivery of anoxic gas mixture

We first assessed the air-tightness of our system by measuring O_2 levels in the experimental bath. The rationale was that if air tight, then little or no O_2 would enter the perfusion system if an anoxic (i.e., pure N_2) mixture was delivered. The O_2 levels were measured with an optical O_2 sensor (Presence, Regensburg, Germany) equilibrated with a normoxic and anoxic gas resulting in a two-point calibration. The normoxic gas used was 5% CO_2 in 95% air and the anoxic equilibration gas used was 5% CO_2 in 95% N_2, with the addition of 250 μM $Na_2S_2O_2$ (sodium dithionide), which reacts with and so consumes all the remaining O_2 in the solution, so that an anoxic solution is ensured for calibration. We then used two test gas mixtures: severe 'hypoxia' 0% (5% CO_2 in 95% N_2) and 'mild' hypoxia 1% (1% O_2, 5% CO_2, 94% N_2).

2.1.2. Sampling for chromatography measurements of anaesthetic in solution

Samples were taken from two sites in the apparatus (Fig. 1). The solution from (a) the bottle into which anaesthetic was bubbled and (b) from the experimental bath was carefully but rapidly drawn up using a 2 ml syringes and then swiftly placed into 2 ml autosampler vials (Finneran Associates, Vineland, USA) until a convex meniscus was formed. The cap was attached immediately excluding any air contamination. The vials were then analysed in batches. We separately confirmed using repeated measurements of the same sample over 24 h that there was no loss of anaesthetic from the autosampler vials, verifying that measurement in batches was appropriate.

2.2. GC–MS measurements

GC–MS analysis was performed using an Agilent 7200 Quadrupole Time-of-Flight mass spectrometer, coupled directly to an Agilent 7890B Gas chromatograph and an Agilent GC Sampler 120 autosampler (Agilent, Stockport, UK). Standards were prepared in a non-polar solvent so as to exploit the high oil:gas partition coefficients of halothane and isoflurane (224 and 98, respectively). Toluene (analytical grade, Fisher, Loughborough, UK) was chosen as it has a higher boiling point (111 °C) than either halothane or isoflurane (50 and 48 °C, respectively) and would elute after the analytes when using standard gas chromatography techniques.

The autosampler was equipped with a 10 μl syringe and its operation was carefully designed to minimise outgassing of analytes. Prior to injection, the syringe was flushed once with toluene then three times with water. The syringe was then cleaned with the sample twice (10 μl of sample was withdrawn and dispensed to waste). The syringe filling speed was set to 0.5 μl/s and sample was drawn up and ejected three times before injecting 10 μl of the sample. Following injection, the syringe was flushed three times with toluene and three times with water.

The gas chromatograph was equipped with a HP-5 column (30 m, 0.25 mm ID, 0.25 μm film thickness, Agilent, Stockport, UK), the carrier gas was helium (BOC, Slough, UK) and the flow rate was 1.2 ml/min. The inlet was set to 300 °C with a split ratio of 100:1. The oven was held at 40 °C for three minutes then ramped at 100 °C/min to 240 °C and held for 2 min. The transfer line was maintained at 300 °C.

The mass spectrometer was operated in electron ionisation (EI) mode with a source temperature 230 °C and electron energy of 70 eV. Mass spectra were collected between 50 and 500 *m/z* and ionisation was disabled after 3.7 min (after all analytes had eluted but before the toluene eluted).

MassHunter software (Agilent, Stockport, UK) was used for instrument control and data analysis. Responses for each analyte were determined using the area of peaks seen in the total ion count (TIC) mass chromatograms. Identities of analyte peaks were confirmed using comparison to the NIST mass spectral library (National Institute of Standards and Technology, Gaithersburg, MD, USA).

3. Results

3.1.1. Assessment of delivery of anoxic gas mixture

When a mild hypoxic gas mixture (1% O_2 bubbled; predicted pO_2 in experimental bath 7.6 mmHg) was delivered, the electrode placed in the experimental bath measured 10.6 mmHg. When severe hypoxia (5% CO_2 in 95% N_2) was used, the electrode measured 3 mmHg. These results confirmed that the apparatus was air-tight with negligible ingress of O_2 from the atmosphere. Furthermore, since we sampled directly from the experimental bath, this also indicated that our flow rates were appropriate and maintained the hypoxia. Furthermore, switches into and out of anoxia/hypoxia were rapid, with the new equilibrium achieved within 3 s (Fig. 2).

3.2. Anaesthetic sampling

Fig. 3 shows that the rate of rise of anaesthetic for each agent in the headspace was rapid and reached equilibrium after just a minute, and remained stable thereafter for >40 min that were tested. Few experimental periods last longer than this.

Whereas anaesthetic concentrations were stable for as long as vapour was bubbled and the system was in equilibrium, sometimes protocols require long interruptions to anaesthetic exposure

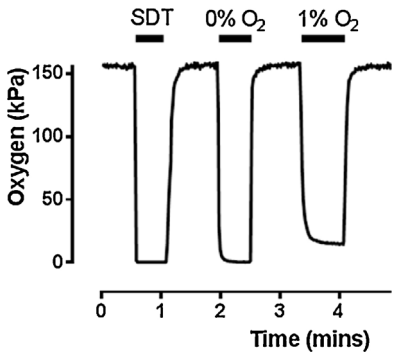

Fig. 2. Delivery of anoxic gas mixture. Estimates of pO_2 in solution in the experimental bath against delivered O_2 concentration. The first gas input (SDT) is severe hypoxia (95% N_2, 5% CO_2) with sodium dithionite, which elicited 0 mmHg. Note the rapid fall and equilibration of hypoxic gas mixtures.

followed by re-exposure. The solution could be bubbled continuously with vapour when not in use, but this wasteful of anaesthetic. Therefore we also assessed the time course for washout of agent from solution (headspace) in two protocols after equilibration as described above. First, we turned the vapourisers off but allowed agent-free gas to bubble into solution. Fig. 4A shows that vapour loss from headspace was very rapid with a half-time of ~50 s regardless of agent or initial concentration. Second, we turned off both vapour and bubbling; we did not seal the bottle air-tight but allowed natural leakage from the small holes in its stopper. We measured headspace gas at 15 min intervals and Fig. 4B shows that under these conditions washout was very slow (Fig. 4B), suggesting that re-equilibration in re-introducing anaesthetic would be faster with this method.

Fig. 5 shows the results of sampling for the two anaesthetic agents from the bottle, and Fig. 6 shows the results for sampling from the experimental bath. It is clear that for both agents there is a strong linear relationship between the vaporisation rate on the vaporiser and the concentration (parts-per-million, ppm) obtained in solution, across a very wide range of concentrations (r^2 range 0.93–0.98). These relationships were found for both sampling from the bottle and the experimental bath. Exact equations were calculated (see figure legends), but approximately the relationship for our apparatus in the experimental bath is ~5 ppm per % vapour, regardless of agent. The variation in results was highest at the higher concentrations, perhaps indicating the influence of sampling error at these higher doses.

Fig. 7 shows that there was no consistent loss of agent across a wide range of concentrations between bottle and perfusion bath for both agents. Statistically this was assessed using factorial analysis of variance, where the difference in concentration of agent between bottle and bath was the 'response' and there were two factors: 'agent' (two levels, one for each anaesthetic) and 'dose' (five levels, one for each concentration). None of the iterations of 'dose', 'agent' or the interactive term were significant ($p > 0.127$), confirming no consistent difference between bottle and bath concentrations either across concentrations or between agents.

We conducted additional experiments in which we bubbled mixtures of agent into solution by placing the vaporisers in series. Anaesthetic mixtures are sometimes used to confirm the additive interactions of agents on cell functions (Hendrickx et al., 2008) but infra-red analysers are unable accurately to measure a mix of agents. We assessed the behaviour of the system in three ways. First, employing three-way taps in the gas lines connecting the vaporisers, we used infra-red analysis to measure continuously the output of each vaporiser separately. This confirmed that dialled

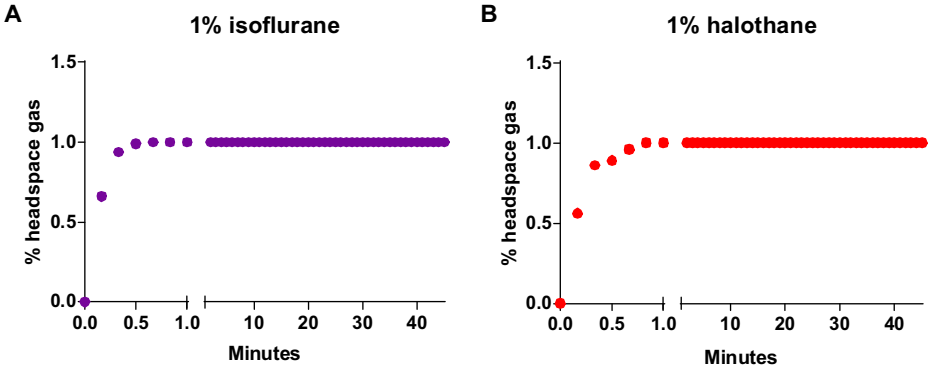

Fig. 3. Representative results of the rate of rise of anaesthetic in headspace gas for 1% of each agent. Recording was taken every 10 s from the infra-red analyser. Measurements were made using 200 ml Tyrode at ~38 °C and similar results (not shown) were obtained for 2% and 4% concentrations of each agent.

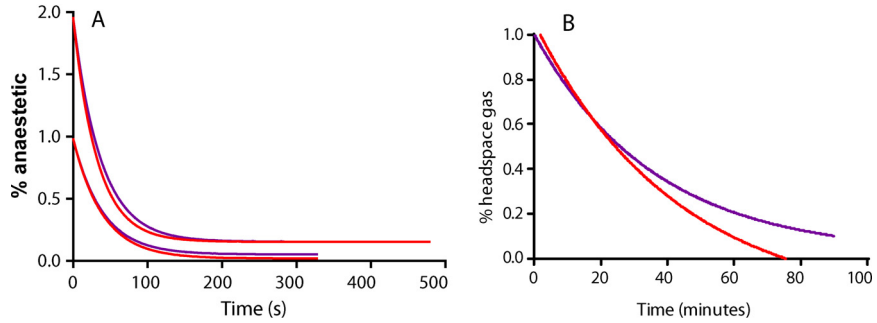

Fig. 4. Washout of agent when anaesthetic bubbling stopped. (A) Time course of loss of headspace vapour when anaesthetic turned off but agent-free bubbling continued. Initial concentrations of 2% and 1% are shown for halothane (red) and isoflurane (purple). For clarity, fitted lines only shown, rather than individual data points. (B) Time course of loss of headspace vapour when both anaesthetic and bubbling turned off (starting concentrations 1% for both agents). Note the much longer timescale on *x*-axis. (For interpretation of the references to colour in this figure legend, the reader is referred to the web version of this article.)

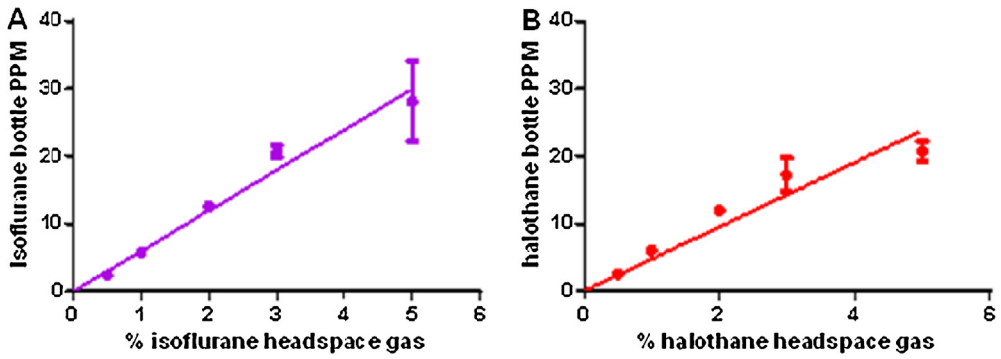

Fig. 5. *Sampling from bottle for anaesthetics.* Panel A: isoflurane; panel B, halothane. Each panel is a plot of anaesthetic concentration measured by GC–MS (ppm) versus % anaesthetic in headspace gas. Each point is the mean of 5–8 samples ± SEM and line fitted by least squares linear regression. For isoflurane, the equation is: PPM = 6.0 × % headspace gas (r^2 = 0.98). For halothane, the equation is: PPM = 4.8 × % headspace gas (r^2 = 0.93).

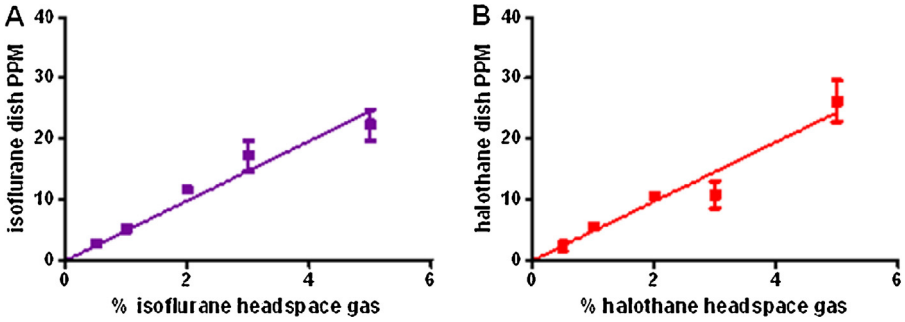

Fig. 6. *Sampling from experimental bath for anaesthetics.* Panel A: isoflurane; panel B, halothane. Each panel is a plot of anaesthetic concentration measured by LGC (ppm) versus % anaesthetic in headspace gas. Each point is the mean of 5–8 samples ± SEM and line fitted by least squares linear regression. For isoflurane, the equation is: PPM = 4.9 × % headspace gas (r^2 = 0.96). For halothane, the equation is: PPM = 4.8 × % headspace gas (r^2 = 0.96).

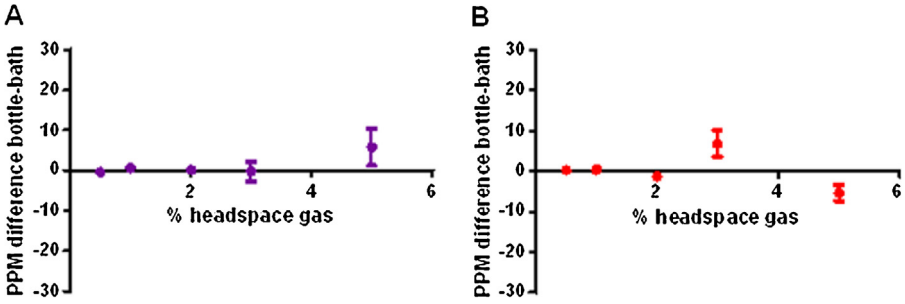

Fig. 7. *Plot of the absolute difference in measured concentration of anaesthetic between bottle and experimental bath.* Panel A: isoflurane; panel B, halothane. Each panel is a plot of the difference in concentration (same scale as Figs 2 and 3) measured by GC–MS for bottle minus bath vs % anaesthetic in headspace gas. A positive value indicates the bottle measurement is higher than the bath (and thus potential loss of agent); a negative value indicates the bath measurement is higher than the bottle (and since anaesthetic cannot have been 'gained', is an index of inherent experimental sampling or measurement error). Each point is the mean of 5–8 samples ± SEM.

concentrations of the proximal vaporiser were not influenced by the presence of a second, distal vaporiser turned on and in series with the first (i.e., no unanticipated back-pressure effects). We used infra-red analysis to confirm that the output of the second, distal vaporiser was not influenced by turning on an empty, proximal vaporiser (i.e., no forward-pressure effects). Second, we used the mass spectrometer (which can separately detect and quantify different agents in a mixture) to confirm that concentrations in the headspace in the mixture were the same as dialled on the vaporisers when mixtures of agent were used, across a range of concentrations. Third, we performed GC–MS measurements as described above, taking samples from the bottle. Fig. 8 confirms that agents dissolve in solution in mixtures, as expected from their individual behaviour.

Finally we tested for the presence of thymol in halothane samples but none was detected in any of the samples using GC–MS (with an accuracy of <1parts per billion; ppb).

4. Discussion

We have described that our system for the 'open' and continuous perfusion with volatile anaesthetic of cells/tissue in our experimental bath achieves stable and reliable concentrations of agents in solution. We have confirmed this for halothane and isoflurane, but there is no reason to suppose that other agents would be differently affected. Importantly, agent concentrations in solution, in the perfusion bath where the cells are bathed, are linearly related to vaporiser dialled concentrations, and with very little variation across a wide range of concentrations (Figs. 5 and 6).

One limitation is that our method only yields anaesthetic concentrations in the clinically relevant range, the limits set by the range of the vaporisers. It also requires that the outputs of the vaporisers are calibrated for gas flow and/or that outputs are continuously measured (e.g., by infrared gas analysis) since vaporiser outputs are sensitive to flow through them. An additional limit is set

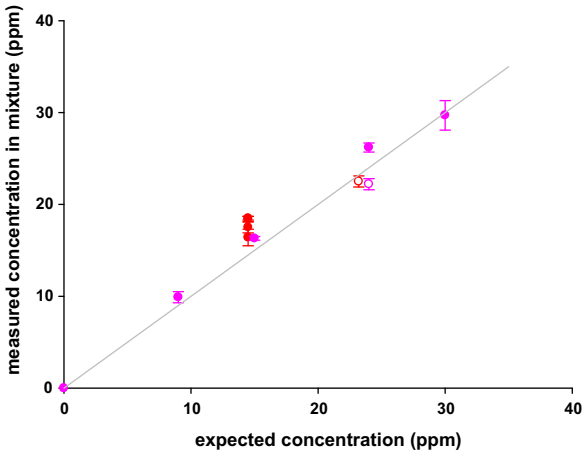

Fig. 8. Concentration of mixtures of anaesthetics in solution. Data are shown (mean ± SEM). The expected concentrations are calculated from the relationships in Figs. 5 and 6 (line of identity shown). The solid circles represent data for a fixed concentration of halothane (2.5%) combined in separate experiments with varying concentrations of isoflurane (1.5%, $n = 5$; 2.5%, $n = 5$; 4%, $n = 5$; and 5%, $n = 3$). Thus the purple solid circles represent the data plotted for isoflurane and the red solid circles data for halothane in the mix (overlapping points for halothane). Also shown is an example of a mixture of 4% halothane ($n = 3$, hollow red) and 4% isoflurane ($n = 3$, hollow purple). (For interpretation of the references to colour in this figure legend, the reader is referred to the web version of this article.)

by the published accuracy range of the infra-red analyser (which for the type we used is 0–5% for each agent). If anaesthetic concentrations outside the vaporiser/analyser range need to be studied, then there is little alternative other than to premix agents in a 'closed' system. However, we are not aware of such techniques being used in combination with the effects of changes in gas composition.

The variation in measured concentrations in solution from ideal (Fig. 7) were more likely be due to our methods of sampling than any shortcomings within the apparatus, because for some concentrations, the bath concentrations were actually slightly higher than in the bottle. It is difficult to sample from this small bath (volume 100 μl). Or, it could represent some inevitable diffusion of vapour from the system. These minor variations were not so large as significantly to influence the linear relationship between desired and actual concentrations (Figs. 5 and 6). It is this linear relationship that is all-important when constructing concentration–response curves to demonstrate drug effects. Indeed, sampling error is a more plausible explanation for this variation as our system is clearly extremely air-tight, because near-anoxic conditions were maintained in the perfusion dish when O_2-free gas ('severe' hypoxia) was used. Adsorptive loss to Teflon or metal tubing has been previously demonstrated not to occur (Herchl, 1970; Suzuki et al., 2005).

We continuously also monitored the concentrations of anaesthetic vapour from the headspace gas above the solution in the bottle, and our verification of the accuracy by GC–MS confirms that therefore, this should be a generally sufficient method of monitoring the input vapour concentrations. Repeated GC–MS measurements are laborious, expensive and clearly unnecessary for our system (although intermittent verification is probably recommended, especially if the apparatus components are refined or renewed). In many experiments involving anaesthetics, it is more important to describe the overall concentration-effect relationships for the cell preparation in question, than it is to ascertain a given effect at an exact anaesthetic concentration. Only if the latter is essential will it be necessary to perform GC–MS on a very frequent basis.

Although we generally perform studies with continuous bubbling of vapour, other experiments might necessitate intermittent interruptions to perfusion by agent (e.g., anaesthetic exposure pre- or post-conditioning to assess hypoxia/reperfusion injury). Our data for washout suggest that anaesthetic concentration will be better retained–for less than ~30 min—if bubbling is stopped during this period, facilitating more rapid re-equilibration (Fig. 4A). If bubbling is continued without vapour, even for less than a minute, loss of agent is very rapid (Fig. 4B).

In terms of the absolute value (in ppm or μM) of anaesthetic concentration in solution for a given percentage vaporiser concentration, a very wide range indeed has been reported in the literature. We measured (in ppm) ~50–150 μM in solution for ~1–3% anaesthetic in the vapour phase (for both agents), which is a slightly wider range, starting at a lower concentration, than that reported by McDougall et al. (2008) of ~100–180 μM for similar vapour concentrations, and close to the ranges reported by Miu and Puil (1989), who noted that measured concentrations were in fact less than half the value of those predicted by calculated partition coefficients. However, all these values are approximately half as much again as those reported by Becker et al. (2012), and a factor of nine times less than found by Roch et al. (2006) and by Pancrazio (1996). We cannot explain these large disparities, except to suggest that they may all be related to the precise composition of solutions used in the respective studies and their solubility for anaesthetics, or sampling error, or vapour loss, or a combination of all of these. In our study, we would expect the intrinsic vapour loss to be greatest between the bottle and the experimental dish, and we would also expect sampling error to be greatest for sampling from the dish, yet these losses were trivial (Fig. 7). Therefore, we are minded to conclude that the data represent the true solubility of the specific Tyrode solution composition we employed.

We also note that the biological action of volatile anaesthetics is regarded as driven by their partial pressure, and not their dissolved content. Thus by way of a 'bioassay' we have previously reported the potent inhibition (through an effect on TASK channels) of the intracellular calcium response in carotid body glomus cells to hypoxia at halothane vapour concentrations of ~1.5%, becoming maximal at ~3% (Pandit and Buckler, 2009), which we estimate to be ~150–300 μM in our solution. Similarly, Sirois et al. (2000) reported near-maximal effects TASK-channel K+ currents at identical partial pressures, although they had employed a 'closed' system of prior dissolution of halothane in air-tight flasks, at higher absolute dissolved concentrations of ~500 μM (Sirois et al., 2000). Our open system therefore resembles how volatile anaesthetics are administered in clinical practice to tissues of the body: the bottle into which agent is first bubbled represents the 'lungs' (Fig. 1), and the remainder of the system (the solution, the tubing, the pump) represents the blood, cardiovascular system and heart, respectively, delivering agent to tissues. Thus, the biological effects upon tissues we examine would not theoretically be influenced by replacing our Tyrode solution with, say, blood even though the absolute anaesthetic carrying capacity of the latter would be much larger.

Finally, we note the complete absence of thymol in solution when halothane is vaporised into it. Thymol is added to halothane at a concentration of 0.01% as a stabiliser and preservative. When the vaporisers are not drained as advised every week, thymol can accumulate (Rosenberg and Alila, 1984). It has been suggested that thymol may be an active ingredient in some of the properties of halothane since it was found to influence GABA-A receptor activity in mouse cortical neurons (Garcia et al., 2006) and decreases the L-type Ca^{2+} and potassium current in canine cardiomyocytes (Magyar et al., 2002). We can now robustly conclude that these results are purely a function of applying halothane mixtures directly to cell preparations in vitro. When halothane is vaporised using conventional equipment, there is simply no vaporisation of thymol. We believe therefore, that this is one additional advantage of our experimental system, in that it avoids the potential confounder that, if

premixed solutions of halothane are used, the thymol effects that others have reported may be seen.

In summary, we report a reliable system for the accurate administration of volatile anaesthetics to cell and tissue samples, with minimal loss of vapour and consistency of anaesthetic stimulus. Furthermore, our system is air tight such that extremely low levels of hypoxia can be co-administered. Finally, rapid switches into and out of hypoxia/euoxia and/or from one agent to another or to no agent can be achieved.

Acknowledgements

All experiments were performed in the Department of Physiology Anatomy & Genetics and the Mass Spectrometry Research Facility CRL, Department of Chemistry, both at University of Oxford. NH, POD and JJP conceived and designed the experiments. NH and POD collected the data. NH and JJP were primarily responsible for data analysis and interpretation, and drafted the manuscript. JW and JM performed and designed all chromatography experiments and critically reviewed the manuscript. POD and KJB assisted in the critical review and revision of the manuscript for important intellectual content. This work was funded by grants from the Medical Research Council, British Journal of Anaesthesia, National Institute of Academic Anaesthesia, Difficult Airway Society (UK) and a personal Higher Education Funding Council (England) New Blood Clinical Senior Lectureship award to JJP.

References

Becker K, Eder M, Ranft A, von Meyer L, Zieglgansberger W, Kochs E, et al. Low dose isoflurane exerts opposing effects on neuronal network excitability in neocortex and hippocampus. PLoS ONE 2012;7:e39346.

Conway KE, Cotten JF. Covalent modification of a volatile anesthetic regulatory site activates TASK-3 (KCNK9) tandem-pore potassium channels. Mol Pharmacol 2012;81:393–400.

Franks NP, Lieb WR. Selective actions of volatile general anaesthetics at molecular and cellular levels. Br J Anaesth 1993;71:65–76.

Garcia DA, Bujons J, Vale C, Sunol C. Allosteric positive interaction of thymol with the GABAA receptor in primary cultures of mouse cortical neurons. Neuropharmacology 2006;50:25–35.

Hendrickx JF, Eger EI 2nd, Sonner JM, Shafer SL. Is synergy the rule? A review of anesthetic interactions producing hypnosis and immobility. Anesth Analg 2008;107:494–506.

Herchl R. The preparation of accurate standard mixtures of inhalation anaesthetic agents. Can Anaesth Soc J 1970;17:624–9.

Jinks SL, Atherley RJ, Dominguez CL, Sigvardt KA, Antognini JF. Isoflurane disrupts central pattern generator activity and coordination in the lamprey isolated spinal cord. Anesthesiology 2005;103:567–75.

Magyar J, Szentandrassy N, Banyasz T, Fulop L, Varro A, Nanasi PP. Effects of thymol on calcium and potassium currents in canine and human ventricular cardiomyocytes. Br J Pharmacol 2002;136:330–8.

McDougall SJ, Peters JH, LaBrant L, Wang X, Koop DR, Andresen MC. Paired assessment of volatile anesthetic concentrations with synaptic actions recorded in vitro. PLoS ONE 2008;3:e3372.

Millman MS, Young M. Kinetics of dissolution of gaseous halothane in Krebs-Ringer's solution. Can J Anaesth 1992;39:980–6.

Miu P, Puil E. Isoflurane-induced impairment of synaptic transmission in hippocampal neurons. Exp Brain Res 1989;75:354–60.

Pancrazio JJ. Halothane and isoflurane preferentially depress a slowly inactivating component of Ca2+ channel current in guinea-pig myocytes. J Physiol 1996;494:91–103.

Pandit JJ. The variable effect of low-dose volatile anaesthetics on the acute ventilatory response to hypoxia in humans: a quantitative review. Anaesthesia 2002;57:632–43.

Pandit JJ. Effect of low dose inhaled anaesthetic agents on the ventilatory response to carbon dioxide in humans: a quantitative review. Anaesthesia 2005;60:461–9.

Pandit JJ, Buckler KJ. Differential effects of halothane and sevoflurane on hypoxia-induced intracellular calcium transients of neonatal rat carotid body type I cells. Br J Anaesth 2009;103:701–10.

Pandit JJ, Winter V, Bayliss R, Buckler KJ. Differential effects of halothane and isoflurane on carotid body glomus cell intracellular Ca2+ and background K+ channel responses to hypoxia. Adv Exp Med Biol 2010;669:205–8.

Roch A, Shlyonsky V, Goolaerts A, Mies F, Sariban-Sohraby S. Halothane directly modifies Na+ and K+ channel activities in cultured human alveolar epithelial cells. Mol Pharmacol 2006;69:1755–62.

Rosenberg PH, Alila A. Accumulation of thymol in halothane vaporizers. Anaesthesia 1984;39:581–3.

Sirois JE, Lei Q, Talley EM, Lynch C 3rd, Bayliss DA. The TASK-1 two-pore domain K+ channel is a molecular substrate for neuronal effects of inhalation anesthetics. J Neurosci 2000;20:6347–54.

Sirois JE, Pancrazio JJ, Lynch C 3rd, Bayliss DA. Multiple ionic mechanisms mediate inhibition of rat motoneurones by inhalation anaesthetics. J Physiol 1998;512:851–62.

Smith RA, Porter EG, Miller KW. The solubility of anesthetic gases in lipid bilayers. Biochim Biophys Acta 1981;645:327–38.

Suzuki T, Uchida I, Mashimo T. Sorptive loss of volatile and gaseous anesthetics from in vitro drug application systems. Anesth Analg 2005;100:427–30.

van den Elsen MJ, Dahan A, Berkenbosch A, DeGoede J, van Kleef JW, Olievier IC. Does subanesthetic isoflurane affect the ventilatory response to acute isocapnic hypoxia in healthy volunteers? Anesthesiology 1994;81:860–7.